SURFACE MODIFICATION OF TITANIUM AND TITANIUM ALLOYS TO ENHANCE BONE HEALING

Janzeer, Yasmeen

Awarding institution:
King's College London

Title: SURFACE MODIFICATION OF TITANIUM AND TITANIUM ALLOYS TO ENHANCE BONE HEALING

Author: Yasmeen Janzeer

SURFACE MODIFICATION OF TITANIUM AND TITANIUM ALLOYS TO ENHANCE BONE HEALING

A thesis submitted to King's College London for the degree of

Doctor of Philosophy

By

Yasmeen Janzeer

Department of Biomaterials, Biomimetics & Biophotonics

King's College London Dental institute

London SE1 9RT

United Kingdom

August 2013

ABSTRACT

Titanium and Its alloys have been used for many years as the material of choice for fabrication of dental, orthopaedic and maxillofacial implants, due to their excellent mechanical properties, biocompatibility, and the ability to osseointegrate with the surrounding bone. In order to improve the bioactivity and osseointegration of titanium implants, especially in compromised bone, surface modification of the implant surface and surface coatings have been introduced. There are different kinds of surface modification, such as, grinding, plasma spraying, sputter coatings, and alkaline treatment. More significantly, immobilization of drugs, such as, bisphosphonates, played an important role in enhancing the bone healing process. The main aim of the study is to develop and identify a facile surface modification method of immobilizing bisphosphonate molecules on commercially pure titanium and its alloy.

10mm discs of commercially pure titanium (CpTi) and titanium-aluminium-vanadium (Ti-6Al-4V) alloy were subjected to different surface treatments experiments; 1) the CpTi and Ti64 alloy surfaces were invested in phosphate bonded investment (Deguvest) and heated up to 900°C simulating superplastic forming process (SPF) creating an interaction layer on the surface upon which they were subjected to immersion in simulated body fluid (SBF) for 7 and 10 days, 2) the titanium surfaces were subjected to alkali treatment with 5M NaOH at 60°C for 24 hours, further more immersed in SBF solution for 7 and 10 days, 3) immobilization of sodium alendronate bisphosphonate on the pre treated titanium surfaces using microseeding method, and 4) tethering of Bioglass® and sodium alendronate bisphosphonate on the titanium surfaces using the electrohydrodynamic spraying method. The surface characterization of the treated surfaces was assessed using scanning electron microscopy (SEM/EDAX), Raman spectroscopy, surface roughness profilometer, and atomic force microscopy (AFM). In vitro cellular bioactivity and cytotoxicity were evaluated on the treated surfaces.

This study established that both the interaction layer and its treatment further with simulated body fluids created a favourable interaction layer on the titanium surfaces, which induced the formation of apatite like layer on the surfaces when soaked in SBF solution. The interaction layer so formed was stable and not lost after physical methods of cleaning, thus can be considered to be a quick and inexpensive method of surface modification of titanium implants, during processing itself, which can enhance the bone healing and result in improved osseointegration. The surface

modification of CpTi and Ti64 achieved with SPF and sodium hydroxide treatment and further treatment with SBF were further used to immobilize alendronate successfully, which yielded a simple method of incorporating bisphosphonates on implant surfaces, without causing any damage to the drug as no heat treatment or chemical crosslinking was required. Based on the cellular response to the investment treated titanium samples, sodium hydroxide treated samples followed by SBF treatment it can be concluded that these surfaces provide favourable conditions for cell growth, proliferation and differentiation when compared to the non-invested samples.

ACKNOWLEDGEMENT

Foremost, I would like to express my sincere gratitude to my wonderful supervisor Dr. Sanjukta Deb for her tremendous, wonderful, and continuous support of my Ph.D study and research, for her patience, motivation, enthusiasm, and immense knowledge. Her guidance helped me in all the time of research and writing of this thesis, for which I am extremely grateful. I could not have imagined having a better advisor and mentor for my Ph.D study. My very sincere thanks goes as well to my second supervisor Professor Lucy Di Silvio for her great invaluable support, advice, expertise and precious help during this research and the writing up stage, for which I am tremendously grateful. I also would like to thank my third supervisor Dr. Trevor Coward and my postgraduate coordinator Professor Gordon Proctor for their invaluable guidance, motivation, and continuous encouragement.

I owe my deepest thank and gratitude to all the people, colleagues and the research group of the Dental Biomaterials, Biomimetics & Biophotonics Department, who have helped me a lot during my four years of this research. The completion of this Ph.D degree would not have been possible without their help and support. My special thanks to Professor Timothy Watson; the head of the department, Mrs Paula Coward; the manager of the cell culture laboratory for her great help, guidance and patience, Mr. Richard Mallett; the manager of the material laboratory for his continuous help and guidance, Mr. Peter Pilecki for his help and training and Mrs Karamjit Rayit. I am grateful as well to Dr. Martyn Sherriff for his kind help and assistance with the statistics of this research, as well Dr. Frederic Festy for offering his time and expertise in the use and training of biophotonic facilities. Not Forgetting, I must also acknowledge Dr. Giuseppe Cama, Dr. Bernadine Idowu and Mr. Hassan Farah for their great assistance and training during my research. I would like to pass my deep gratitude to Professor Mohan Edirisinghe and his team at University College London for the invaluable time and help and for offering to use the Electrohydrodynamic machine, which has been used to set up one of the experiments for this research. My deep thanks goes as well to Tosin Babalola for his great help with the electrohydrodynamic experiment. Finally I would like to thank all my fellow Ph.D students especially in the postgraduate room who became a second family to me. I will never forget the great time I had between them and their continuous support and help making this place a wonderful place for carrying out research work and making friends. My special thanks goes to M. Maghrabi for

the precious support, as well as to Mr. Colin Haylock for his continuous lovely parental support.

I would like also to express my deep appreciation and gratitude to my sponsor Allied Dental Sciences Department, Jordan University of Science and Technology, Jordan for their grant and giving me the chance to pursue my study at King's College London.

Last but not lease, my endless and sincere thanks to my parents and my family for their tremendous encouraging, understanding and patience that supported me and gave me the strength throughout the last four years; I will always indebted to them.

This thesis is specially dedicated to my beloved family

Table of Contents

CONTENT	PAGE NO
ABSTARCT	2
AKNOWLEDGEMENT	4
Table of Contents	6
List of Figures	13
List of Tables	21
CHAPTER ONE – LITERATURE REVIEW	**23**
1.1. Introduction	24
1.2. Titanium and Titanium Alloys	25
1.2.1. Physical and Chemical Properties	25
1.2.2. Mechanical Properties	27
1.2.3. Titanium Oxides	28
1.2.4. Titanium in Dentistry	29
1.2.5. The Interaction between the implant surface and bone	30
1.2.6. Processing Methods of Ti and Ti Alloys	31
1.2.6.1. Casting	31
1.2.6.2. CAD/CAM Technique (Machining)	32
1.2.6.3. Superplastic Forming Process (SPF)	33
1.2.6.3.1. History of Superplasticity	33
1.2.6.3.2. Process of Superplastic Forming	33
1.2.6.3.3. Mechanism of Superplasticity	34
1.2.6.3.4. Advantages and Disadvantages of SPF	35
1.3. Dental Investments	35
1.3.1. Gypsum-bonded Investment Material	36
1.3.2. Phosphate-bonded Investment Material	36
1.3.3. New Investment Material	37
1.3.4. Interfacial Reaction between Ti Castings and Dental Investments	37

1.4. Surface Modifications of Ti and Ti Alloys	38
1.4.1. Mechanical Methods	38
1.4.2. Chemical Methods	39
1.4.2.1. Chemical Treatment	39
1.4.2.2. Electrochemical Treatment (Anodic Oxidation)	41
1.4.2.3. Sol-gel Treatment	42
1.4.2.4. Chemical Vapour Deposition (CVD)	42
1.4.2.5. Biochemical Modification of Titanium and Titanium Alloys	43
1.4.3. Physical Methods	44
1.4.3.1. Thermal Spraying	44
1.4.3.2. Plasma Spraying	44
1.4.3.3. Physical Vapour Deposition	45
1.4.3.4. Glow Discharge Plasma Treatment	46
1.4.3.5. Ion Implantation and Deposition	46
1.4.3.6. Electrohydrodynamic atomization (EHDA)	46
1.5. Bioactive Coatings	48
1.5.1. Inorganic Coatings	48
1.5.1.1. Calcium Phosphates (CaPs)	48
1.5.1.2. Bioactive Glasses	50
1.5.2. Organic biomolecule coatings	51
1.5.2.1. Immobilization of Bisphosphonates on Titanium Substrates	51
1.6. Effect of surface characteristics on cellular response	53
1.7. Aim and objectives of the study	56
CHAPTER TWO- Interaction of Ti and its Alloys with Investment – In vitro Evaluation of Bioactivity	**57**
2.1. Introduction	58
2.2 Materials and Methodology	61
2.2.1. Preparation of Titanium Discs	62
2.2.2. Surface Treatment of the Titanium Discs	63
2.2.2.1. Simulated Body Fluid (SBF) Immersion	63

2.2.2.1.1. Preparation of Simulated Body Fluid (SBF)	63
2.2.3. Surface Characterization	65
2.2.3.1. Surface Roughness Measurement	65
2.2.3.2. Scanning Electron Microscopy/Energy Dispersive X-ray Analysis (SEM/EDS)	66
2.2.3.3. Raman Spectroscopy Analysis	66
2.2.3.4. Atomic Force Microscopy (AFM)	67
2.2.4. In vitro Biological Evaluation	67
2.2.4.1. Assessment of cell viability – MTT (Methyl-tetrazolium) Assay	68
2.2.4.2. Assessment of cell viability – Live and Dead Staining Assay	69
2.2.4.3. Assessment of cell differentiation – Alkaline Phosphatase Assay	69
2.2.4.4. Assessment of cell viability – DNA Quantification Assay	70
2.2.5. Statistical Analysis	70
2.3. Results	71
2.3.1. Surface Roughness Measurement	71
2.3.2. Atomic Force Microscopy (AFM) Observations	72
2.3.3. Scanning Electron Microscopy/Energy Dispersive X-ray Analysis (SEM/EDS)	74
2.3.4. Raman Spectroscopy	77
2.3.5. Evaluation of Cytotoxicity Indirect Method (MTT)	80
2.3.6. Assessment of cell viability – Live and Dead Staining Assay	83
2.3.7. Assessment of cell differentiation – Alkaline Phosphatase Assay	86
2.3.8. Assessment of cell viability – DNA Quantification Assay	87
2.4. Discussion	89
CHAPTER THREE - Surface Modification of Titanium with Sodium Hydroxide and its Effect on In Vitro Cytocompatbility	**97**

3.1. Introduction	98
3.2. Materials and Methodology	100
3.2.1. Specimens preparation	100
3.2.2. Surface Treatments of the Titanium Discs	100
3.2.2.1. Alkali Treatment	100
3.2.2.2. Simulated Body Fluid (SBF) Immersion	100
3.2.3. Surface Characterization	101
3.2.3.1. Surface Roughness Measurement	101
3.2.3.2. Atomic Force Microscopy (AFM)	101
3.2.3.3. Scanning Electron Microscopy/Energy Dispersive X-ray Analysis (SEM/EDS)	101
3.2.3.4. Raman Spectroscopy	101
3.2.4. In vitro Biological Evaluation	101
3.3. Results	103
3.3.1. Surface Roughness Measurement	103
3.3.2. Atomic Force Microscopy (AFM)	104
3.3.3. SEM/EDS observation	107
3.3.4. Raman Spectroscopy	109
3.3.5. In vitro Biological Evaluation	112
3.3.5.1. Evaluation of Cytotoxicity Indirect Method (MTT)	112
3.3.5.2. Live/Dead Assay	115
3.3.5.3. Alkaline Phosphatase Assay- Evaluation of Differentiation	118
3.3.5.4. DNA Assay – Evaluation of Proliferation	119
3.4. Discussion	122
CHAPTER FOUR - Immobilization of Bisphosphonate on Different Surface Treated Ti and its Alloy: In vitro Bioactivity Evaluation	**127**
4.1. Introduction	128
4.2. Materials and Methodology	129
4.2.1. Preparation of Titanium Discs	129

4.2.2. Surface Treatments of Titanium Discs	129
4.2.2.1. Alkali Treatment	129
4.2.2.2. Simulating Superplastic Forming Process Treatment (SPF)	130
4.2.2.3. Simulated Body Fluid (SBF) Immersion	130
4.2.2.4. Preparation and Immobilization of Bisphosphonate (Sodium Alendronate)	130
4.2.3. Surface Characterization	132
4.2.3.1. Surface Roughness Measurement	132
4.2.3.2. Atomic Force Microscopy (AFM)	132
4.2.3.3. Fourier Transform Infrared spectroscopy (FTIR)	132
4.2.3.4. Scanning Electron Microscopy/Energy Dispersive X-ray Analysis (SEM/EDS)	132
4.2.4. In-vitro Biological Evaluation	132
4.2.5. Statistical Analysis	133
4.3. Results	134
4.3.1. Surface Roughness Measurement	135
4.3.2. Atomic Force Microscopy (AFM)	135
4.3.3. Fourier Transform Infrared spectroscopy (FTIR)	139
4.3.4. Scanning Electron Microscopy/Energy Dispersive X-ray Analysis (SEM/EDS)	139
4.3.5. Evaluation of Cytotoxicity Indirect Method (MTT)	143
4.3.6. Assessment of cell differentiation – Alkaline Phosphatase Assay	146
4.3.7. Assessment of cell viability – DNA Quantification Assay	149
4.4. Discussion	153
CHAPTER FIVE - Surface Modification of Commercially Pure Titanium using the Electrohydrodynamic Method	**160**
5.1. Introduction	161
5.2. Materials and Methodology	163
5.2.1. Preparation of Titanium Samples	163
5.2.2. Electrohydrodynamic Deposition of Bioglass®	163

5.2.3. Immobilization of Alendronate Bisphosphonate	164
5.2.4 Surface Characterization	164
5.2.4.1. Scanning Electron Microscopy (SEM) and Energy-Dispersive X-Ray Spectroscopy (EDAX)	164
5.2.4.2. Raman Spectroscopy	165
5.2.5. In-vitro Biological Evaluation	165
5.2.5.1. Cell Viability as assessed by the MTT Assay	165
5.2.5.2. Cell Viability as Assessed by Live-Dead Immune Fluorescence	165
5.2.5.3. Cellular response to sodium alendronate concentration	165
5.2.5.4. Cytoskeletal Staining	166
5.2.5.5. Total DNA Production	166
5.2.5.6. Alkaline Phosphatase (ALP) Activity	166
5.2.5.7. ALP/DNA Ratio	166
5.2.5.8. Alizarin Red Staining	166
5.2.6. Statistical Analysis	167
5.3. Results	168
5.3.1. Surface Characterization	168
5.3.1.1. Scanning Electron Microscopy (SEM) and Energy Dispersive X-Ray Spectroscopy (EDAX)	168
5.3.1.2. Raman Spectroscopy Analysis	169
5.3.2. Cellular Response to Titanium Modified Surfaces	170
5.3.2.1. Evaluation of Cytotoxicity Indirect Method (MTT) on aHOB Cells	170
5.3.2.2. Evaluation of Cytotoxicity Indirect Method (MTT) on HOS Cells	171
5.3.2.3. Cellular response to Sodium Alendronate concentration using MTT assay	172
5.3.2.4. Assessment of alveolar HOB cells viability – Live and Dead Staining Assay	173
5.3.2.5. Assessment of femur HOB cells viability – Live and Dead Staining Assay	174
5.3.2.6. Assessment of HOS cells viability – Live and Dead Staining	175

Assay	
5.3.2.7. Cytoskeletal Staining	176
5.3.2.8. Cell Proliferation as Assessed by Total DNA Production	176
5.3.2.9. Cell Differentiation as Assessed by Alkaline Phosphatase (ALP) Activity	177
5.3.2.10. ALP/DNA Ratio	178
5.3.2.11. Osteoblast Mineral Deposition by Alizarin Red staining	180
5.4. Discussion	181
CHAPTER SIX - Conclusion and Future Work	**187**
6.1. Conclusion	188
6.2. Future Work	190
CHAPTER SEVEN - References	**191**
CHAPTER SEVEN - APPENDICES	202
8.1. Introduction	203
8.2. Materials and Methodology	203
8.2.1. Gene Expression Analysis	203
8.2.1.1. RNA Extraction from Cultured Cells	203
8.2.2.2. Quantification of Extracted RNA and Quantity Analysis	204
8.2.2.3. Reverse Transcriptase of RNA to cDNA	204
8.2.2.4. PCR Amplification	204
8.2.2.5. Gel Electrophoresis	205
8.3. Results and Discussion	206

List of Figures

Figure No	Description	Page No
Fig 1.1	The crystal structure of α phase (hcp), the allotropic β phase structure (bcc) and the allotropic transformation that occurs when heating up to 882.3 °C [1]	26
Fig 1.2	Crystal structure of titanium dioxide phases of rutile, brookite, and anatase, adapted from Pelaez et al. *(Pelaez, M., et al., A review on the visible light active titanium dioxide photocatalysts for environmental applications. Applied Catalysis B: Environmental, 2012. 125(0): p. 331-349)* [2]	29
Fig 1.3	Illustration of Interaction between the biomaterial implant surface and the surrounding tissue adapted from Kurella et al. *(Kurella, A. and N.B. Dahotre, Review paper: Surface Modification for Bioimplants: The Role of Laser Surface Engineering. Journal of Biomaterials Applications, 2005. 20(1): p. 5-50) [3]*	30
Fig 1.4	Illustration of the superplastic forming process SPF adapted from Bonet et al. *(Bonet, J., et al., Numerical simulation of the superplastic forming of dental and medical prostheses. Biomech Model Mechanobiol, 2002. 1(3): p. 177-96) [4].*	34
Fig 1.5	Schematic diagram of biochemical modification of titanium surface adapted from Liu et al [5]. (A) Attachment site by physical or chemical adsorption or covalent linkage without or with cross-polymerization (dashed line); (B) spacer to adjust distance of functional group C from original surface; (C) chemical, biochemical or biological functionality, such as organo-functional group, peptide, protein, etc.	44
Fig 1.6	Schematic diagram of the electrohydrodynamic atomizer (EHDA) system adapted from Li et al. (*Li, X., et al., A novel jet-based nano-hydroxyapatite patterning technique for osteoblast guidance. J R Soc Interface, 2010. 7(42): p. 189-97)* [6]	47
Fig 1.7	Chemical structure of inorganic pyrophosphate and bisphosphonate, adapted from Michaelson et al. [7]	52
Fig 1.8	Structures of the bisphosphonates used in clinical studies approved for commercial use in humans for bone disease classified according to their biochemical mode of action, adapted from Russell et al. [8]	53
Fig 2.1	(A) Titanium stock sheets after abrading with the 800 grit silicon carbide paper, (B) Press and die system used to punch the titanium sheets, (C) titanium stock sheets after punching, and10 mm titanium discs used for the SPF forming	61
Fig 2.2	Representative 2D and 3D of AFM images of the different tested CpTi and Ti64 samples, where the SPF process decrease the Ra value on the CpTi samples, while it increasd it on the Ti64 samples compared to the control. While immersion in SBF seems to increase the surface roughness of these surfaces due to the deposition of apatite like layer.	73

Fig 2.3	SEM/EDS images of CpTi control, CpTi surfaces which were invested simulating superplastic forming process (SPF) and CpTi which were invested simulating superplastic forming process and immersed in simulated body fluid SBF for 10 days.	75
Fig 2.4	SEM/EDS images of Ti64 control, Ti64 surfaces which were invested simulating superplastic forming process (SPF) and Ti64 which were invested simulating superplastic forming process and immersed in simulated body fluid SBF for 10 days.	76
Fig 2.5	Raman spectrum with highlighted peaks of the different treated CpTi (control, invested CpTi simulating superplastic forming process (SPF), and invested CpTi simulating superplastic forming process immersed in simulated body fluid (SBF) for 10 days.	78
Fig 2.6	Raman spectrum with highlighted peaks of the different treated Ti64 (control, invested Ti64 simulating superplastic forming process (SPF), and invested Ti64 simulating superplastic forming process immersed in simulated body fluid (SBF) for 10 days.	79
Fig 2.7	Evaluation of Cytotoxicity Indirect Method/ MTT Day 1 Exposure of CpTi test samples; showing levels of intensity of absorbance at 570nm of the CpTi samples at 24h and 72 elutions, expressed as mean absorbance ± S.D (n=4); the statistical significance was predetermined at $p< 0.05$	80
Fig 2.8	Evaluation of Cytotoxicity Indirect Method/ MTT Day 1 Exposure of Ti64 test samples; showing levels of intensity of absorbance at 570nm of the Ti64 samples at 24h and 72 elutions, expressed as mean absorbance ± S.D (n=4); the statistical significance was predetermined at $p< 0.05$	81
Fig 2.9	Evaluation of Cytotoxicity Indirect Method/ MTT Day 3 Exposure of CpTi test samples; showing levels of intensity of absorbance at 570nm of the CpTi samples at 24h and 72 elutions, expressed as mean absorbance ± S.D (n=4); the statistical significance was predetermined at $p< 0.05$	82
Fig 2.10	Evaluation of Cytotoxicity Indirect Method/ MTT Day 3 Exposure of Ti64 test samples; showing levels of intensity of absorbance at 570nm of the Ti64 samples at 24h and 72 elutions, expressed as mean absorbance ± S.D (n=4); the statistical significance was predetermined at $p< 0.05$	83
Fig 2.11	Live and dead fluorescence staining (Ethidium Homodimer-1) of aHOB cells exposed for 72 hours on CpTi test samples, which were treated simulating SPF process then subjected to immersion in SBF solution for 7 and 10 days. The surfaces are showing a good response of cells with a large number of live cells as it shown in the green staining images and low dead cells as it shown in the red staining images.	84
Fig 2.12	Live and dead fluorescence staining (Ethidium Homodimer-1) of aHOB cells exposed for 72 hours on Ti64 test samples, which were treated simulating SPF process then subjected to immersion in SBF solution for 7 and 10 days. The surfaces are showing a good response of cells with a large number of live cells as it shown in the green staining images and low dead cells as it shown in the red staining images.	85

Fig 2.13	Evaluation of Differentiation of Osteoblast Cells / ALP Assay of CpTi titanium discs which were treated simulating superplastic forming process SPF and then subjected to immersion in SBF solution. The data represents the average for each group as mean absorbance ± SD (n=8); the statistical significance was predetermined at p< 0.05	86
Fig 2.14	Evaluation of Differentiation of Osteoblast Cells / ALP Assay of Ti64 titanium discs which were treated simulating superplastic forming process SPF and then subjected to immersion in SBF solution. The data represents the average for each group as mean absorbance ± SD (n=8); the statistical significance was predetermined at p< 0.05	87
Fig 2.15	Evaluation of Proliferation of Osteoblast Cells / DNA Assay of CpTi titanium discs which were treated simulating superplastic forming process SPF and then subjected to immersion in SBF solution. The data represents the average for each group as mean absorbance ± SD (n=8); the statistical significance was predetermined at p< 0.05	87
Fig 2.16	Evaluation of Proliferation of Osteoblast Cells / DNA Assay of Ti64 titanium discs which were treated simulating superplastic forming process SPF and then subjected to immersion in SBF solution. The data represents the average for each group as mean absorbance ± SD (n=8); the statistical significance was predetermined at p< 0.05	88
Fig 3.1	Ti discs fitted within the bent wire B) Ti discs placed in vials to be soaked in sodium hydroxide C) Ti discs suspended in sodium hydroxide to ensure all surfaces were exposed to the sodium hydroxide solution over the 24 h period.	100
Fig 3.2	Representative 2D and 3D of AFM images of the different CpTi surface treated groups; alkali treated surfaces (NaOH), which were immersed in SBF solution showed higher surface roughness compared to the non-treated surfaces, which were immersed in SBF as well.	105
Fig 3.3	Representative 2D and 3D of AFM images of the different Ti64 surface treated groups; alkali treated surfaces (NaOH), which were immersed in SBF solution showed higher surface roughness compared to the non-treated surfaces, which were immersed in SBF as well.	106
Fig 3.4	Qualitative SEM images and EDAX analysis of CpTi and Ti64 different treated samples; showing that treating titanium surfaces with NaOH enhance the deposition of apatite like layer when immersed in SBF (CpTi NaOH SBF and Ti64 NaOH SBF) compared to non-treated surfaces immersed in SBF (CpTi SBF and Ti64 SBF).	108
Fig 3.5	Raman spectra of the different treated CpTi samples; control with no treatment, NaOH treated, immersion in SBF only and immersion in SBF after alkali treatment.	110
Fig 3.6	Raman spectra of the Ti64 samples; control with no treatment, NaOH treated,Ti64 immersed in SBF only and SBF treatment after alkali treatment.	111
Fig 3.7	Evaluation of Cytotoxicity Indirect Method/ MTT Day 1 Exposure of CpTi test samples; showing levels of intensity of absorbance at 570nm of the Ti64 samples at 24h and 72 elutions, expressed as mean absorbance ± S.D (n=4); the	112

	statistical significance was predetermined at p< 0.05. An increase in	
Fig 3.8	Evaluation of Cytotoxicity Indirect Method/ MTT Day 1 Exposure of Ti64 specimens exposed to only to SBF treatment and sodium hydroxide treatment followed by SBF immersionexpressed as mean absorbance ± S.D (n=4); the statistical significance was predetermined at p< 0.05. An increase in cell metabolic activity was observed on all test samples and non-toxic control (TCP) compared to the toxic control(10% alcohol).	113
Fig 3.9	Evaluation of Cytotoxicity Indirect Method/ MTT Day 3 Exposure of CpTi specimens exposed to only SBF treatment and sodium hydroxide treatment followed by SBF immersionexpressed as mean absorbance ± S.D (n=4); the statistical significance was predetermined at p< 0.05. The results showed that the eluants at 24 h lowered the cell activity indicating a fall in cell metabolic activity, resulting from a potential leachable from the materials in the elution fluid due to longer elution time.	114
Fig 3.10	Evaluation of Cytotoxicity Indirect Method/ MTT Day 1 Exposure of Ti64 specimens exposed to only to SBF treatment and sodium hydroxide treatment followed by SBF immersionexpressed as mean absorbance ± S.D (n=4); the statistical significance was predetermined at p< 0.05. A decrease in cell metabolic activity was observed on all test samples and non-toxic control (TCP) compared to the toxic control(10% alcohol).	115
Fig 3.11	Live and dead fluorescence staining (Ethidium Homodimer-1) of aHOB cells exposed for 72 hours on CpTi samples. The images show that the surfaces treated with sodium hydroxide followed by SBF treatment had a large number of live cells in comparison to the SBF treated samples only.	116
Fig 3.12	Live and dead fluorescence staining (Ethidium Homodimer-1) of aHOB cells exposed for 72 hours on Ti64 samples. The images show that the surfaces treated with sodium hydroxide followed by SBF treatment had a large number of live cells in comparison to the SBF treated samples only.	117
Fig 3.13	Evaluation of Differentiation of Osteoblast Cells / ALP Assay of CpTi titanium discs, which were treated with NaOH and immersed in SBF for 7 and 10 days. The data represents the average for each group as mean absorbance ± SD (n=8); the statistical significance was predetermined at p< 0.05.	118
Fig 3.14	Evaluation of Differentiation of Osteoblast Cells / ALP Assay of Ti64 titanium discs, which were treated with NaOH and immersed in SBF for 7 and 10 days. The data represents the average for each group as mean absorbance ± SD (n=8); the statistical significance was predetermined at p< 0.05.	119
Fig 3.15	Evaluation of Proliferation of Osteoblast Cells / DNA Assay of CpTi samples which have been treated with NaOH and immersed in SBF for 7 and 10 days. The data represents the average for each group as mean absorbance ± SD (n=8); the statistical significance was predetermined at p< 0.05	120

Fig 3.16	Evaluation of Proliferation of Osteoblast Cells / DNA Assay of Ti64 samples which have been treated with NaOH and immersed in SBF for 7 and 10 days. The data represents the average for each group as mean absorbance ± SD (n=8); the statistical significance was predetermined at p< 0.05.	120
Fig 4.1	Schematic illustration of the different surface treatment on the CpTi and Ti64 discs, with three main experimental groups (non-treated, alkali treated and SPF), which were immersed in SBF solution for 7 and 10 days, subsequently alendronate sodium was immobilised on their surfaces	131
Fig 4.2	Representative 2D and 3D of AFM images of the different tested CpTi samples, where the SPF process decrease the Ra value on the CpTi samples, the immersion in SBF seems to increase the surface roughness of these surfaces	137
Fig 4.3	Representative 2D and 3D of AFM images of the different tested Ti64 samples, where the SPF process seems to increase the Ra value on the Ti64 samples, the immersion in SBF seems to increase the surface roughness of these surfaces due to the deposition of apatite like layer. Alendronate deposition seems to decrease the surface roughness by forming a more uniform layer on the surface.	138
Fig 4.4	FTIR spectrum of CpTi, which was subjected to immobilization of sodium alendronate bisphosphonate after it was invested and heated simulating superplastic forming process (SPF).	139
Fig 4.5	Figure 4.8: SEM/EDS images of CpTi control, CpTi surfaces which were subjected to simulated superplastic forming process (SPF) only and CpTi discs SPF and immersed in simulated body fluid SBF for 10 days with subsequent immobilization with bisphosphonate (sodium alendronate)	141
Fig 4.6	SEM/EDS images of Ti64 control, CpTi surfaces which were subjected to simulated superplastic forming process (SPF) and CpTi discs which were subjected to simulated superplastic forming process (SPF) and immersed in simulated body fluid SBF for 10 Days with subsequent immobilization with bisphosphonate (sodium alendronate)	142
Fig 4.7	Evaluation of Cytotoxicity Indirect Method/ MTT Day 1 Exposure of CpTi test samples; showing levels of intensity of absorbance at 570nm of the CpTi samples at 24h and 72 elutions, expressed as mean absorbance ± S.D (n=4); the statistical significance was predetermined at p< 0.05	143
Fig 4.8	Evaluation of Cytotoxicity Indirect Method/ MTT Day 1 Exposure of Ti64 test samples; showing levels of intensity of absorbance at 570nm of the Ti64 samples at 24h and 72 elutions, expressed as mean absorbance ± S.D (n=4); the statistical significance was predetermined at p< 0.05	144
Fig 4.9	Evaluation of Cytotoxicity Indirect Method/ MTT Day 3 Exposure of CpTi test samples; showing levels of intensity of absorbance at 570nm of the CpTi samples at 24h and 72 elutions, expressed as mean absorbance ± S.D (n=4); the statistical significance was predetermined at p< 0.05	145
Fig 4.10	Evaluation of Cytotoxicity Indirect Method/ MTT Day 3 Exposure of Ti64 test samples; showing levels of intensity of absorbance at 570nm of the Ti64 samples at 24h and 72 elutions, expressed as mean absorbance ± S.D (n=4); the	146

	statistical significance was predetermined at p< 0.05	
Fig 4.11	Evaluation of Differentiation of Osteoblast Cells / ALP Assay of CpTi titanium disks which have been treated with NaOH and immersed in SBF for 7 and 10 days, and then subjected to immobilisation of 2mg/ml sodium alendronate. The data represents the average for each group as mean absorbance ± SD (n=8) (p<0.05).	147
Fig 4.12	Evaluation of Differentiation of Osteoblast Cells / ALP Assay of Ti64 titanium disks which have been treated with NaOH and immersed in SBF for 7 and 10 days, and then subjected to immobilisation of 2mg/ml sodium	147
Fig 4.13	Evaluation of Differentiation of Osteoblast Cells / ALP Assay of CpTi titanium samples, which were simulated superplastic forming SP, and then subjected to immobilisation of 2mg/ml sodium alendronate. The data represents the average for each group as mean absorbance ± SD (n=8)	148
Fig 4.14	Evaluation of Differentiation of Osteoblast Cells / ALP Assay of Ti64 titanium samples, which were simulated superplastic forming SPF, and then subjected to immobilisation of 2mg/ml sodium alendronate. The data represents the average for each group as mean absorbance ± SD (n=8)	149
Fig 4.15	Evaluation of Proliferation of Osteoblast Cells / DNA Assay of CpTi Samples which have been treated with NaOH and immersed in SBF for 7 and 10 days, and then subjected to immobilisation of 2mg/ml sodium alendronate. The data represents the average for each group as mean absorbance ± SD (n=8)	150
Fig 4.16	Evaluation of Proliferation of Osteoblast Cells / DNA Assay of Ti64 Samples which have been treated with NaOH and immersed in SBF for 7 and 10 days, and then subjected to immobilisation of 2mg/ml sodium alendronate. The data represents the average for each group as mean absorbance ± SD (n=8)	150
Fig 4.17	Evaluation of Proliferation of Osteoblast Cells / DNA Assay of CpTi Samples, which were simulated superplastic forming SPF and then subjected to immobilisation of 2mg/ml sodium alendronate. The data represents the average for each group as mean absorbance ± SD (n=8)	151
Fig 4.18	Evaluation of Proliferation of Osteoblast Cells / DNA Assay of Ti64 Samples, which, were simulated superplastic forming SPF and then subjected to immobilisation of 2mg/ml sodium alendronate. The data represents the average for each group as mean absorbance ± SD (n=8)	152
Fig 5.1	Schematic illustration of the experimental group investigated in this study, Ti: Titanium, BG: Bioglass®, BPs: Bisphosphonate (sodium alendronate)	163
Fig 5.2	Schematic diagram illustrating EHDA process of depositing Bioglass® coating, where the coating solution is sprayed through the needle onto the surface of the substrate under predetermined conditions and power supply. [9]	164
Fig 5.3	SEM images and EDAX analysis. A: The micrograph of CpTi as received at magnifications of 100x with the insert showing a magnification of 2000x. B: CpTi specimen coated with Bioglass® 45S5 using EHDA process that shows the irregular	168

	particles embedded on the surface. C: CpTi coated with Bioglass® 45S5 by EHDA and treated with alendronate (B and C show 100x magnification in main image with an insert at 5000x magnification in top right	
Fig 5.4	Raman spectra obtained on: (A) Ti-Uncoated surface, (B) Ti surface coated with Bioglass (BG) and (c) Ti surface coated with Bioglass® and alendronate sodium immobilized (BG BP).	169
Fig 5.5	Evaluation of Cytotoxicity Indirect Method/ MTT 24h and 72h elution times of the test samples on aHOB cells; showing levels of intensity of absorbance at 570nm of the test samples at 24 and 72 exposures, expressed as mean absorbance ± S.D (n=3); the statistical significance was predetermined at p<0.0	170
Fig 5.6	Evaluation of Cytotoxicity Indirect Method/ MTT 24h and 72h elution times of the test samples on HOS cells; showing levels of intensity of absorbance at 570nm of the test samples at 24h and 72h exposures, expressed as mean absorbance ± S.D (n=3); the statistical significance was predetermined at p<0.05.	171
Fig 5.7	Evaluation of Cytotoxicity Indirect Method/ MTT 24 and 72 hour Exposure of alveolar HOBs, femur HOBs, and HOS cells cultured in different concentrations of sodium alendronate (BP). Showing levels of intensity of absorbance at 570nm of the test samples at 24h and 72 elutions, expressed as mean absorbance ± S.D (n=3); t statistical significance was predetermined at p<0.05.	172
Fig 5.8	Live (green) and dead (red) fluorescence staining (Ethidium Homodimer-1) of aHOB cells exposed for 24, 72 hours and 7 days on CpTi test samples (Thermanox®= nontoxic control)	173
Fig 5.9	Live (green) and dead (red) fluorescence staining (Ethidium Homodimer-1) of femur HOB cells exposed for 24, 72 hours and 7 days on CpTi test samples (Thermanox®= non-toxic control)	174
Fig 5.10	Live (green) and dead (red) fluorescence staining (Ethidium Homodimer-1) of femur HOB cells exposed for 24, 72 hours and 7 days on CpTi test samples (Thermanox®= nontoxic control)	175
Fig 5.11	Immunofluorescent staining of cytoskeletal structure showing cell morphology at x20 magnification. Microtubule is stained with anti-β-tubulin (red). Nuclei are counter stained with DAPI (blue). A) HOB cells staining on uncoated Ti surfaces, B) HOB cells staining on BG coated surfaces, and C) HOB cells staining on BG+BPs coated surfaces.	176
Fig 5.12	Evaluation of Proliferation of aHOB Cells / DNA Assay of CpTi titanium discs The data represents the average for each group as mean absorbance ± SD (n=3); the statistical significance was predetermined at p<0.05	177
Fig 5.13	Evaluation of Proliferation of aHOB Cells / ALP Assay of CpTi titanium discs The data represents the average for each group as mean absorbance ± SD (n=3), and the statistical significance was predetermined at p<0.05	178

Fig 5.14	Alkaline phosphatase/ DNA activity in HOB cells, deduced from separate ALP and DNA cultures over 21 days.	179
Fig 5.15	Total DNA production and ALP activity for the control and test samples at day 14 (extracted from Figures 5.11 and 5.12)	179
Fig 5.17	Alizarin Red Qualitative analysis of HOB cell mineral (calcium) deposition. Mineral (Calcium) stained in red. (n=2, one representative disc is displayed).	180
Fig 8.1	Schematic illustration of the experimental group investigated in this study, Ti: Titanium, BG: Bioglass, BPs: Bisphosphonate (sodium alendronate)	203
Fig 8.2	Gene expression of four different genes: ALP, Osteocalcin, RUNX2 and GAPDH (as a control) from RNA extracted at day 14. The table represents the corresponding bands to the tested samples.	206

List of Tables

Table No	Description	Page No
1.1	The chemical composition of the different grades of commercially pure titanium and the titanium alloys used for implants, adapted from McCraken et al. (McCracken, M., Dental Implant Materials: Commercially Pure Titanium and Titanium Alloys. Journal of Prosthodontics, 1999. 8(1): p. 40-43) [10]	27
1.2	The mechanical properties of titanium, titanium alloys, and other natural and implant materials, adapted from Niinomi et al. (Niinomi, M., Mechanical properties of biomedical titanium alloys. Materials Science and Engineering: A, 1998. 243(1–2): p. 231-236) [11].	28
1.3	Table 1.3: Surface modification methods for titanium and its alloys implants, adapted from Liu et al. [5] and Kurella et al. [3].	40
1.4	Table 1.4: Examples of CaP phases for biomedical applications along with their chemical formula and Ca/P ratio.	48
1.5	Table 1.5: Common methods of producing Calcium Phosphate/HA coatings on Titanium surfaces, adapted from Narayanan et al. (Narayanan, R., et al., Calcium phosphate-based coatings on titanium and its alloys. J Biomed Mater Res B Appl Biomater, 2008. 85(1): p. 279-99) [12]	49
2.1	Table 2.1: The composition and manufacturer information of the dental investment Deguvest SR used for investing the Ti and Ti6AlV4 discs using simulated superplastic forming process	62
2.2	Table 2.2: A comparison of ionic concentrations in SBF and Blood Plasma adapted from kokubo et al. [13]	64
2.3	Table 2.3: Reagent amounts for preparation of SBF solution (1L, 7.4 pH) according to Kokubo recipe [13]	65
2.4	Table 2.4: Average surface roughness (Ra) measurements using a profliometer of CpTi and Ti64 samples (n=4) ± standard deviation (SD) before and after treatment with SBF on invested and non- invested specimens	71
2.5	Table 2.5: Surface roughness parameter for the different surface treated titanium disc groups obtained under AFM. The results were statistically analyzed using one-way Anova analysis (GraphPad Prism software). The Statistical significance was predetermined at ($p < 0.05$) and n=4 (± SD). There was no significant difference between the control and the different treated surfaces for both CpTi and Ti64 samples.	72
2.6	Table 2.6: Concentrations of Ca and P (Atomic %) of CpTi and Ti64 test samples which were invested simulating superplastic forming process and immersed in SBF for 10 days obtained from EDS analysis.	74
3.1	Table 3.1: The experimental and sub groups of the different treated surfaces which were immersed in SBF solution. For each group both CpTi and Ti64 specimens were used.	103
3.2	Table 3.2: Surface roughness measurements (Ra ± SD) for the different treated CpTi and Ti64 samples (n=4).	103

3.3	Table 3.3: Surface roughness Ra for the different surface treated titanium disc groups obtained with AFM, n=4 (± SD).	104
3.4	Table 3.4: Concentrations of Ca and P (Atomic %) of CpTi and Ti64 samples treated with NaOH and immersed in SBF.	107
4.1	Table 4.1: The experimental and sub groups of the different treated surfaces which were subjected to immobilisation of BPs.	134
4.2	Table 4.2: Surface roughness parameter (Ra) measurements for CpTi and Ti64 samples (n=4) ± SD.	135
4.3	Table 4.3: Surface roughness (Ra) of the different surface treated titanium disc groups obtained under AFM. The results were statistically analyzed using one-way Anova analysis (GraphPad Prism software). The statistical significance was predetermined at ($p < 0.05$) and n=4 (± SD). There was no significant difference between the control and the different treated surfaces for both CpTi and Ti64 samples.	136
4.4	Table 4.4: Concentrations of Ca and P (Atomic %) of CpTi and Ti64 samples	140
8.1	Table 5.1: Primer sequences for RT-PCR, ALP: alkaline phosphatase, OSC: osteocalcin, RUNX2: Runt-related transcription factor 2, and GAPDH: Glyceraldehyde 3-phosphate dehydrogenase	205

CHAPTER ONE

Literature Review

1.1 Introduction

Implant biomaterials have progressed dramatically during the last century. These can be broadly classified into metallic, ceramic, and composite systems. Metallic biomaterials consisting of various steel formulations resulted in unfavorable tissue reactions and turned out to be a failure during the early years of the twentieth century. It was not until the 1920s that materials scientists were able to find a material that was compatible with a biological environment [14]. Currently, most artificial joints consist of a metallic component (either titanium alloy or Co–Cr alloys) articulating against a polymer (typically ultrahigh molecular weight polyethylene, UHMWPE). Co-Cr alloys have excellent wear resistance and are stable due to the formation of a passive and self-replenishing chromium oxide, a few atomic layers thick. Although, Cr–Co alloys have good wear resistance; the low density of titanium and its alloys drove research into their applications as implants in the 1930s [3]. Apart from this, titanium alloys are increasingly used as implant materials in dentistry and orthopaedics because of their excellent biocompatibility, which is attributed to a passive layer of titanium dioxide on the surface [5].

Ceramics are referred in implantology as bioceramics, which are refractory in nature and possess high compressive strength. Bioceramics comprise of a group of materials for medical applications, mainly for implants in orthopaedics, maxillofacial surgery and dental implants. They form a diverse class of biomaterials that include three types, namely bioinert high strength ceramics, bioactive ceramics which form direct chemical bonds with bone or even with soft tissue of a living organism and various bioresorbable ceramics that actively participate in the metabolic processes of an organism with predictable results [15]. Bioinert ceramics such as alumina and zirconia maintain their physical and mechanical properties even in biological environments, whereas calcium phosphate and tricalcium phosphate (TCP) degrade upon implantation in a biological environment and hence are considered biodegradable whilst hydroxyapatite (HA) can be crystallized from calcium phosphate. Hydroxyapatite, certainly the most widely researched biomaterial is closely related to the mineral phase of bone and teeth, which accounts for its biocompatibility and application as a bone replacement material. However, the major drawback of HA is its poor mechanical properties, limiting it to low load-bearing applications, coatings, or porous implants. The latest classes of bioceramic materials are bioactive in nature, examples include Bioglass® and Cervital®. These materials induce a biological bonding at the interface between the material and the tissue, and their major application is in the coating of metal prostheses [3, 15].

Polymers such as polyethylene terephthalate, polytetrafluoroethylene, ultrahigh molecular weight polyethylene (UHMWPE) and lactide-co-glycolide, are considered for a wide range of biomedical applications (orthopaedic, dental, cardiovascular, and soft tissue), because of their ease of manufacture, low cost and adequate mechanical and physical properties. However, compared to metallic and ceramic systems, polymers tend to possess low mechanical strength and poor wear resistance.

1.2. Titanium and Titanium Alloys

Titanium is currently one of the most important metals used in the healthcare industry. Gregor first discovered the element in England in 1790, although it did not receive its name until Klaproth named it after the mythological first sons of the earth, the Titans, in 1795. Not until the refining process was developed did commercial production become viable. In 1925, van Arkel refined the ore using titanium tetraiodide, producing a metal with acceptable properties and ductility. In the 1930s, Krol developed commercial extraction procedures that are still used today [3, 5, 10].

1.2.1. Physical and Chemical Properties

Chemically, titanium is one of the transition elements in Group IV that has an atomic number of 22 and an atomic weight of 47.9. [5]. It has a high melting point (1668 °C) and possesses a hexagonal closely packed crystal structure (hcp) α up to a temperature of 882.3 °C. Titanium transforms into a body centered cubic structure (bcc) β above this temperature [2]. Titanium alloys may be classified as alpha (α), near- α, α + β, metastable β, or stable β depending upon the room temperature microstructure. According to this, alloying elements of titanium fall into three categories: (1) α -stabilizers, such as Al, O, N, C; (2) β -stabilizers, such as Mo, V, Nb, Ta (isomorphous), Fe, W, Cr, Si, Co, Mn, H (eutectoid), and (3) neutrals, such as Zr. The alpha and near- α titanium alloys exhibit superior corrosion resistance but have limited low temperature strength, whilst, the ‘α + β’ alloys exhibit higher strength due to the presence of both the α and β phases. The properties of the materials depend on the composition, relative proportions of the ‘α and β’ phases, thermal treatment, and thermo–mechanical processing conditions [1, 5, 16]. This has brought on the discovery of low-rigidity Ti alloys such as Ti-13Nb-13Zr, Ti-12Mo-6Zr-2Fe, Ti-15Mo-5Zr-3Al, Ti-15Mo, and Ti-35Nb-7Zr-5Ta. These alloys have proved to be effective in preventing bone atrophy and enhancing bone remodeling, however the high amount of spring back and low fatigue strength makes them undesirable as implant material. Ti-6Al-4V alloy and commercial pure Ti thus remain currently the most popular materials for implantation purposes. [17].

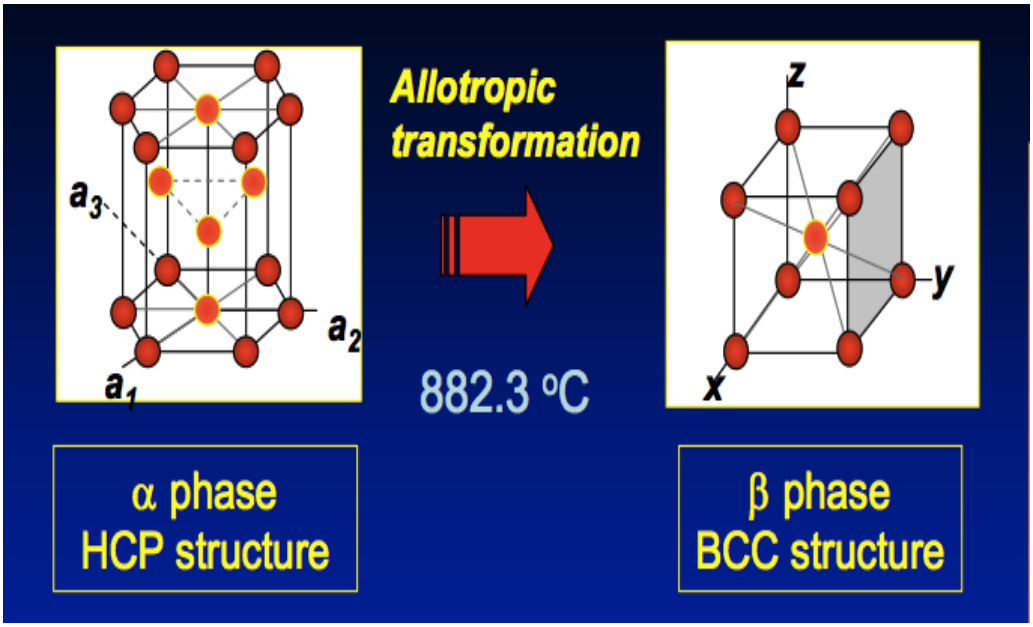

Figure 1.1: The crystal structure of α phase (hcp), the allotropic β phase structure (bcc) and the allotropic transformation that occurs when heating up to 882.3 °C **[1].**

CpTi in fact is an alloy of titanium with up to 0.4 % oxygen. Elements such as; oxygen, nitrogen and carbon have a greater solubility in the hexagonal close-packed structure of the α-phase than in the cubic form of the β-phase. These elements form interstitial solid solutions with titanium and help to stabilize the α-phase. When aluminum and vanadium are added to titanium in only small quantities, the strength of the alloy increases over that of CpTi. Aluminum is considered to be α'-stabilizer, with vanadium acting as a' β'-stabilizer. When these metals are added to titanium, the temperature at which α- β transition occurs is depressed, such that both the α and β forms can exist at room temperature. Thus, Ti-6Al-4V has a two-phase structure of α and β grains. [10].

The ASTM (the American Society for Testing and Materials) for Surgical Implants recognizes four grades of commercially pure titanium and two titanium alloys [10]. The two alloys are Ti-6Al-4V and Ti-6Al-4V extra low interstitial (ELI). The commercially pure titanium are classified into commercially pure grade I, grade II, grade III, and grade IV. All six of these materials are commercially available as dental implants. The chemical composition of CpTi and Ti6Al4V alloy is summarized in Table 1.1 [10, 17].

Titanium	N	C	H	Fe	O	Al	V	Ti
Cp Grade I	0.03	0.1	0.015	0.02	0.18	-	-	balance
Cp Grade II	0.03	0.1	0.015	0.03	0.25	-	-	balance
Cp Grade III	0.03	0.1	0.015	0.03	0.35	-	-	balance
Cp Grade IV	0.03	0.1	0.015	0.05	0.40	-	-	balance
Ti6Al4V	0.05	0.08	0.015	0.30	0.20	5.5-6.75	3.5-4.5	balance
Ti6Al4V ELI	0.05	0.08	0.012	0.10	0.13	5.5-6.5	3.5-4.5	balance

Table 1.1: The chemical composition of the different grades of commercially pure titanium and the titanium alloys used for implants, adapted from McCraken et al. *(McCracken, M., Dental Implant Materials: Commercially Pure Titanium and Titanium Alloys. Journal of Prosthodontics, 1999. 8(1): p. 40-43)* [10].

1.2.2. Mechanical Properties

The mechanical properties of the different grades of CpTi and its alloys are summarized in Table 1.2 [11]. It is important to note that while the modulus of elasticity of Cp grade I titanium to Cp grade IV titanium ranges from 102 to 104 GPa (a change of only 2%), the yield strength increases from 170 to 483 MPa (a gain of 180%), due to the residual oxygen in the metal. The characteristic trend of increasing strength with relatively constant modulus continues when comparing Cp titanium with titanium alloys. The elastic modulus of the alloys is slightly higher (113 MPa compared with 104 MPa of Cp grade IV titanium), but the yield strength increases over 60% to 795 MPa for ELI alloys and 860 MPa for Ti-6Al-4V alloys. Typically, fatigue strength limits are less than 50% of the ultimate tensile strength [18]. Compared to Co-Cr-Mo alloys, the titanium alloy is almost twice as strong and has half the elastic modulus. Compared to 316L stainless steel, the Ti-6Al-4V alloy is roughly equal in strength, but again, it has half the modulus. Strength is beneficial because materials can better resist occlusal forces without fracture or failure. Lower modulus is desirable because the implant biomaterial better transmits forces to the bone [18, 19].

Material	Modulus (GPa)	Tensile strength (MPa)	Yield Strength (MPa)	Elongation (%)	Density (g/cc)
CpTi grade I	102	240	170	24	4.5
CpTi grade II	102	345	275	20	4.5
CpTi grade III	102	450	380	18	4.5
CpTi grade IV	104	550	483	15	4.5
Co-Cr-Mo	240	700	450	8	8.5
316 L steel	200	965	690	20	7.9
Cortical Bone	18	140	n/a	1	0.7
Dentine	18.3	52	n/a	0	2.2
Enamel	84	10	n/a	0	3.0

Table 1.2: The mechanical properties of titanium, titanium alloys, and other natural and implant materials, adapted from Niinomi et al. ***(Niinomi, M., Mechanical properties of biomedical titanium alloys. Materials Science and Engineering: A, 1998. 243(1–2): p. 231-236)*** **[11].**

1.2.3. Titanium Oxide

Bone anchored implants have revolutionized oral healthcare with the surface characteristics playing a major role in molecular interactions, cellular response and bone regeneration. Most of the surface and structural properties are associated with the surface oxide that always covers the metal. The chemical composition of surface oxides on titanium is usually titanium dioxide, TiO_2, which is responsible for the chemical stability and corrosion-resistance of titanium under normal physiological conditions. Surface oxides on titanium can vary in thickness from a few nanometers up to several micrometers, depending on the method of preparation and the temperatures involved. They can have a microstructure that is amorphous (non-crystalline) or crystalline. At least three different crystalline TiO_2 phases are possible, anatase, rutile and brookite, all of which have different chemical properties and crystalline structures. The primary source and the most stable form of TiO_2 is rutile. In all three forms, titanium (Ti^{4+}) atoms are coordinated to six oxygen (O^{2-}) atoms, forming a TiO_6 octahedra (Figure 1.2) [2, 20].

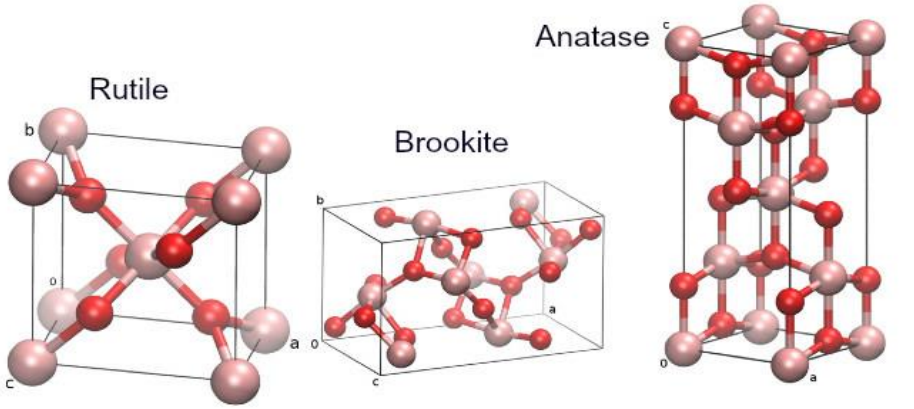

Figure 1.2: Crystal structure of titanium dioxide phases of rutile, brookite, and anatase, adapted from Pelaez et al. *(Pelaez, M., et al., A review on the visible light active titanium dioxide photocatalysts for environmental applications. Applied Catalysis B: Environmental, 2012. 125(0): p. 331-349)* [2]

The effect of the phase composition of the surface oxide is a largely unexplored field as there are difficulties in analyzing the often very thin oxide layer of the implants with regards to phase composition. There are a variety of methods allowing the identification of phase composition of the surface oxide layer. However, many of these methods require flat surfaces and/or rather thick oxides, which are crystalline. Few techniques are available for the analysis of the native oxides of screw-shaped, clinically used titanium implants, having complex macro-geometries and increased micro roughness [2].

1.2.4. Titanium in Dentistry

In 1965, the Swedish doctor Per-Ingvar Brånemark whilst investigating the blood microcirculation in rabbit tibia with an observational camera made of titanium, noticed that the metal and bone were perfectly integrated, that made the cameras very difficult to remove. Based on this observation, Brånemark developed special cylinders to be implanted in rabbit and dog tibiae; which became, later, a secure, modified and optimized base to receive long-term fixed prosthesis in maxilla and mandible for human application [21-23]. In the same year, a 10-year follow-up study was initiated in Gothenburg, Sweden, to evaluate the clinical results of the application of this technique in humans [24]. In 1982, Brånemark presented the results of his research with implants, where the results showed a near 97% success rate. Brånemark definitively introduced the technique of osseointegrated titanium implants, not only in dentistry, but also in the medical area [25]. Titanium implants have also been used with success for years in the fabrication of dental prostheses

such as single crown and bridge frameworks, inlays/onlays, removable and partial denture bases, as well as a material for endosseous and subperiosteal implants and implant-retained structures in dental implantology and for fixed appliances in orthodontics [25, 26]. Dental endosseous implants have been widely used also to retain maxillofacial and craniofacial prostheses since the introduction of the osseointegration concept, which have minimized some of the disadvantages associated with traditional retention methods (i.e. adhesives, eyeglasses) and provided patients with predictable aesthetics and durability, improved prosthesis retention and stability [27, 28].

1.2.5. The Interaction between the implant surface and bone

The interaction between the tissue and the implant surface is a dynamic process. Generally, water, free biomolecules and dissolved ions, surround the implant surface during the initial few seconds after implantation. The healing process initiates with change in the composition of the surrounding biofluid and adsorption of a layer of biomolecules, as shown in Figure 1.3. Following this, cells reach the surface and the adsorbed layer dictates the way the cells respond. As time progresses, the type of cells and their activities on the surface change, resulting in a tissue integration or fibrous capsule formation [3].

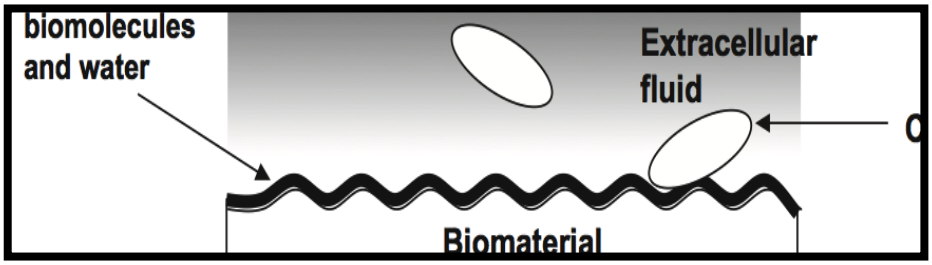

Figure 1.3: Illustration of Interaction between the biomaterial implant surface and the surrounding tissue adapted from Kurella et al. ***(Kurella, A. and N.B. Dahotre, Review paper: Surface Modification for Bioimplants: The Role of Laser Surface Engineering. Journal of Biomaterials Applications, 2005. 20(1): p. 5-50) [3]***

Osseointegration refers to the direct contact between a bone and an implant without the intervention of a soft tissue. For effective osseointegration, the surface micro-texture and its chemistry play a vital role. The physical textural features at atomic, molecular and macro levels act as contact areas for biological units such as proteins, cells, tissues, etc. The different types of bonding associated with each of these biological units influence the classified integration of a surface into its bonding environment. At the same time, it is important to realize that the chemical activity of the implant surfaces also provokes responses from the biomolecules. Different

levels of bonding are initiated by different chemical species and thus affect the adhesion properties. A material undergoes different chemical reactions at the surface depending on the environment and thus complicates the understanding of the exact nature of the interactions [3, 16]. Commercially pure titanium is highly reactive and its surface composition is substantially different from the bulk that forms spontaneously, several oxides when exposed to air, water, or an aqueous biological environment among which TiO_2 is the most common one.

Based on the general knowledge about molecule implant surface interactions, the relevant surface properties should be expected to include both structural and chemical properties from the macroscopic scale all the way down to the atomic level of implant surfaces, and this has led researchers to pay an increasing attention to issues regarding the preparation and characterization of biomaterial surfaces, and a steady increase in the use of surface analytical techniques in dental implants surfaces [29].

Traditionally scanning electron microscopy and X-ray diffraction with Raman spectroscopy (where visible light scattering is analysed) requires a thick and crystalline oxide to overcome the noise level in order to identify the phase of the oxide. In the case of amorphous oxides, no information is retrieved and it is difficult to distinguish between amorphous or crystal- line oxides thinner than a few tens of nanometres [30]. The same applies to X-ray diffraction (where the scattering of X-rays is analysed): a larger flat area is needed to overcome the noise level. The use of transmission electron microscopy (TEM) allows accurate measurements of the lattice parameters as well as analysis of the micro- structure and grain sizes of the surface layer by high resolution TEM (HRTEM). A novel tool in modern scanning electron microscopy (SEM) is electron backscattering diffraction detection. This technique allows electron diffraction analysis of surface films, without extensive sample preparation[31]. However, the usefulness of this technique for acquiring structural information of real implant surfaces yet remains to be demonstrated.

1.2.6. Processing Methods of Ti and Ti Alloys

1.2.6.1. Casting

Titanium requires special melting and casting technology. There are three main types of titanium casting systems: casting under pressure/vacuum with separated chambers of melt and casting; casting under pressure/vacuum with a single chamber of melt and casting; casting under vacuum/centrifugation. Also, dental titanium casting can be accomplished through the methods of centrifugation or

pressure/vacuum. The metal is melted with an electric plasma arc or through inductive heating in a chamber full of inert gas or under vacuum. The molten metal is then transferred to the refractory mould through the centrifuge or through filling under pressure/vacuum [25, 32].

Investment materials with low reactivity are used to prevent superficial reactions with the molten metal while materials with high expansion are used to compensate the high shrinkage of titanium. For this purpose, it is preferable to use titanium alloys. The most common is the Ti–6Al–4V alloy, mainly because of its simple reproducibility [21].

This method is commonly used to fabricate crowns, bridge frameworks and full or partial denture frameworks. The cost of the titanium casting equipment is considerably higher than that for standard dental casting equipment. Special dental investment materials with low reactivity are used to prevent surface reaction with the molten metal due to the high affinity of the molten titanium to the dental investments that causes the formation of a reactive layer (alpha-case). In addition cast titanium restorations are more susceptible to corrosion [25, 32, 33].

1.2.6.2. CAD/CAM Technique (Machining)

Due to the initial problems with casting titanium dental restorations, manufacturing of dental titanium restorations by cutting metal from bullet stock of pure metal or alloy was seen as an alternative method of processing. Such techniques utilize the CAD-CAM (Computer-aided design/Computer-aided manufacturing) system and comprise a computerized system of reconstruction that uses a scanning technique primarily in combination with machining techniques of titanium and/or porcelain in the prosthetic laboratory. The different systems can use either CAD-CAM or a wax pattern combined with CAM. Some examples of known systems are: HintELs®, Procera®, DCS President® System, Cad. Esthetics®, KaVo Everest® System, microDenta®, Cercon brain® and Cerec® [21]. These techniques are based on a model scanning, which is digitalized for the production of a design by the software. This design represents the final shape of the desired structure. Therefore, through the data obtained from the representation of the final structure shape, the framework is fabricated by industrial machining equipment using a single block of titanium [25, 32, 33]. The CAD / CAM systems have been used mostly for the manufacturing of prosthetic fixed restorations, such as inlays, onlays, veneers and crowns. Although this method is successful in fabricating dental restorations, it is expensive and time consuming [25, 32, 34].

1.2.6.3. Superplastic Forming Process (SPF)

Superplasticity is a phenomenon exhibited by some materials whereby at high temperatures and strain rates it is possible to achieve very high ductility. This enables products to be made with high dimensional precision with little or no spring back associated with cold forming. Structural superplasticity is observed in fine-grained alloys (the average grain size does not exceed 10 μm) under proper conditions of high temperature (greater than about one-half the absolute melting point), and controlled strain-rate (within the strain-rate range 10^{-4} to 10^{-2} s^{-1}) [4].

Commercial applications of superplastic forming are restricted to aluminium and titanium alloys. In the aircraft and automotive industries, superplastic forming shows promise as a main approach for producing light, complex-shaped parts. For dental and medical prostheses, dimensional precision, biocompatibility, very light weight and structural strength are paramount, and superplastically formed titanium alloy, Ti-6Al-4 V, meets all these crucial requirements [35, 36].

1.2.6.3.1. History of Superplasticity

It was not until 1962, when Underwood from the United States started to investigate the superplasticity phenomenon, performing different experiments in order to understand the feasibility of this technology for production purposes. In the late 1964 Backofen, Turner & Avery, published a paper in which they described the "extraordinary formability" exhibited when fine-grain zinc-aluminium eutectoid (Zn 22 Al) was subjected to bulge testing under appropriate conditions. They concluded their research findings with the following insightful comment "even more appealing is the thought of applying to superplastic metals forming techniques borrowed from polymer and glass processing." Since then their insightful thought has become a substantial reality with thousands of tons of metallic sheet materials now being superplastically formed each year [37].

1.2.6.3.2. Process of Superplastic Forming

The production of SPF dental and cranial prostheses depends on the ability to apply the correct loading conditions to the titanium disc. The loading conditions are dependent upon the argon gas pressure profile and temperature that are determined using a geometrical model for SPF. The superplastic behaviour of a material can be characterized by its constitutive equations that illustrate the relationship between the flow stress and strain rate during forming at a particular temperature [38]. As an example of the process, the production of a superplastically formed dental prosthesis requires a die, replicating the reverse of the dental

impression, made from dental casting investment material. The die is inserted into a steel furnace chamber and induction heated to about 800–900 ˚C. The furnace is then opened to insert the 140-mm diameter titanium alloy sheet, the temperature is further raised, usually to between 830–930 ˚C, a clamping pressure of 4.8 MN/m^2 is applied and the gas pressure above the titanium sheet is raised in accordance with the pressure–time cycle. The pressure cycle runs automatically and consists of 32 pre-set data points obtained from the numerical simulation. On completion of the pressure cycle, the machine reverts to the lower clamping force until the temperature drops to the temperature for titanium sheet extraction, between 700 ˚C–900 ˚C [4, 38].

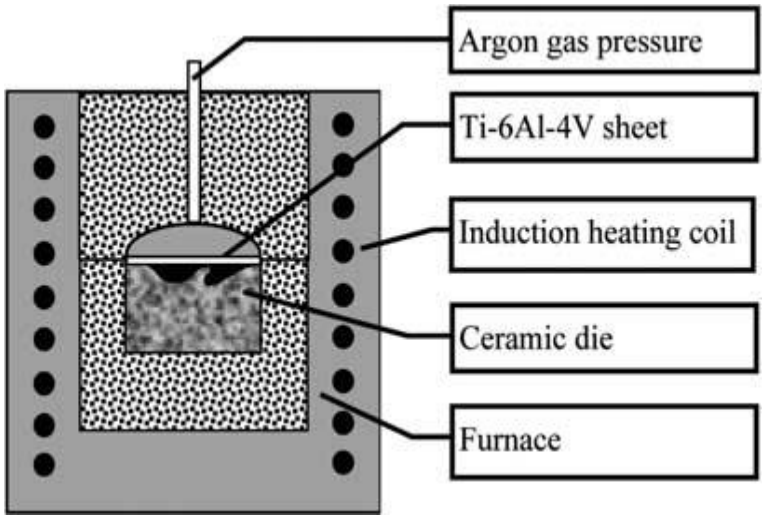

Figure 1.4: Illustration of the superplastic forming process SPF adapted from Bonet et al. *(Bonet, J., et al., Numerical simulation of the superplastic forming of dental and medical prostheses. Biomech Model Mechanobiol, 2002. 1(3): p. 177-96) [4].*

1.2.6.3.3. Mechanism of Superplasticity

Polycrystalline solids exhibit two main types of superplastic forming either a fine structure or internal stress superplasticity. The primary mechanism of fine structure superplasticity is due to superplastic deformation in grain boundary sliding accommodated by dislocation lids. In the case of internal superplasticity, internal stresses develop when low external stresses are applied and tensile plasticity occurs as a result. The mechanism is that of slip-creep and thus does not require fine grain size. The potential for processing bulk material to form the very fine grain sizes required to form parts at the high strain rates is desirable in manufacturing. This allows the grains to rearrange to produce large strains without substitutional grain elongation. The ability to form fine-grained structures in bulk materials is important to broaden the uses of superplasticity. The various theories of

superplastic mechanisms are based on (a) stress-induced transport of vacancies through the lattice, (b) stress-induced vacancy transport through grain boundaries, (c) dislocation movement in grain interiors, (d) combined processes of dislocation climb and slip, and (e) grain boundary sliding. Individual experimental investigation can support each of these mechanisms, but these models are not completely general for all materials [39]

1.2.6.3.4. Advantages and Disadvantages of SPF

Either aspects of superplastic behaviour; the large deformations, or the low forces required would, itself, be sufficient to give a material considerable advantages over non-superplastic materials of similar basic cost and service properties. This offers superplastic materials great advantages such as; complex shapes can be formed in single operation, fine details can be reproduced and close tolerances can be held. Tooling and cost are much lower than for conventional metal forming processes. In addition; superstructures with consistent passive fit without the need for sectioning and re-soldering can also be produced. Furthermore superstructures can be made of titanium alloys that are similar in nature to the implant material and abutment components (commercially pure titanium), thus reducing potential galvanic effect. The titanium alloy has the added advantages of being extremely lightweight and strong in comparison to gold alloys. Other advantages are that superplastically formed material need to be heated to 0.6 Tm (K), so that problems associated with thermal mismatch of investment materials, casting shrinkage and porosity can be minimized. In addition, the slow strain rates of between $5 \times 10^{-4}\ s^{-1}$ and $1 \times 10^{-4}\ s^{-1}$ used for forming the components reduce the possibility of internal stresses leading to dimensional changes on cooling [36, 37].

On the other hand, there are some disadvantages of superplastic forming especially for some reactive, high melting point materials because of the tendency to oxidize and may also mean higher tooling costs than those for lower forming temperature. Deformation speeds have to be kept low for the strain rates to remain within the superplastic range and special alloy compositions and thermomechanical treatment may be necessary to induce superplastic behaviour and to ensure the work piece will remain superplastic throughout the forming process [36, 40].

1.3. Dental Investments

Dental investment materials have long been used in the manufacture of a whole variety of customised prostheses for dental restorative procedures [36]. Generally, two types of investments are employed, depending on the melting range of the alloy. They are the gypsum-bonded and phosphate-bonded investments [41].

Casting titanium for dental applications has acted as a major stimulant to development of investment materials, thus responding to the challenge of casting titanium, new investment materials such as; magnesia and alumina based phosphate investment materials have been developed to overcome some major problems of the casting [40].

1.3.1. Gypsum-bonded Investment Material

Gypsum-bonded investments are the mould materials most commonly employed in the casting of dental gold alloys with liquidus temperatures no higher than 1080 °C [41]. Gypsum materials set by the reaction of calcium sulphate hemihydrate with water to yield calcium sulphate dihydrate. It is an exothermic reaction and the setting occurs via the process of crystallization [40, 41]. Since these materials have a tendency to decompose at high temperature, phosphate bonded investments have been used as an alternative for many years in dentistry for the fabrication of dental castings using high melting temperature dental alloys [40].

$$2(CaSO_4.1/2H_2O) + H_2O \rightarrow 2(CaSO_4.2H_2O)$$

calcium sulphate hemihydrate + water calcium sulphate dihydrate

(Setting reaction of gypsum [36])

1.3.2. Phosphate-bonded Investment Material

The phosphate-bonded investments consist essentially of two main groups of ingredients; (1) fillers which usually consist of quartz and/or cristobalite, and (2) binders which are essentially basic MgO and acidic $NH_4\ H_2\ PO_4$. The setting reactions and further thermal reactions are the results of the initial interaction between MgO and $NH_4H_2PO_4$, Allan and Asgar et al [42] positively identified struvite (crystalline $MgNH_4PO_4 \cdot 6H_2O$) in the set investment and proposed a simple reaction to account for its formation [40]:

$$NH_4H_2PO_4 + MgO + 5H_2O \rightarrow NH_4MgPO_4.\ 6H_2O$$

Ammonium hydrogen + Magnesium oxide + water → struvite phosphate

(Setting reaction of phosphate bonded investment)

Nieman and Sarma et al. [43] proposed a mechanism of the reaction; where the acid phosphate dissolves rapidly and saturates the solution, which lower the pH and thus enhances the dissociation of the magnesia. This dissociation raises the pH and colloidal struvite particles form to produce setting by the formation of a gel [44]. Soudee and Pera et al. [45], suggested another mechanism for the reaction; quoting that the nucleation of the struvite takes place on the surface of the magnesia particles, and grows outward using hydrate magnesium ions from the solution. When the surface of the magnesia is fully covered with these ions, magnesium ions can no longer be released, which describes the setting phase [45]. Scrimgeour et al. [46, 47] has reported on the phases and compounds that occur in phosphate bonded investment materials in the as received condition, during setting and after burn-out with the purpose of discovering whether such compounds are the same in each material across a range of products. This research has shed new light on the composition of set materials that was thought to be well understood. The primary reason for the new information is due to the use of P solid-state MAS-NMR, which can determine the phosphorus compounds, their state and crystallinity [48, 49].

1.3.3. New Investment Materials

The investment of titanium raises two major problems due to its high reactivity and melting point. In order to achieve more accurate castings, new investment materials have been developed such as; magnesia and alumina based investment materials (i.e. Selevest D®, Selevest DM® Investments), which contain about one third aluminous cement binder so negligible change on setting should be expected. In compression, these materials are said to be approximately twice as strong as conventional phosphate-bonded investments [40, 50-52].

1.3.4. Interfacial Reaction between Ti Castings and Dental Investments

Titanium has a high melting point and high chemical reactivity with oxygen and nitrogen (atmospheric air) as well as with other elements of the investment materials. The reactions between molten metal and some of the elements of the phosphate-bonded and other silica-based investment materials (oxygen, phosphorus, and silicon) result in the formation of a surface contamination layer referred to as the ‘‘a-case,’’ consisting of compounds of titanium, primarily with silicone (Si), phosphorus (P), and oxygen (O) [53]. This layer is porous and brittle and is considered unfavourable because of reduced fatigue, ductility, and corrosion

resistance [54]. The microhardness of the α-case is up to 3 times greater than that of bulk titanium. It is also reported that this layer may have a surface depth of up to 200 μm and result in low bond strength between cast titanium and dental porcelain [55-57]. To minimize the extent of the α-case, new investment materials consisting of oxides with a higher chemical affinity to oxygen than titanium, such as MgO and Al_2O_3, were introduced. Though, a thin contamination zone of approximately 20 to 40 μm [25, 58, 59] forms on Ti surfaces even with these newly developed magnesia investments [55].

1.4. Surface Modifications of Ti and Ti Alloys

After titanium implants are inserted into bone, they readily adsorb proteins (i.e. albumin, fibronectin and fibrinogen) from biological fluids (after interaction with water and ions). Afterwards neutrophils and macrophages interrogate the implant, followed by the formation of foreign body giant cells from activated macrophages, and then the migration of osteoprogenitor cells to the implant site and differentiate into osteoblasts that make bone [60-62]. However, a thin non-mineral layer generally separates titanium and bones, and the bond associated with osseointegration is attributed to mechanical interlocking of the titanium surface roughness and pores in the bones. In order to make titanium biologically bond to bones and in cases of poor bone quality and quantity (i.e. bone resorption due to bone metastasis, hypercalcemia of malignancy) [63], surface modification methods have been proposed to improve the bone conductivity or bioactivity of titanium [60-62, 64].

The main reasons to carry out various surface modifications on implant materials for biomedical applications are; (1) to clean the implant material surface from contaminations prior to implantation procedure, (2) to increase the bioactivity, cell growth and tissue attachments after implantation, (3) to increase the hardness of implant to reduce wear rate especially in articulation joint applications, (4) to Initiate passive layer to prevent excessive ion release into body environment, (5) to promote antibacterial effect, and (6) to increase fatigue strength of implants. Surface modification methods can be classified into various methods and a summary of them is listed in Table 1.3:

1.4.1. Mechanical Methods

Common mechanical surface modification methods are: machining, grinding, polishing, and blasting. They involve physical treatment, shaping, or removal of the materials surface. The typical objective of mechanical modification is to achieve specific surface topographies and roughness, remove surface contamination, and/or

improve adhesion in consequent bonding steps [61]. Albrektsson et al. [65] and Ronold et al. [66] suggested that the surface roughness (Ra) in the interval 0.5-1.5 μm shows stronger bone response after the implantation than the smoother or rougher implants. Those observations are in contrast with the results obtained by Fini et al. [67], where positive results were obtained with the surface roughness as high as 21.4 μm. Their results were confirmed during in vivo experiments using titanium implants with various different roughness 16.5 – 21.4 μm inserted in the cortical and trabecular bone of goats. They suggest that the rougher surfaces exhibit a more prolonged effect over time. Surface roughness enhances cell attachment, proliferation and differentiation of osteogenic cells and is the key factor for the osseous integration of metallic implants [68-70]. One of the most common method of achieving desired surface roughness is blasting titanium surface with the SiC particles (SiC), alumina particles (A_2O_3) and biphasic calcium phosphates particles (BCP), hydroxyapatite and ß-Tricalcium phosphate [71]. However, one of the main disadvantages of blasting is that the possibility of surface contamination and local inflammatory reactions of surrounding tissues as a result of dissolution of the abrasive particles such as A_2O_3 particles into the host bone [72].

1.4.2. Chemical Methods

1.4.2.1. Chemical Treatment

This treatment is based on chemical reactions occurring at the interface between the titanium surface and a solution. The common treatments are alkali, acid, hydrogen peroxide H_2O_2, heat and passivation treatments [73] . Acid treatment is used to pre-treat titanium. A combination of acids which are; 10-30 vol% of HNO_3 and 1-3 vol% of HF in distilled water has been recommended as a standard solution for pre-treatment [5, 74]. Takeuchi et al investigated the effect of three acidic solutions ($Na_2S_2O_8$, H_2SO_4, and HCl) on the titanium surface, and found that HCL solution demonstrated the best decontamination method for the surface preparation process of titanium and it could easily dissolve titanium salts and not weaken the surface [75]. Acidic pretreatment commonly leads to a thin surface oxide layer TiO_2 (< 10 nm), and some residues such as; fluorine and hydrogen. In addition, acid treatment can be used in a combination with other surface treatment, which can improve the properties of titanium. Wen et al, reported that the bioactivity of Ti alloy could be improved by using two-step chemical treatments (HCL+ H_2SO_4, and alkaline solution) [76].

Surface Modification	Modified Layer	Objective
Mechanical methods ❖ Machining ❖ Grinding ❖ Polishing ❖ Blasting	Rough or smooth surface formed by subtraction process	Produce specific surface topographies; clean and roughen surface; improve adhesion in bonding
Chemical methods ❖ Chemical treatment ➢ Acidic treatment ➢ Alkaline treatment ➢ Hydrogen peroxide treatment ❖ Sol–gel ❖ Anodic oxidation ❖ CVD (Chemical Vapour Deposition) ❖ Biochemical methods	<10 nm of surface oxide layer ~1 µm of sodium titanate gel ~5 nm of dense inner oxide and porous outer layer ~10 µm of thin film, such as calcium phosphate, TiO_2, and silica ~10 nm to 40 µm of TiO_2 layer, adsorption and incorporation of electrolyte anions ~1 µm of TiN, TiC, TiCN, diamond and diamond-like carbon thin film Modification through silanized titania, photochemistry, self-assembled monolayers, protein-resistance, etc.	Remove oxide scales and contamination Improve biocompatibility, bioactivity Improve biocompatibility, bioactivity Improve biocompatibility, bioactivity or bone conductivity Produce specific surface topographies; improve corrosion resistance; improve biocompatibility, bioactivity or bone conductivity Improve wear resistance, corrosion resistance and blood compatibility Induce specific cell and tissue response by means of surface-immobilized peptides, proteins, or growth factors
Physical methods ❖ Thermal spray ❖ Flame spray ❖ High velocity oxygen fuel (HVOF), ❖ Detonation gun spraying (DGUN) ❖ Physical Vapour Deposition (VPD) ➢ Evaporation ➢ Ion plating ➢ Sputtering ❖ Ion implantation and deposition ➢ Beam-line ion implantation ➢ PIII ❖ Glow discharge plasma treatment	~30 to 200 µm of coatings, such as titanium, HA, calcium silicate, Al_2O_3, ZrO_2, TiO_2 ~1 µm of TiN, TiC, TiCN, diamond and diamond-like carbon thin film ~10 nm of surface modified layer and/or ~µm of thin film Modify surface composition; ~1 nm to ~100 nm of surface modified layer	Improve wear resistance, corrosion resistance and biological properties Improve wear resistance, corrosion resistance and blood compatibility Improve wear, corrosion resistance, and biocompatibility Clean, sterilize, oxide, nitride surface; remove native oxide layer

Table 1.3: Surface modification methods for titanium and its alloys implants, adapted from Liu et al. [5] and Kurella et al. [3].

Alkali treatment was first introduced by Kim et al [77], along with heat treatment to improve the bioactivity of the titanium surface. In this method the specimens are first immersed in a 5M NaOH or KOH solution for 24 h, followed by rinsing with distilled water and ultrasonic cleaning for 5 min, and then dried in an oven at 40 °C for 24 h and finally heated to around 600–800 °C for 1 h [77]. This method enables the formation of sodium titanate layer on the surface of the titanium substrate; therefore the surface can act as a place for the subsequent in vitro nucleation of calcium phosphates from SBF solution, mimicking the earliest surface reaction stages after implantation [79]. Ho et al, showed that titanium and its alloys with untreated surfaces do not induce calcium phosphates precipitation after soaking in SBF solution [80].

The other common chemical treatment method is the hydrogen peroxide (H_2O_2) treatment, which offers a good pre-treatment method for apatite formation through the chemical dissolution and oxidation of the titanium surface. An amorphous titania gel layer can be produced by treating titanium in a H_2O_2/0.1 M HCl solution [81, 82]. The reaction between titanium and the H_2O_2 solution results in the formation of a layer of amorphous titania gel on the Ti surface, and the thickness of the titania gel layer depends almost linearly on the duration of the chemical treatment, where subsequent heat treatment above 300°C gradually changes the amorphous gel into crystalline one. The best results have been achieved using heat treatment between 400 and 500°C as the titania gel would have anatase structure exhibiting excellent bioactivity[5, 83, 84]. Gotfredsen et al. [85] confirmed that a micro-scale rough surface prepared by grit blasting and subsequent acid-etching was able to initiate rapid and increased bone growth whilst Buser et al. [86] suggested that SLA (sandblasted/acid-etched) modified implants could further reduce the healing time to 3–4 weeks. Kokubo et al. [87] and Kim et al. [88] also reported that NaOH-treated titanium had good bone conductivity.

1.4.2.2. Electrochemical Treatment (Anodic Oxidation)

Anodic oxidation is a well-established method to produce different types of protective oxide films on metals. It includes electrode reactions in combination with electric field driven metal and oxygen ion diffusion leading to the formation of an oxide film on the anode surface. Different diluted acids (H_2SO_4, H_3PO_4, acetic acid and others) can be used as electrolytes in the process. The anodic oxide can have interconnected pores (0.5–2 μm in diameter) and intermediate roughness (0.60–

1.00 µm) [89]. The main advantage of anodizing titanium is improved adhesion and bonding and it can also be used to increase the oxide thickness to increase corrosion protection and decrease ion release, coloration, and porous coatings [61]. Anodic spark deposition (ASD) is a novel anodic oxidation technique to deposit ceramic coatings on the surface of metals [61, 90]. The treatment involves high voltage conditions, electrolytic solutions containing chemical species that are incorporated into the oxide and promote an increase in the oxide hardness and further mechanical treatments aimed at compacting and further hardening the oxide layer [91, 92]. BioSpark™ is a developed ASD process that includes two consecutive ASD treatments performed in a solution containing phosphate ions and in a solution rich in calcium ions. Sandrini et al. [93] reported that BioSpark™ enhances protein adsorption and osteoblasts activity better than the traditional ASD method. Short-term cellular response studies demonstrated that BioSpark™-treated surfaces supported well MG63 osteoblastic-like cell adhesion and proliferation when compared with smooth, sandblasted or acid-etched Ti surfaces [93, 94].

1.4.2.3. Sol-gel Treatment

A sol is a colloid suspension of solid particles in a liquid and a gel is a substance that contains a continuous solid skeleton enclosing a continuous liquid phase. In this method, the chemical reactions do not occur at the interface between the sample surface and solution or gel, but rather in the solution. The sol–gel process can be divided into five main steps: (1) hydrolysis and poly-condensation (2) gelation (3) aging (4) drying (5) densification and crystallization [61]. The sol–gel process is widely used to deposit thin (<10 µm) ceramic coatings. Because of the advantages of this method (such as; low processing temperature, homogeneity, the possibility of coating on substrates with large areas, and low cost), sol–gel films, as hydroxyapatite, TiO_2, SiO_2 and related films have been developed, used and widely studied [95-99].

1.4.2.4. Chemical Vapour Deposition (CVD)

Chemical vapour deposition is a process involving chemical reactions between chemicals in the gas phase and the sample surface resulting in the deposition of a non-volatile compound on the substrate. It can thus be distinguished from physical vapour deposition (PVD) processes, such as evaporation and reactive sputtering, which involve the adsorption of atomic or molecular species on the substrate [61, 100]. CVD coatings are typically fine-grained, impervious, high purity and harder than coatings produced by other methods. Therefore, CVD is a process of interest

for the fabrication of microelectronic devices or coating objects with complex geometry and has also been widely used to modify the mechanical and biological properties of titanium and titanium alloys. [100, 101].

1.4.2.5. Biochemical Modification of Titanium and Titanium Alloys

Biochemical modification applies the biological and biochemical knowledge on cellular function, adhesion, differentiation and remodelling. Puleo and Nanci et al defined the biochemical modification as; “Biochemical surface modification endeavours to utilize current understanding of the biology and biochemistry of cellular function and differentiation’’ [102]. The objective of biochemical surface modification is to immobilize proteins, enzymes or peptides on biomaterials for the purpose of inducing specific cell and tissue responses. However, it is necessary that while biochemical modification improves the biocompatibility of the surface, the bulk properties cannot be negatively affected, and so the concept of a bio-mimetic surface has been introduced. The most common techniques which have been used on titanium and its alloys are; silanized titania, photo-chemistry, self-assembled monolayers, and protein resistant and protein immobilization [5]. Self-assembled monolayers technique has become an important technique to produce surfaces with a very well defined chemical composition, and are often been used as model surfaces for various biological assays including the study of cell-surface interaction and the influence of the surface chemistry on the spontaneous mineralization caused by contact with simulated body fluid (SBF). Recently, self-assembled monolayers of alkaline phosphates or phosphonates have been used on titanium surfaces to modify selected physico-chemical properties of the surface, such as wettability and electrical charge [61, 103].

Protein-resistant and protein immobilization technologies are frequently used to modify the surface of titanium and titanium alloys, where the integration of the implant with the newly formed tissue is desired. Hence, the adsorption of cell-adhesive proteins or bioactive proteins is an important aspect of the healing process. Bone morphogenetic protein has been reported to be immobilized on the surface of Ti6Al4V to enhance the bioactivity [104]. The amount of protein and the strength of binding to metallic biomaterials can be controlled by the choice of the surface treatment and immobilization chemistry, however limitations such as denaturation of the protein or loss can occur [5, 104].

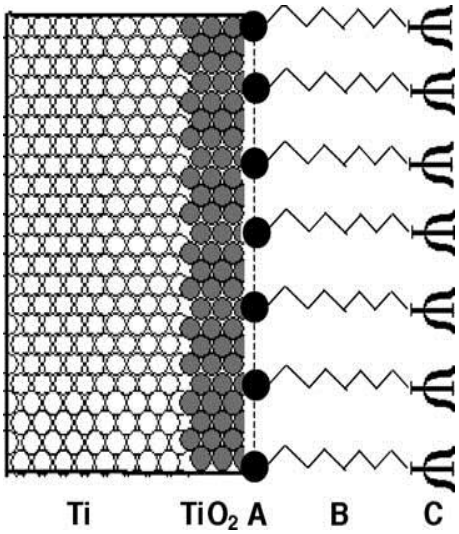

Figure 1.5: Schematic diagram of biochemical modification of titanium surface adapted from Liu et al [5]. (A) Attachment site by physical or chemical adsorption or covalent linkage without or with cross-polymerization (dashed line); (B) spacer to adjust distance of functional group C from original surface; (C) chemical, biochemical or biological functionality, such as organo-functional group, peptide, protein, etc.

1.4.3. Physical Methods

Physical methods employed to modify the surface of titanium do not involve any chemical reactions. In such cases, the formation of surface modified layer, films or coatings on titanium and its alloys are mainly attributed to the thermal, kinetic, and electrical energy of the modification process [61].

1.4.3.1. Thermal Spraying

Thermal spraying is a process in which materials are thermally melted into liquid droplets and introduced energetically to the surface on which the individual particles stick and condense. Thermal spraying is often divided into flame spraying and plasma spraying depending on the device used to create a high temperature flame or a plasma jet. In flame spraying, the temperature is limited by the internal heat of combustion of the fuel gas, while plasma spraying, using electrical energy as the source to create the plasma can provide very high temperature [105, 106].

1.4.3.2. Plasma Spraying

Plasma spraying, a type of thermal spraying, is often used to form ceramic coatings, and it includes atmospheric plasma spraying (APS) and vacuum plasma spraying (VPS). The process uses an electrical arc to melt and spray materials onto a surface. The formation of a plasma coating consists of several stages, which affect the properties of the sprayed layer. The method of powder transport to the plasma

torch and the shape and granularity of powder then affect the paths of the particles and the velocity. The mechanical, chemical and thermal conditions of the substrate also determine the overall characteristics and properties of the sprayed layer. Plasma spraying is widely used to produce hydroxyapatite coatings on different prosthesis or implants. However, one of the main disadvantages of this method is the relatively poor bonding between a plasma sprayed HA coating and titanium because of the difference in the coefficient of thermal expansion of HA (13.3×10^{-6} K^{-1}) coating and titanium substrate (8.5×10^{-6} K^{-1}) resulting in high residual stress leading to delaminating of the coating [107].

Bioactive glass can also be deposited onto titanium and its alloys using plasma spraying. The bioactive glass coating retains the properties of the original glass with respect to the amorphous structure and the behaviour in a hydrolytic environment [108], however it can be assumed there is some amount of the formation of a glass-ceramic phase. Liu et al. [109] introduced the idea of using plasma spraying to produce a bioactive wollastonite and dicalcium silicate coating on titanium. The results showed that the wollastonite and dicalcium silicate coatings can promote the proliferation of osteoblast and possess excellent biocompatibility. The reason may be the local chemical environment, which is suitable for the proliferation of osteoblasts as a result of dissolution of wollastonite and dicalcium silicate coatings.

1.4.3.3. Physical Vapour Deposition

Physical vapour deposition is a process where the materials are evaporated or sputtered to form atoms, molecules or ions under vacuum that are subsequently transported to the substrate surface, on which condensation and sometimes some reactions with the materials surface take place leading to film growth. The steps involved in this process are: (1) generation of particles from the target materials (2) transport and film growth (3) particle energy, density, substrate temperature and reactive gas properties. Physical vapour deposition processes include evaporation, sputtering, and ion plating. Evaporation is carried out in vacuum, and in the sputtering process, positive argon ions produced in a glow discharge bombard the target materials (cathode) dislodging atoms that enter into the vapour phase and are deposited onto the substrate. In the ion plating process, the materials are vaporized as in evaporation, but they pass through a gaseous glow discharge on its way to the substrate for increased ionization. The use of this method is mainly aimed to improve the hardness and wear resistance of the material as well as reduce the friction. On the other hand this method can be difficult to coat undercuts and is expensive [110].

1.4.3.4. Glow Discharge Plasma Treatment

Glow discharge plasma is a low-temperature, low-pressure gas in which ionization is controlled by energetic electrons. It is used for the surface modification of bulk polymers and production of thin polymer coatings (plasma polymerization). Plasma treatments have for some time been a relatively common method to increase the surface energy and clean the surface of biomaterials before biological evaluation studies [111].

1.4.3.5. Ion Implantation and Deposition

It is a process in which energetic ions are introduced into the surface layer of a solid substrate via bombardment. The use of energetic ions affords the possibility of introducing a wide range of atomic species independent of thermodynamic factors therefore making it possible to obtain impurity concentrations and distributions of particular interest. Ion implantation includes conventional beam-line ion implantation and plasma immersion ion implantation (PIII) [61, 112]. Ion implantation can produce surface-modified layers. The wear resistance and bone conductivity can be improved by nitrogen and calcium ion implantation, respectively. Thin films can also be used to improve bone conductivity, corrosion resistance, and wear resistance. Examples are apatite, TiO_2, and TiN, respectively [61, 112].

Hanawa et al. [113] found that calcium ion implantation improved the ability of titanium to induce the formation of calcium phosphate precipitates and their experiments in vivo confirmed that calcium ion-implanted titanium was superior to un-implanted titanium from the perspective of bone conduction. Loinza et al. [114] reported that the surface hardness increased by 100% and wear resistance also improved significantly after oxygen plasma implantation into titanium has been conducted to fabricate titanium oxide. Xie et al. [115] demonstrated titanium surface became rougher and Ti–OH was introduced after sequential water and hydrogen implantation in order to modify the biocompatibility of titanium and improve the related properties of it [70].

1.4.3.6. Electrohydrodynamic atomization (EHDA)

Recently, attention has been paid to various low temperature thin film techniques, to extend the clinical applications of CaP coatings. EHDA is one of such techniques. It is a simple, economical process carried out at room temperature, which is capable of producing uniform coatings [116]. Its ease of use and compatibility with micro-fabrication technology has made it highly attractive. The process consists of a nozzle (needle) that is connected to a high voltage supply and a ground electrode. A suspension or solution containing the desired coating material is fed through the

nozzle at a controlled flow rate through a syringe pump. A copper template with the desired pattern is placed over the ground substrate. The electric field created between the nozzle (electrode) and the substrate, forms a liquid jet from the needle. This breaks up into smaller droplets as the applied voltage increases, and it eventually breaks up into fine and uniform droplets in the nano- or micro-meter scale. The spray collects on the ground substrate and template to produce a fine coating that can be controlled by varying process parameters such as flow rate and applied voltage. After coating, the solvent evaporates away and the template can be removed, leaving the inverted template pattern on the substrate (Figure 1.5) [116-118].

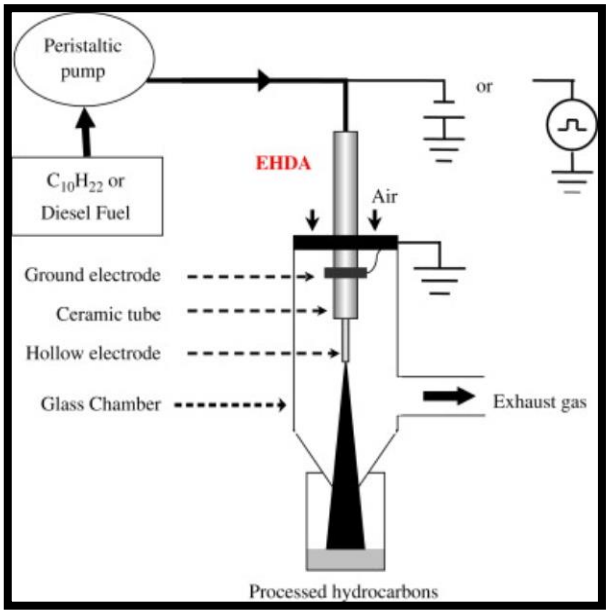

Figure 1.6: Schematic diagram of the electrohydrodynamic atomizer (EHDA) system adapted from Li et al. (*Li, X., et al., A novel jet-based nano-hydroxyapatite patterning technique for osteoblast guidance. J R Soc Interface, 2010. 7(42): p. 189-97)* [6].

The process has been successfully used to create hydroxyapatite layers on titanium. Li et al. [116] established a procedure to optimize EHDA coating of titanium with nano- hydroxyapatite to form a uniform coating. By altering needle size, distance between needle and coating substance, flow rate and applied voltage, they were able to influence the morphology of nHA coatings. Cellular response to EHDA coatings on different substrates has been assessed. Huang et al. [119] successfully deposited nano-sized titanium containing hydroxyapatite onto Ti surfaces. This surface was able to support human osteoblast cell attachment and growth whilst also providing anti-infective properties.

1.5. Bioactive Coatings

Bioactive surface treatment is generally applied on titanium alloys in order to combine the mechanical strength of metals with the excellent biological properties of inorganic (i.e. calcium phosphate and bioactive glass) or organic (i.e. bisphosphonates) coatings [120, 121].

1.5.1. Inorganic Coatings

1.5.1.1. Calcium Phosphates (CaPs)

CaPs have been highly popular biomaterials due to their similarity with the mineral phase of bone. Hydroxyapatite and carbonate apatites are highly abundant inorganic phases in the human body. Apatite has the formula $Ca_5(PO_4)_X$, x being any of several mono and/or divalent anions (OH^-, F^- or carbonate). Various CaP phases exist including; tricalcium phosphate, hydroxyapatite and carbonate apatite (Table 1.4). HA is the most commonly used phase due to its similarity to natural bone. CaP ceramics possess bioactive properties enabling them to interact with bone to form chemical bonds with the tissue. On implantation, an ion-exchange reaction occurs between these implants and surrounding body fluids resulting in the formation of a carbonate apatite layer, identical chemically and crystallographically to that of the mineral phase of bone [122] .This apatite layer is known to enhance the bone healing process [123]. Thus, they have osteoconductive properties (ability to support bone growth over its surface).

Name/Abbreviation	Formula	Ca/P ratio
Hydrate Calcium Phosphate/ brushite (DCP)	$CaHPO_4.2H_2O$	1.0
Octacalcium phosphate (OCP)	$Ca_8(HPO_4)_2(PO_4)_4.5H_2O$	1.33
Tricalcium phosphate (α or β TCP)	$Ca_3(PO_4)_2$	1.5
Hydroxyapatite (HA)	$Ca_{10}(PO_4)_6(OH)_2$	1.67

Table 1.4: Examples of CaP phases for biomedical applications along with their chemical formula and Ca/P ratio.

CaP ceramics are however too brittle to be used as bulk materials especially under conditions of biomechanical loading. Hence, in order to exploit their biological properties, they are often used to coat stronger metallic substrates [124]. Various techniques have been developed for introducing CaP coatings on metallic substrates. Narayan et al. [12] broadly classified these techniques into 5 types summarized in Table 1.5, including common techniques . Currently, the most

successful method for introducing CaP coatings is the plasma-spraying technique, largely due to the rapid deposition rate and ability to coat large surface areas. It involves injecting a CaP material in powder form into a high temperature plasma flame, which rapidly heats and accelerates the material at a high velocity towards the surface of the substrate. An electric arc ionizes the gas, creating high-pressure plasma [125]. There are however still some major concerns regarding this technique. For one, coating thickness needs to be at least 50μm to achieve complete coverage. These thick coatings usually result in weak adhesion. Due to extremely high temperatures and rapid cooling, phase changes of CaP are highly unpredictable. A mixture of crystalline and amorphous CaP phases usually results, as well as an inhomogeneous microstructure. Thus, alternative methods of coating continue to receive considerable attention, including electrohydrodynamic deposition [125].

Category	Techniques	Methods/Features of the Process
Wet Process	Immersion in SBF	Simple immersion in SBF of coated or uncoated or activated titanium surfaces produces HA
	Other wet chemical methods	Addition of stoichiometric calcium to stoichiometric phosphorus yields calcium phosphates
	Sol-gel method	HA coatings are less porous and show better performance
High temp. Process	Plasma spraying	Produces thick, inhomogeneous HA coatings
	Ion-beam method	Thin HA coatings produced on Ca and P implanted Ti surface
	Laser method	Thin coatings with diverse compositions and crystallinities and high fatigue strength
	RF sputtering	Thin but dense HA coatings with strong adhesion and compact microstructure
Electrochemical	Cathodic deposition	Synthesis of thick coatings of HA on cathodic Ti from electrolyte containing Ca and P
Phase Conversion	Hydrothermal	High pressure steam treatment of coatings on Ti (containing Ca and P) produces HA

Table 1.5: Common methods of producing Calcium Phosphate/HA coatings on Titanium surfaces, adapted from Narayanan et al. *(Narayanan, R., et al., Calcium phosphate-based coatings on titanium and its alloys. J Biomed Mater Res B Appl Biomater, 2008. 85(1): p. 279-99)* [12]

1.5.1.2. Bioactive Glasses

Bioactive glasses have the ability to develop a mechanically strong bond to bone. These ceramics possess similar biocompatibility and osteoconductive properties to HA. In physiological conditions, they form a hydroxycarbonate apatite layer on their surfaces, which the body recognizes as bone-like and deposit tissue. This formation of an apatite layer is preceded by the dissolution of the glass network, leading to the formation of a silica-rich gel layer, thought to be essential for their biocompatibility [126]. Bioactive glasses are particularly attractive, especially when compared to conventional hydroxyapatite ceramics, because they have been shown to possess osteoinductive properties (stimulate new bone growth) [127].

Coating metal surfaces with 45S5 Bioglass® has been difficult. For instance, plasma spray methods usually fail due to a resulting weak glass/metal interface and rapid dissolution in body fluids when implanted. A barrier to using these glasses for coatings is the high thermal expansion coefficients of Bioglass® compositions relative to those of titanium-alloys resulting in cracking of the glass when there is thermal stress [128]. Attempts to coat by enameling technique also failed due to the glass crystallizing significantly resulting in lack of adhesion to the substrate [129]. There has been some success in coating tailored bioactive glasses, in the system SiO_2–Na_2O–K_2O–CaO–MgO–P_2O_5, on titanium substrates [130]. Stan et al. [126] reported highly adherent bioactive glass thin films by RF magnetron sputtering at low temperature.

Recently, a group of researchers achieved successful deposition of 45S5 Bioglass® via an innovative thermal spray process; high-velocity suspension flame spraying (HVSFS) [131]. This technique involves a modified high-velocity oxygen fuel torch to process a liquid suspension. Glass powders were dispersed in a water and isopropanol suspension and thermally sprayed onto pre-heated Ti plates. Fine particles in suspension were easy to melt and create small, thin, strongly adherent coating. The bioactivity of HVSFS coatings was characterized by soaking in SBF and interaction with osteoblast-like cells was assessed by in-vitro cytotoxicity and cytocompatibility tests. Raman spectroscopy revealed composition of coating identical to bulk 45S5 Bioglass® (no structural alteration), however it is possible that there is partial conversion of the glass. Interaction with SBF was also similar to bulk 45S5 Bioglass®, resulting in the formation of a carbonated hydroxyapatite layer. In-vitro tests indicated that the surfaces were suitable for human osteoblast-like cell adhesion and proliferation [131].

1.5.2. Organic biomolecule coatings

The immobilization of proteins, enzymes and peptides on implant surfaces currently receives considerable amounts of interest. Biologically functional molecules are being introduced to enhance bone regeneration at the implant-bone interface. Currently explored approaches include the immobilization of extracellular matrix (ECM) proteins (e.g. collagen and fibrin), deposition of bone growth factors and other cell signaling agents and the immobilization of DNA for structural reinforcement [132]. Most reported methods use physical adsorption, physical entrapment or covalent entrapment to immobilized these molecules on to Ti surfaces. Natural bone being composite (inorganic CaP and collagen) in nature has also more recently prompted inorganic-organic coatings with composite compositions such as, collagen-CaP with some degree of success[133].

1.5.2.1. Immobilization of Bisphosphonates on Titanium Substrates

Bisphosphonates (BPs) are a major class of drugs used to treat various bone related diseases (such as osteoporosis, metastasis and hypercalcaemia). They prevent bone resorption by inhibiting osteoclast activity including their activity and differentiation [134]. Orally administered BPs have been used to prevent osteoclast function at bone-implant interface as osteoclast activity (premature bone resorption and remodeling) at implant site can adversely affect implant fixation and recovery time [135]. These drugs are also desirable in osteoporotic conditions and will therefore be beneficial to most patients of advanced age who need implant treatment. One of the major problems associated with the oral administration of BPs is their low oral bioavailability. Thus, several delivery systems have been proposed to improve their absorption and to direct them to sites other than bone tissues [136]. In the case of placement of implants/prosthetic components in bone effect of these drugs can be maximized if they are ideally delivered directly at the bone-implant interface. Systemic use of BPs is also associated with undesirable effects such as gastrointestinal ulceration and jaw osteonecrosis [137]. Literature shows some evidence that orthopedic implants fail due to a lack of initial attachment of the implant to the bone, and there has indeed been some evidence that these drugs enhance osteoblast proliferation and differentiation when coated on titanium surfaces [138]. If a certain initial stabilization of the implant cannot be achieved because the supporting bone is resorbed, the implant can migrate, resulting in the need for a second surgery.

BPs have been reported to have a high affinity for natural and synthetic HAs [139]. They have a P-C-P structure with variable lateral chains R1 and R2. R1 is involved with their binding to bone mineral and R2 conducts antiresorptive activities. If the two bonds are located on the same carbon atom, resulting in a P–C–P structure, the compounds are called geminal bisphosphonates. They are therefore analogues of pyrophosphate that contain a carbon instead of an oxygen atom (Figure 1.7) [140]. The P-C-P structure allows a great number of possible variations, either by changing the two lateral chains on the carbon or by esterifying the phosphate groups. Thus bisphosphonates are available in different structures such as; alendronate, clodronate, etidronate, ibandronate, pamidronate, and risedronate, which are currently approved for commercial use in humans for bone disease (Figure 1.8). Each bisphosphonate has its own chemical, physicochemical, and biological characteristics [140].

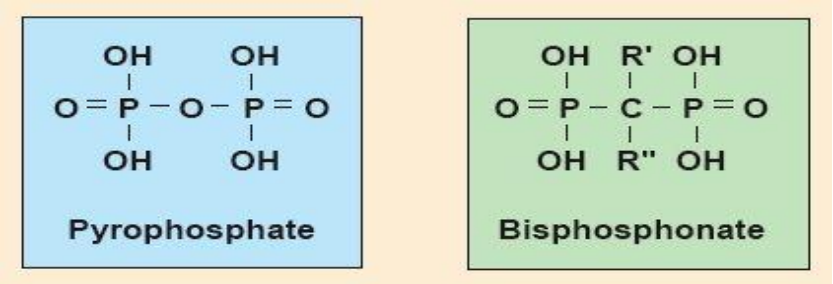

Figure 1.7: Chemical structure of inorganic pyrophosphate and bisphosphonate, adapted from Michaelson et al. [7]

The mechanism of action of bisphosphonates is that of inhibiting osteoclast cell activity. When osteoclasts resorb bone, the resorbing cell internalizes the bisphosphonate, thus, the bisphosphonates become targeted on the osteoclasts. Nitrogen-containing bisphosphonates, such as pamidronate, alendronate, and ibandronate decrease bone resorption through the inhibition of an enzyme in the mevalonate pathway and by forming a toxic ATP-analogue in the osteoclasts. The result appears to be that osteoclasts either undergo apoptosis or at least lose their bone resorbing capacity. A common method for binding bisphosphonates to implant surfaces is to use hydroxyapatite or other calcium compounds on the surface [141]. Phosphate groups in the bisphosphonate molecule have a strong affinity to calcium phosphate molecules, so incorporation of these molecules onto implants could be achieved using calcium phosphate coatings such as hydroxyapatite, or calcium phosphate coatings obtained by biomimetic coating procedure [142].

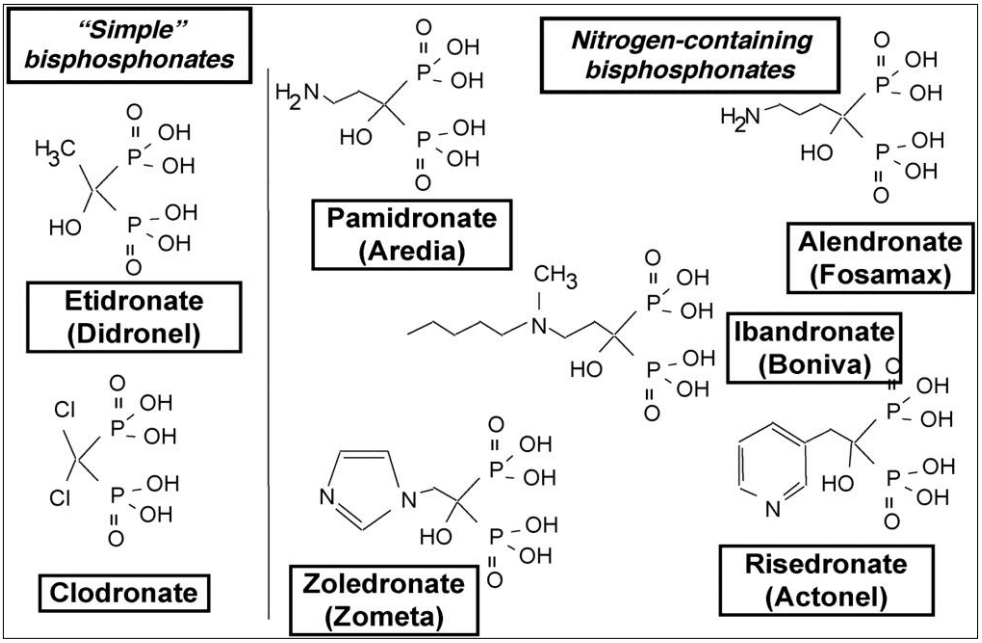

Figure 1.8: Structures of the bisphosphonates used in clinical studies approved for commercial use in humans for bone disease classified according to their biochemical mode of action, adapted from Russell et al. [8]

Gao et al. [143] conducted an in-vivo study to assess bone response to surface immobilized bisphosphonates on hydroxyapatite-coated titanium in ovariectomized rats (OVX rats - commonly used model for osteoporosis). Ti substrates were plasma sprayed with HA and then immersed in different BPs (pamidronate, ibandronate and zoledronic acid). After implantation for 3 months, the three BPs triggered pronounced bone-implant integration and early bone formation around implants in the OVX rats. Bisphosphonates have also been coated on the surface of titanium alone or on PDLLA-, heparin- or hydroxyapatite-coated titanium implants which have been shown to inhibit osteoclasts in vitro, resulting in enhanced stability of implants in rat models [144-146]. Furthermore, it has been suggested that the different BPs used in the study exhibited different levels of efficacy. These results provide evidence that BPs if present locally may enhance implant fixation in osteoporotic bone, as well as their previously reported positive effects normal bone [143].

1.6. Effect of surface characteristics on cellular response

The success of dental implants quality depends on the mechanical, chemical, physical, and topographic characteristics of the implant surface. These different properties interact and determine the activity of the attached cells that are adjacent to the dental implant surface [147]. Commercially dental implants have been designed to provide shapes and textures that may enhance the cellular activity and

direct bone apposition [148]. The amount of bone to implant contact (BIC) is very important in the long- term success of dental implants; thus maximizing the BIC has become a goal of treatment, through modification of implant surface roughness factor [149].

Albrektsson et al. [150] showed that among the factors influencing BIC such as topography, chemistry, wettability and surface energy the most important factor is the wettability of the surface. Surface wettability is largely dependent on surface energy and influences the degree of contact with the physiological environment [151]. Several studies have confirmed that implants with rough surfaces show better bone apposition and BIC than implants with smooth surfaces, and has a positive influence on cell migration and proliferation, which in turn leads to better bone healing [152, 153].

Buser et al. [86] supported the use of alterations in surface chemistry to modify the osseointegration of the cells on implant surface. Specifically, an investigation utilizing sandblasted, large-grit, acid-etched (SLA) surfaces that were chemically different but had the same physical properties was conducted to assess BIC as a measure of osseointegration. The chemically enhanced SLA surface demonstrated significantly enhanced bone implant contact during the first 4 weeks of bone healing, with 60% more bone than the standard SLA surface after 2 weeks [86]. However, Anselm et al. [154] demonstrated that primary human osteoblast cells and mouse osteoblastic cells line showed more spreading and higher proliferation and adhesion on smooth surface rather than rough surface of Ti6Al4V alloy [154]. Though, most of the literature showed that bone to implant contact was enhanced along with increased surface roughness though an optimum surface roughness is thought to exist with Ra value believed to be between 1-2 μm [65, 150, 152, 153]. Several explanations can be given to justify the mentioned discrepancies in the biologic effects of substrate surface roughness, such as small but very relevant differences in surface topography, different animal models and different surgical techniques [155].

Haung et al. [156] reported the effect of surface roughness of ground Ti on the initial adhesion of osteoblast-like U-2 OS cells. They showed that after two hours of cell incubation, the specimens with surface roughness value (*R*a: 0.15 μm) showed the best cell and adhesion and spreading compared to the other specimens with a surface roughness values of (*R*a: 0.05 and 0.07 μm). Deligianne et al. [157] investigated the effect of surface roughness of the titanium alloy Ti–6Al–4V (Ti alloy) on the short- and long-term response of human bone marrow cells in vitro and on

protein adsorption. Three different values in a narrow range of surface roughness were used for the subse (*Rα*: 0.320, 0.490 and 0.874 μm). This study showed that, cell attachment and proliferation were surface roughness sensitive and increased as the roughness of Ti alloy increased. Protein radiolabeling showed that human serum albumin was adsorbed preferentially onto the smooth substratum. XPS technique showed that the rough substratum bound a higher amount of total protein and fibronectin (10-fold) than did the smooth one.

Dowling et al. [158] studied the effect of surface wettability and topography on the adhesion of the human MG63 osteosarcoma cells. Surfaces with water contact angle from hydrophilic (12°) to super-hydrophobic (155°) were obtained through a combination of modifying surface roughness (Ra). The surface roughness values in the range of 19–2365 nm were obtained by grinding the surface. The nanometer thick siloxane coatings were deposited using an atmospheric pressure plasma system. It was observed that higher polymer surface roughness enhanced cell adhesion, but had a negative effect on cell spreading.

An in vivo study by Sul et al. [159] investigated the effect of surface characterization of oxidized implants on the bone response in rabbit tibia. It showed that after six weeks of immediate loading on an implant placed in rabbit tibia, the mean bone removal torque (RTVs) values showed the highest on CpTi surfaces with roughness value range between 0.7 to 1.0 μm, compared to CpTi control samples with surface roughness values of 0.55 μm [159]. Another study by Curtis et al reported that the interaction of an investment material, namely Croform with titanium whilst used in the superplastic forming process resulted in a surface that exhibited enhanced proliferation of osteoblast like cells [36]. These findings indicated that investment materials may have a beneficial effect under SPF process, contradictory to previously reported studies.

1.7. Aim and objectives of the study

The main aim of the study is to develop and identify a facile method of immobilizing bisphosphonate molecules on commercially pure titanium and its alloy.

More specifically:

1. To utilize the interaction layer that may form during superplastic forming of commercially pure titanium and the Ti6Al4V alloy in order to modify the surface that can enhance biofunctionality and be further used to tether bisphosphonates. This would provide the opportunities to make SPF technology available to patients with the ability to modify surface by simple technologies to optimize biological properties of prostheses for dental/medical and maxillofacial applications.

2. To study the effect of alkali treatment without subsequent heat treatment of commercially pure titanium and the Ti6Al4V to modify the surfaces and investigate the effect on biological properties to allow tethering of heat sensitive molecules such as alendronate.

3. To investigate the effect of tethering alendronate onto modified surfaces of CpTi and Ti6Al4 using the SPF interaction layer and sodium hydroxide treated samples after interaction with simulated body fluid by using in vitro cell culture tests.

4. Application of electrohydrodynamic deposition of bioactive glass on CpTi and Ti6Al4V and then using alendronate to bind to the surface and its effect on the biological properties using in vitro cell culture techniques

The hypothesis of the study is that the interaction between titanium alloy and investment material during SPF (simulated) results in the formation of an interaction layer that can be exploited for further surface modification to enhance cellular response and biofunctionality. The alkali treatment of commercially pure titanium and Ti6Al4V without heat treatment still allows the formation of a reaction layer in presence of simulated body fluids that can be utilized to attach bisphosphonates. Finally, electrohydrodynamic coating may be used to bind bioactive glasses without changing the chemistry of the glass to be further explored to bind bisphosphonates such as alendronate.

CHAPTER TWO

Interaction of Ti and its Alloys with Investment – In vitro Evaluation of Bioactivity

2.1. Introduction

Dental and craniomaxillofacial implants are used to reconstruct, rehabilitate and restore form and function to the edentulous or partially edentulous jaws and the craniomaxillofacial skeleton of the patient. Implants are also used to replace maxillofacial parts [16, 160-162], which not only plays a significant role in restoring lost masticatory function but also promotes self-esteem especially in patients with orofacial defects. With advances in imaging techniques, diverse geometry of implants are required for reconstruction thereby creating a need for the fabrication of custom made maxillofacial devices.

Titanium naturally forms a thin oxide layer in air [60]. The excellent chemical inertness, corrosion resistance, and even biocompatibility of titanium and titanium alloys are thought to result from the chemical stability and structure of this titanium oxide film which is usually only a few nanometres thick [5]. Titanium implants readily adsorb proteins (i.e. albumin, fibronectin and fibrinogen) from biological fluids (after interaction with water and ions) on placement in bone. Subsequently, neutrophils and macrophages interrogate the implant, followed by the formation of foreign body giant cells from activated macrophages, and then the migration of osteoprogenitor cells to the implant site and differentiate into osteoblasts that result in the formation of bone [6-8]. However, a thin non-mineral layer generally separates the bone-titanium interface, and the bond associated with osseointegration is attributed to mechanical interlocking of the surface roughness of titanium and pores in the bone surface. Although titanium implants demonstrate a good clinical success rate, the treatment is offered to patients after careful selection, which precludes a number of patient groups such as diabetics, osteoporosis, bone disorders or cardiovascular conditions. Thus, the modification of titanium to fabricate implant surfaces is of interest and being explored in order to promote osseointegration, faster healing time, higher bone-to-implant contraction and longevity. Furthermore, in order to make titanium biologically bond to bone, in patients with poor bone quality and quantity (i.e. bone resorption due to bone metastasis, hypercalcemia of malignancy) [163], mechanical, chemical and physical methods of surface modification have been proposed to improve the bone conductivity and bioactivity of titanium [5, 60, 62, 64]. The manufacturing process to devise dental implants or maxillofacial prostheses from titanium is important and considerable effort has been focussed on the laboratory processes such as methods of casting, machining, bonding to porcelain etc. Although titanium has several advantages over cobalt-chrome alloys

in it being lightweight with excellent biocompatibility, one of the problems associated with casting titanium is that it is able to react with the elements of the investment materials that results in a hard and brittle reaction layer [164]. Superplastic forming process is one of the techniques that has been used to process titanium for manufacturing dental prostheses, and the technology now finds a place for manufacturing dental and maxillofacial prostheses with a good degree of accuracy that also lends itself to manufacturing custom made prostheses, using CAD-CAM technology. The production of a superplastically formed dental prosthesis requires a die, replicating the reverse of the dental impression, made from dental casting investment material [162].

As dental investments are used to fabricate dental prostheses using the superplastic forming process; it is very important to understand the interfacial reaction between the investment and the titanium surface. The high melting point and chemical reactivity with oxygen and nitrogen (atmospheric air) as well as with other elements of the investment materials is often associated with the formation of a contamination layer. The structure and chemical stability of the die material has a significant effect on the depth of contamination. The quartz, alumina and zirconia insert produce the least interaction between the die and the alloy. The titanium casting investment was shown to reduce the extent of contamination in comparison to silica-based investments; however, doubts remained over its hot strength during forming due to marked slumping during superplastic forming [36]. Typically, the SPF forming of such shapes takes between 15 minutes and three hours at temperatures ranging from 700 – 950˚C, during which time chemical reactions may occur. Titanium is a highly reactive metal that under normal ambient conditions is protected by a passive oxide film. At high temperatures such as these, the oxide becomes soluble in the metal, and the protection is decreased, so reaction with the substrate is expected to occur [36]. In order to make a super plastically formed superstructure, which is of the exact dimensions as the implants, i.e. a passive fit, the dimensional changes associated with each stage of construction must be carefully controlled. With regard to the investment used, the overall expansion must match the thermal contraction of the alloy as it cools from the forming temperature (typically 900˚C), resulting in a zero net dimensional change [35]. As superplastic forming of titanium and its alloys are now being used for clinical applications (e.g. dental and maxillofacial prostheses) it is important to assess the interaction of the investment material with the Ti and its alloys during this process. Thus, to study the interaction of the investment with the Ti, the surface characteristics were determined

followed by an in vitro cell culture study to assess the effect of the interaction layer on the cytocompatibility. Furthermore as there is already some evidence of surface contamination with ions during superplastic forming [36, 165] surface modifications have been carried out to examine the effect of formation of an active calcium phosphate layer on the surface of these discs. The superplastic forming of titanium was simulated due to the fact that a large number of small shaped disc specimens were required for the study. The SPF equipment is designed for larger sheets or blocks and this would require punching of the specimens post SPF forming thus altering the interaction layer. Simulation of SPF is established [4, 166] and several studies have used this technique to study the effect of SPF mainly due to the availability of the equipment in few centres.

2.2 Materials and Methodology

2.2.1. Preparation of Titanium Discs

150X150 and 0.5 mm thickness commercially pure titanium stock sheets (CpTi) (TI003150, Goodfellow Company, UK), and 140 mm diameter and 0.5 mm thickness titanium alloy Ti6Al4V stock sheets (RTI International Metals Ltd, Staffordshire, UK) were used. The titanium sheets were abraded mechanically on both sides using silicon carbide (SiC) abrasive paper (800 Grit), in order to remove any debris, marks or imperfections on the surface to produce a uniform surface. Then they were punched into 10 mm diameter titanium discs using 3000 lb lever press and die system (RS Supplies, Corby, UK) (Figure 2.1). The 10 mm diameter disks were then polished using a dry electro-polishing machine (EcoMaxi Otec, Prazisionfinish GmbH, Germany), cleaned and then hand polished again using diamond-based paste (Struers diamond paste) in order to polish the surface and minimise any scratches or imperfections. The samples were then subjected to a sequential cleaning protocol ultrasonically, starting with rinsing in distilled water, acetone, ethanol and finally again with distilled water for 20 minutes each, after which, they were placed on glass dishes and dried in an oven at 40°C for 30 minutes.

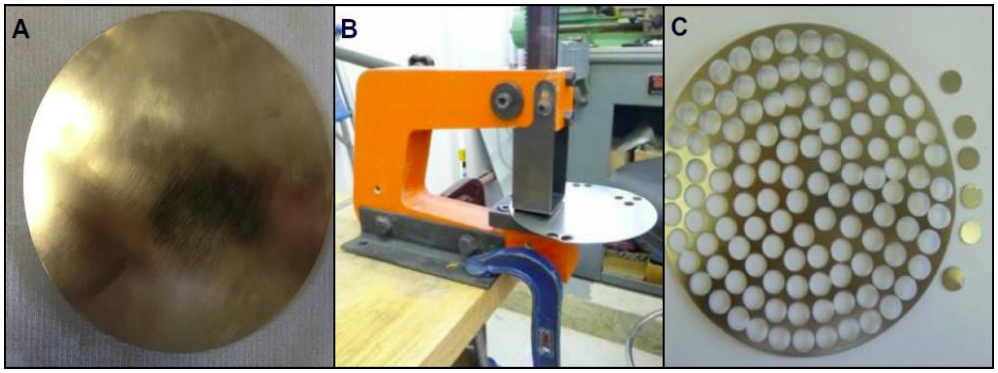

Figure 2.1: (A) Titanium stock sheets after abrading with the 800 grit silicon carbide paper, (B) Press and die system used to punch the titanium sheets, (C) titanium stock sheets after punching, and10 mm titanium discs used for the SPF forming

Superplastic simulation process: The samples of the CpTi and Ti6Al4V were embedded in Deguvest SR phosphate bonded investment (DeguDent, Germany) moulds, and heated in an oven up to 900°C and held for 20 minutes at this temperature, simulating the superplastic forming process, Deguvest was used in this experiment, as previous research findings showed high surface interaction with Ti. The name of the manufacturer, the treatment procedure, and the binder are

summarised in (Table 2.1). Deguvest is a phosphate-bonded investment that utilizes the reaction of a blend of $NH_4H_2PO_4$ and MgO powders mixed with water. Allan and Asgar et al. [167] positively identified struvite (crystalline $MgNH_4PO_4 \cdot 6H_2O$) in the set investment and proposed a simple reaction to account for its formation.

$NH_4H_2PO_4 + MgO + 5H_2O \rightarrow NH_4MgPO_4 \cdot 6H_2O$ [43]

Investment	Manufacturer	Use	Treatment Procedure	Binder	Chemical Composition
Deguvest 	DeguDent GmbH Germany	Casting Precious Metals	Furnace	Phosphate	$NH_4H_2PO_4$ + MgO

Table 2.1: The composition and manufacturer information of the dental investment Deguvest SR used for investing the Ti and Ti6AlV4 discs using simulated superplastic forming process

The phosphate bonded investment was prepared as recommended by the manufacturer and the powder: liquid ratio were measured before the mix was hand spatulated quickly to obtain a homogenous mix, after which it was vacuum mixed for 60 seconds at 25-30 mmHg negative pressure (Continental power vacuum mixer, Whipmix Corp, Kentucky,USA). The mixture was then poured into plastic moulds and the 10 mm diameter cleaned titanium discs were embedded in the investment mixture and distributed sequentially and it was ensured that the surfaces were totally covered by the investment material. The moulds were allowed to set at room temperature (21°C) for about one hour, then the set investments were released from the plastic moulds and heated in an electric furnace to the superplastic forming temperature of 900°C at a rate of 5°C/min to simulate the superplastic forming process (SPF), and then held at 900°C for 20 minutes. In SPF process, 20 minutes is the expected range of time where the pressure is maintained for the superplastic manufacturing of prostheses at 900°C [36]. After the heat treatment, the moulds were allowed to cool to room temperature before the cold investment moulds were removed to retrieve the embedded titanium discs. The discs were then subjected to a cleaning process using stainless steel pins in a mixture of water and very small amount of detergent, in order to remove the superficial investment residue, which

might be found on the titanium surfaces. The process of cleaning was performed using magnetic polishing machine called EcoMaxi for 30 minutes (Otec, Prazisionfinish GmbH, Germany). This process allows the titanium discs to be cleaned mechanically, using hundreds of small stainless steel pins that whirl through the machine containing water, cleaning the titanium surfaces when they come into contact.

After the discs were cleaned, they were again subjected to the sequential cleaning regime which was mentioned earlier (Section 2.2.1), ultrasonically rinsed with distilled water, followed by acetone, ethanol and rinsed again with distilled water, then followed air drying at room temperature. The cleaned titanium discs were grouped and packed into proper sealed bags to prevent possible damage or contamination to the treated surfaces before being sent for sterilisation for the purpose of biological evaluation. The SPF simulated commercially pure titanium and Ti6Al4V titanium alloy discs, which were embedded in the Deguvest phosphate bonded investment denoted as CpTi SPF and Ti64 SPF respectively, where the untreated titanium discs were denoted as CpTi Control and Ti64 Control respectively.

2.2.2. Surface Treatment of the Titanium Discs

2.2.2.1. Simulated Body Fluid (SBF) Immersion

Bioactive materials have been shown to form an apatite layer on interaction with simulated body fluid [13]. A bone-like apatite layer is shown to form on the surface of bioactive materials when bonding to living bone. Thus surface modification of titanium and it alloys were carried out by immersion of control (non-invested) and invested titanium discs in SBF fluid with ion concentrations nearly equal to those of human blood plasma and examined for formation of an interaction layer.

2.2.2.1.1. Preparation of Simulated Body Fluid (SBF)

The preparation of the SBF solution was based on the Kokubo recipe (1990). The concentrations of the ions of the SBF solution compared to those of human blood plasma are shown in Table 2.2. A volume of around 700 mL of ultra-pure water was placed into a 1000 ml beaker, which was placed on an electrical base stirrer with a magnetic stirrer inside. Each chemical was mixed in water until number 8, one by one in the order shown in Table 2.3. After each reagent completely dissolved, the solution was placed in a water bath at a temperature maintained between 36.5 and

38°C, and the pH level was measured, after that $(CH_2OH)_3CNH_2$ buffer was added little by little with less than 1 g in order to avoid local increase in the pH of the solution. The final pH was adjusted to 7.4 using Titrate 1kmol/dm3-HCl solution. The final volume was adjusted to 1000 ml by addition of ultrapure water with constant stirring, and then the solution was stored in polyethylene bottle at 4°C for a maximum one month prior to use.

Ions	SBF ($mmol/dm^3$)	Blood Plasma ($mmol/dm^3$)
SO_4^{-2}	0.5	0.5
HPO_4^{-2}	1.0	1.0
HCO_3^-	4.2	27.0
Cl^-	147.8	103.0
Mg^{+2}	1.5	1.5
Ca^{+2}	2.5	2.5
Na^+	142.0	142.0
K^+	5.0	5.0

Table 2.2: A comparison of ionic concentrations in SBF and Blood Plasma adapted from kokubo et al. [13]

The non-invested (control) and invested groups, were immersed in 10 ml of SBF solution at 37°C for 10 days, in which period, the solution was changed every two days. After soaking for the required time, the discs were removed rinsed gently with distilled water and then left to dry in a desiccator, then they were placed in sealed bags and vials to be used for surface evaluation.

Order	Reagent	Amount
1	NaCl	7.996 g
2	$NaHCO_3$	0.350 g
3	KCl	0.224 g
4	$K_2HPO_4.3H_2O$	0.228 g
5	$MgCl_2.6H_2O$	0.305 g
6	1 kmol/m^3 HCl	40 cm3
7	$CaCl_2$	0.278 g
8	Na_2SO_4	0.071 g
9	$(CH_2OH)_3CNH_2$	6.057 g
10	1 kmol/m^3 HCl	Appropriate amount to adjust the pH

Table 2.3: Reagent amounts for preparation of SBF solution (1L, 7.4 pH) according to Kokubo recipe [13]

2.2.3. Surface Characterization

2.2.3.1. Surface Roughness Measurement

The surface roughness analysis of the titanium sample discs in microns (μm) before and after surface treatment was assessed and quantified with a contact profilometer surface analysis instrument, TESA Rugosurf 10G surface roughness gauge (TESA technology; Hexagon Metrology, Switzerland). The mean roughness was measured and recorded at a traverse speed with a diamond probe tip stylus of 5μm. For each of the 10 mm titanium sample discs, the roughness parameters were measured at four different locations and a total of three discs from each group of the titanium samples, were analysed to obtain an accurate assessment. In the current study, the surface roughness parameter is presented as Ra, which is the most common, used surface parameter to express implant surface roughness [65]. Ra is defined as average surface roughness or arithmetic mean deviation of the roughness profile, which is the area between roughness profile and its mean line, or the integral of the absolute value of the roughness profile heights (peaks and valleys) and then averaging them all over the entire cut-off/evaluation length [168]. The centerline normally corresponds to the section through the profile, which cuts off the equal areas above and below it.

2.2.3.2. Scanning Electron Microscopy/Energy Dispersive X-ray Analysis (SEM/EDS)

The treated titanium discs were observed using scanning electron microscopy (SEM) (Hitachi S3500N, UK Hitachi High-Technologies), accompanied with an energy dispersive X-ray spectroscopy machine (EDAX) (Oxford instruments Microanalysis, UK). However two different scanning electron microscopes (FEI Quanta ™ FEG) with differing EDAX software were used during the course of the study due to availability and the equipment being out of action. SEM/EDAX analysis offered high-resolution imaging with nanometre resolution of surface structure. Although the field emission SEM could be operated in low vacuum environment mode, high vacuum mode was used to optimize EDAX analysis. The samples were prepared for the SEM/EDS analysis by mounting them on 12mm pin stubs and were coated with Leit-C Conducting Carbon Cement. The atomic chemical analysis was obtained by X-rays produced from the interaction of primary electron beams from SEM with the surface atoms, producing characteristic measurements from elements present on surface.

2.2.3.3. Raman Spectroscopy Analysis

Using Raman spectroscopy in biological studies to determine the chemical properties of biological materials, such as bone, presents several advantages especially over the infrared spectroscopy (IR). Raman microspectroscopy is able to explore samples at the micrometer scale. As measurements are obtained with a reflection optical arrangement, as there is no limitation regarding the transparency or thickness of the specimen. In addition, it offers superior resolution on the order of 0.6–1 μm compared to FTIR's resolution of 5–10 μm. In this study, Raman spectroscopy measurement was performed on the titanium surfaces using the Renishaw inVia Raman microscope system (Renishaw plc, Wotton-under-Edge, UK). The measurements were recorded at room temperature using laser beam of 785 nm excitation wavelength. The titanium samples were scanned from 100 to 3000 cm^{-1} range at spatial resolution of 1 μm with 600 lines/mm grating. Prior to the measurements, the Raman spectroscopy system was calibrated using 520 cm^{-1} Raman peak of polycrystalline Si standard. The measurements data were recorded and analysed using Wire 3.0 software Streamline® mapping capability (Renishaw, UK).

2.2.3.4. Atomic Force Microscopy (AFM)

Atomic force microscopy (AFM) is a very high-resolution type of scanning microscopy, with demonstrated resolution in the order of fractions of a nanometer, more than 1000 times better than the optical diffraction limit. This technique offers a three dimensional scanning of surfaces compared to SEM and Raman. On the other hand AFM can only image a small area in comparison with the image scanned by the SEM technique. The scanned area is limited to an area of around 100x100 μm^2 (X and Y dimensions) with a maximum height of 10 µm. The AFM consists of a cantilever with a sharp tip (probe) at its end that is used to scan the specimen surface. The cantilever is typically silicon or silicon nitride with a tip radius of curvature on the order of nanometers. In the current study, a commercial AFM (Tropometrix Explorer SPM, Veeco Metrology LLC, Santa Barbara, CA USA) was used to perform three-dimensional and morphological topography analysis of the treated titanium surfaces, using the standard tapping mode and the tip was conventional conical shape NSC35, single beam, etched silicone probe with cantilever spring constant in the range of 3.5 to 8.5 N/m. The images obtained were processed and analysed using Gwyddion© 2.19 (http://www.gwyddion.net, Czech Metrology Institute) data analysis software, and SPIP©6.0.13 (Scanning Probe Image Processor, nanoScience instruments, http://www.nanoscience.com).

2.2.4. In vitro Biological Evaluation

Human primary alveolar osteoblast cells (HOB) were used for the biological evaluation; these were isolated from alveolar bone obtained from dental patients undergoing surgical procedures (ethics approved and consent given). The cells were prepared following a protocol previously described by Di-Silvio et al [169]. Briefly, HOB cells were cultured in 25 cm^2 tissue culture flasks in Dulbecco's Modified Eagle's Medium (DMEM) supplemented with 10 % foetal calf serum, non-essential amino acids MEM (1%), 2 mM L-glutamine and, 5 ml of Penicillin-streptomycin in 500 ml of media (10,000 units penicillin and 10mg streptomycin per ml) ascorbic acid (0.075g), L-glutamine (2 mM), and HEPES (0.02M). Then incubated at 37˚C 5% CO_2 humidified incubator. The growth of the cells was checked twice weekly, once confluent they were split. Medium was changed and the flasks were maintained in a humidified atmosphere at 37˚C and 5% CO_2. At 70% to 80% of cells confluence, the DMEM was removed from the flasks and discarded; the flasks were rinsed with 2-4 ml of PBS in order to clean the flask from any remaining medium left. The cells were then detached by adding 2 ml of trypsin, incubated for 5 minutes and observed under the microscope to ensure cell

detachment. A 10 ml of medium was added to the flask and then transferred into sterilized universal. Cell pellets were obtained by centrifugation. Cells were split and transferred into 75 cm^3 flasks. A cell counting was performed visually using a haemocytometer, where 100 µl of trypan blue was added to 100 µl of cell suspension, placed onto the haemocytometer and counted under the microscope. Following cell counting a 50 µl of cell suspension of 2 x 10^5 was ready to be seeded onto each disc sample surface for quantitative evaluation.

2.2.4.1. Assessment of cell viability – MTT (Methyl-tetrazolium) Assay

This assay was used to measure the metabolic activity of cells and does so by the reduction of MTT (3-(4,5-Dimethylthiazol-2-yl]-2,5-diphenyl tetrazolium bromide) to formazan, thus giving a purple colour. This mostly happens in mitochondria and as such, it is in effect a measure of mitochondrial activity. It was used also to determine any cytotoxicity effect of the titanium surfaces being in contact with the investment material, due to any potential toxic leachable materials from the test samples. For the elution studies, the test samples were placed into labelled bijou using sterile forceps, and 3 mm of sterile complete DMEM media were added. The lids were sealed with parafilm and placed onto the roller mixer for 24 and 72 hours (elution time). After the required time of 24 h and 72 h, the media was removed and frozen until further analysis. aHOB cells were trypsinised, counted and then seeded into 96 well plate at a density of 1 x 10^4 cell/100 µl per well. The plates were placed in the incubator for 24 hours in order to allow for cell confluence. After 24 hours of incubation, the plates were removed from the incubator and then the media were removed from the wells by pipetting using a 100 µl pipette. The MTT solution was prepared by mixing 50 mg of MTT powder (Sigma, UK), dissolved in 5 ml PBS (Sigma, UK) and next filtered. Then MTT assays were performed as follows; a 96 well plate for 24 h, 96 well plate for 72h, and 96 well plate for positive control (10% alcohol diluted in media). 100µl of the eluant was added to the designed wells. The plates then were returned to the incubator and left for 24 hours and 72 hours as required. After the required exposure time, the media was removed from the 96 well plate and a 100 µl of the MTT solution was added to each well and placed in the incubator for 4 hours. After the 4 hours of incubation, the media was removed and 100 µl of DMSO was added to each plate, wrapped with aluminium foil, and then placed on a shaker for 5 minutes. Finally the absorbance was read at 570 nm test wavelength with 630 nm using the Dynex mircoplate reader.

2.2.4.2. Assessment of cell viability – Live and Dead Staining Assay

A two-colour fluorescence assay was used to determine; 1) live cell number: live cells have intracellular esterases that convert nonfluorescent, cell-permeable calcein acetoxymethyl (calcein AM) to the intensely fluorescent calcein. Cleaved calcein is retained within cells. 2) Dead cell number: dead cells have damaged membranes; the ethidium homodimer-1 (EthD-1) enters damaged cells and is fluorescent when bound to nucleic acids. EthD-1 produces a bright red fluorescence in dead cells. Fluorescent staining solution was prepared by mixing; 8 µl 1mM of Caclin Am, 4 µl of Ethidium and 4 ml of phenol free media. After incubation of cells, the media was removed from the wells, and the samples washed with PBS, 250 µl of the fluorescent solution was added per each well, and then placed in the incubator for 1 hour. The samples were arranged into two 24 well plates (24 hours and 72 hours), HOB cells were seeded at density of 2 x 10^5 per µl at passage number 12, and then placed in the incubator to allow cell attaching to the surfaces. Finally the plates were observed under Olympus® fluorescent microscope (Suffolk UK), where Green fluorescent is indication of live cells and Red one is for dead cells.

2.2.4.3. Assessment of cell differentiation – Alkaline Phosphatase Assay

Alkaline phosphatase is a membrane-bound enzyme and is used as a marker of osteoblast differentiation. In the current study, alkaline phosphatase (ALP) was performed on the different surface modification treatments to evaluate the differentiation of osteoblast cells on the surfaces. The assay was carried out with cell lysates collected at different time points (Days 1, 3, 7, 14, 21 and 28) using the freeze/thaw cycle, in which aHOB cells were trypsinised, counted and seeded at 1 x 10^6 per 50 µl; the medium was replaced at 2-day intervals throughout the experiment. At each time point the plates were removed from the incubator and placed into a laminar flow cabinet, the media was discarded and the wells were gently washed with 1 ml PBS (Phosphate Buffered Saline, Serotec. UK) then 1 ml of distilled water was added in each well, then the plates were frozen for 15 minutes at –80°C and transferred to an incubator at 37°C for 20 minutes. Following each cycle, cells were thoroughly mixed. This freeze/thaw technique was repeated twice more. Subsequently the cell lysate was frozen into small vials; such samples were used for the ALP activity measurements after 1, 3, 7, 14, 21 and 28 days in culture, by adding 50 µl of each cell lysates from the test materials into appropriate 96 well plate and then the addition of 50 µl of substrate reagents solution. Glycine solution

was prepared by dissolving 0.75 g of glycine powder into 90 ml of distilled water adjusted to pH of 10.3 and then the volume was made up to 100 ml. The substrate agent was obtained with 20 mg p-nitrophenol phosphate, 17 mg magnesium chloride hexahydrate, 40µl Triton-X 100 and made up to 5 ml with 0.1M glycine. A standard curve was prepared fresh by diluting of 200 mg p-nitrophenol phosphate in 0.1M glycine solution (pH 10.3), to give a range of different concentration values of standards (50, 25, 12.5, 6.25, 3.125, 1.563, 0.782, and 0 µg/ml). 100 µl of each p-nitrophenol standards was then aliquoted into 96 well plate accordingly, and then the plates were placed on a shaker for 2 minutes and read at 0 and 20 minutes using Dynex plate reader at wavelength of 410 nm.

2.2.4.4. Assessment of cell viability – DNA Quantification Assay

DNA assay is a method used to measure cell turnover and proliferation, hence an indicator of cell turnover in the presence or absence of a test material. DNA assay was carried out on the different surface treatment samples of CpTi and Ti6Al4V alloy as HOB cells were lysed at 6 time points (Days 1, 3, 7, 14, 21 and 28) using a freeze/thaw method which was described above in the previous section. Total DNA was assessed using a fluorometric assay incorporating bisbenzimidazole (Hoechst 33258). A fluorescent effect is produced due to the interaction of the reagent with cell DNA. The fluorescence intensity is proportional to the amount of DNA and thus the number of cells in the sample. The aHOB cells were trypsinized and placed into new wells. DNA was extracted at each time point using a freeze/thaw technique. Hoechst 33258 was allowed to react with the lysate and DNA standards (calf thymus DNA, Sigma) of concentrations 0, 0.31, 0.63, 1.25, 2.5, 5, 10, and 20 µg/ml in saline sodium citrate buffer (pH 7.0). Measurement of fluorescence was performed by using a plate Chameleon V (Hidex) and subsequently the DNA content was calculated from the standard curve.

2.2.5. Statistical Analysis

The data were statistically analysed using analysis of variance (ANOVA) for assessing the significance level of the differences between the experimental groups. All statistical analysis was performed with commercial statistical software GraphPad Prism (version 6.0c). The probability of p being below 0.05 was considered to be statistically significant. Results were represented graphically as mean values with standard deviation.

2.3. Results

2.3.1. Surface Roughness Measurement

Surface roughness measurements were obtained for four samples per each surface treated group, and calculated as mean value, which are presented in Table 2.4.

CpTi Group	**Average *Ra* ± SD (µm)**	**Ti64 Group**	**Average *Ra* ± SD (µm)**
CpTi Control	0.414 ± 0.176	Ti64 Control	0.217 ± 0.09
CpTi SPF	0.160 ± 0.075	Ti64 SPF	0.420 ± 0.128
CpTi SPF SBF 10D	0.389 ± 0.08	Ti64 SPF SBF 10D	0.431 ± 0.113

Table 2.4: Average surface roughness (Ra) measurements using a profliometer of CpTi and Ti64 samples (n=4) ± standard deviation (SD) before and after treatment with SBF on invested and non- invested specimens

The protocol to generate an average roughness on the surfaces of both untreated CpTi and Ti-6Al-4V prior to simulating the SPF process was defined, such that the interaction layer that occurred, would be formed on similar rough surfaces thus, making it possible to compare the data and conduct the cell culture studies on surfaces with similar surface roughness. As a large number of specimens were required for the study initially all specimens were subjected to profilometry and as reproducible surface roughness could be obtained by following the polishing regime, 4 samples from each group were used to report the results. The surfaces of CpTi and Ti64 obtained after polishing with the SiC paper resulted in CpTi surfaces to have a more rough topography in comparison to the alloy, which can be related to the surface hardness of the two different metals. The Ra of CpTi control of a value of 0.414 µm decreased to a roughness value of 0.160 µm when these surfaces were invested in Deguvest simulating superplastic forming process. While the roughness value of invested Ti64 surfaces of 0.420 µm showed an increase in the surface roughness compared to the control one. Immersion of invested surfaces in SBF solution for 10 days showed an increase in the surface roughness of both CpTi and Ti64.

2.3.2. Atomic Force Microscopy (AFM) Observations

The roughness parameters obtained under AFM for the different treated titanium disc groups in this study are summarized in Table 2.5. Different values were observed between the samples due to the different treatments. Figure 2.2 shows the qualitative characterization with two-dimensional and three-dimensional images of the corresponding surface topography of the differently treated titanium samples, which have been observed under AFM. The CpTi control had the highest Ra of 0.213 µm followed by the invested CpTi simulating superplastic forming process (SPF) which were immersed in SBF solution of 0.179 µm compared to the other samples. When CpTi was invested simulating superplastic forming process only (SPF) it showed that the surface had less surface roughness compared to the control with Ra of 0.164 µm. However, Ti64 surfaces, which were invested simulating superplastic forming process, appeared to increase the surface roughness compared to the Ti64 control.

CpTi Group	**AFM (Average Ra ± SD µm)**	**Ti64 Group**	**AFM (Average Ra ± SD µm)**
CpTi Control	0.213 ± 0.019	Ti64 Control	0.080 ± 0.013
CpTi SPF	0.164 ± 0.015	Ti64 SPF	0.152 ± 0.024
CpTi SPF SBF 10D	0.179 ± 0.038	Ti64 SPF SBF 10D	0.159 ± 0.026

Table 2.5: Surface roughness parameter for the different surface treated titanium disc groups obtained under AFM. The results were statistically analyzed using one-way Anova analysis (GraphPad Prism software). The Statistical significance was predetermined at ($p < 0.05$) and n=4 (± SD). There was no significant difference between the control and the different treated surfaces for both CpTi and Ti64 samples.

Sample name	2D AFM Image	3D AFM Image
CpTi Control	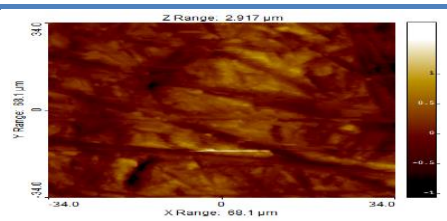	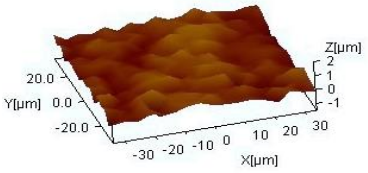
CpTi SPF	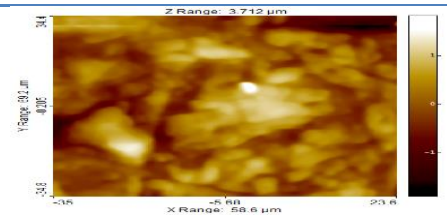	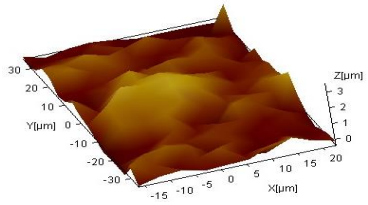
CpTi SPF SBF 10D	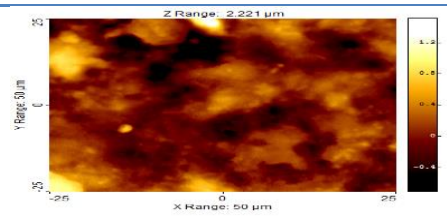	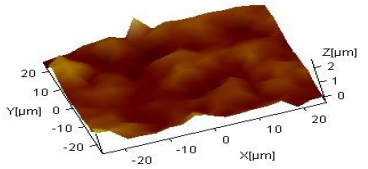
Ti64 Control	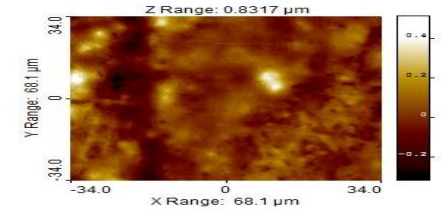	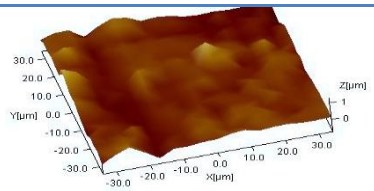
Ti64 SPF	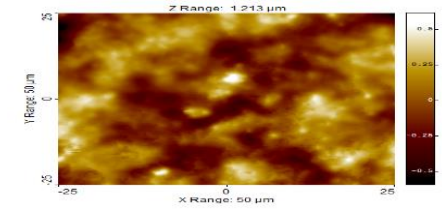	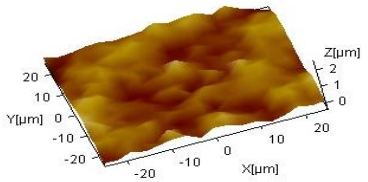
Ti64 SPF SBF 10D	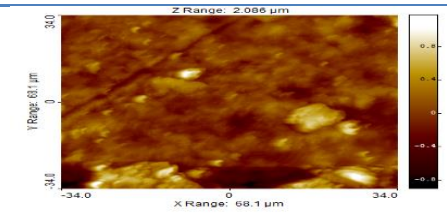	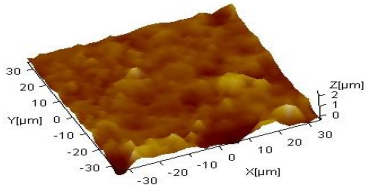

Figure 2.2: Representative 2D and 3D of AFM images of the different tested CpTi and Ti64 samples, where the SPF process decrease the Ra value on the CpTi samples, while it increasd it on the Ti64 samples compared to the control. While immersion in SBF seems to increase the surface roughness of these surfaces due to the deposition of apatite like layer.

2.3.3. Scanning Electron Microscopy/Energy Dispersive X-ray Analysis (SEM/EDS)

Qualitative surface characterization of the titanium surface topography was visualised using electron microscopy (SEM). The SEM images of the treated and untreated surface morphologies of CpTi and Ti6Al4V titanium discs are shown in Figures 2.3 and 2.4 respectively. And the Ca/P ratio for the samples is presented in Table 2.6. The CpTi and Ti64 titanium control samples were relatively smooth with some imperfections and scratches due to the sandblasting and polishing processes. It was observed that these marks and imperfections were finer on the CpTi control than the Ti64 control surfaces. The simulated superplastic forming process (SPF) samples showed a deposition of a layer. The EDS analysis of this layer on these surfaces showed the presence of phosphorus ions due to the chemical reaction between the titanium surface and the phosphate-bonded investment. Although titanium is a highly reactive metal under ambient conditions, is protected by a passive oxide film. However at high temperatures such as the SPF processing temperature, the oxide becomes soluble in the metal, and the protection is decreased, so reaction with the investment is expected to occur. The simulated superplastic forming process (SPF) CpTi and Ti64 samples which were immersed in simulated body solution (SBF) for 10 days showed a deposition of apatite like layer on their surfaces, whilst the CpTi and Ti64 which were not subjected to SPF treatment prior to SBF interaction did not show the formation of an interaction layer. The Ca/P ratio of the apatite like layer on the invested and immersed in SBF CpTi and Ti64 surfaces was 1.13 and 1.14 respectively which is lower than the bone mineral apatite layer of Ca/P ratio 1.67.

Sample Name	Ca	P	Atomic Ca/P ratio
CpTi SPF SBF 10D	3.29	3.72	1.13
Ti64 SPF SBF 10D	4.95	5.63	1.14

Table 2.6: Concentrations of Ca and P (Atomic %) of CpTi and Ti64 test samples which were invested simulating superplastic forming process and immersed in SBF for 10 days obtained from EDS analysis.

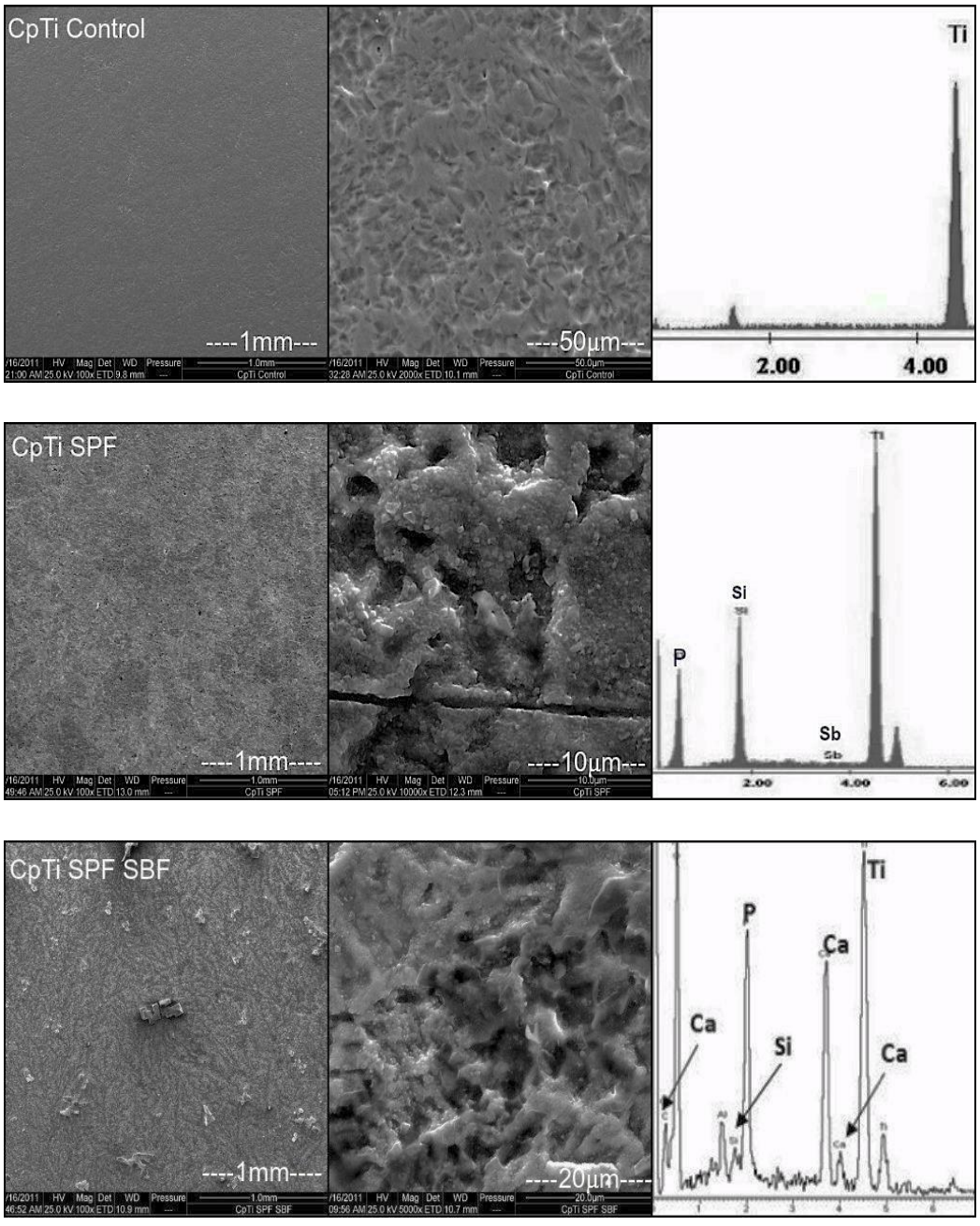

Figure 2.3: SEM/EDS images of CpTi control, CpTi surfaces which were invested simulating superplastic forming process (SPF) and CpTi which were invested simulating superplastic forming process and immersed in simulated body fluid SBF for 10 days.

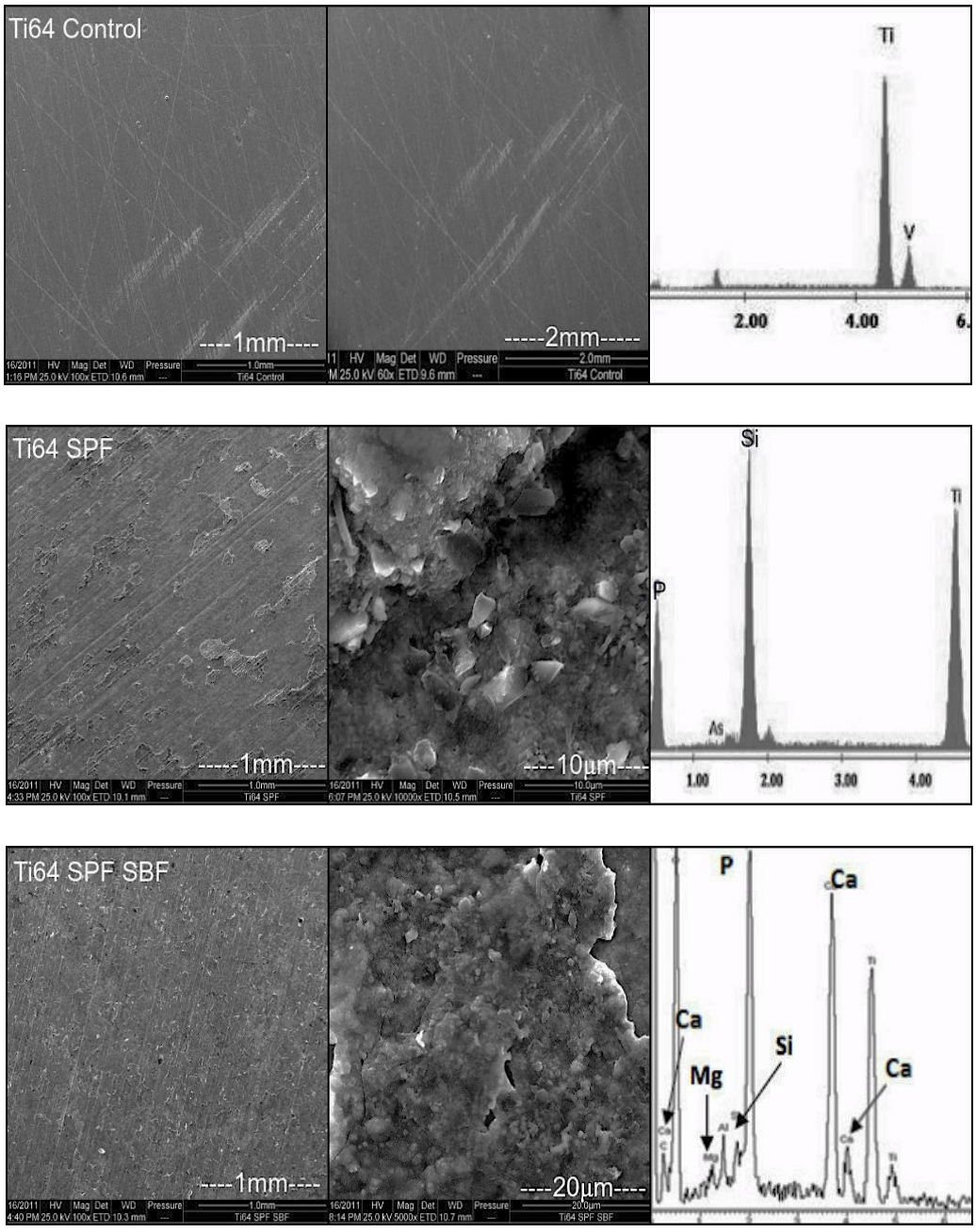

Figure 2.4: SEM/EDS images of Ti64 control, Ti64 surfaces which were invested simulating superplastic forming process (SPF) and Ti64 which were invested simulating superplastic forming process and immersed in simulated body fluid SBF for 10 days.

2.3.4. Raman Spectroscopy

Raman high resolution scanning of the different titanium sample surfaces were measured in order to determine the chemical composition of the treated surfaces after simulation of superplastic forming process (SPF), as well as to investigate the presence of the apatite like layer on the surface which may have formed due to the SBF immersion treatment. High resolution of Raman scans of the SPF CpTi and Ti64 titanium surfaces, which were in contact with investment materials, showed the presence of different titanium dioxides crystallographic phases, which are composed mainly of rutile and anatase as recorded in the 100-800 cm^{-1} region of the Raman spectrum, as shown in Figures 2.5 and 2.6. Raman spectra of CpTi and Ti64 surface invested in Deguvest (phosphate bonded investment), consisted of two strong bands at 145 and 148 cm^{-1} respectively which correspond to anatase phase and medium bands at 223 and 222 cm^{-1}, 447 and 449 cm^{-1}, 608 and 602 cm^{-1} respectively which correspond to rutile phase. Weak bands at between 329 and 404 cm^{-1} were observed on CpTi and Ti64 invested surfaces, which correspond to brookite phase. Very weak bands were observed in the range between 801 and 975 cm^{-1} on titanium samples, which were invested simulating superplastic forming process (SPF) and immersed in SBF for 10 days compared to the only invested ones as there was no distinguishing band of the apatite-like layer between 957 and 962 cm^{-1}compared to the Raman peak of the hydroxyapatite in bone tissue

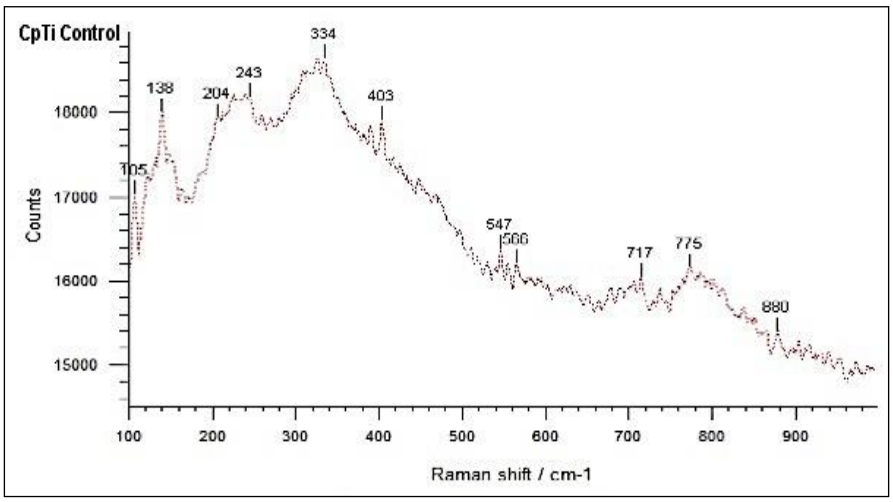

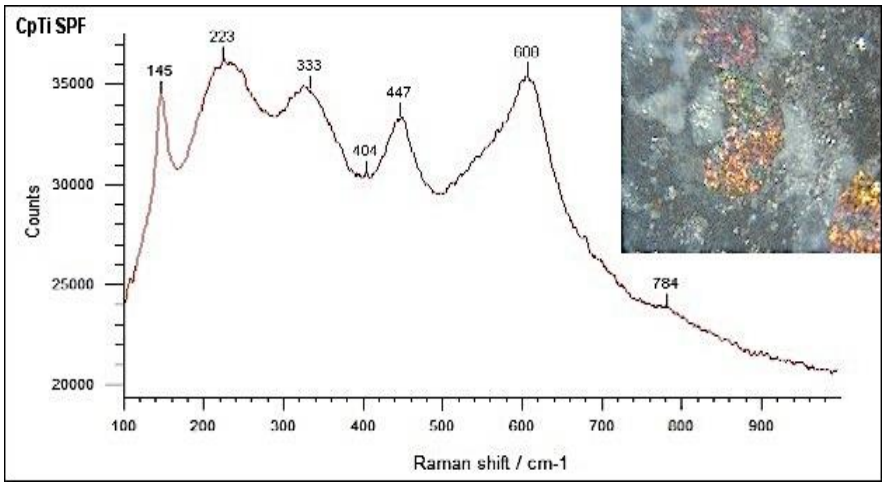

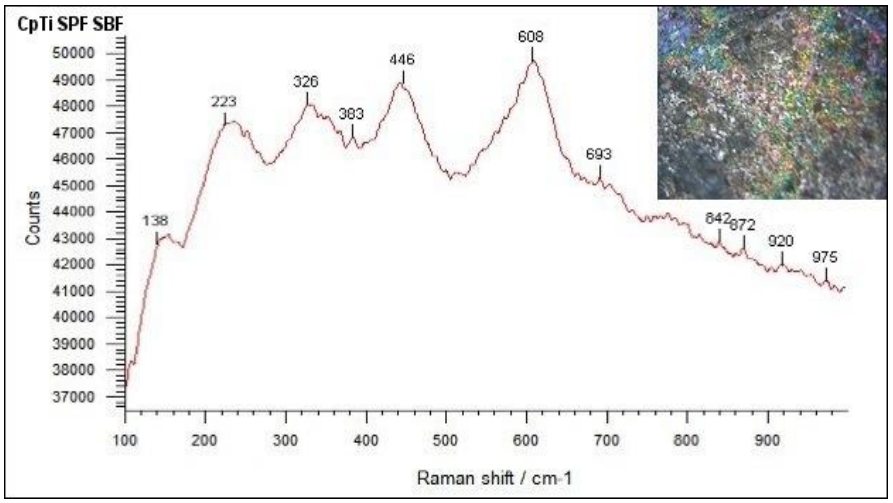

Figure 2.5: Raman spectrum with highlighted peaks of the different treated CpTi (control, invested CpTi simulating superplastic forming process (SPF), and invested CpTi simulating superplastic forming process immersed in simulated body fluid (SBF) for 10 days.

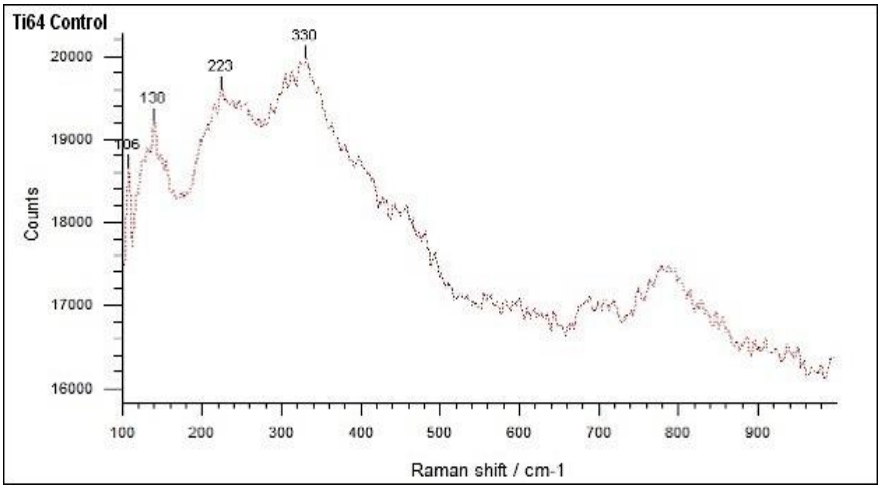

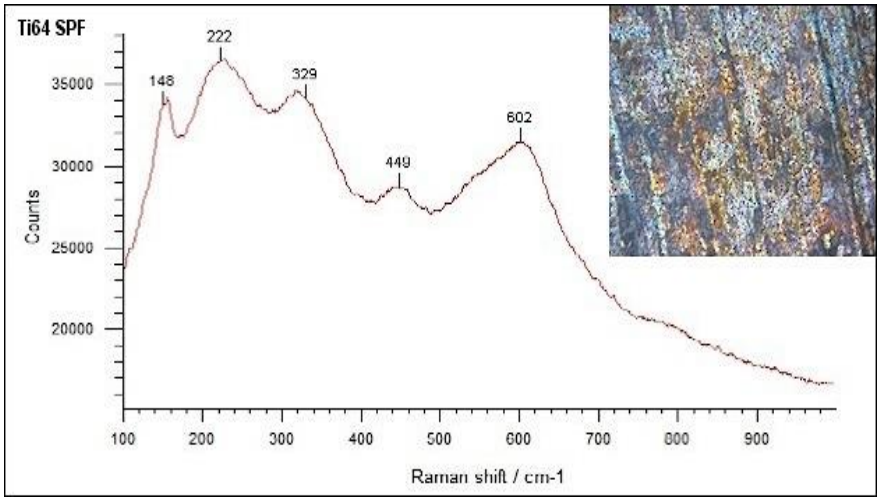

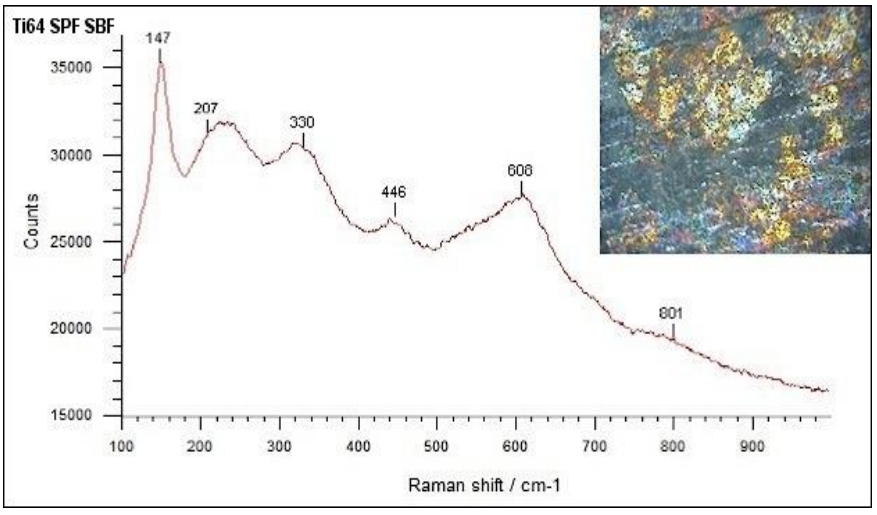

Figure 2.6: Raman spectrum with highlighted peaks of the different treated Ti64 (control, invested Ti64 simulating superplastic forming process (SPF), and invested Ti64 simulating superplastic forming process immersed in simulated body fluid (SBF) for 10 days.

2.3.5. Evaluation of Cytotoxicity Indirect Method (MTT)

MTT, Day 1 Exposure:

Samples were eluted for 24 hours for indirect exposure, where two elution time points were obtained (24h elution and 72h elution), in order to detect if any leaching products could affect the cell behaviour. After one day of MTT exposure, different metabolic cell activity levels were observed between the different groups.

For the CpTi samples, at the 24h elution time point, a comparison of the samples was made to media+cells sample (negative control). All samples showed higher cell activity level than the negative control. CpTi samples which had been heated simulating SPF and then immersed in SBF solution for 10 days showed the higher cell metabolic activity. At 72h elution time, there was a decrease in the cell metabolic activity obtained in all the samples, particularly, CpTi samples by CpTi samples, which had been heated simulating (SPF). In general all the test samples were similar but higher when compared to the control (Figure 2.7). The longer elution period may have resulted in the release of some leachables that affected the cell metabolic activity, but as a measure of cytotoxicity, this was not an indicator of cytotoxic effect compared with the positive control (10% alcohol). The results were statistically analysed showing that there was no significant differences ($p>0.05$) in osteoblast cells response between the negative control (media + cells) and the different surface treatment surfaces tested.

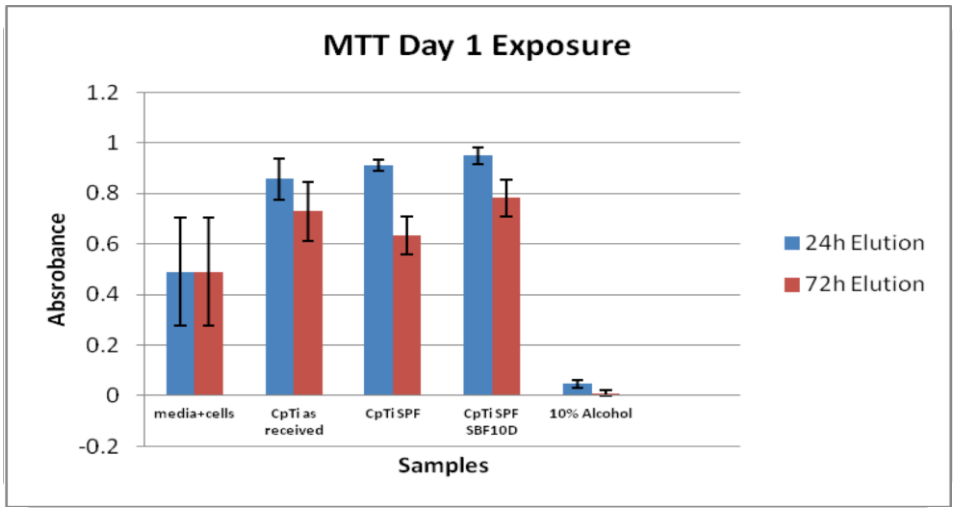

Figure 2.7: Evaluation of Cytotoxicity Indirect Method/ MTT Day 1 Exposure of CpTi test samples; showing levels of intensity of absorbance at 570nm of the CpTi samples at 24h and 72 elutions, expressed as mean absorbance ± S.D (n=4); the statistical significance was predetermined at $p< 0.05$

For the Ti64 samples, at the 24h elution time point, a comparison of the test samples was made to media+cells sample (negative control). All samples showed not significant increase cell metabolic activity level than the negative control. Ti64 samples which were heated simulating (SPF) showed better cell response followed by the Ti64 samples which was heated simulating SPF and then immersed in SBF solution for 10 days. At 72h elution time, there was a decrease in the cell activity obtained by all the test samples. Generally, all test samples showed similar results compared to each other and higher cell activity compared to the negative control (media+cells) and as a measure of cytotoxicity the samples were not toxic compared to the positive control (10% alcohol) (Figure 2.8). The results were statistically analysed and showed that there was no significant differences ($p>0.05$) in osteoblast cells response between the negative control (media + cells) and the different surface treatment surfaces tested.

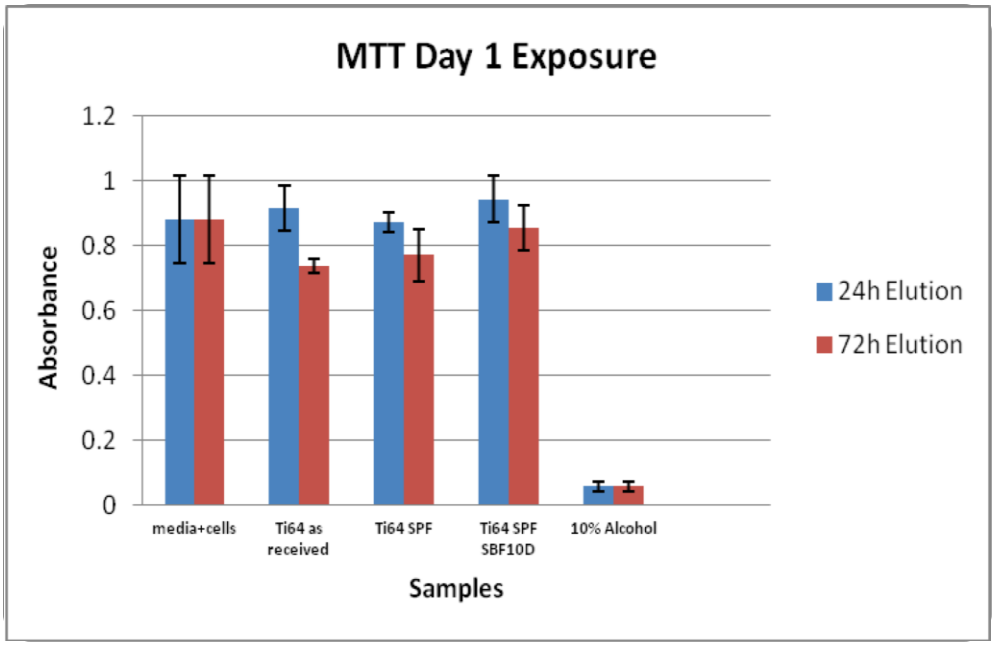

Figure 2.8: Evaluation of Cytotoxicity Indirect Method/ MTT Day 1 Exposure of Ti64 test samples; showing levels of intensity of absorbance at 570nm of the Ti64 samples at 24h and 72 elutions, expressed as mean absorbance ± S.D (n=4); the statistical significance was predetermined at $p< 0.05$

MTT, Day 3 Exposure:

Samples were eluted for 72 hours for indirect exposure, where two elution time points were obtained (24h elution and 72h elution), in order to detect if any leaching

products could affect the cell behaviour. After 3 days of MTT exposure, various cell activity levels were observed between the different groups. For the CpTi samples, at the 24h elution time point, a comparison of the samples was made to media+cells sample (negative control). All samples showed higher cell metabolic activity level compared to the negative control. CpTi as received showed the higher cell metabolic activity, followed by CpTi samples, which heated simulating SPF. At 72h elution time, there was an increase in the cell activity obtained by all the samples, except the CpTi as received samples. Generally there was an increase in the cell activity at the 72h elution time (Figure 2.9). Statistically there was no significant difference ($p>0.05$) in osteoblast cells response between the negative control (media + cells) and the different surface treatment surfaces tested.

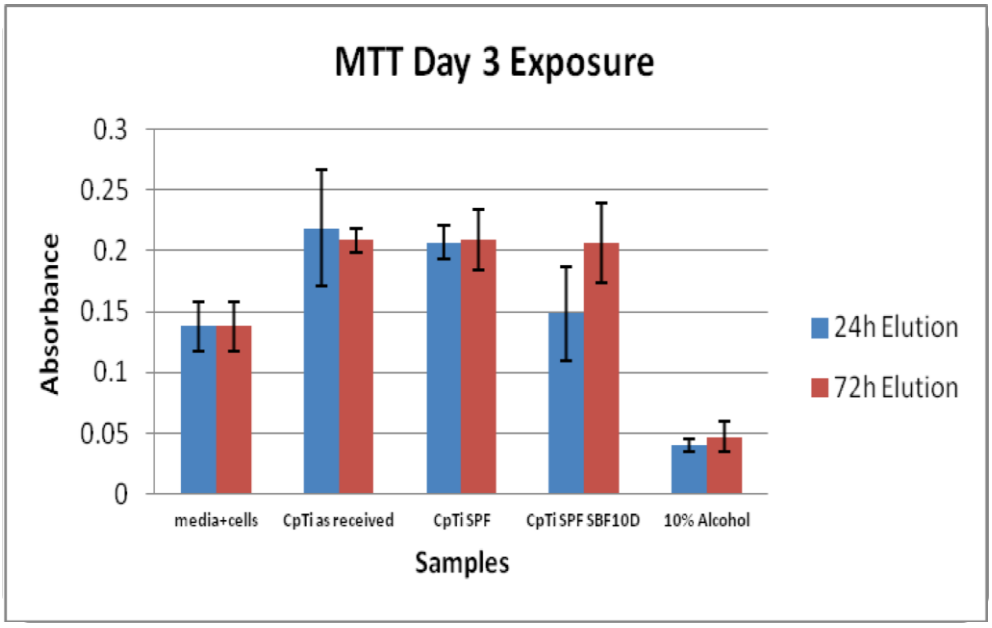

Figure 2.9: Evaluation of Cytotoxicity Indirect Method/ MTT Day 3 Exposure of CpTi test samples; showing levels of intensity of absorbance at 570nm of the CpTi samples at 24h and 72 elutions, expressed as mean absorbance ± S.D (n=4); the statistical significance was predetermined at $p< 0.05$

For the Ti64 samples, at the 24h elution time point, a comparison of the samples was made to media+cells sample (negative control). All samples showed lower cell activity level compared to the negative control, except the Ti64 samples, which heated simulating the SPF process then immersed in SBF solution for 10 days. At 72h elution time point, there was a significant drop in the cell activity for all samples (Figure 2.10). Statistically there was significant difference ($p<0.05$) in osteoblast

cells response at 72h elution time of the different treated samples compared to the negative control (media + cells).

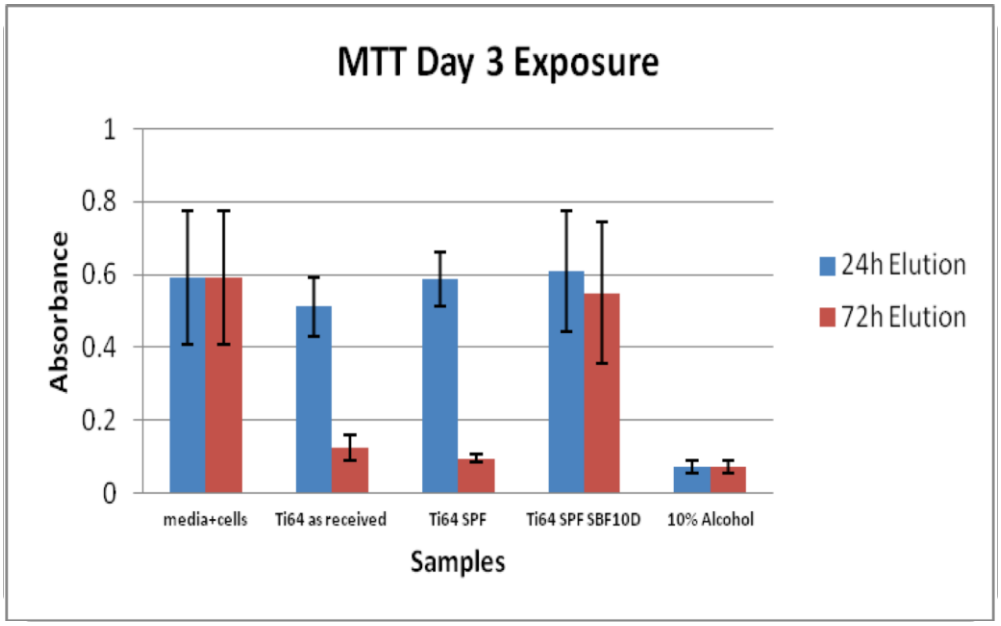

Figure 2.10: Evaluation of Cytotoxicity Indirect Method/ MTT Day 3 Exposure of Ti64 test samples; showing levels of intensity of absorbance at 570nm of the Ti64 samples at 24h and 72 elutions, expressed as mean absorbance ± S.D (n=4); the statistical significance was predetermined at p< 0.05

2.3.6. Assessment of cell viability – Live and Dead Staining Assay

Live/dead cells were measured for the tested samples for 24h and 72h of incubation. All different test samples showed good response with a large number of live cells, and few numbers of dead cells. This emphasizes the cytocompatibility of the CpTi and Ti6Al4V materials in their contact with the osteoblast cells. Different surface treatments of CpTi and Ti64 showed that they are not inducing cytotoxic effect on the cell viability. Images of live/dead cells of the different test sample are shown in Figures 2.11 and 2.12.

Group	Live Cells	Dead Cells
Thrx Discs	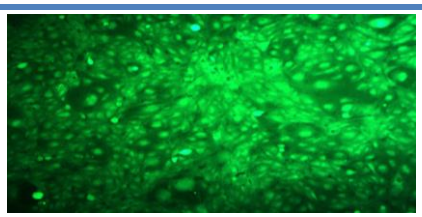	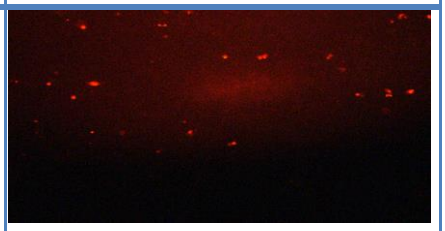
CpTi as received	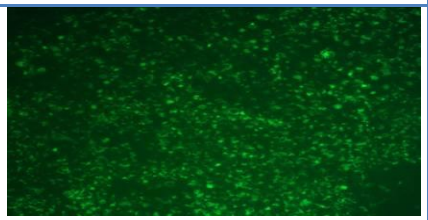	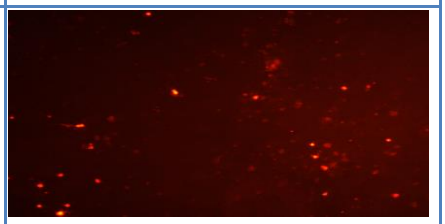
CpTi SPF	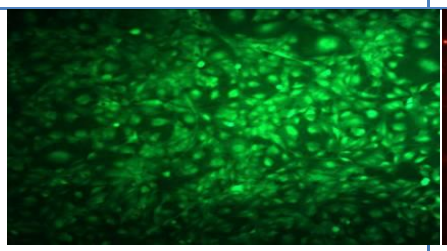	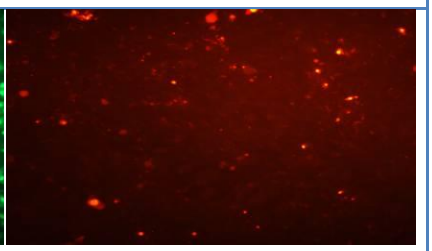
CpTi SPF SBF 7D	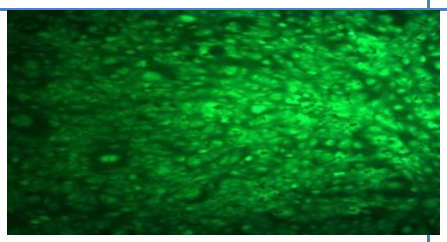	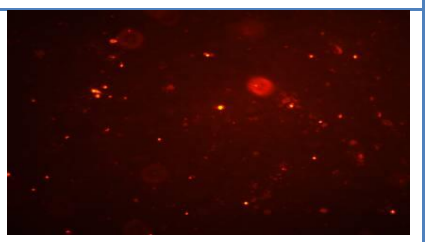
CpTi SPF SBF 10D	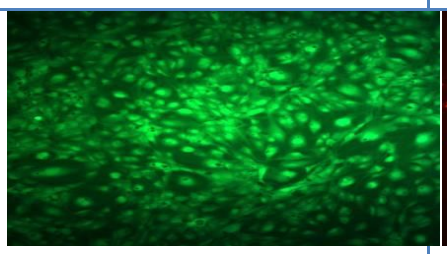	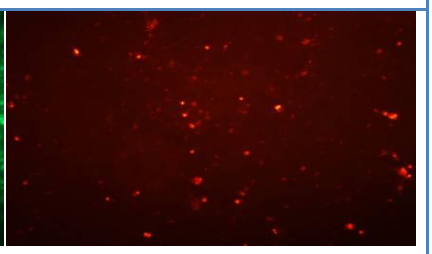

Figure 2.11: Live and dead fluorescence staining (Ethidium Homodimer-1) of aHOB cells exposed for 72 hours on CpTi test samples, which were treated simulating SPF process then subjected to immersion in SBF solution for 7 and 10 days. The surfaces are showing a good response of cells with a large number of live cells as it shown in the green staining images and low dead cells as it shown in the red staining images.

Group	Live Cells	Dead Cells
Thrx Disks	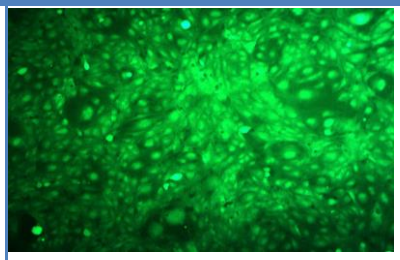	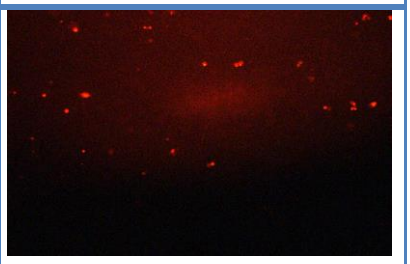
Ti64 as received	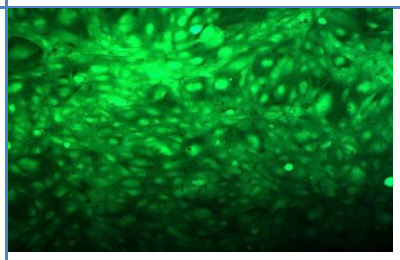	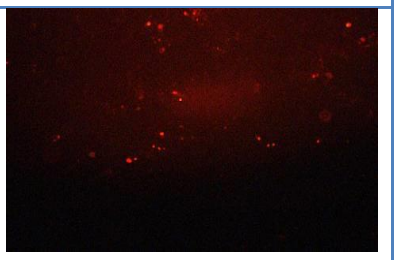
Ti64 SPF	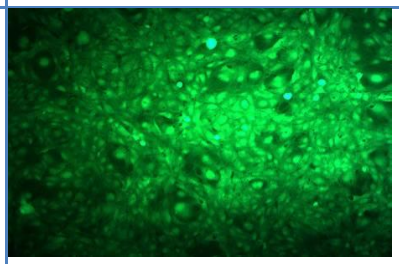	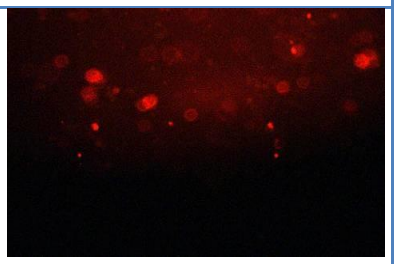
Ti64 SPF SBF 7D	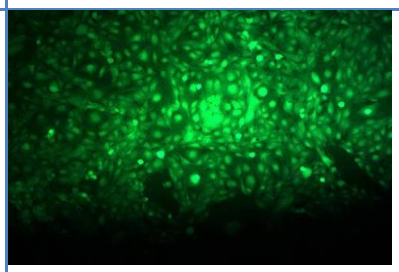	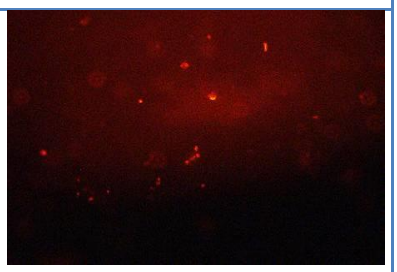
Ti64 SPF SBF 10D	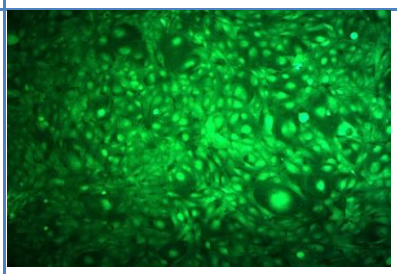	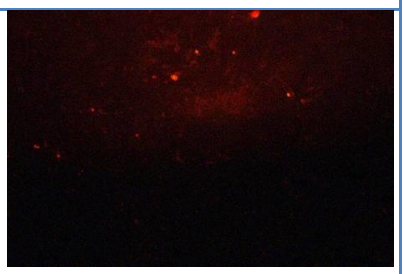

Figure 2.12: Live and dead fluorescence staining (Ethidium Homodimer-1) of aHOB cells exposed for 72 hours on Ti64 test samples, which were treated simulating SPF process then subjected to immersion in SBF solution for 7 and 10 days. The surfaces are showing a good response of cells with a large number of live cells as it shown in the green staining images and low dead cells as it shown in the red staining images.

2.3.7. Assessment of cell differentiation – Alkaline Phosphatase Assay

Alkaline phosphatase activity was used as marker of osteoblast phenotype. This assay was performed on the different surface modified titanium surfaces to evaluate the differentiation potential of osteoblast cells on the surfaces, at 6 time points; days 1 , 3, 7, 14, 21 and 28. The ALP assay of the CpTi samples (Figure 2.13) showed a slight increase in the ALP activity on the different test samples from day 1 to day 28. The control, CpTi control and the SPF heat-treated CpTi samples showed ALP response activity that peaked at day 28, while when these surfaces immersed in SBF solution, the ALP response activity peaked at day 7 which was statistically significant compared to the positive control (Thrx).

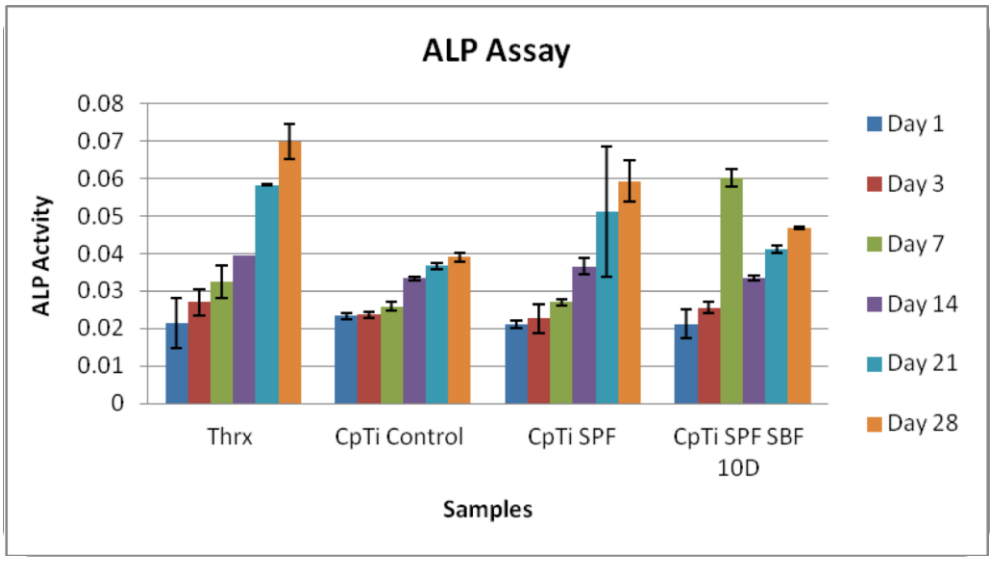

Figure 2.13: Evaluation of Differentiation of Osteoblast Cells / ALP Assay of CpTi titanium discs which were treated simulating superplastic forming process SPF and then subjected to immersion in SBF solution. The data represents the average for each group as mean absorbance ± SD (n=8); the statistical significance was predetermined at p< 0.05

The ALP assay of the Ti64 test samples (Figure 2.14) showed a general increase in the ALP activity on the different samples from day 1 to day 28. The control, Ti64 control and the SPF heat treated Ti64 samples showed a peak of ALP activity at day 28, while the SPF samples which were immersed in SBF showed an ALP peak at day 21. However there was no significant difference between the different test samples and the positive control.

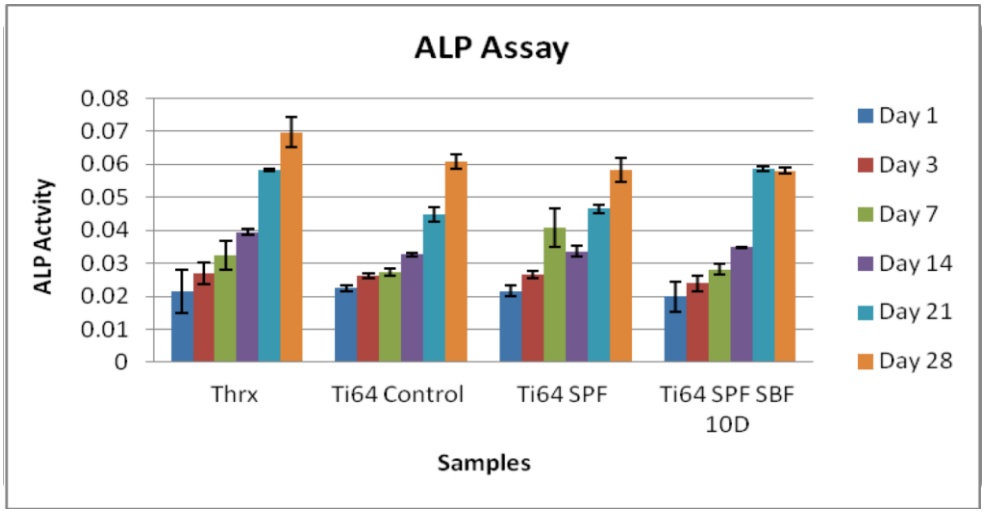

Figure 2.14: Evaluation of Differentiation of Osteoblast Cells / ALP Assay of Ti64 titanium discs which were treated simulating superplastic forming process SPF and then subjected to immersion in SBF solution. The data represents the average for each group as mean absorbance ± SD (n=8); the statistical significance was predetermined at p< 0.05

2.3.8. Assessment of cell viability – DNA Quantification Assay

DNA assay is a method used to measure cell turnover and proliferation hence an indicator of cell activity in the presence or absence of a test material. DNA assay was carried out on the different surface treatment samples of CpTi and Ti6Al4V alloy at 6 time points (Days 1, 3, 7, 14, 21, and 28).

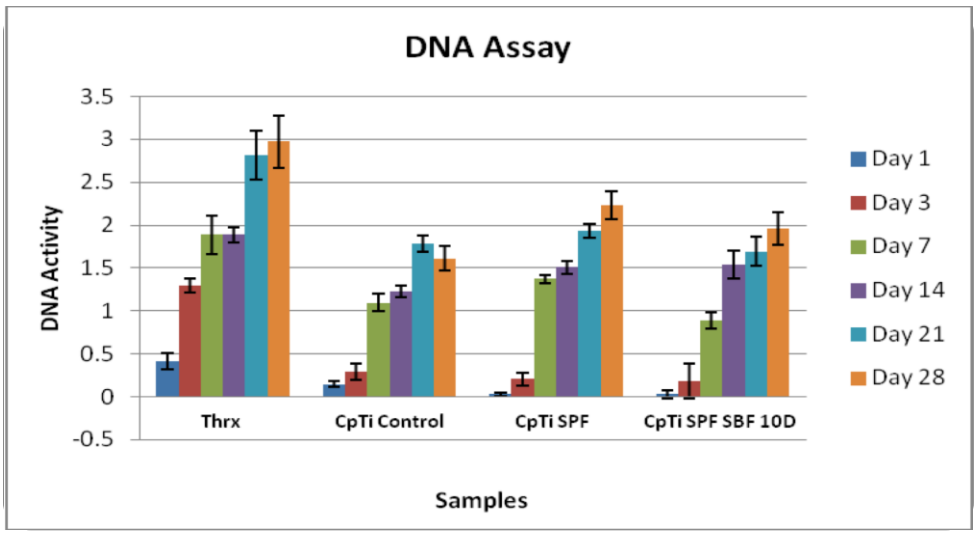

Figure 2.15: Evaluation of Proliferation of Osteoblast Cells / DNA Assay of CpTi titanium discs which were treated simulating superplastic forming process SPF and then subjected to immersion in SBF solution. The data represents the average for each group as mean absorbance ± SD (n=8); the statistical significance was predetermined at p< 0.05

The DNA activity assay of the CpTi samples showed general increase of cell proliferation through the 28 days of the DNA assay. All the different surface treatments showed higher cellular response compared to the sample surface with no treatment (CpTi Control) as expected. The heat-treated SPF process showed similar results to the heat-treated samples, which were immersed in SBF solution for 10 days. However, all the test sample surfaces showed significantly decrease in cellular response compared to the positive control (Thrx).

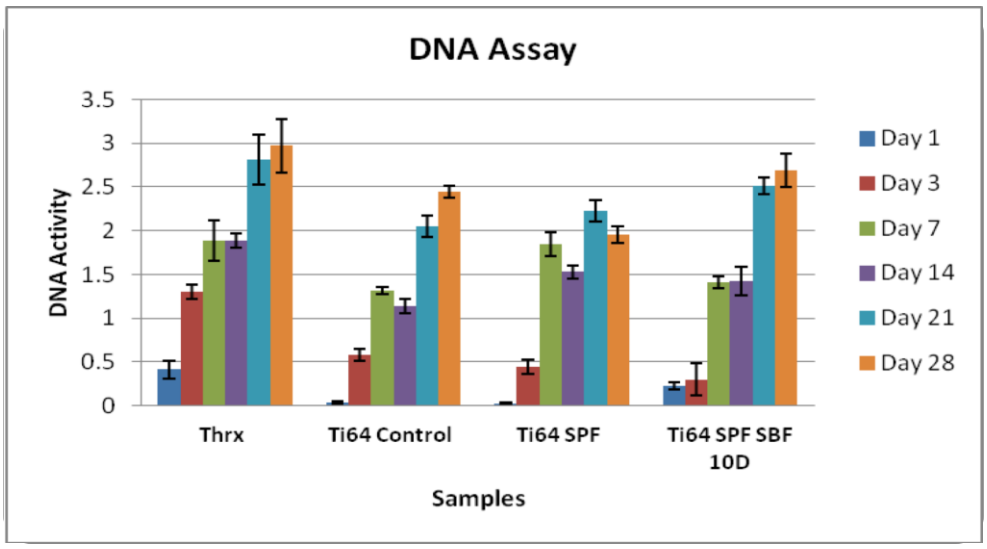

Figure 2.16: Evaluation of Proliferation of Osteoblast Cells / DNA Assay of Ti64 titanium discs which were treated simulating superplastic forming process SPF and then subjected to immersion in SBF solution. The data represents the average for each group as mean absorbance ± SD (n=8); the statistical significance was predetermined at p< 0.05

The DNA activity assay of the Ti64 samples showed general increase of cell proliferation through the 28 days of the DNA assay. All the different surface treatments showed higher cellular response compared to the sample surface with no treatment (Ti64 Control) as expected. The heat-treated SPF process showed similar results to the heat-treated samples, which were immersed in SBF solution for 10 days. However, there was no significant difference between the different treated samples and the positive control (Thrx).

2.4. Discussion

Traditionally titanium is coated with hydroxyapatite to enhance the bioactivity of the surface. There are many methods employed for the deposition of thin film coatings of hydroxyapatite, such as plasma spraying [170] HA coatings [171], sputtering [172], dip coating [173, 174], electrophoretic deposition [175] and electrochemical deposition [176]. As most coating techniques employ high temperatures due to post sintering requirements, it can lead to deterioration of the metallic substrate [177] and inclusion of drugs or biological molecules are not possible.

With the fast revolution of dental and maxillofacial implants, the need for customized prostheses has been growing due to the demand and requirement for a unique prosthesis to the individual resulting in better fit and overall treatment. One of the most recent and interesting method to achieve customisation of dental and maxillofacial prostheses, is the use of superplastic forming process (SPF) utilising computer technology for design and fit [178]. In the current study, we investigated the formation of the interaction layer following contact with a phosphate bonded investment material during SPF processing where the titanium sheet is pressed at high temperature on investment die under gas pressure. The SPF process was simulated due to the large number of samples required for the study to avoid punching specimens post superplastic forming of larger sheets in order not to alter the invested surface.

The CpTi and Ti64 discs invested in the phosphate bonded investment material showed evidence of the interaction layer, which was similar to that first noted by Curtis et al. [36]. The formation of the phases rutile, anatase and brookite was also in agreement as previously reported by Curtis et al. [36] A titania (TiO_2) film of 7 – 8 nm forms a passive and corrosion resistant film on the alloy surface that gives the material excellent implant characteristics and chemical stability, post-implantation. It is well known that titania exists in four different allotropic forms, amorphous titania, brookite, anatase and rutile. It has been suggested that rutile is mainly desirable for blood compatibility, whereas anatase has more efficient photocatalytic properties and can be used for biomimetic formation of bonelike apatite [179, 180]. Despite this, anodic oxidation of titanium surfaces has clearly indicated that apatite deposition occurs on both rutile and anatase surfaces [181]. The discs post investment with the interaction layer were further subjected to immersion in simulated body fluid to assess if the interaction layer had the ability to act as a

surface that would be conducive to the formation of an apatite like layer on the surfaces in vitro (SBF), thus improving its bone bonding ability in vivo. The results of this study, indicated that no apatite was formed on both CpTi and Ti64 that were non-invested (control) surfaces, whilst, an apatite like deposit was observed on titanium surfaces that were embedded in the dental investment material followed by heat treatment, and then immersed in simulated body fluid SBF for 10 days (CpTi SPF SBF and Ti64 SPF SBF) (Fig 2.2, Fig 2.3). This indicated that CpTi and Ti64 surfaces in contact with investment material simulating superplastic forming process SPF have the ability to form an apatite like layer in SBF. The possible explanation of this observation is due to the presence of contamination layer on the surface of the heat-treated surfaces due to the interaction between the phosphate-bonded investment and the titanium at high temperatures. Typically, the SPF forming takes between 15 minutes and 3 hours at temperatures ranging from 700 – 950˚C, during which time chemical reactions may occur. At high temperatures such as these, the oxide becomes soluble in the metal, and the protection is decreased, so reaction with the substrate is expected to occur [36]. The reaction between the molten metal and some of the elements of the phosphate-bonded and other silica-based investment materials (oxygen, phosphorus, and silicon) result in the formation of a surface contamination layer referred to as the ‘‘α-case,’’ consisting of compounds of titanium, primarily with silicon (Si), phosphorus (P), and oxygen (O) [53]. These elements can induce the formation of CaP nuclei when the surface is immersed in SBF solution due to the deposition of soluble ions of Ca and P of the SBF onto the invested surface. The formation of an apatite layer on titanium and its alloys subjected to heat treatment has been reported in the literature [88, 168, 182]. The Ca/P ratio of the formed apatite gradually increased to 1.65 (similar to bone apatite) with time after immersion in SBF. This apatite layer on the titanium surface when implanted into the animal body has been shown to tightly bind to the surrounding bone [167, 181, 183]. In the current study, the Ca/P atomic ratio obtained was much lower compared to the Ca/P ratio of bone mineral or that of stoichiometric hydroxyapatite [$Ca_{10}(PO_4)_6(OH)_2$], i.e. 1.13 and 1.14 for CpTi SPF SBF and Ti64 SPF SBF respectively. These very low Ca/P ratio precipitates could be possibly in the range of those amorphous calcium phosphates. In more acidic solutions ACPs can contain HPO_4^{-2} ions instead of PO_4^{-3}, leading to a lower Ca/P ratio, such phases are unstable and convert very rapidly into dicalcium phosphate dihydrate (DCPD) (CaH-$PO_4 2H_2O$) [184]. According to this, in the current study the titanium surfaces were invested in phosphate bonded investment (Deguvest), which contains the HPO_4^{-2} ions as it shown in its chemical composition $MgNH_4PO_4 \cdot 6H_2O$ that may

lead to decrease the Ca/P ratio on these surfaces. Takadama et al. [180] showed that Ca/P ratio of 1.4 is in the range of amorphous calcium phosphates which will eventually stabilizes into crystalline apatite, may contains a small quantity of Mg and has a Ca/P atomic ratio of 1.65, similar to bone apatite. According to Kokubo et al. [185], since the amorphous calcium phosphate is metastable, it will eventually transform into a stable crystalline apatite phase. This explanation was supported as well by Yang et al. [186] and Wang et al. [183]. They demonstrated that prolonged immersion of treated titanium in SBF for up to four weeks would subsequently convert amorphous to crystalline bone-like apatite. Therefore, understanding the surfaces, the factors and the mechanisms whereby bioactivity can be enhanced will assist in the development of bioactive titanium for clinical applications. Considering the observations and findings from these previous studies, we believe that titanium and its alloys in contact with investment materials as such of high temperature (e.g. as in SPF) are potentially bioactive, as shown by their ability to form apatite-like deposits on their surfaces. Therefore, this formation of apatite-like deposition on titanium surfaces in SBF in vitro could be one measure of its surface bioactivity in vivo. Thus, titanium processed by SPF where the material is in contact with the investment material could yield a bioactive surface at low cost and time saving process in one step without subsequent steps required to modify the surface. In addition as the entire prosthesis formed under the SPF conditions the interaction layer is not limited to certain regions as is one of the limitations of spray coating processes.

Raman spectroscopy is mainly based on in-elastic scattering of the light, which is used to detect stoke and anti-stoke scattering in which the photon's energy is reflected upon collision with a molecule of the illuminated materials. In the current study, Raman spectroscopy was used to analyse the surface reaction layer on the titanium discs, and the surface oxide layer formed. Raman spectra of CpTi and Ti64 surface invested in Deguvest (phosphate bonded investment), consisted of two strong bands at 145 and 148 cm^{-1} respectively which correspond to anatase phase and medium bands at 223 and 222 cm^{-1}, 447 and 449 cm^{-1}, 608 and 602 cm^{-1} respectively which correspond to rutile phase. However, the strong peak arising from rutile due to similar Raman absorption bands may mask the phosphate group stretching. Weak bands between 329 and 404 cm^{-1} were observed on CpTi and Ti64 invested surfaces, which correspond to brookite phase. There was no distinguishing band of the apatite-like layer between 957 and 962 cm^{-1} compared to

the Raman peak of the hydroxyapatite in bone tissue in the SBF treated groups which may be attributed to the low concentration of Ca and P of the apatite like which might be formed on the SPF surfaces after immersion in SBF solution. However very weak bands were observed in the range between 801 and 975 cm^{-1} on titanium samples, which were immersed in SBF for 10 days compared to the only invested ones (SPF), which may be due to an amorphous deposition of an apatite layer. These observations can be explained, that the Raman spectrum of other elements presented on the surface of invested titanium were more prominent than the other peaks, as these surfaces subjected to heat treatment at high temperature, then the presence of these oxide phases can be stronger than other deposits on the surface. In support of these findings, Curtis et al. and Omar et al. [166], showed in a similar study of SP700 and Ti6Al4V alloys invested in Wirovest and Deguvest investments simulating superplastic forming process, that the samples which were invested in Deguvest investments didn't show a strong Rutile phase compared to those invested in Wirovest. And explained this in accordance to Scrimgeour et al. [47] who have fully characterized the phases in specific investment materials using 31P solid-state MAS-NMR spectroscopy for phosphate bonded investments. So, based on the observations and the findings of Scrimgeour, it is possible that since pyrophosphates is the dominant phase in Wirovest investment; these compounds may be responsible for the increased apatite density compared to Deguvest investment.

The surface roughness measurement for all the treated surfaces obtained under profilometer showed different surface roughness values between the groups. The CpTi control surface showed a surface roughness of 0.414 µm, which is higher, compared to the Ti64 control surface roughness of 0.217 µm under same surface roughness protocol, which was performed on these surface prior to simulating the SPF process. This could be due to that the alpha-case on the ductile cpTi can be ground much easier than its bulk interior structure, whereas the less ductile Ti-6Al-4V, the grinding rate is much higher than that of cpTi, and the alpha-case and its interior structure are at similar levels since the fracture toughness of its alpha-case and the bulk material is not large enough. The CpTi when subjected to investment with Deguvest using a simulated superplastic forming method with a roughness value of 0.160 µm yielded a fairly smooth surface in comparison to the alloy Ti64 with a roughness value of 0.420 µm. This can be explained by the fact that the starting surface of CpTi contained more troughs and crests and the interaction layer covered the defects. The invested Ti64 titanium discs showed a higher surface

roughness compared to the CpTi invested ones, as well as compared to the control, which is possibly due to the investment interacting on a smoother surface yielding deposits from the interaction layer that were causing a more non-uniform surface. The immersion of invested titanium discs in SBF solution for 10 days showed an increase of surface roughness of the CpTi samples with a value of 0.389 µm compared to the surface roughness of Ti64 samples with a value of 0.431 µm, which can be explained due to the deposition of apatite like layer on the invested interaction layer which may cause some roughness on these surfaces.

The roughness parameter obtained under AFM for the different treated titanium surfaces In this study the surface roughness obtained with homogenous surfaces with an average Ra values close to 0.5 µm. Different values have been observed between the samples due to the different treatments that the surfaces were subjected to. The CpTi control surface had the highest Ra of 0.213 µm followed by the invested CpTi simulating superplastic forming process (SPF) which was immersed in SBF solution of Ra value of 0.179 µm compared to the other samples. When CpTi was invested simulating superplastic forming process only (SPF) it showed that the surface had less roughness compared to the control one with Ra value of 0.164 µm, this might be due to the layer which were deposited on the surface due the interaction between the titanium surface and the investment mold at high temperatures. While the opposite trend can be observed with Ti64 samples as the investing of TI64 surfaces simulating superplastic forming process (SPF) appeared to increase the surface roughness of Ra value of 0.152 µm compared to the control surface roughness of Ra value of 0.08 µm. this is could be due to the relatively smooth surface of TI64 control prior investing this surface where the deposited interaction layer can cause a rougher surface With roughness parameter kept constant, the Ra values obtained from AFM measurements showed a varied range which may be attributed to scanning of small sections i.e. 20 µm x 20 µm of the entire surface in comparison to surface profilometry, where the line measurement was about 4 mm. Therefore, it is probable that the area measured with AFM contains within the valley, bump, or fell on the flat surface. A study by Bathomarco et al. [187] has shown that roughness is a scale dependent parameter, where they showed that the roughness value in all their titanium samples presents a similar trend, i.e. the roughness of all samples is seen to increase for scan length in the range from 10 µm to approximately 50 µm. they concluded that only when the

scan size/length exceeded 50 µm, the surface roughness becomes constant and is independent on the scanning length.

Biological evaluation at a cellular level was also conducted as an initial screening test on these invested titanium surfaces. In vitro cell study allows evaluation of the biocompatibility of a material in relation to its final use in vivo. As previously mentioned, the human alveolar osteoblast cells were used in this study, as they are most appropriate for biomaterial-cell interactions or bone metabolism for dental bone tissue engineering. Furthermore, primary osteoblast-like cells are representative of the cell type in contact with the material in vivo. The success of a material to be used in the body relies on the efficiency and the stability of its interaction with the bone cells or osteoblasts. The behaviour of alveolar HOB cells on these different titanium surfaces were examined by MTT an indirect cytotoxicity assay, which showed a reduction in cell metabolic activity (Figure 2.7, 2.8, 2.9 and 2.10) after incubation for 72 hours eluants, which was probably due to some toxic leachables or contaminant released from the test materials. Any toxic leachables are likely to be either the grinding media during the cleaning process, or the investment material debris from the die or the mould. However, this surface wash off released from the test materials in the 24 and 72 hours eluants did not have a detrimental effect on the aHOB cells, as the cells continued to behave normally in the subsequent time points of the MTT tests. According to literature [188-191], it has been shown that investment materials may evoke a detrimental effect due to the increase in the brittleness and hardness on titanium surfaces and subsequent formation of a so-called a 'contamination' layer. However this study showed that superplastic forming with a phosphate bonded investment did not evoke a detrimental response, which is contrary to other reported findings.

Live/dead fluorescent staining highlighted further evidence of cytocompatibility of the different materials. From the live/dead staining results as shown in Figures 2.11 and 2.12, the notable abundance of green fluorescent cells (live cells) than the red ones (dead cells) confirmed that the both the untreated and treated CpTi and Ti64 were cytocompatible. The results showed that aHOB cells cultured on Deguvest invested samples and immersed in SBF solution for 72 hours, were able to adhere with a large number of viable cells. As previously discussed, these surfaces showed the presence of different phases of titanium, namely, anatase and rutile, in addition to the apatite-like deposit, which formed as a result of the interaction with the SBF solution. This is in agreement with the results reported by Sul et al [192],which showed that the titanium implant with a mixture of rutile and anatase TiO_2, showed

better bone response that anatase structure. However, as the live-dead staining is a qualitative method it was not possible to distinguish between the different surface treatment groups in this study.

The expression of alkaline phosphatase ALP was used as a phenotypic biochemical marker of differentiation on the titanium surfaces. ALP is well known as an early marker of maturation, osteogenesis and differentiation of osteoblast cells [193]. As a rule, the number of cells should achieve a threshold of confluency before maturation and differentiation of the cell to take place. aHOB cell differentiation was observed on all different treated titanium surfaces, as indicated by ALP production. The expression of ALP over the observation period of 28 days indicated that the osteoblasts on the control surface and the invested surfaces reached their peak on day 28, except for the CpTi and Ti64 invested surfaces, which were immersed in SBF reached their peaks on day 7 and day 21 respectively. This can be explained due to the presence of apatite-like layer on the surface of these samples, which were induced by the SBF solution, and this layer then induces the osteoblast differentiation earlier than cells cultured on the other surfaces. As is known that extracellular matrix undergoes a series of modifications in composition and organization, coupling with down regulation of proliferation, which leads to a progression of cells into a more mature osteoblast and makes it capable for mineralisation. These findings are in accordance with a very recent study by Lee et al [194], who showed that heat treated titanium alloy surfaces exhibited a higher ALP activity than non-heated surfaces.

The cellular proliferation behaviour of aHOB cells was evaluated by direct contact assay of DNA synthesis test. The results of the DNA production for the current study demonstrated that aHOB cells on the invested titanium samples increased throughout the entire period of investigation and was comparable with that of negative control (Thx). The SPF SBF invested samples exhibited higher DNA production in the case of Ti alloy, which may be due to the surface chemistry of the titanium in contact with investment materials that influenced the aHOB cell adhesion and proliferation. The presence of elements such as phosphorus (P) and magnesium (Mg) on invested titanium surfaces may have contributed to the aHOB cell proliferation behaviour on these surfaces. This is particularly true due to fact that Mg is an important element for human body function. Studies have shown that the Mg is one of many important elements required for the cell adhesion and proliferation [195].

In general, this study showed that simulating superplastic forming process could create a favourable interaction layer on the titanium surfaces, which induces the formation of apatite like layer on the surfaces when soaked in SBF solution. This can be considered to be a quick and inexpensive method of surface modification of titanium implants, during processing itself, which can enhance the bone healing thus resulting in improved osseointegration.

CHAPTER THREE

Surface Modification of Titanium with Sodium Hydroxide and its Effect on In vitro Cytocompatibility

3.1. Introduction

Titanium and its alloys are widely used for dental and orthopaedic implants under load-bearing conditions, which are known to show a mechanically stable interface with bone that is attributed to the thin film (2–7 nm) of amorphous native oxide (TiO_2) formed on the surface. In addition to being stable in the physiological environment, titanium oxides increase calcium ion interactions, which are important for protein and subsequent osteoblast adhesion [169, 188, 196]. However, Ti and its alloys are considered as foreign substances; therefore, osteogenesis is generally inactive on Ti surfaces. Thus, to overcome this problem a great deal of effort has been made to render titanium bioactive[169, 188, 196, 197].

Coating titanium with hydroxyapatite has been one of the most widely investigated approach, which is a calcium phosphate considered to play an important role in the formation and properties of bone. Because of this, HA is proposed as a suitable coating material to provide stronger early fixation of dental prostheses. Enhanced bone bonding can be achieved with bioactive materials, which form a stable connection with bone through a natural formation of hydroxyapatite (HA) on their surface, which then acts as a bonding layer and integration occurs at an atomic or molecular scale. Although hydroxyapatite coatings on implants have a reliable long-term survival, there are concerns about their reliability under loads, which can be overcome by reinforcing the HA layer mechanically with metal oxides such as zirconia and alumina [185, 197]. Surface modification is known to effectively activate osteogenesis on Ti and various methods have been employed (Chapter1). Hydroxyapatite coatings can be produced by different methods, such as plasma spraying and physical vapour deposition (PVD) techniques, however the main drawback of these methods is the difficulty in coating of complex implant geometries.

Biomimetic methods to fabricate apatite coatings on implants overcomes these drawbacks and typically, substrates with active surfaces are immersed in a simulated body fluid at physiological pH and temperature (approximately 37°C), to obtain an apatite layer that forms, crystallize and grow on these surfaces. This method allows deposition of CaP coatings on many different objects, such as sponges, cements, metal surfaces or fixation rods and also gives a possibility of co-precipitating ions, drugs, macromolecules and biological molecules together with the inorganic layer. Furthermore by varying immersion conditions, coatings with a wide range of thicknesses and composition can be obtained [77, 189, 190]. Chosa et al.

[198] reported that titanium and its alloys do not encourage calcium phosphates precipitation after soaking in simulated body fluid (SBF). However a simple emerging method of rendering the surface of titanium bioactive is the alkali-heat treatment, first described by Kokubo et al to yield a bioactive surface [199, 200]. The soaking of titanium and its alloys in aqueous solution of 5M sodium hydroxide at 60^0C for 24 hours and subsequent heat treatment usually at temperatures over 600^0C was reported to form a surface that induced nucleation of bone like apatite when placed in simulated body fluid. The mechanism of the formation of apatite on bioactive titanium is of interest and is thought that the alkali treatment of titanium prior to treatment with SBF encourage the formation of an apatite layer possibly due to the formation of a sodium titanate layer on the metal surface by the sodium hydroxide and heat treatment, which releases its Na^+ ions into the surrounding fluid via an ion exchange with H_3O^+ in the fluid to form Ti-OH groups (approximately half an hour after the immersion). The Ti-OH groups then immediately interact with the calcium ions from the fluid and calcium titanate is formed [77]. The calcium titanate incorporates the calcium ions, as well as, phosphate ions, therefore, forming the apatite nuclei. Once formed, the apatite nuclei grow by consuming the calcium and phosphate ions from the SBF solution [77, 169]. However, a review of the literature indicates conflicting data on the mandatory requirement of the heat treatment post sodium hydroxide treatment, although most studies apply heat treatment of the Ti and its alloys, it is reasonable to assume that degradation of the mechanical properties of the bulk substrate may occur at the temperatures used.

This chapter is aimed at investigating the surface characteristics of the biomimetic apatite like-bone that may be formed on the surface of commercially pure titanium (CpTi) and Ti6Al4V titanium alloy (Ti64) after immersion in simulated body fluid. The groups selected for the study involved the prolonged treatment of native CpTi and and Ti6Al4V titanium alloy (Ti64) in simulated body fluid (SBF) as well as the effect of sodium hydroxide pre-treatment without heat treatment followed by deposition of apatite for the purpose of investigating the potential of modified substrates for the in vitro response of osteoblast cells (aHOB cells) and thus the osseointegration and bone healing process. Heat treatment was not used as a comparative group as the main aim was to establish if an apatite layer would form on the bioactive surface of titanium. No bulk mechanical properties were determined in this study as it was out of the scope of the current study.

3.2. Materials and Methodology

3.2.1. Specimen preparation

150 mmX150 mm and 0.5 mm thickness commercially pure titanium stock sheet (CpTi), and 140 mm diameter and 0.5 mm thickness titanium alloy Ti6Al4V stock sheets were used and prepared for treatment as previously described in chapter two.

3.2.2. Surface Treatments of the Titanium Discs

3.2.2.1. Alkali Treatment

Alkali treatment was performed on sanded and cleaned CpTi and Ti64 10 mm diameter titanium discs, which were grouped and soaked in 6 ml of 5M solution of sodium hydroxide (NaOH) at 60°C for 24 hours. The discs were placed in vials using a bent stainless steel wire, which was fitted to the edge of each titanium disc in order to expose both surfaces with NaOH (Figure 3.1). After 24 hours the discs were removed and rinsed gently with distilled water and allowed to dry at room temperature.

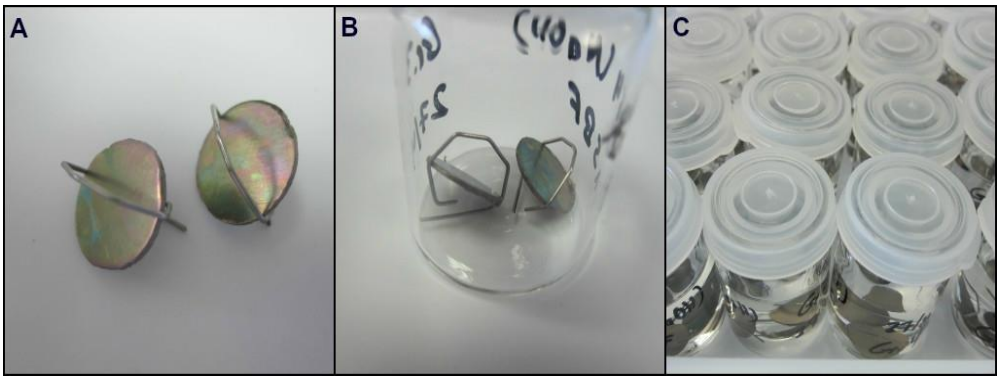

Figure 3.1: A) Ti discs fitted within the bent wire B) Ti discs placed in vials to be soaked in sodium hydroxide C) Ti discs suspended in sodium hydroxide to ensure all surfaces were exposed to the sodium hydroxide solution over the 24 h period.

3.2.2.2. Simulated Body Fluid (SBF) Immersion

The SBF solution was prepared based on Kokubo recipe (1990) as described in chapter two. Both non treated and alkali treated titanium disc groups, were immersed in 10 ml of SBF solution at 37°C for 7 and 10 days respectively. Then they were rinsed gently with distilled water and then left to dry in a desiccator.

3.2.3. Surface Characterization

3.2.3.1. Surface Roughness Measurement

The surface roughness analysis of the titanium sample discs in microns (μm) before and after surface treatment was assessed and quantified with a contact profilometer surface analysis instrument. The mean roughness was measured and recorded at a traverse speed with a diamond probe tip stylus of 5μm. For each of the 10 mm titanium sample discs, the roughness parameters were measured at four different locations and a total of four discs from each group of the titanium samples, were analysed to obtain an average value.

3.2.3.2. Atomic Force Microscopy (AFM)

A commercial AFM was used to perform three-dimensional and morphological topography analysis of the treated titanium surfaces, as previously described in chapter two. Four areas were scanned for each sample.

3.2.3.3. Scanning Electron Microscopy/Energy Dispersive X-ray Analysis (SEM/EDS)

The surface of the treated titanium discs were studied using scanning electron microscopy (SEM) (Hitachi S3500N) accompanied with an energy dispersive X-ray spectroscopy machine (EDS), obtaining high-resolution imaging with nanometre resolution of surface structure as described in chapter two.

3.2.3.4. Raman Spectroscopy

Raman spectroscopy was used to analyse the nature of surface layer on the titanium discs and chemical composition. In this study, the Raman spectroscopy measurement was performed on the titanium surfaces using the Renishaw inVia Raman microscope system (Renishaw plc, Wotton-under-Edge, UK). Details are provided in chapter 2.

3.2.4. In vitro Biological Evaluation

Human primary alveolar osteoblast cells (aHOB) were used for the biological evaluation; these were isolated from alveolar bone obtained from dental patients and were prepared following a protocol previously described by Di-Silvio et al [169]. The protocol of culturing, incubating, splitting and counting cells is described in detail chapter two. Once the cells were counted and the density of cells was

determined, a 50 µl of cell suspension was ready to be seeded onto each disk sample surface for the following biological assays; assessment of cell viability – MTT assay, assessment of cell viability – live and dead staining assay, assessment of cell differentiation – alkaline phosphatase assay (ALP), and assessment of cell viability – DNA activity assay. The methodology of each assay is described in chapter two.

3.3. Results

The surface treatments carried out on the CpTi and Ti64 discs are shown in Table 3.1.

Name of Group	Name of Sample	Surface Treatment
1. Control	Non Treated	No surface treatment
2. Alkali treatment (NaOH)	NaOH SBF 7D	Treated with 5M NaOH for 24h and immersed in SBF solution for 7 days
	NaOH SBF 10D	Treated with 5M NaOH for 24h and immersed in SBF solution for 10 days
3. Cleaned non-treated	SBF 7D	Cleaned non treated immersed in SBF for 7 days
	SBF 10D	Cleaned non treated immersed in SBF for 10 days

Table 3.1: The experimental and sub groups of the different treated surfaces which were immersed in SBF solution. For each group both CpTi and Ti64 specimens were used.

3.3.1. Surface Roughness Measurement

Surface roughness measurements were obtained for the different titanium sample discs and calculated as mean value, which are presented in the Table 3.2.

CpTi Group	Average *Ra* ± SD (µm)	Ti64 Group	Average *Ra* ± SD (µm)
CpTi Control	0.404 ± 0.176	Ti64 Control	0.217 ± 0.074
CpTi NaOH SBF 7D	0.253 ± 0.069	Ti64 NaOH SBF 7D	0.283 ± 0.089
CpTi NaOH SBF 10D	0.296 ± 0.065	Ti64 NaOH SBF 10D	0.312 ± 0.091
CpTi SBF 7D	0.383 ± 0.085	Ti64 SBF 7D	0.201 ± 0.063
CpTi SBF 10D	0.376 ± 0.052	Ti64 SBF 10D	0.241 ± 0.096

Table 3.2: Surface roughness measurements (Ra ± SD) for the different treated CpTi and Ti64 samples (n=4).

The average roughness of the CpTi discs after the various treatments indicated that immersion in SBF solution post alkali treatment decreased the Ra value from 0.404 µm to 0.253 µm and 0.296 µm for 7 days and 10 days respectively. However, non-alkali treated surfaces exhibited Ra values almost similar to that of control specimens after immersion in SBF. The Ti64 alloy samples, showed varied results of Ra values, but in general the alkali treated surfaces showed an increase in the surface roughness parameter after immersion in SBF solution of Ra value of 0.283 µm and 0.312 µm after 7 and 10 days respectively, whilst the Ra values were almost unchanged when non-alkali treated surfaces were immersed in SBF.

3.3.2. Atomic Force Microscopy (AFM)

The roughness parameters obtained under AFM for the different treated titanium discs in this study are summarized in Table 3.3, where four different scans were measured for each sample and the average was calculated.

CpTi Group	**AFM (Average Ra ± SD µm)**	**Ti64 Group**	**AFM (Average Ra ± SD µm)**
CpTi Control	0.213 ± 0.019	Ti64 Control	0.080 ± 0.013
CpTi NaOH SBF 7D	0.138 ± 0.023	Ti64 NaOH SBF 7D	0.100 ± 0.016
CpTi NaOH SBF 10D	0.156 ± 0.014	Ti64 NaOH SBF 10D	0.140 ± 0.023
CpTi SBF 7D	0.221 ± 0.017	Ti64 SBF 7D	0.073 ± 0.012
CpTi SBF 10D	0.204 ± 0.032	Ti64 SBF 10D	0.092 ± 0.016

Table 3.3: Surface roughness Ra for the different surface treated titanium disc groups obtained with AFM, n=4 (± SD).

The average roughness values of CpTi and Ti64 samples with and without sodium hydroxide treatment followed by SBF immersion shown in Table 3.3 indicates variable data however the data needs to be dealt with caution as only selected areas are used for AFM scanning. Figures 3.2 and 3.3 show the qualitative characterization in two-dimensional and three-dimensional images of the corresponding surface topography of the different treated titanium samples observed under AFM. For the CpTi groups, the control had the highest Ra of 0.213 µm followed by the non-alkali treated surfaces which were immersed in SBF solution for 7 and 10 days of Ra average value of 0.221 µm and 0.204 µm

respectively. Immersion of alkali treated surfaces in SBF solution seemed to decrease the surface roughness values of 0.138 µm and 0.156 µm for 7 and 10 days immersed surfaces respectively. For the Ti64 group, it was realized that the alkali treated surfaces, which were immersed in SBF solution for 7 and 10 days showed a rougher surfaces of Ra value of 0.100 µm and 0.140 µm respectively, compared to the other samples.

Sample name	2D AFM Image	3D AFM Image
CpTi Control	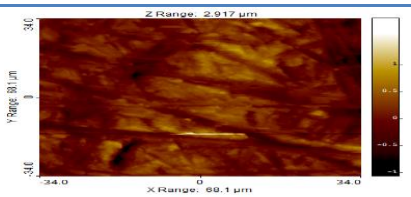	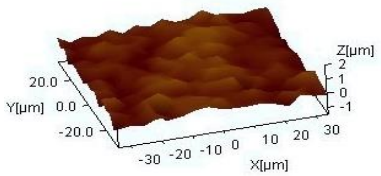
CpTi SBF 7D	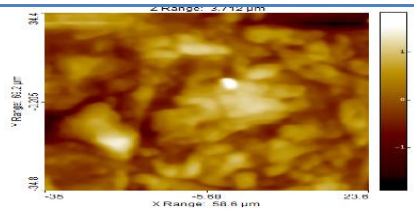	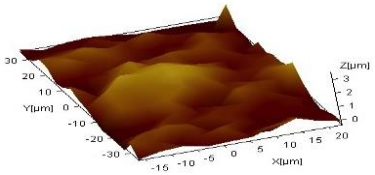
CpTi SBF 10D	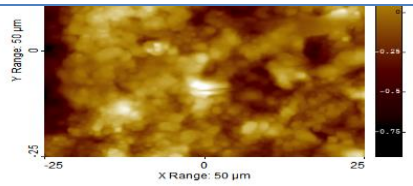	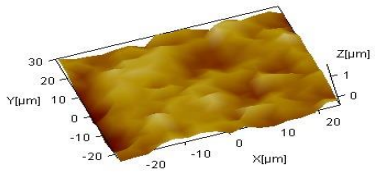
CpTi NaOH SBF 7D	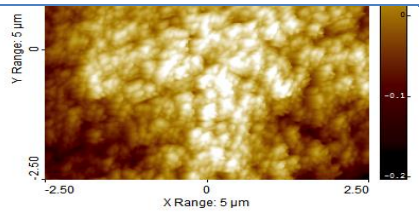	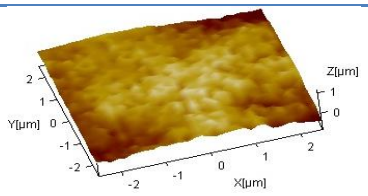
CpTi NaOH SBF 10D	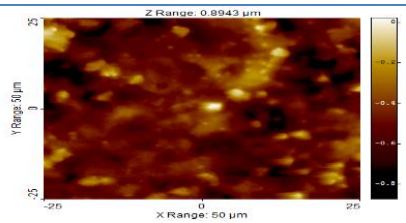	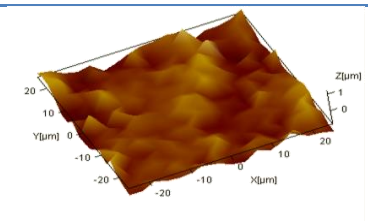

Figure 3.2: Representative 2D and 3D of AFM images of the different CpTi surface treated groups; alkali treated surfaces (NaOH), which were immersed in SBF solution showed higher surface roughness compared to the non-treated surfaces, which were immersed in SBF as well

Sample name	2D AFM Image	3D AFM Image
Ti64 Control	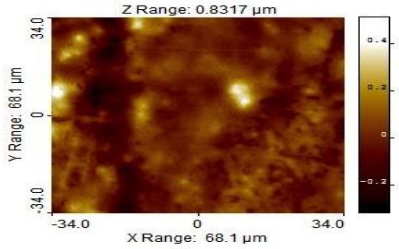	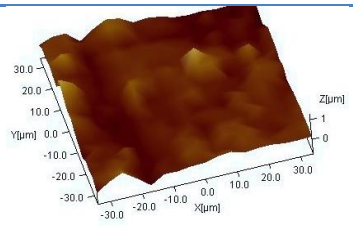
Ti64 SBF 7D	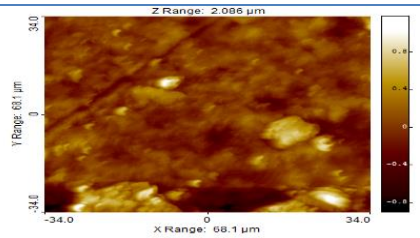	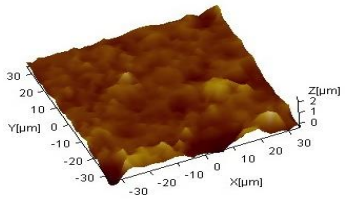
Ti64 SBF 10D	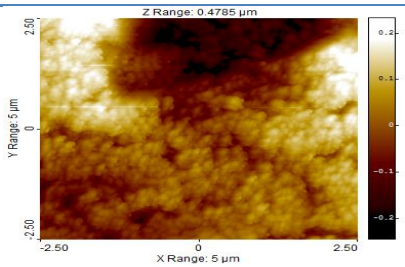	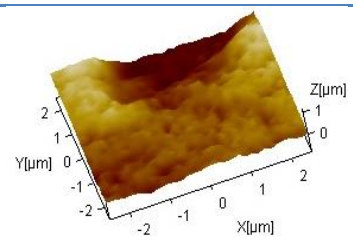
Ti64 NaOH SBF 7D	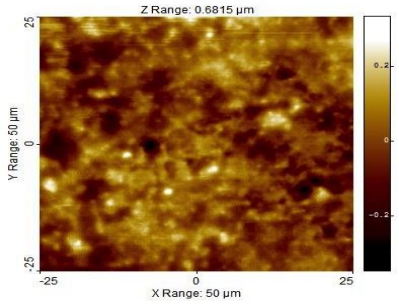	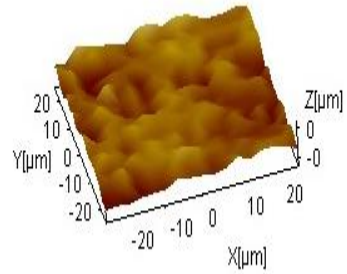
Ti64 NaOH SBF 10D	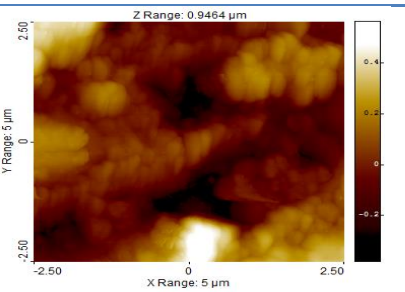	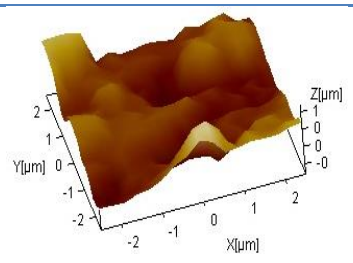

Figure 3.3: Representative 2D and 3D of AFM images of the different Ti64 surface treated groups; alkali treated surfaces (NaOH), which were immersed in SBF solution showed higher surface roughness compared to the non-treated surfaces, which were immersed in SBF as well.

3.3.3. SEM/EDS observation

Qualitative surface characterization of the surface topography of the experimental discs of Ti is illustrated using electron microscopy (SEM). The SEM images of the surface morphologies of the CpTi and Ti64 control, NaOH treated with SBF immersion for 10 days and non-treated CpTi and Ti64 immersed in SBF for 10 days, are shown in Figure 3.4. The titanium control samples were relatively smooth with some imperfections and scratches observed due to the sandblasting and polishing processes. It was noted on the alkali treated CpTi and Ti64 specimens that were immersed in SBF for 10 days, showed the formation of a layer, which had the appearance of a mineral deposit, in comparison to the specimens exposed to SBF immersion without an alkali treatment. The interaction of sodium hydroxide with Ti surfaces is believed to result in the formation of sodium a titanate layer rendering the surface active. This surface can induce the formation of apatite-like layer compared to the non-alkali treated, in which case only trace amount of mineral like deposits are apparent. The EDS analysis of the same samples showed the presence of traces of Ca and P ions on the surface especially on the sodium hydroxide treated titanium specimens, which were immersed in SBF solution indicating the apatite-like layer. Table 3.6 shows the Ca/P ratio of alkali treated surfaces, which were immersed in SBF solution, as non-treated surfaces, which were immersed in SBF showed no traces of apatite, like deposition as expected. However, these ratios are very low compared to the bone mineral Ca/P ratio of 1.67.

Sample Name	Ca	P	Ca/P (Atomic %) Ratio
CpTi NaOH SBF 10D	7.19	9.04	1.26
Ti64 NaOH SBF 10D	5.38	7.23	1.34

Table 3.4: Concentrations of Ca and P (Atomic %) of CpTi and Ti64 samples treated with NaOH and immersed in SBF.

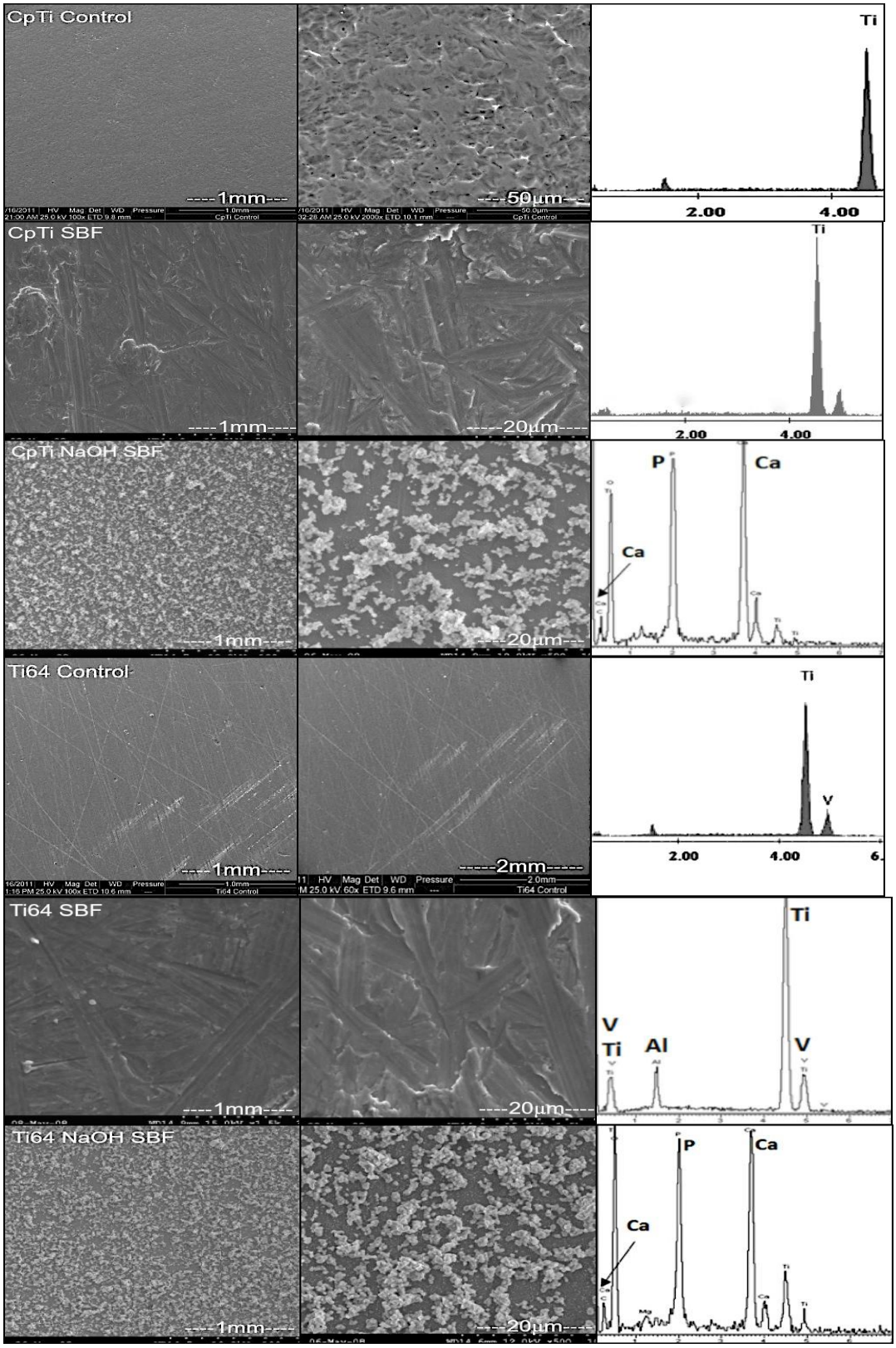

Figure 3.4: Qualitative SEM images and EDAX analysis of CpTi and Ti64 different treated samples; showing that treating titanium surfaces with NaOH enhance the deposition of apatite like layer when immersed in SBF (CpTi NaOH SBF and Ti64 NaOH SBF) compared to non-treated surfaces immersed in SBF (CpTi SBF and Ti64 SBF).

3.3.4. Raman Spectroscopy

Raman high resolution scanning spectroscopy of the different titanium sample surfaces were carried out in order to determine the chemical composition of the treated surfaces after alkaline treatment with NaOH, as well as to investigate the presence of the apatite like layer on the surface which may have formed due to the SBF immersion treatment. High resolution Raman scans of the alkali and non-alkali treated CpTi and Ti64 titanium surfaces are shown in Figures 3.5 and 3.6. The Raman spectra showed the presence of different phases of TiO_2 such as rutile, anatase and brookite. It was observed that Raman spectra of all alkali treated CpTi and Ti64 surfaces, showed strong bands at 134 cm^{-1} and 138 cm^{-1} that correspond to the anatase phase. Medium intensity bands were observed at 216 cm^{-1} and 223 cm^{-1} and weak bands around 460 cm^{-1} and 470 cm^{-1}, which correspond to the rutile phase. Raman mapping showed that both alkali treated CpTi and Ti64 surfaces were mainly covered with rutile and anatase phases.

The alkali treatment at 60° C can lead to the formation of sodium titanate which can be distinguished on these surfaces by the corresponding peak approximately between 712 and 773 cm^{-1}, which can be seen in the Raman spectrum of alkali treated surfaces. While, these peaks can't be found in the Raman spectrum of the non-alkali treated surfaces. There was no distinguishing peak of the apatite-like layer between 957 and 962 cm^{-1} compared to the Raman peak of the hydroxyapatite in bone tissue. But there were peaks close to this range between 785 and 868 cm^{-1}, which were more prominent on titanium samples when treated with NaOH and then immersed in SBF for 10 days compared to the other samples. The absence of the peaks can be related to the low intensity of the peaks and the noise in the spectra masked the peaks.

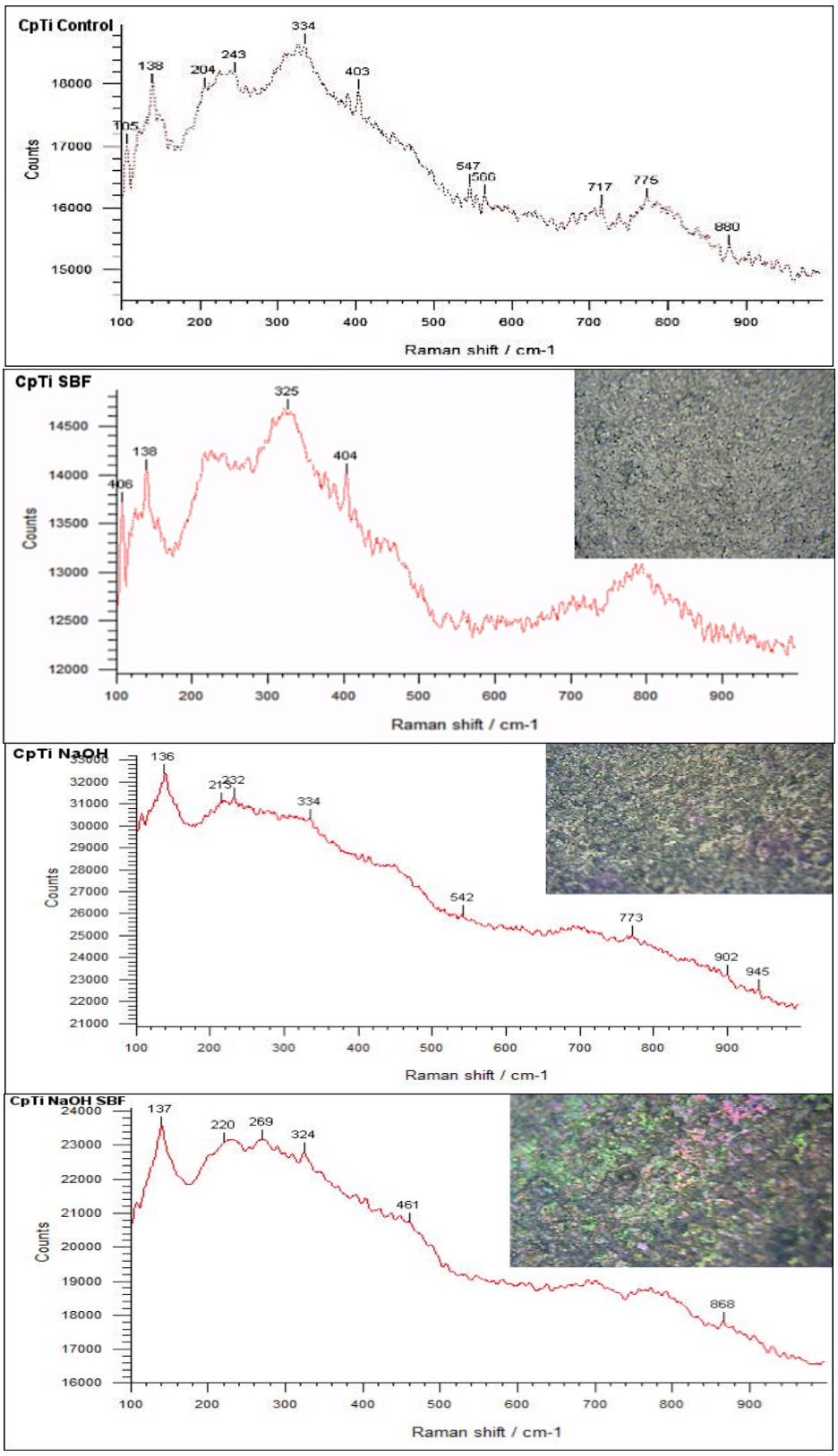

Figure 3.5: Raman spectra of the different treated CpTi samples; control with no treatment, NaOH treated, immersion in SBF only and immersion in SBF after alkali treatment.

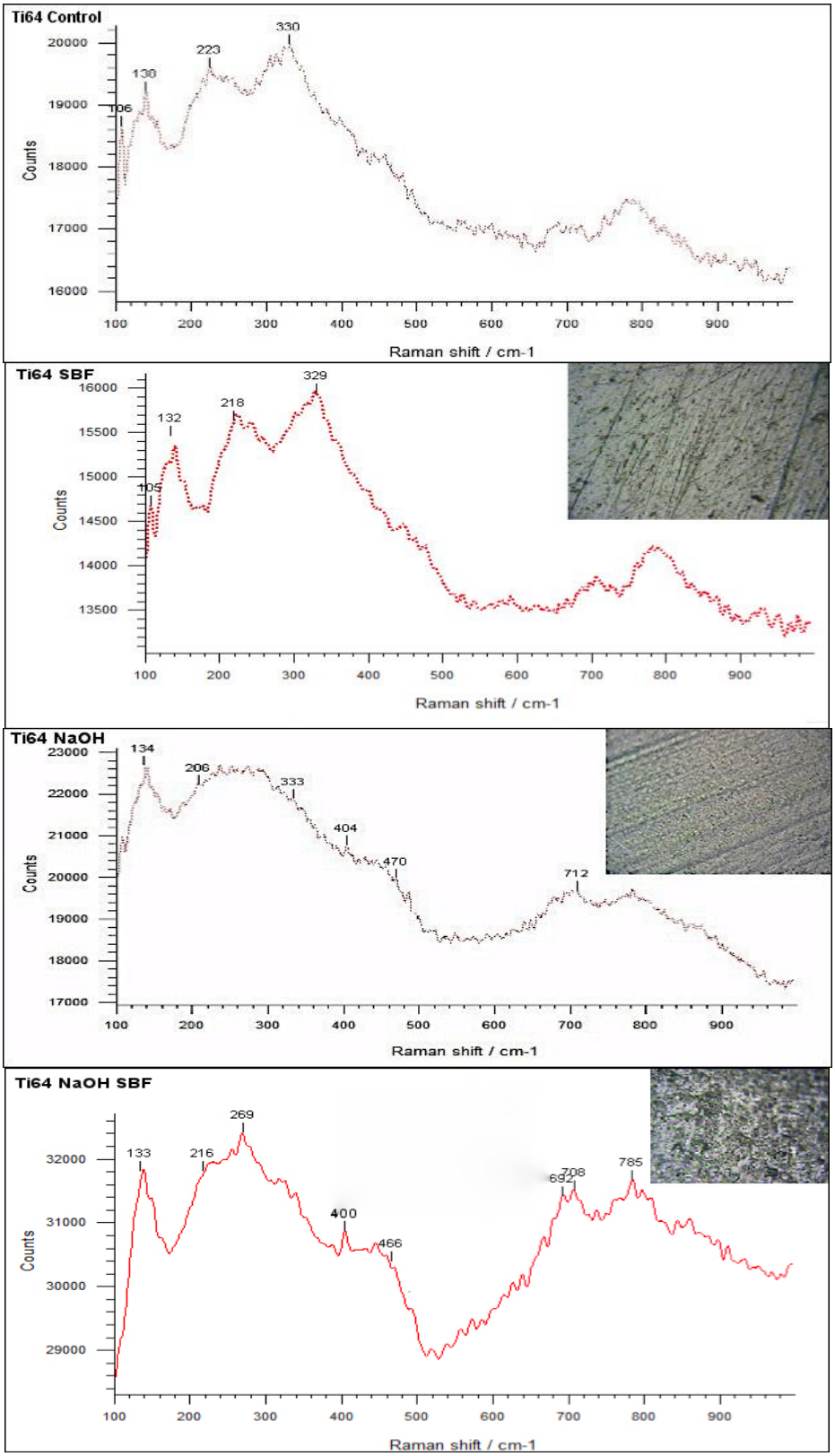

Figure 3.6: Raman spectra of the Ti64 samples; control with no treatment, NaOH treated,Ti64 immersed in SBF only and SBF treatment after alkali treatment.

3.3.5. In vitro Biological Evaluation

3.3.5.1. Evaluation of Cytotoxicity Indirect Method (MTT)

MTT, Day 1 Exposure:

Elutions collected at 24 hours were exposed to aHOB cells for 24 and 72 hours in order to detect if any leaching products could affect cell behaviour. After one day of MTT exposure, various absorbance levels were observed between the different groups. For the CpTi samples, at the 24h elution time point, a comparison of the samples was made to media cell sample (negative control). All samples showed lower cell metabolic activity than the negative control (media + cells). CpTi samples immersed in SBF solution for 7 days showed best cell activity, followed by CpTi samples which have been pre-treated with NaOH and immersed in SBF for 7 Days. At 72h elution time, there was a decrease in the cell metabolic activity obtained by all the samples, particularly, CpTi samples immersed in SBF solution for 10 Days (Figure 3.7). There was no significant difference in osteoblast cells response between the negative control (media + cells) and the different surface treatment surfaces tested

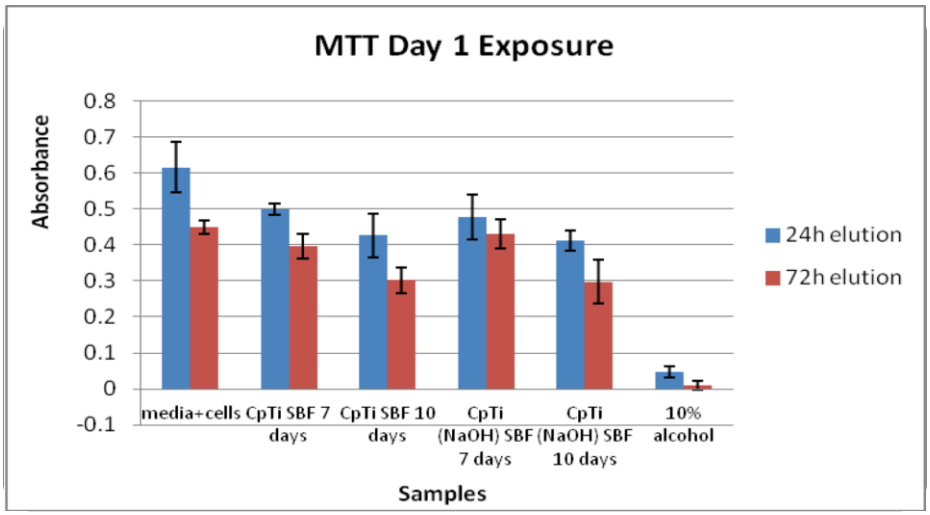

Figure 3.7: Evaluation of Cytotoxicity Indirect Method/ MTT Day 1 Exposure of CpTi test samples; showing levels of intensity of absorbance at 570nm of the Ti64 samples at 24h and 72 elutions, expressed as mean absorbance ± S.D (n=4); the statistical significance was predetermined at p< 0.05. An increase in cell metabolic activity was observed on all test samples and non-toxic control (TCP) compared to the toxic control(10% alcohol).

For the Ti64 samples, at the 24h elution time point, a comparison of the samples was made to media cell sample (negative control). All samples showed lower cell metabolic activity than the negative control (media+cells). Ti64 samples immersed in SBF solution for 7 days and NaOH treated Ti64 samples and immersed in SBF for 7 days showed higher cell metabolic activity than those immersed in SBF for 10 days. At 72h elution time, there was a decrease in the cell metabolic activity obtained by all the samples, this could be that with time these surfaces are leaching some toxic leachables, which may affect the cell activity (Figure 3.8). There was no significant differences in osteoblast cells response between the negative control (media + cells) and the different surface treatment surfaces tested.

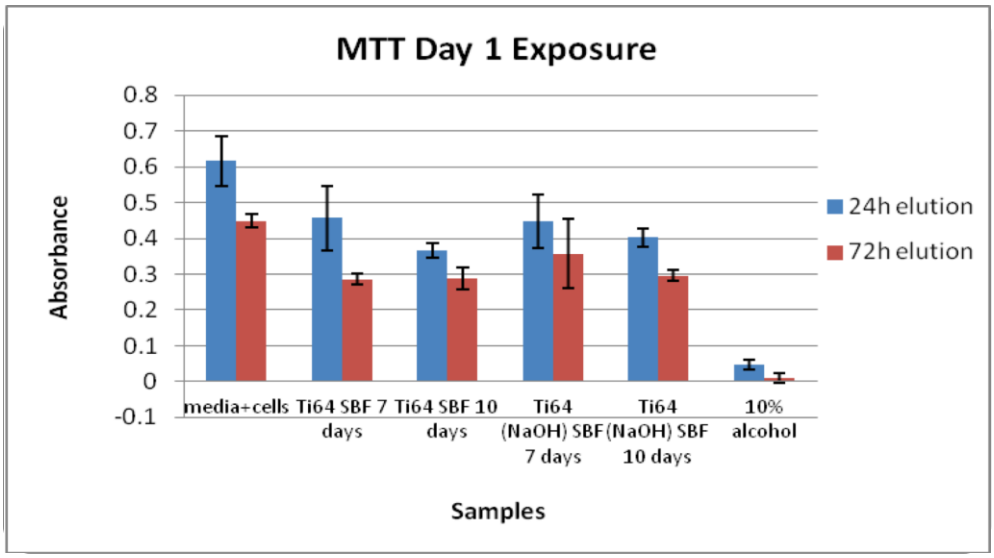

Figure 3.8: : Evaluation of Cytotoxicity Indirect Method/ MTT Day 1 Exposure of Ti64 specimens exposed to only to SBF treatment and sodium hydroxide treatment followed by SBF immersionexpressed as mean absorbance ± S.D (n=4); the statistical significance was predetermined at p< 0.05. An increase in cell metabolic activity was observed on all test samples and non-toxic control (TCP) compared to the toxic control(10% alcohol).

MTT, Day 3 Exposure:

Samples were eluted for 72 hours for indirect exposure, where two elution time points were measured (24h elution and 72h elution), in order to detect if any leaching products could affect the cells behaviour. After 3 days of MTT exposure, various cell metabolic activity were observed between the different groups.

For the CpTi samples, at the 24h elution time point, a comparison of the samples was made to media cell sample (negative control). All samples showed lower cell metabolic activity level than the negative control. CpTi samples immersed in SBF solution for 7days and CpTi samples pre-treated with NaOH and immersed in SBF for 7 days showed the best cell metabolic activity. At 72h elution time, there was an increase in the cell activity obtained by all the samples, particularly, CpTi samples immersed in SBF solution for 7 Days (Figure 3.9). There was no significant difference in osteoblast cells response between the negative control (media + cells) and the different surface treatment surfaces tested.

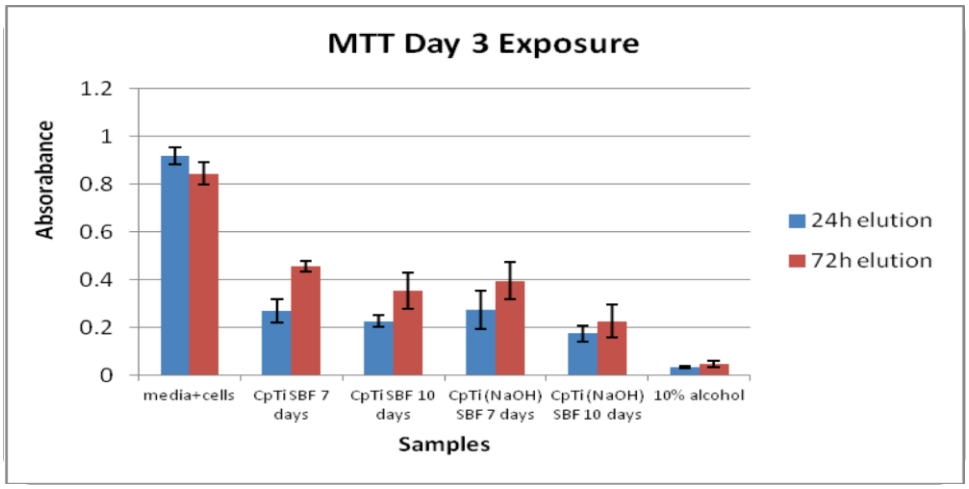

Figure 3.9: Evaluation of Cytotoxicity Indirect Method/ MTT Day 3 Exposure of CpTi specimens exposed to only SBF treatment and sodium hydroxide treatment followed by SBF immersionexpressed as mean absorbance ± S.D (n=4); the statistical significance was predetermined at p< 0.05. The results showed that the eluants at 24 h lowered the cell activity indicating a fall in cell metabolic activity, resulting from a potential leachable from the materials in the elution fluid due to longer elution time.

For the Ti64 samples, at the 24h elution time point, a comparison of the samples was made to media cell sample (negative control). All samples showed lower cell metabolic activity level than the negative control. Ti64 samples immersed in SBF solution for 7 days and Ti64 samples pre-treated with NaOH and immersed in SBF for 7 days showed the best cell metabolic activity. At 72h elution time, there was an increase in the cell activity obtained in all the samples, particularly, Ti64 samples immersed in SBF solution for 7 days (Figure 3.10). There was no significant difference in osteoblast cells response between the negative control (media + cells) and the different surface treatment surfaces tested.

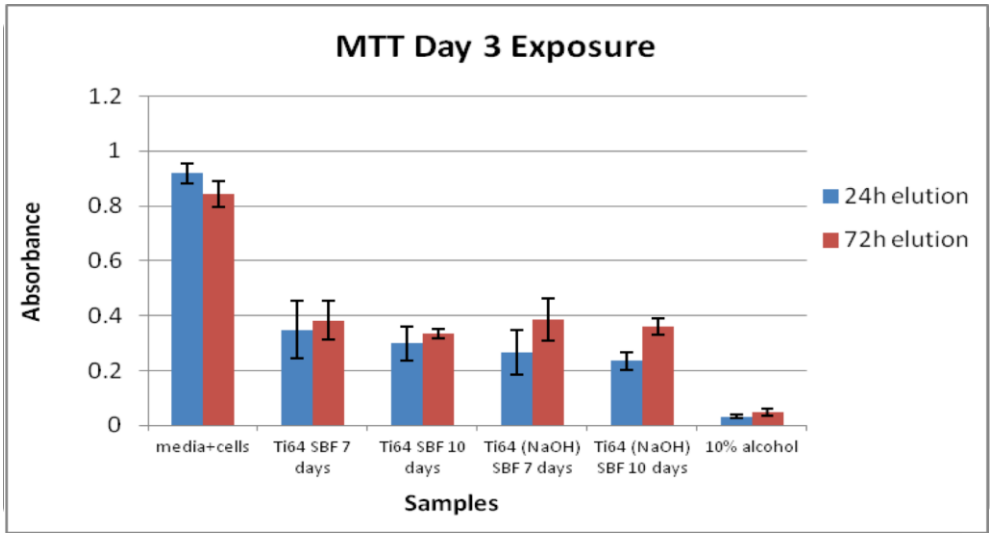

Figure 3.10: Evaluation of Cytotoxicity Indirect Method/ MTT Day 1 Exposure of Ti64 specimens exposed to only to SBF treatment and sodium hydroxide treatment followed by SBF immersionexpressed as mean absorbance ± S.D (n=4); the statistical significance was predetermined at p< 0.05. A decrease in cell metabolic activity was observed on all test samples and non-toxic control (TCP) compared to the toxic control(10% alcohol).

3.3.5.2. Live/Dead Assay

This assay measures the cell viability through the number of live and dead cells. It is a two-fluorescence assay, where green fluorescent is indication of live cells and red one is for dead cells. Live/dead cells were measured for the tested samples for 24h and 72h of incubation. All different samples showed good behaviour, large numbers of live cells with few dead cells. This emphasizes the cytocompatibility of the CpTi and Ti6Al4V materials in contact with the osteoblast cells.

Figures 3.11 and 3.12 show the live/dead staining images of the different treated surfaces, where it can be observed that treating CpTi and Ti64 samples with NaOH followed by immersion in SBF solution enhances the number of live cells, which is an indication of greater cell viability.

Group	Live Cells	Dead Cells
Thrx Disks	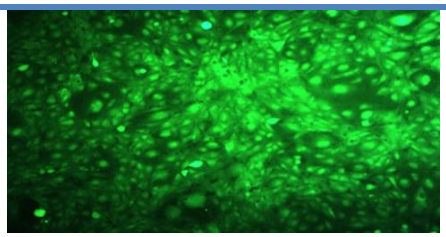	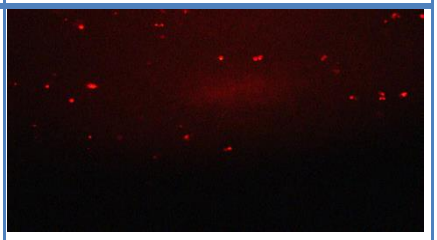
CpTi as received	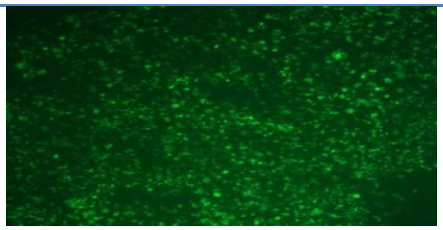	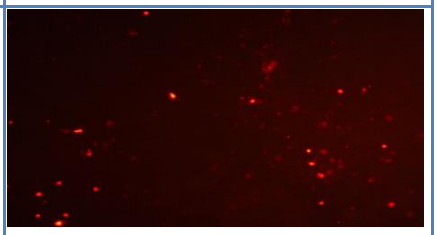
CpTi SBF 7D	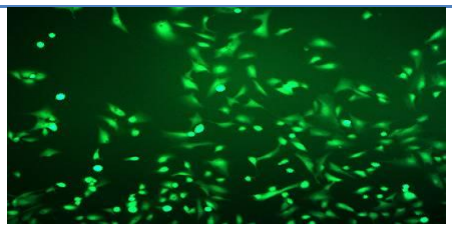	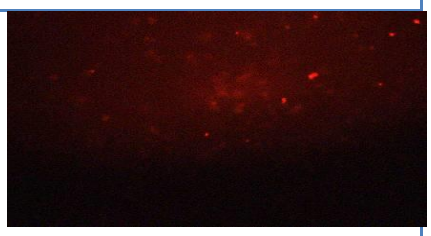
CpTi SBF 10D	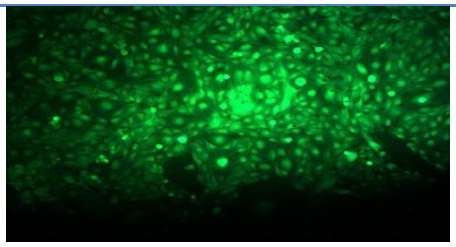	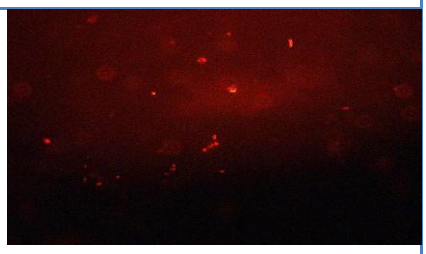
CpTi NaOH SBF 7D	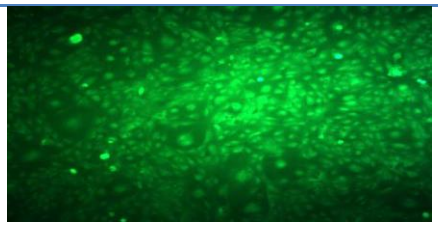	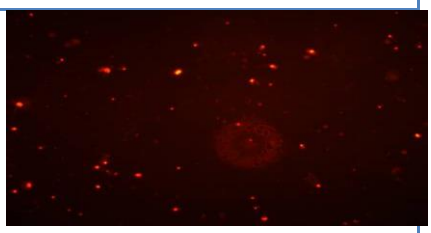
CpTi NaOH SBF 10D	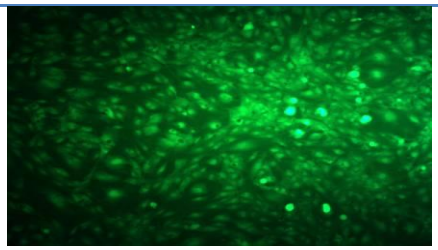	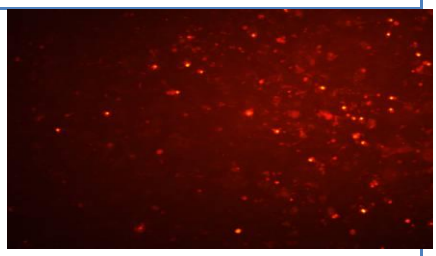

Figure 3.11: Live and dead fluorescence staining (Ethidium Homodimer-1) of aHOB cells exposed for 72 hours on CpTi samples. The images show that the surfaces treated with sodium hydroxide followed by SBF treatment had a large number of live cells in comparison to the SBF treated samples only.

Group	Live Cells	Dead Cells
Thrx Disks	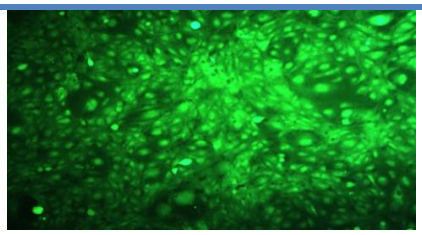	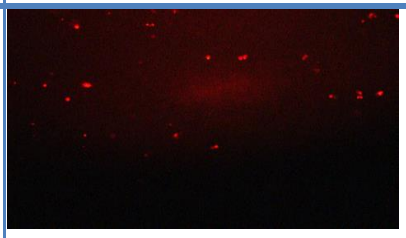
Ti64 as received	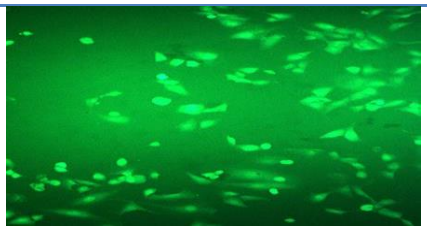	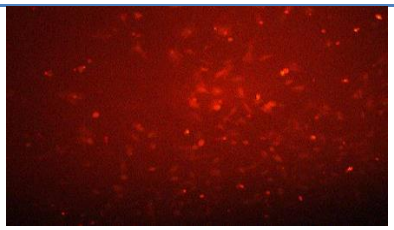
Ti64 SBF 7D	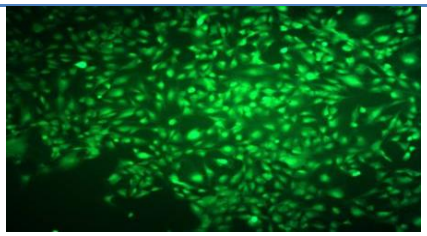	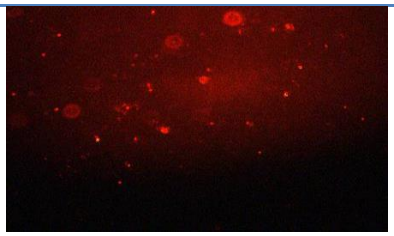
Ti64 SBF 10D	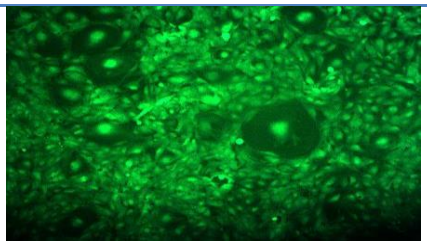	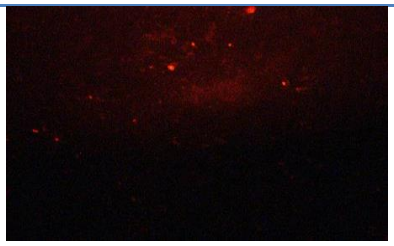
Ti64 NaOH SBF 7D	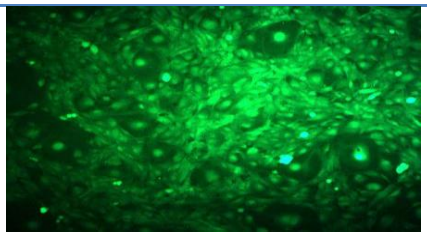	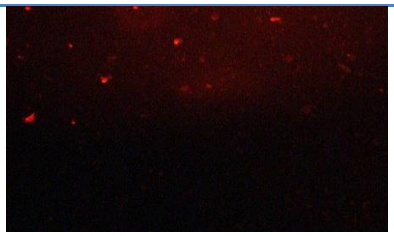
Ti64 NaOH SBF 10D	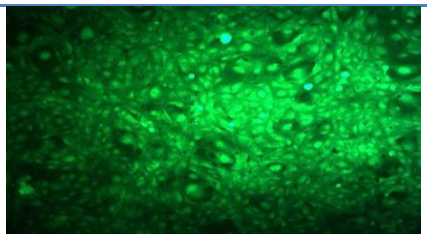	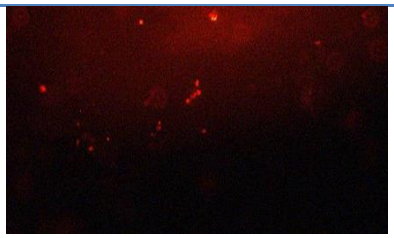

Figure 3.12: Live and dead fluorescence staining (Ethidium Homodimer-1) of aHOB cells exposed for 72 hours on Ti64 samples. The images show that the surfaces treated with sodium hydroxide followed by SBF treatment had a large number of live cells in comparison to the SBF treated samples only.

3.3.5.3. Alkaline Phosphatase Assay- Evaluation of Differentiation

Alkaline phosphatase (ALP) activity was measured as an early indicator of differentiation of primary aHOB cells seeded directly onto the titanium samples. The specific activity of ALP measured from the osteoblast cell lysate was investigated over a period of 28 days for 6 times points (Days 1, 3, 7, 14, 21 and 28). The ALP assay results are illustrated in Figures 3.12 and 3.13 for the CpTi and Ti64 groups.

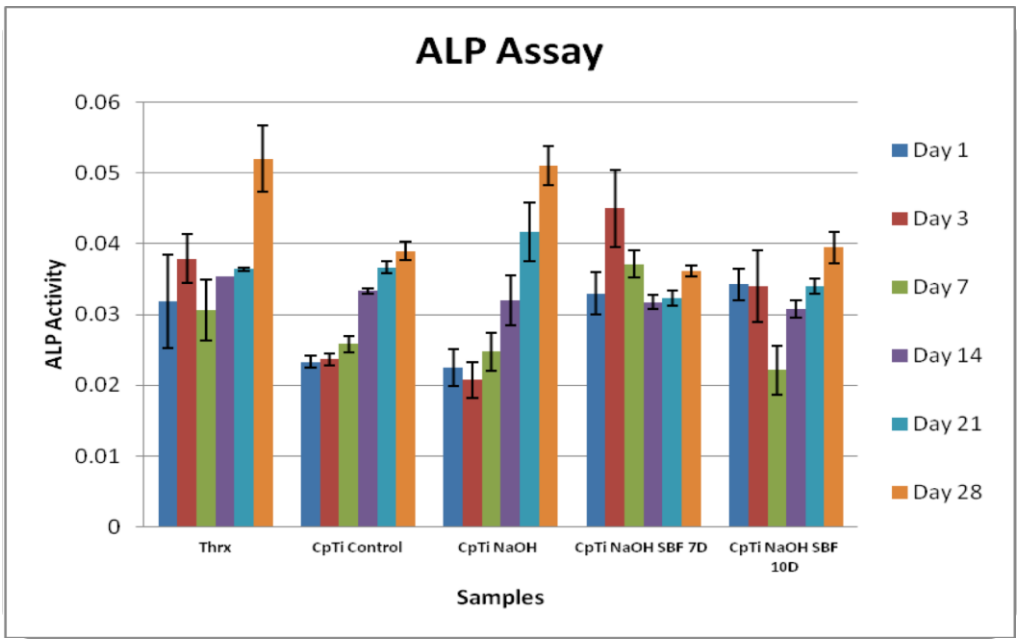

Figure 3.13: Evaluation of Differentiation of Osteoblast Cells / ALP Assay of CpTi titanium discs, which were treated with NaOH and immersed in SBF for 7 and 10 days. The data represents the average for each group as mean absorbance ± SD (n=8); the statistical significance was predetermined at p< 0.05.

The ALP assay on the CpTi samples (Figure 3.13) showed a general increase in the ALP activity on the different samples from day 1 to day 28. The control specimens of CpTi and the thermanox as well as the NaOH treated samples showed increasing ALP activity with time, which peaked at 28 days, whereas the experimental groups exhibited some variation. The NaOH treated surfaces and immersed in SBF for 7 days showed an early peak at day 3, whereas there was a significant drop in ALP activity at day 7 for the NaOH treated surfaces and immersed in SBF for 10 days.

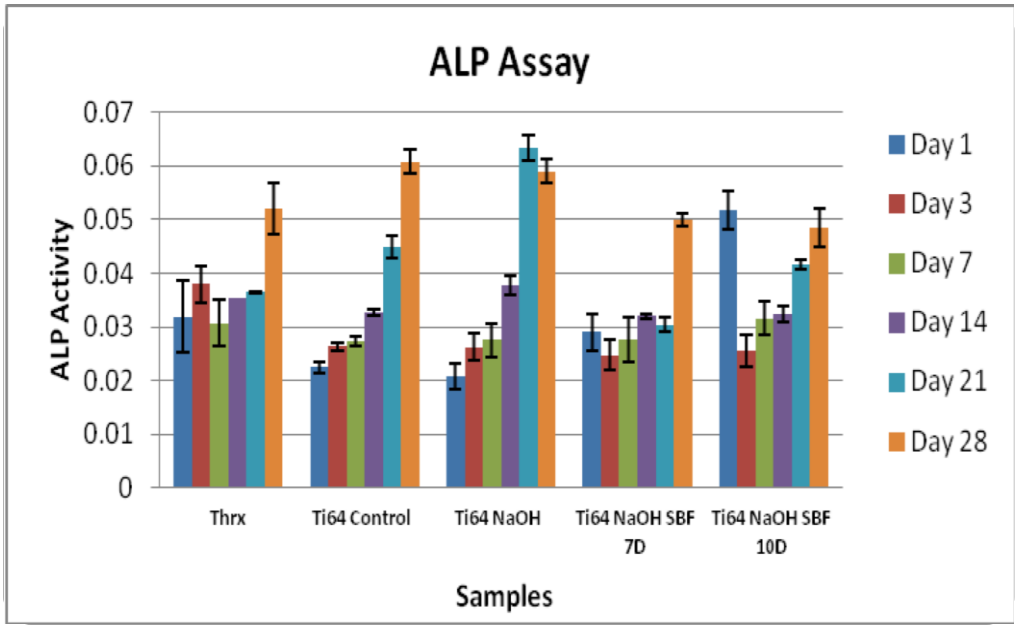

Figure 3.14: Evaluation of Differentiation of Osteoblast Cells / ALP Assay of Ti64 titanium discs, which were treated with NaOH and immersed in SBF for 7 and 10 days. The data represents the average for each group as mean absorbance ± SD (n=8); the statistical significance was predetermined at p< 0.05.

The ALP assay of the Ti64 samples (Figure 3.14) showed a general increase in the ALP activity on the different samples from day 1 to day 28. All surface treated samples showed increasing ALP activity with time, which peaked at 28 days, except the NaOH treated surfaces which were immersed in SBF for 10 days, which peaked at day 1. The NaOH treated surfaces showed a significant peak at day 21 compared to the positive control and other samples.

3.3.5.4. DNA Assay – Evaluation of Proliferation

DNA assay is a method used to measure cell turnover and proliferation hence an indicator of cell activity in the presence or absence of a test material. DNA assay was carried out on the different surface treated samples of CpTi and Ti6Al4V alloy at 6 time points (Days 1, 3, 7, 14, 21 and 28). The DNA assays results are shown in Figures 3.15 and 3.16 for the CpTi and Ti64 groups.

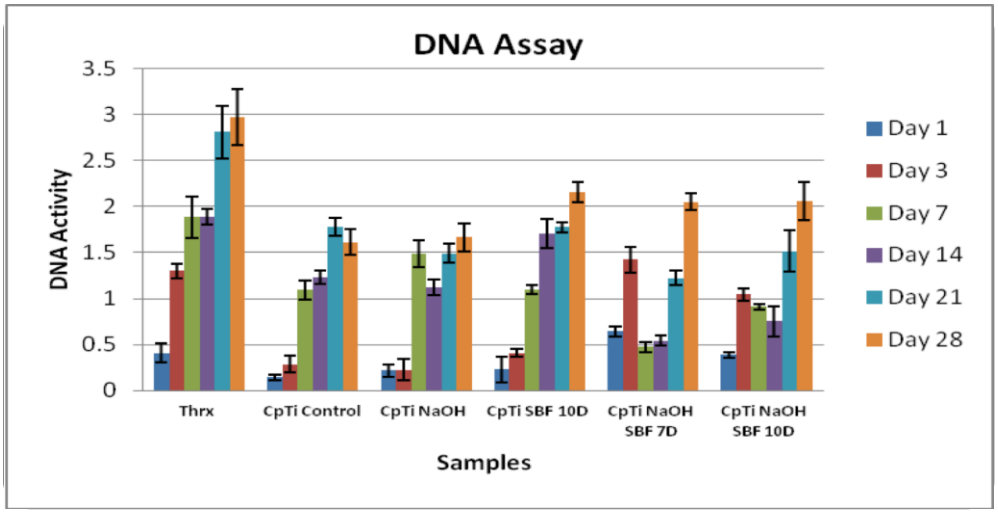

Figure 3.15: Evaluation of Proliferation of Osteoblast Cells / DNA Assay of CpTi samples which have been treated with NaOH and immersed in SBF for 7 and 10 days. The data represents the average for each group as mean absorbance ± SD (n=8); the statistical significance was predetermined at p< 0.05

The DNA activity assay of the CpTi samples showed general variable behaviour of cell proliferation through the 28 days of the DNA assay. Most of the different surface treatments showed higher results compared to the sample surface with no treatment (CpTi Control). All the experimental samples showed a peak at day 28. However, the general cell proliferation is lower than the positive control, which was significant for the control, and the NaOH treated CpTi samples. The cleaned and the NaOH pre-treated CpTi samples, which were immersed in SBF solution for 10 days showed the best results compared to the other treatment samples.

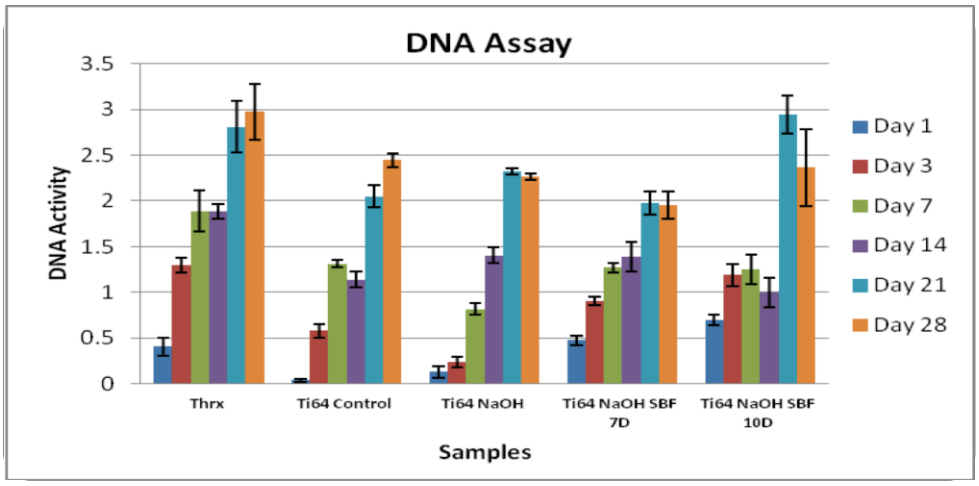

Figure 3.16: Evaluation of Proliferation of Osteoblast Cells / DNA Assay of Ti64 samples which have been treated with NaOH and immersed in SBF for 7 and 10 days. The data represents the average for each group as mean absorbance ± SD (n=8); the statistical significance was predetermined at p< 0.05.

The DNA activity assay of the Ti64 samples showed general increase of cell proliferation through the 28 days of the DNA assay. All the experimental samples showed a cell proliferation peak at day 21, whereas, the positive control and Ti64 control showed a peak at day 28. There was a significant difference in the cell activity peak at day 21 between NaOH treated surfaces, which were immersed in SBF for 7 and 10 days.

3.4. Discussion

For successful implantation, the surface characteristics of the implant is an important factor since the cascade of biological reactions that occur are closely related to the surface that is first exposed in the body [188, 196]. Biomedical and materials researchers have tried to design the ideal surface to ensure long-lasting anchorage of implants. All bioactive materials developed for implants up to 1990 were based on calcium phosphate ceramics [185]. It was later revealed that materials that form a calcium phosphate layer, usually called a bonelike apatite, on their surfaces in the living body bond to living bone through this apatite layer, as it seems to activate bone morphogenetic proteins and osteogenic cells that result in bone formation [197]. Apatite formation on a material can be induced by formation of functional groups such as TiOH, SiOH, TaOH, and ZrOH on its surface.

Alkali-heat treatment is a simple and cost-effective method to modify titanium implant surfaces as well as coating titanium with apatite. Several studies showed that, by treating commercially pure titanium and titanium alloys surfaces with NaOH followed by heat treatment makes titanium a bioactive material. They found that treatment of titanium with different concentrations of NaOH (4–10M) at 60°C for about 24h followed by heat treatment at 400–800°C for 1–24h produces a layer of sodium titanate gel [77, 189, 190]. This gel layer induces nuclei for the deposition of bone-like apatite crystals when immersed in a simulated body fluid (SBF) solution. The gel layers formed are characterized by irregular topography and high degree of open porosity on the submicron scale [191].

In the current study, commercially pure titanium and Ti64 titanium alloy were treated with 5M NaOH for 24 hours at 60°C, then subjected to immersion in simulated body fluid SBF for 7 and 10 days at room temperature to investigate the effect of NaOH treated surfaces on the enhancement of apatite-like formation on titanium surfaces after immersion in SBF solution. The results showed that the average roughness of the CpTi discs after the various treatments indicated that the immersion in SBF solution after alkaline treatment of the surface, decreased the Ra value, which may be due to the interaction and deposited apatite-like layer which is expected to be present on the surface due to the immersion in SBF. However, non-alkali treated surfaces resulted in lowest values of Ra after immersion in SBF which is due to the inability of these surfaces to imbibe an apatite-like layer on the surface because of the lack of any sites to promote nucleation. The Ti64 alloy samples, showed a variable results of Ra values, but in general the alkali treated surfaces showed an

increase in the surface roughness after immersion in SBF solution whilst the Ra values decreases or remained unchanged on non-alkali treated surfaces immersed in SBF. The trend in the Ti64 differs from the roughness parameters observed for the CpTi specimens, which is arguably due to the smoother surface of the control specimens at the outset raising the roughness to an extent after a deposition layer is formed.

The AFM surface evaluation showed that the CpTi alkali treated surfaces soaked in SBF solution decrease the surface roughness values, which might be due to reaction of titanium with the sodium hydroxide, forming a layer of sodium titanate, which can induce the apatite formation after immersion in SBF solution resulting in a deposition of more uniform layer reducing the surface roughness. While, the Ti64 surfaces that were alkali treated and soaked in SBF solution showed an increase in the surface roughness, which can be due to the porous sodium titanate surface network which is formed from the alkaline treatment on the smoother surface of the Ti64 alloy, thus enhancing the deposition of apatite-like layer on the surface from the SBF immersion resulting in a rougher surfaces. These results are in agreement with studies by Kokubo et al, where a bone-like apatite deposition is reported on titanium orthopaedic implants post sodium hydroxide and heat treatment followed by immersion in a simulated body fluid (SBF). Na^+ ions from the titanate layer are exchanged for H_3O^+ ions from the surrounding SBF. This causes the formation of TiOH groups, which combine with Ca^{2+} ions to form amorphous calcium titanate. The subsequent reaction with PO_4^{3-} ions forms amorphous calcium phosphate, which eventually transforms into bone-like apatite. Similar findings have been reported by Kim et al. [88] and Kokubo et al [185]. However the observations from this study suggests that the heat treatment post alkali treatment may not be necessary for the interaction.

The Raman spectroscopy results in this study showed the presence of corresponding bands of anatase and rutile titanium oxide phases at 133-138 cm^{-1} and 460-470 cm^{-1} respectively, as well the presence of peaks ranging between 785 and 868 cm^{-1}, which was more prominent on titanium, samples that were treated with NaOH and then immersed in SBF for 10 days compared to the other samples. Almost similar results have been reported by Kokubo et al. [185] where there were peaks arising between 700 and 850 shift /cm^{-1} on NaOH treated surfaces and soaked in SBF solution. They attributed this to the heat treatment accompanied with the alkaline treatment, which formed sodium titanate that can be seen on these

surfaces, however in this study similar peaks were detected without heat treatment indicating that sodium titanate formed and was retained just via the sodium hydroxide treatment. Ravelingien et al. [201] investigated the effect of different heat treatments on the bioactivity of alkali treated titanium surfaces, and showed the presence of Raman spectra bands corresponding to anatase and rutile phases at 223 and 447 cm^{-1} respectively and a Raman peak around 700 cm^{-1} corresponding to sodium titanate for alkali treated surfaces which were soaked in 5M NaOH for 24 hours at 60° C.

The surface morphologies of the non-treated, alkali treated, and soaked in SBF surfaces, have been evaluated as well by SEM/EDS characterisation, which showed that titanium control samples were relatively smooth with some imperfections and scratches due to the sandblasting and polishing processes. It was observed that these marks and imperfections were finer on the CpTi control than the Ti64 control surfaces. The SEM images of the NaOH treated samples showed the presence of a deposited layer on the surface, which is believed to be a layer of sodium titanate and the presence as well of a deposited apatite-like layer on the surfaces, which were immersed in SBF solution. As expected the immersion of the discs in simulated body fluid (SBF) irrespective of NaOH treatment yielded a rougher surface that is attributed to the formation of the apatite layer which is thought to be induced by the super-saturation of calcium phosphate salts within the medium. A deposition process commences on immersion in the SBF solution due to a heterogeneous nucleation. This is further confirmed by the SEM-EDX that provides evidence of calcium and phosphate species; the changes at this stage due to the surface chemistry rather than the differences in surface roughness. EDAX analysis measured a range between 1.26 and 1.34 Ca/P ratio in the bioactive layer for alkali treated titanium samples that were soaked in simulated body fluid (SBF). The values are much lower and vary from the stoichiometric ratio in hydroxyapatite of a Ca/P ratio of 1.67, which may be related to the other calcium phosphates such as TCP, (OCP: $Ca_8H_2(PO_4)_6 \cdot 2H_2O$).

Yousefpour et al (2006) [177] investigated the formation of bioactive layer alkaline-acid treated titanium in simulated body fluid, and showed that different Ca/P ratio can be obtained according the treatment of the surface. An EDAX analysis of the bioactive layer of the different treated methods showed a Ca/P ratio O.6 on alkaline treated surfaces with 5M NaOH stating that it could be to other forms of calcium

phosphates such as TCP [177]. Chen et al. [202] investigated the bioactivity and cytocompatibility of Ti and TiZr after alkali and heat treatment followed by Ca-ion-deposition via SBF soaking. They observed the formation of a compact apatite coating on the surface modified Ti and TiZr alloys which enhanced the cell adhesion and proliferation using human osteoblast like cells (SaOS2) on the treated titanium surfaces compared to the untreated ones [202].

In the current study, the viability, proliferation and differentiation evaluation of primary aHOB cells on the different treated titanium samples were examined by MTT indirect cytotoxicity assay, live/dead staining, alkaline phosphatase activity and DNA activity. For the indirect cytotoxicity tests performed as shown in Figures 3.7, 3.8, 3.9, and 3.10. The reduction in cellular metabolic activity after incubation of 72 hours eluted media was probably due to some toxic leachables or contaminant released from the test materials. This toxic materials leaching are likely to be either the grinding media from the cleaning process, or the presence of Na^+ ions from NaOH treatments, which was not cleaned probably of the surface. However, these eluants released from the test materials in the 24 and 72 hours eluted media didn't or was not sufficient to have a harmful effect on the aHOB cells, as the cells still appear to continue their activity in the other cellular tests. From the live/dead staining results in Figures 3.11 and 3.12, it was observed that there were notably more green fluorescent cells than the red one on all samples. The results showed that aHOB cells cultured on NaOH treated samples and immersed in SBF solution for 72 hours, had a favourable surface cell proliferation indicated by the large number of live cells.

The expression of alkaline phosphatase ALP was used as aHOB phenotypic biochemical marker of differentiation on the titanium surfaces. aHOB cell differentiation was observed on all different treated titanium surfaces, as indicated by ALP production. The expression of ALP over the observation period of 28 days, indicated The ALP assay of the CpTi samples (Figure 3.13) showed a general increase in the ALP activity on the different samples from day 1 to day 28. The control specimens of CpTi and the thermanox as well as the NaOH treated samples showed increasing ALP activity with time, which peaked at 28 days, whereas the experimental groups exhibited some variation. The NaOH treated surfaces and immersed in SBF for 7 days showed an early peak at day 3, whereas there was a significant drop in ALP activity at day 7 for the NaOH treated surfaces and immersed in SBF for 10 days. The ALP assay of the Ti64 samples (Figure 3.14) showed a general increase in the ALP activity on the different samples from day 1 to

day 28. All surface treated samples showed increasing ALP activity with time, which peaked at 28 days, except the NaOH treated surfaces which were immersed in SBF for 10 days, which peaked at day 1. The NaOH treated surfaces showed a significant peak at day 21 compared to the positive control and other samples. This can be due to the presence of apatite-like layer on the surface of these samples, which were induced by the SBF solution, as this layer can motivate the osteoblast differentiation earlier than cells cultured on the other surfaces. These findings are in accordance with a very recent study by Lee et al. [198], which showed that alkaline heat treated titanium alloy surfaces exhibit a higher ALP activity than non alkaline heated surfaces.

The cellular proliferation behaviour of aHOB cells was evaluated by direct contact assay of DNA synthesis test. The DNA activity of osteoblast cells cultured on the NaOH treated surfaces yielded some variation between the different groups. The CpTi and Ti64 samples which were treated with NaOH seems to induce the cell activity indicated by the DNA activity on these surfaces, however immersion of these surfaces in SBF solution could increase the cell activity depending on the time required for immersion as it can be recognised clearly between the NaOH treated surfaces which were immersed in SBF for 7 and 10 days, as the latter showed a higher cell activity.

Takemoto et al [193] in an in vivo study, showed that both treated and untreated porous Ti cylinders were implanted in rabbit femoral condyles. Unexpectedly, there was no significant difference in bone in- growth at the early post-implantation times of 2 and 4 weeks. Over time, however, the alkali- and heat-treated implants showed increased osseointegration, whereas the untreated implants did not. A very recent study by Hamodeh et al [188], showed that increasing the alkali treatment period and heat treatment temperature positively affected surface roughness and formation of a bioactive sodium titanium oxide (sodium titanate) layer on the titanium surface, especially after heat treatment at 800°C. There was a significantly higher calcium deposition on alkaline heat treated surfaces than the non-treated ones, indicating that the alkali and heat treatment of titanium implant materials created better treatment conditions for obtaining a bioactive implant material.

Thus this study demonstrated that treatment of the Ti and Ti64 with sodium hydroxide yielded a bioactive surface and heat treatment was not essential to obtain the bioactivity. In vitro cell culture showed that further treatment of these sodium hydroxide treated surfaces with SBF enhanced in vitro cytocompatibility.

CHAPTER FOUR

Immobilization of Bisphosphonate on Different Surface Treated Ti and its Alloy: In vitro Bioactivity Evaluation

4.1. Introduction

A variety of surface modifications have been developed to facilitate bone tissue responses toward titanium surfaces including control of surface topography, hydroxyapatite coatings and biomolecular immobilization. In recent years, another approach to stimulate bone-titanium interactions has been the tethering of peptides on the Ti surface; however, the adhesion layer between the titanium and these peptides is weak and tends to breakdown. One example of improving cell-material response is to incorporate bone morphogenic proteins (BMPs) attempted, known to play an important role in bone regeneration [203]. Although BMP-2 has successfully been used to stimulate bone regeneration, the use of BMP-2 is expensive, a high dose is required (1 mg BMP-2/mL defect) and it has a short half-life in vivo. To overcome these limitations, BMP-2 delivery systems such as collagen gels, sponges, scaffolds, and fibrin gels for long-lasting, local release of BMP-2 have been suggested [204, 205]. However, these systems are associated with problems such as uncontrolled release rates, release of BMP-2 for only a short period, and a high initial bolus of release [206].

Another interesting approach to modify or coat the implant surface is to immobilize drugs for example bisphosphonates; which inhibit osteoclast activity thus resulting in faster bone regeneration around implants [207]. Bisphosphonates are currently the most effective inhibitors of bone resorption, which were first used clinically to treat Paget's disease [208]. Today, bisphosphonates are the drugs of choice in the treatment of osteoporosis and hypercalcemia of malignancy and evaluated for treating inflammation-related bone loss, fibrous dysplasia, as well as other disorders of the musculoskeletal system (osteogenesis imperfecta) [208]. Bisphosphonates are compounds characterized by two C–P bonds.

In dental implants, bisphosphonates have been used clinically in patients lacking sufficient bone support (e.g. severely resorbed alveolar ridges). It has been shown that a chemically associated bisphosphonate zoledronate onto calcium phosphate compounds inhibits osteoclastic activity, thus reducing bone resorption [209, 210]. Experimental in vivo studies using bisphosphonate-incorporated titanium surfaces have demonstrated a significant increase in the amount of supporting bone surrounding the implants [163, 211]. However, other experimental studies have demonstrated only a slight increase in implant osseointegration [212, 213]. The major concern of using bisphosphonates in implants is the controlled and sustained release of these antiresorptive agents from the titanium implant surface. However,

the ideal dose of these drugs should be carefully determined because an increase in peri-implant bone density has been reported to be bisphosphonate concentration-dependent, as it was found that growth and pro-differentiation effects are exerted at lower concentrations of bisphosphonates ranging from 10^{-9} M to 10^{-6} M, whereas the inhibitory effects are found at concentrations higher than 10^{-5} M [214, 215]. Furthermore, an unexpected potential adverse effect of these drugs is a possible association with the osteonecrosis of jaw bone [142].

This chapter aims to utilize the surface modified CpTi and Ti64 obtained after SPF processing, sodium hydroxide treatments followed by SBF immersion (as discussed in chapters 2 and 3) to study if immobilisation of bisphosphonate molecule (Alendronate, Sodium Salt) can be effected on these surfaces and investigating the in vitro response of osteoblast cells on the titanium surface, thus the osseointegration and bone healing process.

4.2. Materials and Methodology

4.2.1. Preparation of Titanium Discs

150mmX150mm and 0.5 mm thickness commercially pure titanium stock sheet (CpTi), and 140 mm diameter and 0.5 mm thickness titanium alloy Ti6Al4V stock sheets were used and prepared for treatment as was previously described in chapter two.

4.2.2. Surface Treatments of Titanium Discs

In this study, two major titanium disc groups were prepared for immobilization of bisphosphonate; invested titanium discs simulating superplastic forming process (SPF) and alkali treatment of titanium discs (NaOH), where both of them were immersed in simulated body fluid (SBF) solution (Figure 4.1).

4.2.2.1. Alkali Treatment

Alkali treatment was performed only on untreated and non-invested titanium samples, which were prepared along with the preparation of the other titanium groups. Sanded and cleaned CpTi and Ti64 10 mm diameter titanium discs were grouped and soaked in 6 ml of 5M solution of Sodium Hydroxide (NaOH) at 60°C for 24 hours, subsequently rinsed and allowed to dry at room temperature.

4.2.2.2. Simulating Superplastic Forming Process Treatment (SPF)

The cleaned discs of the CpTi and Ti6Al4V were embedded in Deguvest SR phosphate bonded investment (DeguDent, Germany) moulds, and heated in an oven up to 900°C and held for 20 minutes at this temperature, simulating the superplastic forming process as previously described in chapter two.

4.2.2.3. Simulated Body Fluid (SBF) Immersion

A bone-like apatite layer is formed on the surface of bioactive materials when bonding to living bone. This apatite layer can be reproduced on the titanium surface in simulated body fluid with ion concentrations that nearly equal to those of human blood plasma. The SBF solution was prepared based on Kokubo recipe (1990) as described previously in chapter two. The non-treated/control, alkaline treated and simulated superplastic forming process (SPF) discs, were immersed in 10 ml of prepared SBF solution at 37°C for 7 and 10 days respectively.

4.2.2.4. Preparation and Immobilisation of Bisphosphonate (Sodium Alendronate)

In the current study sodium alendronate was selected as the bisphosphonate to be immobilized on the different treated titanium samples, as it considered one of the most commercial bisphosphonates in treating bones disease and in the research field. The different surface treated Ti discs were dried, and divided into different groups to be further treated with sodium alendronate as illustrated in Figure 4.1. Sodium alendronate (CALBIOCHEM, EMD Biosciences, Inc, CA, USA) solution of the desired concentration (2mg/ml) was prepared by dissolving the required amount of sodium alendronate in distilled water with continuous magnetic stirring. 100 µl of the prepared solution was micro-seeded on each disk and allowed to dry in an electrical oven at 40°C, after which, the samples were moved carefully and allowed to cool at room temperature, then divided into groups for surface characterisation and biological evaluation. The samples for the biological evaluation were sterilised by autoclaving method, in which they were subjected to a high-pressure saturated steam at 121 °C for around 30 minutes.

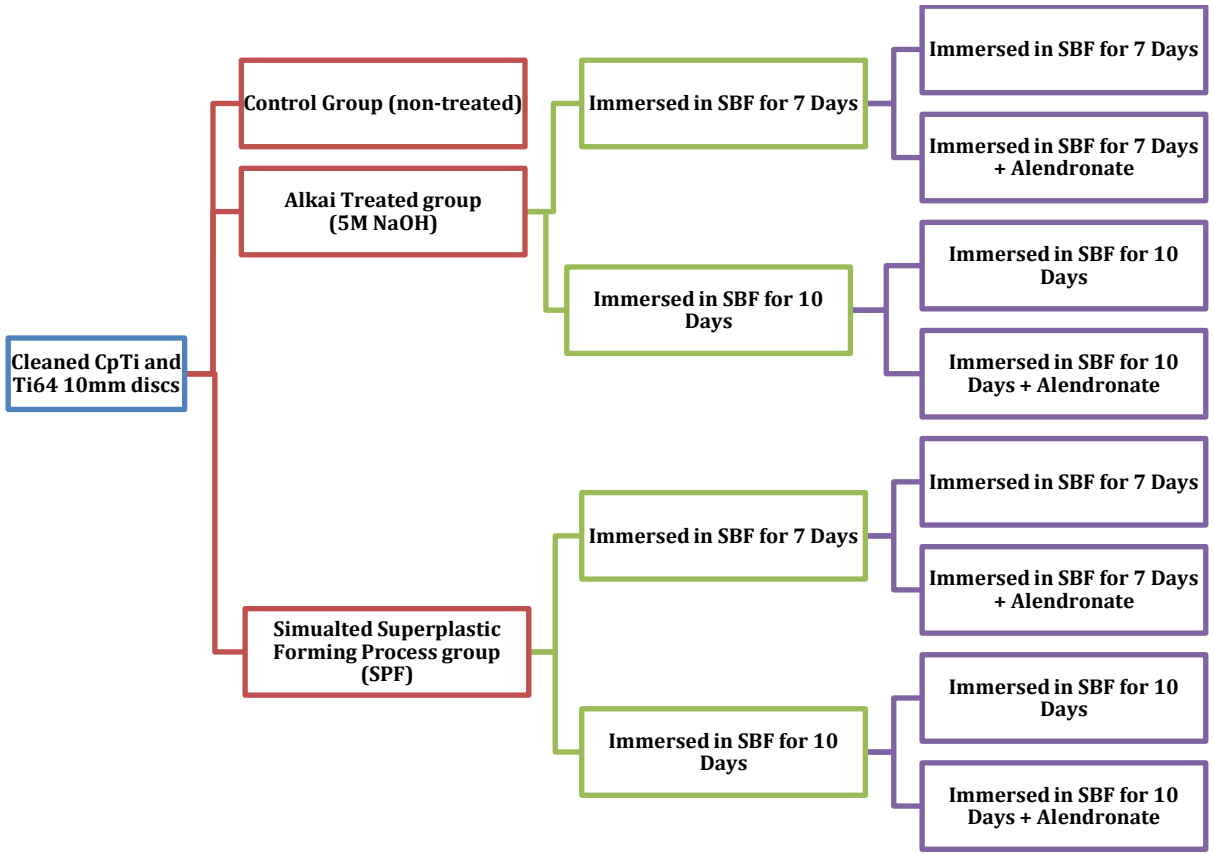

Figure 4.1: Schematic illustration of the different surface treatment on the CpTi and Ti64 discs, with three main experimental groups (non-treated, alkali treated and SPF), which were immersed in SBF solution for 7 and 10 days, subsequently alendronate sodium was immobilised on their surfaces.

4.2.3. Surface Characterization

4.2.3.1. Surface Roughness Measurement

The surface roughness analysis of the titanium discs in microns (μm) before and after surface treatment was assessed and quantified with a contact profilometer surface analysis instrument, TESA Rugosurf 10G surface roughness gauge. The mean roughness was measured and recorded at a traverse speed with a diamond probe tip stylus of 5μm. For each of the 10 mm titanium sample discs, the roughness parameters were measured at four different locations and a total of three discs from each group of the titanium samples, were analysed to obtain an accurate assessment.

4.2.3.2. Atomic Force Microscopy (AFM)

In the current study, a commercial AFM was used to perform three-dimensional and morphological topography analysis of the treated titanium surfaces, as previously described in chapter two. Four areas were scanned for each sample, and the images obtained were processed and analysed using Gwyddion© 2.19 and SPIP©6.0.13 data analysis software.

4.2.3.3. Fourier Transform Infrared spectroscopy (FTIR)

To further analyze surface composition, Fourier transform infrared spectroscopy (FTIR) was used. A PerkinElmer Spectrum One FT-IR spectrometer was used (PerkinElmer, Massachusetts, USA) to analysis the chemical surface composition of the treated surfaces.

4.2.3.4. Scanning Electron Microscopy/Energy Dispersive X-ray Analysis (SEM/EDS)

The surfaces of the treated titanium discs were evaluated and studied using scanning electron microscopy (SEM) (Hitachi S3500N) accompanied with an energy dispersive X-ray spectroscopy machine (EDS), obtaining high-resolution imaging with nanometre resolution of surface structure. The technique is described in chapter two.

4.2.4. In-vitro Biological Evaluation

Human primary alveolar osteoblast cells (aHOB) were used for the biological evaluation. The sterilized samples were prepared for the following biological assays; assessment of cell viability – MTT assay, assessment of cell differentiation – alkaline phosphatase assay (ALP), and assessment of cell viability – DNA activity assay. The methodology of each assay has been previously described in chapter two.

4.2.5. Statistical Analysis

The data were statistically analysed using analysis of variance (ANOVA) for assessing the significance level of the differences between the experimental groups. All statistical analysis was performed with commercial statistical software GraphPad Prism (version 6.0c). The probability of p being below 0.05 was considered to be statistically significant. Results were represented graphically as mean values with standard deviation.

4.3. Results

The surface treatments carried out on the CpTi and Ti64 discs are shown in Table 4.1. The alkali (NaOH) treatment was carried out to compare the effect of the superplastic forming with investment materials and subsequently subjected to similar treatments, the sub groups forming the controls within each type of surface treatment groups.

Name of Group	**Name of Sample**	**Surface Treatment**
1. Control	Non Treated	No surface treatment
2. Alkali treatment (NaOH)	NaOH	treated with 5M NaOH for 24h
	NaOH SBF 7D	Treated with 5M NaOH for 24h and immersed in SBF solution for 7 days
	NaOH SBF 7D BPs	Treated with 5M NaOH for 24h, immersed in SBF solution for 7 days then 2mg/ml alendronate bisphosphonate was immobilised
	NaOH SBF 10D	Treated with 5M NaOH for 24h and immersed in SBF solution for 10 days
	NaOH SBF 10D BPs	Treated with 5M NaOH for 24h, immersed in SBF solution for 10 days then 2mg/ml alendronate bisphosphonate was immobilised
3. Simulating Superplastic Forming (SPF)	SPF	Invested in Deguvest investment and heated up to 900°C simulating superplastic forming
	SPF SBF 7D	Invested in Deguvest investment, heated up to 900°C and immersed in SBF solution for 7 days
	SPF SBF 7D BPs	Invested, heated up to 900°C, immersed in SBF for 7 days then 2mg/ml alendronate bisphosphonate was immobilised
	SPF SBF 10D	Invested in Deguvest investment, heated up to 900°C and immersed in SBF solution for 10 days
	SPF SBF 10D BPs	Invested, heated up to 900°C, immersed in SBF for 10 days then 2mg/ml alendronate bisphosphonate was immobilised

Table 4.1: The experimental and sub groups of the different treated surfaces which were subjected to immobilisation of alendronate sodium bisphosphonate.

4.3.1. Surface Roughness Measurement

Surface roughness measurements were obtained for the different titanium sample discs and calculated as mean value, which are presented in the Table 4.2.

CpTi Group	**Average *Ra* ± SD (µm)**	**Ti64 Group**	**Average *Ra* ± SD (µm)**
CpTi Control	0.404 ± 0.176	Ti64 Control	0.217 ± 0.09
CpTi SPF	0.160 ± 0.075	Ti64 SPF	0.420 ± 0.128
CpTi SPF BPs	0.230 ± 0.113	Ti64 SPF BPs	0.251 ± 0.102
CpTi SPF SBF 10D	0.389 ± 0.08	Ti64 SPF SBF 10D	0.431 ± 0.113
CpTi SPF SBF10D BPs	0.235 ± 0.097	Ti64 SPF SBF 10D BPs	0.271 ± 0.073
CpTi NaOH SBF 10D	0.296 ± 0.065	Ti64 NaOH SBF 10D	0.312 ± 0.091
CpTi NaOH SBF BPs	0.167 ± 0.07	Ti64 NaOH SBF BPs	0.266 ± 0.082

Table 4.2: Surface roughness parameter (Ra) measurements for CpTi and Ti64 samples (n=4) ± SD.

The average roughness of the CpTi discs after the various treatments indicated that the simulated plastic forming decreased the Ra value for the CpTi samples from 0.404 to 0.160 µm, while the Ti64 showed the opposite trend as the Ra values increased from 0.217 to 420 µm when simulated superplastic forming process. However immersion of SPF samples in simulated body fluid solution SBF increased the surface roughness compared to the SPF samples for both CpTi and Ti64 samples. On the other hand, the alkali treatment of CpTi and Ti64 samples showed to decrease the surface roughness after immersion in SBF solution. However immobilisation of alendronate sodium bisphosphonate over the entire surface may result in lowering the average roughness.

4.3.2. Atomic Force Microscopy (AFM)

The roughness parameters obtained under AFM for the different treated titanium discs in this study are summarized in Table 4.3, where four different scans were measured for each sample and the average was calculated. Different values were observed between the samples due to the different surface treatments as expected. Figures 4.2 and 4.3 indicate the qualitative characterization in two-dimensional and three-dimensional images of the corresponding surface topography of the different treated titanium samples observed under AFM.

For the CpTi groups, the control had the highest Ra of 0.213 µm followed by the CpTi simulated superplastic forming process (SPF) which were immersed in SBF solution of Ra average value of 0.179 µm compared to the other samples. When CpTi was simulated superplastic forming process only (SPF) it showed that the surface had lower surface roughness of Ra value of 0.164 µm compared to the control one with Ra value of 0.213 µm, this might be due to the layer which were deposited on the surface due the interaction between the titanium surface and the investment mould at high temperatures. The alkaline treated surfaces that were immersed in SBF solution showed a relatively higher surface roughness of 0.156 µm and 0.140 µm for CpTi and Ti64 samples respectively. This might be due to reaction of titanium with the sodium hydroxide, forming a layer of sodium titanate, which can induce the apatite formation after immersion in SBF solution resulting in a rough surface. It was observed that the surfaces, which were immobilized with sodium alendronate bisphosphonate, decreased the surface roughness value compared to the same surfaces before immobilization of BPs. For the Ti64 group, it was realized that the simulated superplastic forming process (SPF) samples, which were further immersed in SBF solution, showed the highest surface roughness value of 0.159 µm, whilst the control surface showed the lowest value of 0.08 µm. As well as for the CpTi samples, it was observed that the immobilization of sodium alendronate also decreased the surface roughness values of the treated surfaces compared to the same surfaces before the immobilization process, which probably is due to the uniform attachment of the BP to form a molecular layer on the surface.

CpTi Group	**AFM (Average Ra ± SD µm)**	**Ti64 Group**	**AFM (Average Ra ± SD µm)**
CpTi Control	0.213 ± 0.019	Ti64 Control	0.080 ± 0.013
CpTi SPF	0.164 ± 0.015	Ti64 SPF	0.152 ± 0.024
CpTi SPF BPs	0.106 ± 0.023	Ti64 SPF BPs	0.092 ± 0.015
CpTi SPF SBF 10D	0.179 ± 0.038	Ti64 SPF SBF 10D	0.159 ± 0.026
CpTi SPF SBF10D BPs	0.149 ± 0.02	Ti64 SPF SBF 10D BPs	0.104 ± 0.017
CpTi NaOH SBF	0.156 ± 0.03	Ti64 NaOH SBF	0.140 ± 0.023
CpTi NaOH SBF BPs	0.132 ± 0.016	Ti64 NaOH SBF BPs	0.094 ± 0.015

Table 4.3: Surface roughness (Ra) of the different surface treated titanium disc groups obtained under AFM. The results were statistically analyzed using one-way Anova analysis (GraphPad Prism software). The statistical significance was predetermined at ($p < 0.05$) and n=4 (± SD). There was no significant difference between the control and the different treated surfaces for both CpTi and Ti64 samples.

Sample name	2D AFM Image	3D AFM Image
CpTi Control	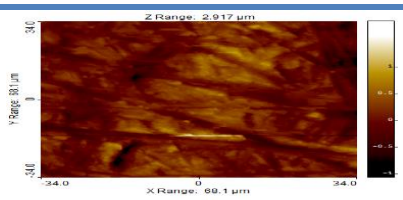	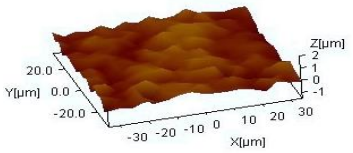
CpTi SPF	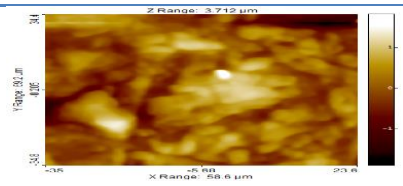	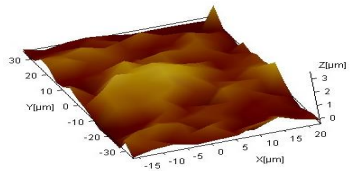
CpTi SPF BPS	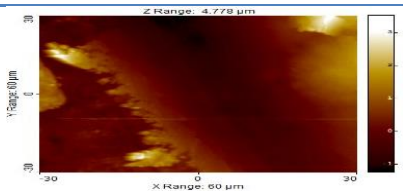	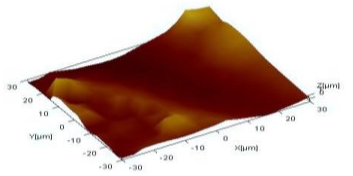
CpTi SPF SBF 10D	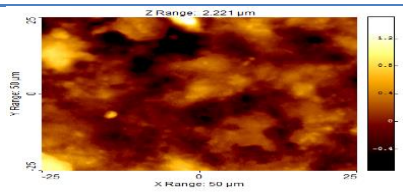	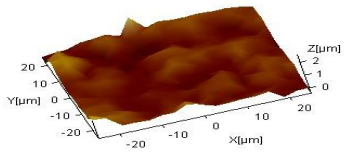
CpTi SPF SBF 10D BPs	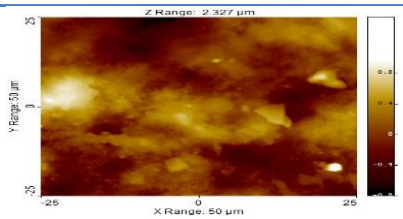	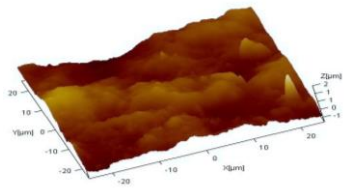
CpTi NaOH SBF	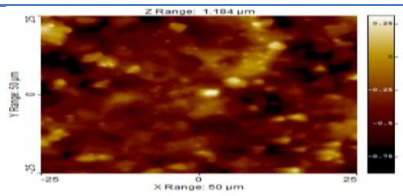	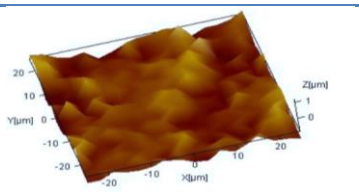
CpTi NaOH SBF BPs	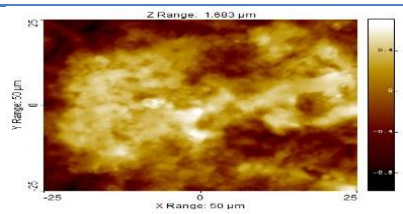	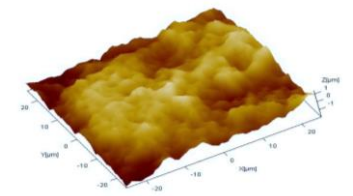

Figure 4.2: Representative 2D and 3D of AFM images of the different tested CpTi samples, where the SPF process decrease the Ra value on the CpTi samples, the immersion in SBF seems to increase the surface roughness of these surfaces due to the deposition of apatite like layer. Alendronate deposition seems to decrease the surface roughness by forming a more uniform layer on the surface.

Sample name	2D AFM Image	3D AFM Image
Ti64 Control	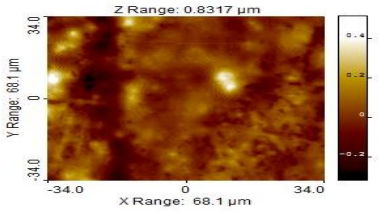	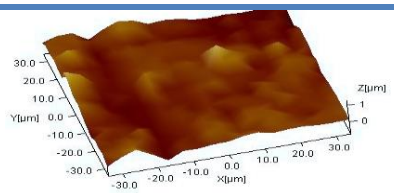
Ti64 SPF	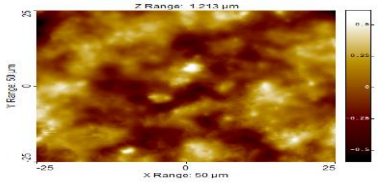	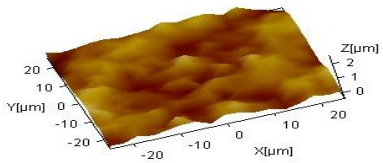
Ti64 SPF BPS	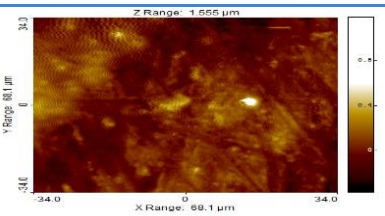	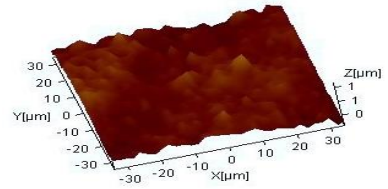
Ti64 SPF SBF 10D	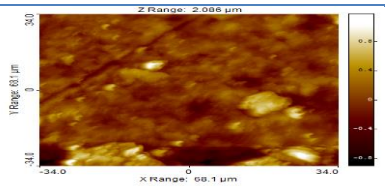	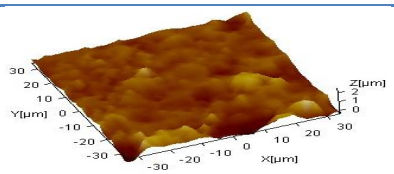
Ti64 SPF SBF 10D BPs	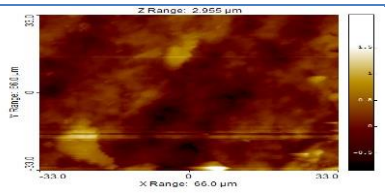	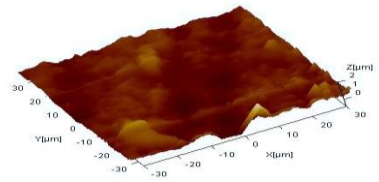
Ti64 NaOH SBF	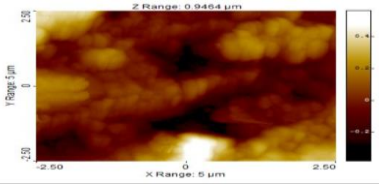	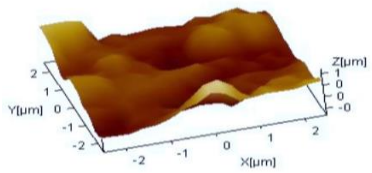
Ti64 NaOH SBF BPs	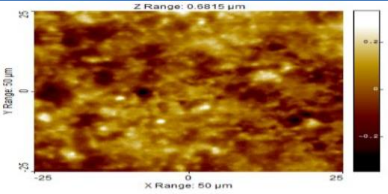	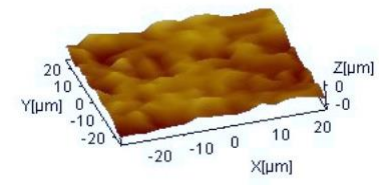

Figure 4.3: Representative 2D and 3D of AFM images of the different tested Ti64 samples, where the SPF process seems to increase the Ra value on the Ti64 samples, the immersion in SBF seems to increase the surface roughness of these surfaces due to the deposition of apatite like layer. Alendronate deposition seems to decrease the surface roughness by forming a more uniform layer on the surface.

4.3.3. Fourier Transform Infrared spectroscopy (FTIR)

Fourier transform infrared spectroscopy (FTIR) was used to analyse the surface chemical composition of the treated surfaces. Although it was very difficult to detect an apatite layer on the treated surfaces probably due to the low ratio of Ca/P on the surfaces which were obtained from the SEM/EDS analysis. FTIR analysis of invested samples simulating superplastic forming process which were subjected to immobilisation of bisphosphonate showed the presence of P-O and -NH_2 groups on the surfaces which are an indication of the presence of alendronate arising from the phosphate and the amino group. Figure 4.4 shows the different peaks, which were detected from the FTIR spectrum of CpTi SPF BPs sample as an example.

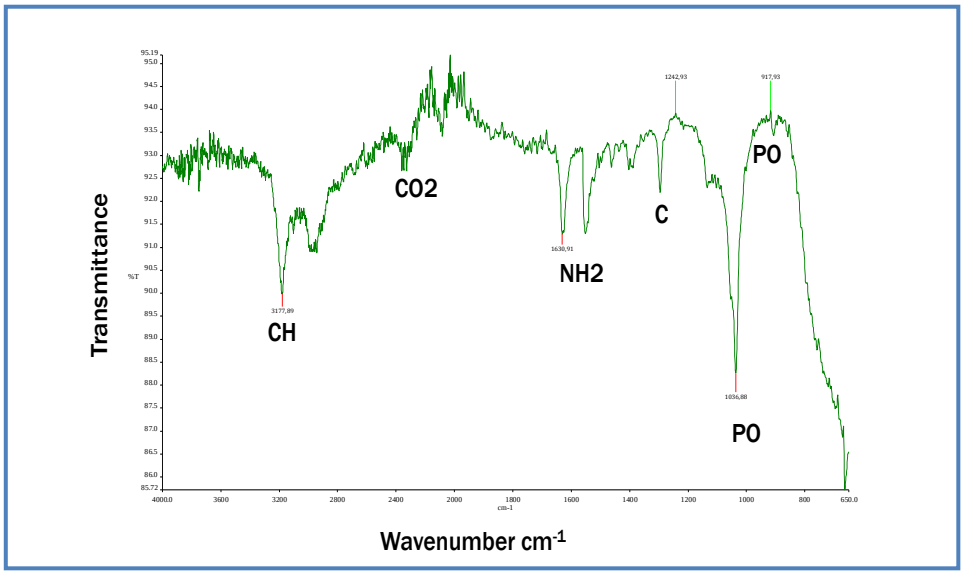

Figure 4.4: FTIR spectrum of CpTi, which was subjected to immobilization of sodium alendronate bisphosphonate after it was invested and heated simulating superplastic forming process (SPF).

4.3.4. Scanning Electron Microscopy/Energy Dispersive X-ray Analysis (SEM/EDS)

Qualitative surface characterization of the titanium surface topography was visualised using electron microscopy (SEM). The SEM images of the samples treated with NaOH, invested surfaces, and the untreated (Ti as received) surfaces morphologies of CpTi and Ti6Al4V titanium discs are shown in Figures 4.5 and 4.6 respectively. The CpTi and Ti64 titanium control samples were relatively smooth with some imperfections and scratches due to the sandblasting and polishing processes.

The simulated superplastic forming process (SPF) samples showed evidence of deposition of a layer. As titanium is a highly reactive metal that under normal ambient conditions is protected by a passive oxide film, at high temperatures such as the SPF process temperature, the oxide becomes soluble in the metal, and the protection is decreased, so reaction with the investment is expected to occur. The simulated superplastic forming process (SPF) CpTi and Ti64 samples which had been immersed in simulated body solution (SBF) for 10 days showed a deposition of apatite like layer on their surfaces according to the EDS analysis of these surfaces which showed the presence of Ca and P ions, whilst the CpTi and Ti64 which were not subjected to SPF treatment prior to SBF interaction did not show the formation of an interaction layer. The EDS analysis of the surfaces, which were treated with sodium alendronate (bisphosphonate) showed the presence of Na, P, O and N, which is an indication of the presence of these molecules on the surface as the chemical structure of sodium alendronate is $C_4H_{12}NNaO_7P_2 \cdot 3H_2O$. The Ca/P atomic ratio for all samples is summarized in Table 4.4.

Sample Name	**Ca**	**P**	**Ca/P (Atomic %) Ratio**
CpTi SPF SBF 10D	3.29	3.72	1.13
CpTi SPF SBF 10D BPs	1.54	1.69	0.9
CpTi NaOH SBF 10D	7.19	9.04	1.26
CpTi NaOH SBF 10D BPs	1.90	1.85	1.10
Ti64 SPF SBF 10D	4.95	5.63	1.14
Ti64 SPF SBF 10D BPs	2.43	2.56	0.94
Ti64 NaOH SBF 10D	5.38	7.23	1.34
Ti64 NaOH SBF 10D BPs	2.35	2.64	0.89

Table 4.4: Concentrations of Ca and P (Atomic %) of CpTi and Ti64 samples

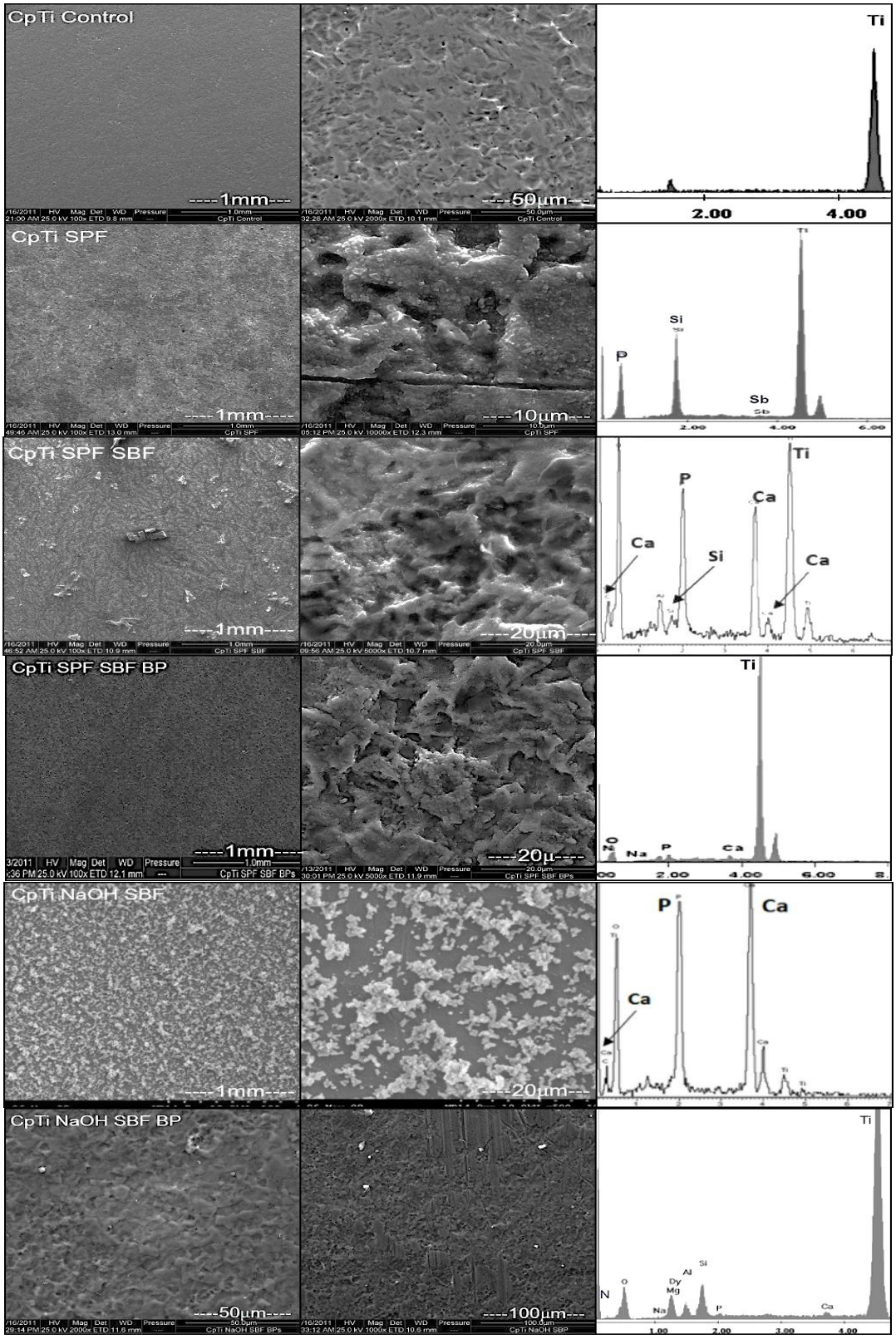

Figure 4.5: SEM/EDS images of CpTi control, CpTi surfaces which were subjected to simulated superplastic forming process (SPF) only and CpTi discs SPF and immersed in simulated body fluid SBF for 10 days with subsequent immobilization with bisphosphonate (sodium alendronate)

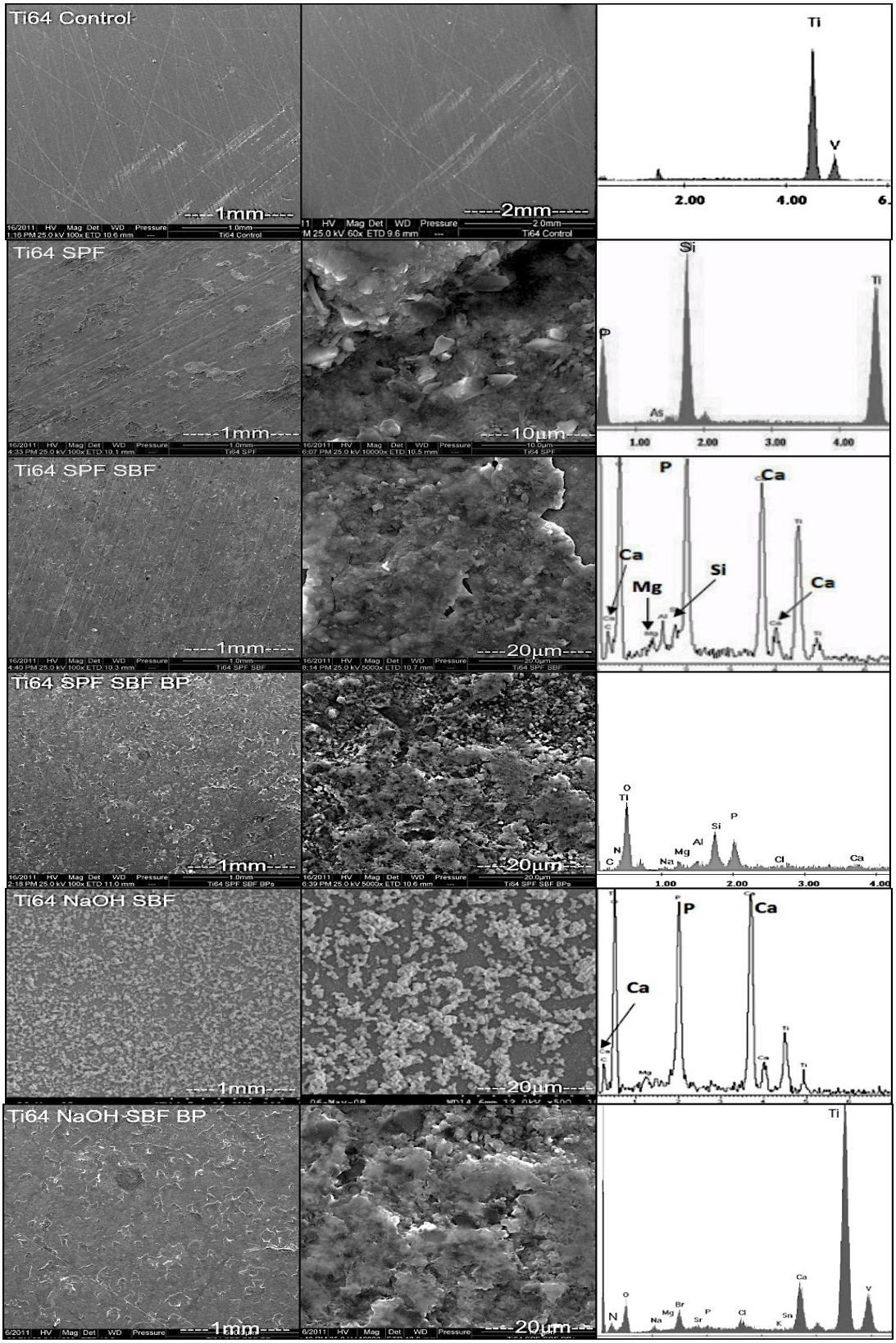

Figure 4.6: SEM/EDS images of Ti64 control, CpTi surfaces which were subjected to simulated superplastic forming process (SPF) and CpTi discs which were subjected to simulated superplastic forming process (SPF) and immersed in simulated body fluid SBF for 10 Days with subsequent immobilization with bisphosphonate (sodium alendronate)

4.3.5. Evaluation of Cytotoxicity Indirect Method (MTT)

This assay was used to determine the effect of any potential toxic leachables from the surface treatments carried out on the Ti and alloy specimens on cells.

MTT, Day 1 Exposure:

Samples were eluted for 24 hours for indirect exposure, where two elution time points were obtained (24h elution and 72h elution), in order to detect if any leachable products could affect the cells behaviour. After one day of MTT exposure, various absorbance levels were observed between the different groups (Figure 4.7)

For the CpTi samples, at the 24h elution time point, a comparison of the samples was made to negative control comprising culture medium+cells. All samples showed higher cell metabolic activity compared to the negative control. CpTi samples were heated to simulate SPF and then immersed in SBF solution for 10 days, followed by immobilization of sodium alendronate accompanied with the samples together with SPF treatment only with sodium alendronate immobilisation, showed the highest cell metabolic activity. A reduction in cell metabolic activity was observed after following exposure to 72h of eluants, in all samples, particularly, CpTi samples which were heated simulating (SPF). The drop in the cell activity was indicative of a fall in cell metabolic activity resulting from a potential leachable from the test material in the elution fluid. The results were statistically analysed and showed that there was no significant differences ($p>0.05$) in osteoblast cells response between the negative control (medium+ cells) and the different surface treatment surfaces tested

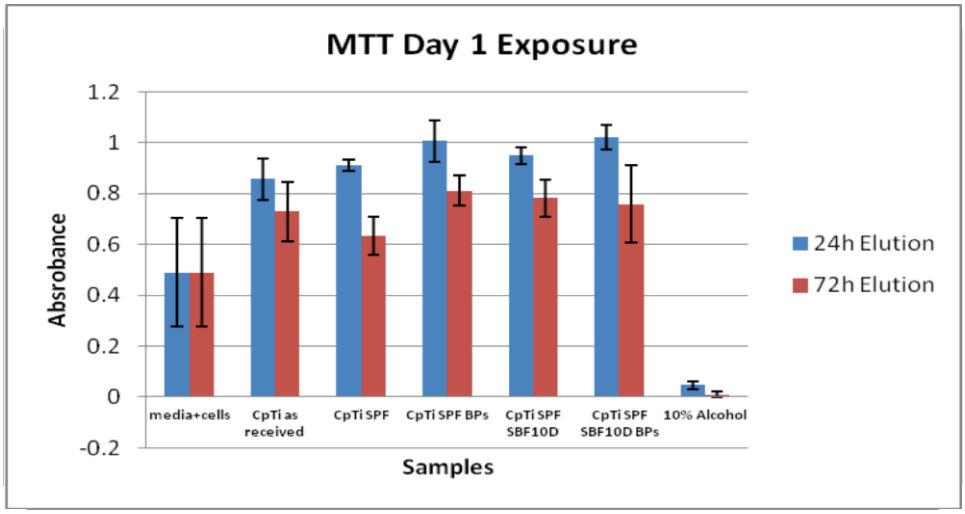

Figure 4.7: Evaluation of Cytotoxicity Indirect Method/ MTT Day 1 Exposure of CpTi test samples; showing levels of intensity of absorbance at 570nm of the CpTi samples at 24h and 72 elutions, expressed as mean absorbance ± S.D (n=4); the statistical significance was predetermined at $p< 0.05$

For the Ti64 samples, at the 24h elution time point, a comparison of the samples was made to the negative control medium +cells sample. All samples showed higher cell metabolic activity than the negative control that was not statistically significant. Ti64 samples, which were subjected to simulated SPF treatment and then immobilised with sodium alendronate, showed the higher cell activity followed by the Ti64 samples, which were heated simulating SPF, and then immersed in SBF solution for 10 days. At 72h elution time, there was a decrease in the cell metabolic activity obtained for all test samples. The drop in the cell activity was indicative of a fall in cell metabolic activity resulting from a potential leachable from the test material in the elution fluid (Figure 4.8). The results were statistically analysed and showed that there was no significant differences ($p>0.05$) in osteoblast cells response between the negative control (medium+ cells) and the different surface treatment surfaces tested.

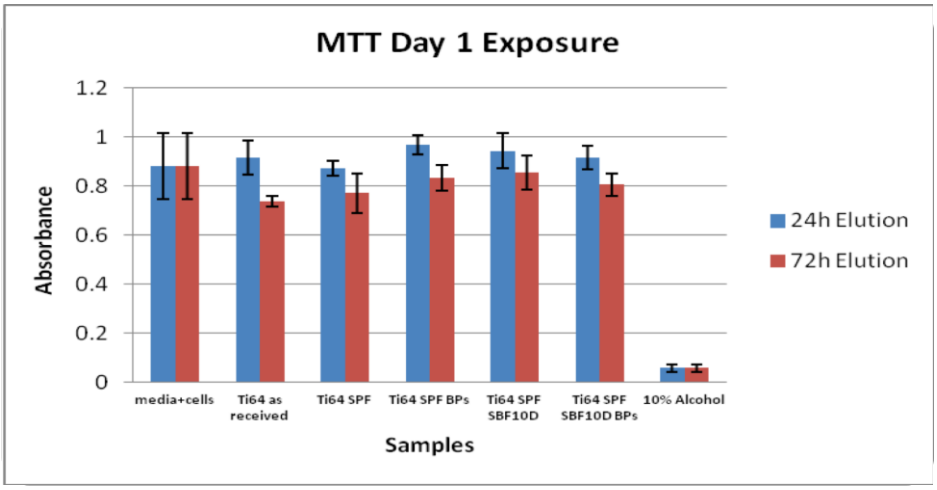

Figure 4.8 : Evaluation of Cytotoxicity Indirect Method/ MTT Day 1 Exposure of Ti64 test samples; showing levels of intensity of absorbance at 570nm of the Ti64 samples at 24h and 72 elutions, expressed as mean absorbance ± S.D (n=4); the statistical significance was predetermined at $p< 0.05$

MTT, Day 3 Exposure:

Samples were eluted for 72 hours for indirect exposure, where two elution time points were measured (24h elution and 72h elution), in order to detect if any leachable products could affect the cells behaviour. After 3 days of MTT exposure, variable cell metabolic activity was observed between the different groups.

For the CpTi samples, at the 24h elution time point, a comparison of the samples was made to negative control (medium+cells). All samples showed higher cell metabolic activity than the negative control. CpTi as received, showed the higher cell activity, and followed by CpTi samples, which were heated simulating SPF. At 72h elution time,

there was an increase in the cell metabolic activity obtained by all the samples, except the CpTi as received samples, which was not significant statistically (Figure 4.9). There was no statistically significance between the different samples compared to the control.

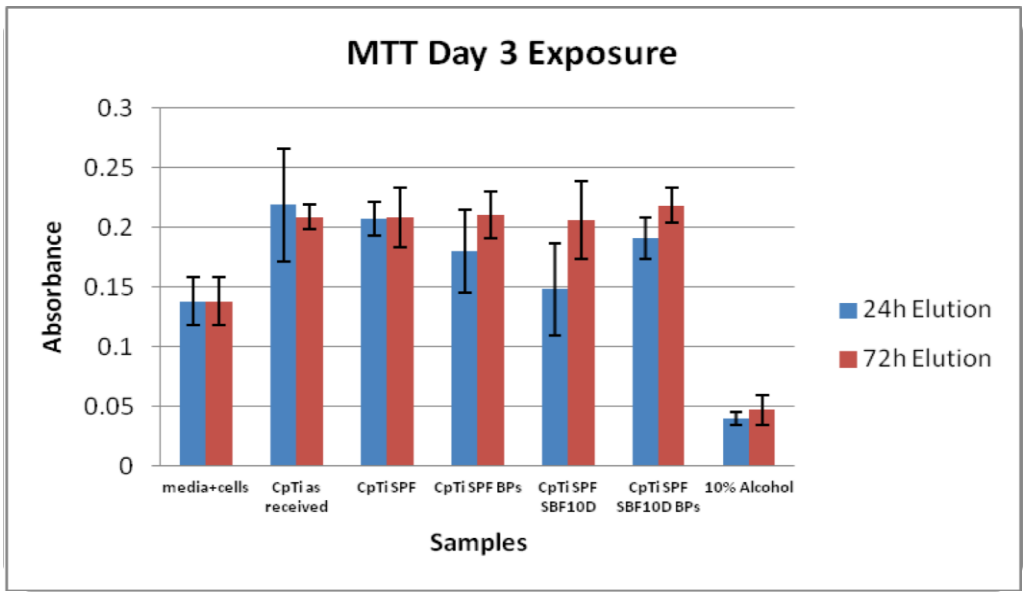

Figure 4.9: Evaluation of Cytotoxicity Indirect Method/ MTT Day 3 Exposure of CpTi test samples; showing levels of intensity of absorbance at 570nm of the CpTi samples at 24h and 72 elutions, expressed as mean absorbance ± S.D (n=4); the statistical significance was predetermined at p< 0.05

For the Ti64 samples, at the 24h elution time point, a comparison of the samples was made to negative control (medium+cells). Most of samples showed reduction in the metabolic cell activity compared to the negative control, where the Ti64 samples which were heated simulating the SPF process then immersed in SBF solution for 10 days and subjected to immobilisation of sodium alendronate showed the best cell metabolic activity and higher than the negative control. At 72h elution time point, there was a significant drop in the cell activity for all samples, except for the Ti64 samples that were heated simulating SPF process and immersed in SBF solution for 10 days. The drop in the cell activity was indicative of a fall in cell metabolic activity resulting from a potential leachable from the test material in the elution fluid (Figure 4.10). There was significant drop ($p<0.05$) in osteoblast cells response to sample surfaces after 72h of eluant time for all samples except Ti64 SPF SBF samples compared to the negative control (medium + cells).

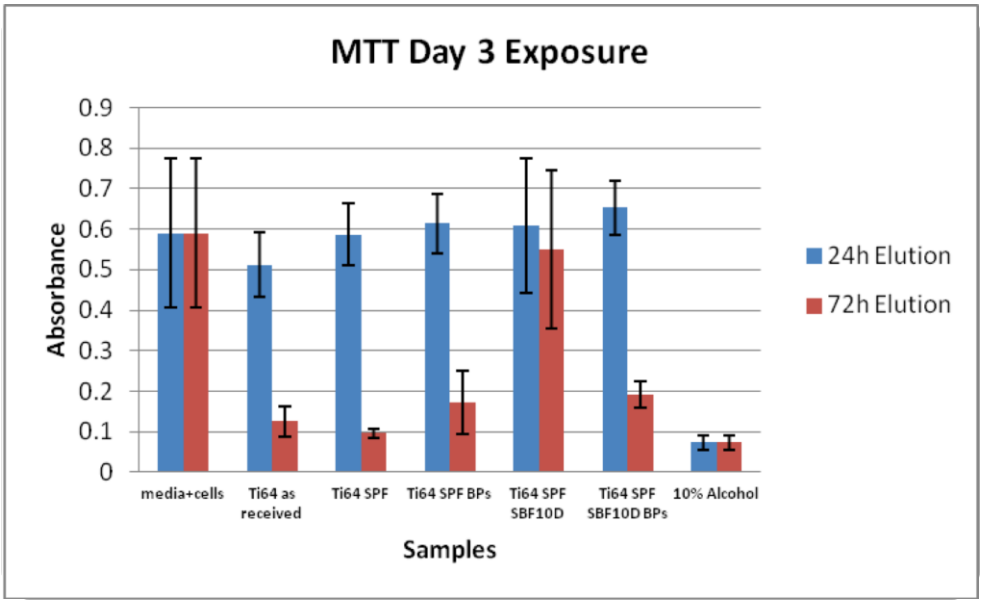

Figure 4.10 : Evaluation of Cytotoxicity Indirect Method/ MTT Day 3 Exposure of Ti64 test samples; showing levels of intensity of absorbance at 570nm of the Ti64 samples at 24h and 72 elutions, expressed as mean absorbance ± S.D (n=4); the statistical significance was predetermined at p< 0.05

4.3.6. Assessment of cell differentiation – Alkaline Phosphatase Assay

Alkaline phosphatase (ALP) activity was measured as an early indicator of differentiation of primary aHOB cells seeded directly onto the titanium samples. The specific activity of ALP measured from the osteoblast cell lysate was investigated over a period of 28 days for 6 times points (Days 1, 3, 7, 14, 21 and 28).

The ALP activity of cells on the CpTi test samples (Figure 4.11) showed a general increase from day 1 to day 28. The control specimens of CpTi and the thermanox samples showed increasing ALP activity with time, which peaked at 28 days, whereas the experimental groups exhibited some variation. The bisphosphonate immobilized surfaces showed a significant drop in ALP activity at day 28 for both CpTi NaOH SBF 7 and 10 Days compared to the positive control (thermanox). There was no significant difference in ALP activity on BPs immobilized surfaces compared to the one with no BPs, except for CpTi NaOH SBF10D BPs, where there was a significant drop in ALP activity at day 28 compared to the same treated surfaces with no bisphosphonate.

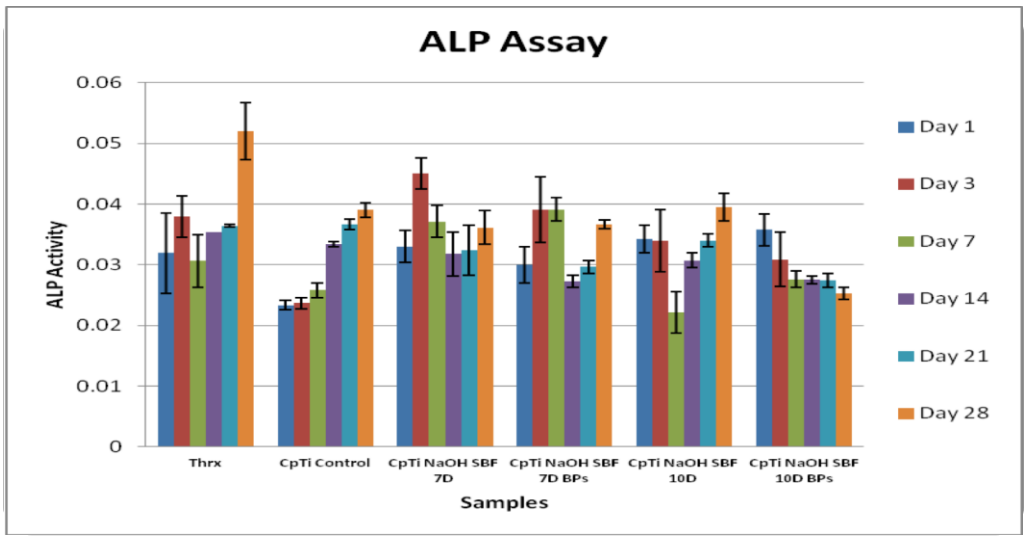

Figure 4.11: Evaluation of Differentiation of Osteoblast Cells / ALP Assay of CpTi titanium disks which have been treated with NaOH and immersed in SBF for 7 and 10 days, and then subjected to immobilisation of 2mg/ml sodium alendronate. The data represents the average for each group as mean absorbance ± SD (n=8) (p<0.05).

The ALP activity of cells cultured on the Ti64 samples (Figure 4.12) showed a general increase on the different test samples from day 1 to day 28. All the samples showed ALP activity peak at day 28 except for the test samples, which were NaOH treated then immersed in SBF for 10 days, where it peaked at day 1. There was no significant difference between bisphosphonate-immobilised surfaces compared to the surfaces with no bisphosphonate.

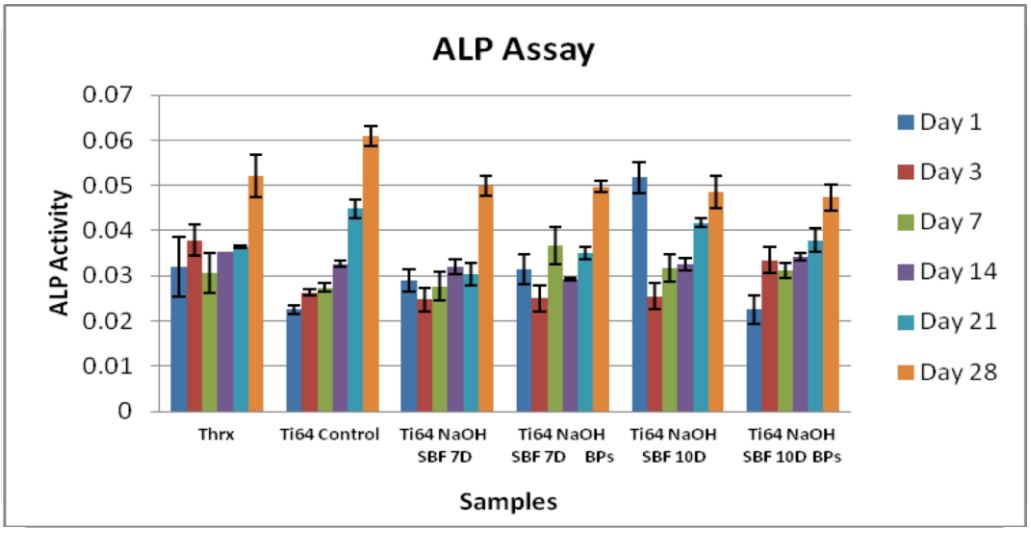

Figure 4.12: Evaluation of Differentiation of Osteoblast Cells / ALP Assay of Ti64 titanium disks which have been treated with NaOH and immersed in SBF for 7 and 10 days, and then subjected to immobilisation of 2mg/ml sodium alendronate. The data represents the average for each group as mean absorbance ± SD (n=8)

The ALP activity of cells cultured on the CpTi samples (Figure 4.13) showed a general increase on the different samples from day 1 to day 28. The aHOB cell differentiation measured by ALP activity peaked at day 28 for all samples. The CpTi surfaces, which were immobilised with bisphosphonate after simulation of superplastic forming process (SPF) showed close values of ALP activity between the different time points. The bisphosphonate on these surfaces showed a stable ALP activity without a significant decrease in the cell activity from day 1 to day 14, where at day 21 and day 28 there was a significant decrease in ALP activity on the bisphosphonate immobilised surfaces compared to none immobilised one.

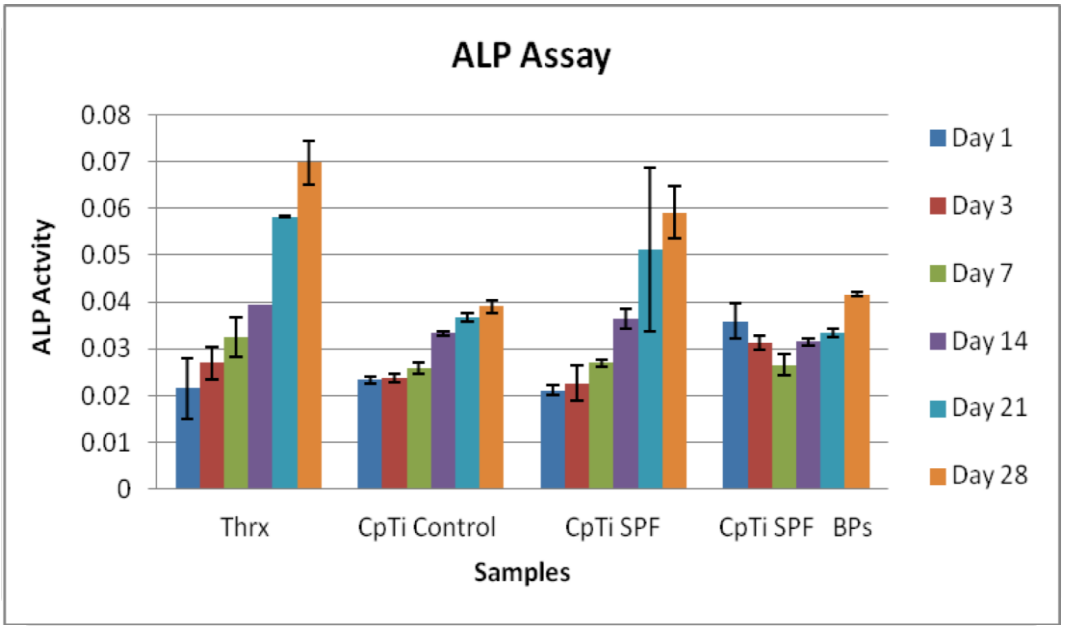

Figure 4.13: Evaluation of Differentiation of Osteoblast Cells / ALP Assay of CpTi titanium samples, which were simulated superplastic forming SP, and then subjected to immobilisation of 2mg/ml sodium alendronate. The data represents the average for each group as mean absorbance ± SD (n=8)

The ALP activity of the cells cultured on of the Ti64 samples (Figure 4.15) showed a general increase in the ALP activity on the different samples from day 1 to day 28. The control, Ti64 control, and the simulated superplastic forming process (SPF) samples showed a peak of ALP activity at day 28. The bisphosphonate immobilised surfaces showed a significant increase in ALP activity at day 1 , while there was a significant decrease in ALP activity from day 7 till day 21 compared to surfaces which were not immobilised with bisphosphonate.

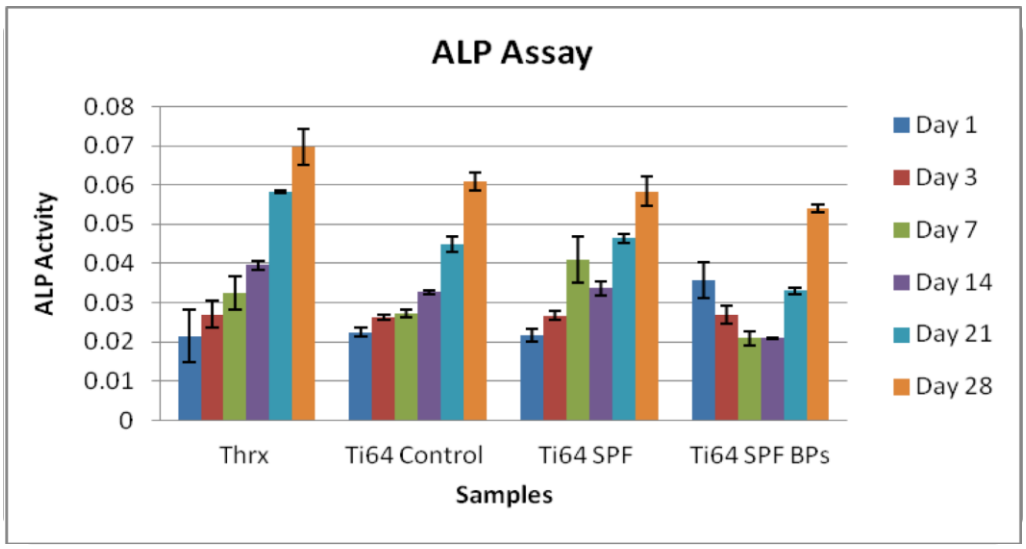

Figure 4.14: Evaluation of Differentiation of Osteoblast Cells / ALP Assay of Ti64 titanium samples, which were simulated superplastic forming SPF, and then subjected to immobilisation of 2mg/ml sodium alendronate. The data represents the average for each group as mean absorbance ± SD (n=8)

4.3.7. Assessment of cell viability – DNA Activity Assay

DNA is a measure cell turnover and proliferation, hence an indicator of cell activity in the presence or absence of a test material. DNA assay was carried out on the different surface treated samples of CpTi and Ti6Al4V alloy at 6 time points (Days 1, 3, 7, 14, 21 and 28).

Total DNA of cells cultured on the CpTi samples (Figure 4.15) showed a varied response of osteoblast cell proliferation in correspondence to the different treated titanium surfaces. The control, CpTi control and CpTi that were immersed in SBF solution and the NaOH pretreated CpTi samples which were then immersed in SBF showed that cell proliferation activity increased through the time points till 28 days. The immobilisation of sodium alendronate bisphosphonate on the CpTi samples, which were pre-treated with NaOH and then immersed in SBF for 7 and 10 days, showed a decrease in the cell proliferation activity as shown by the drop in DNA at 28 days. Total DNA of aHOB cells cultured on the NaOH pre-treated surfaces which were immersed in SBF for 7 days and subjected to immobilisation of bisphosphonate showed a significant increase at day 3 and a significant decrease at day 21 and day 28 compared to the non-alendronate containing surfaces, a similar trend being observed on the NaOH pre-treated surfaces which were immersed in SBF for 10 days.

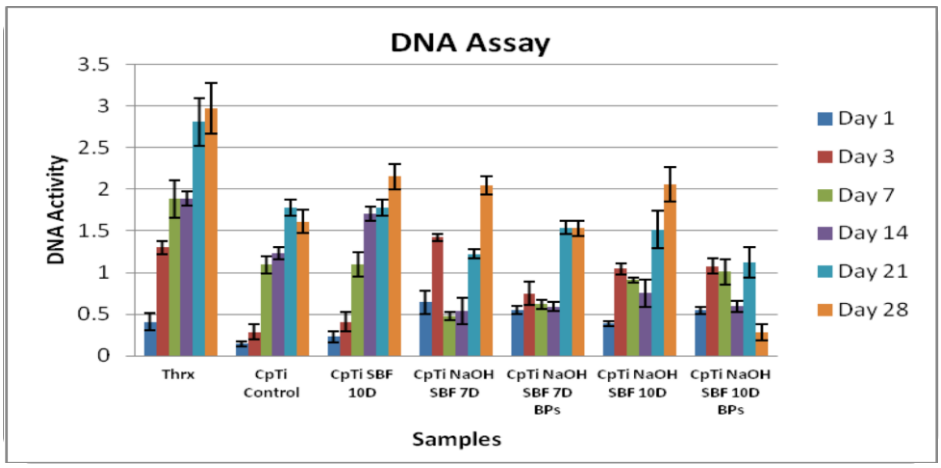

Figure 4.15: Evaluation of Proliferation of Osteoblast Cells / DNA Assay of CpTi Samples which have been treated with NaOH and immersed in SBF for 7 and 10 days, and then subjected to immobilisation of 2mg/ml sodium alendronate. The data represents the average for each group as mean absorbance ± SD (n=8)

Total DNA of osteoblast cells cultured on the Ti64 samples (Figure 4.16) showed a varied response of proliferation in compared to the different treated titanium surfaces. All samples showed a general increase in total DNA of the osteoblast cells which all peaked at day 28. Total DNA of aHOB cells cultured on the NaOH pre-treated surfaces which were immersed in SBF for 7 days and subjected to immobilisation of bisphosphonate showed a significant decrease at day 21 and a significant increase at day 28 compared to the non BP containing surface, while the NaOH pre-treated surfaces which were immersed in SBF for 10 days and subjected to immobilization of bisphosphonate, showed a significant decrease at day 21 compared to the non BP containing surface.

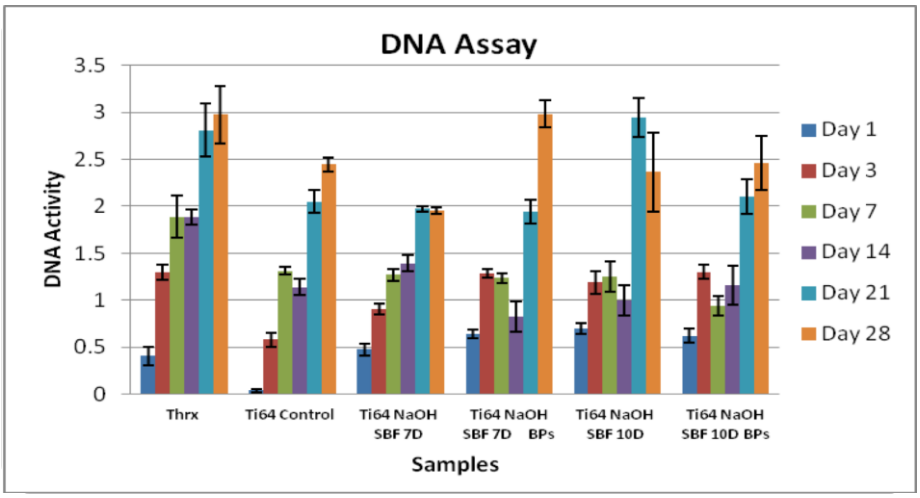

Figure 4.16: Evaluation of Proliferation of Osteoblast Cells / DNA Assay of Ti64 Samples which have been treated with NaOH and immersed in SBF for 7 and 10 days, and then subjected to immobilisation of 2mg/ml sodium alendronate. The data represents the average for each group as mean absorbance ± SD (n=8)

Total DNA of cells cultured the CpTi samples (Figure 4.17) showed a general increase in osteoblast cell proliferation compared to the different treated titanium surfaces. The immobilisation of sodium alendronate bisphosphonate on the CpTi samples that were simulated superplastic forming process (SPF) seems to significantly increase the cell proliferation activity during the 28 days. The immobilisation of bisphosphonate on simulated superplastic forming surfaces significantly increased the DNA activity of osteoblast cells on these surfaces at days 3, 21 and 28.

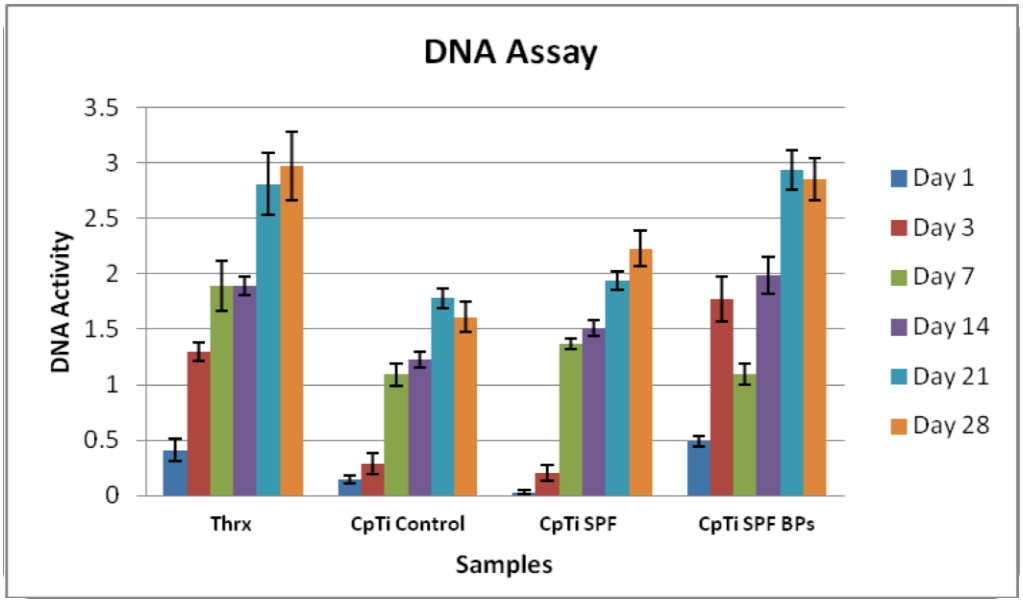

Figure 4.17: Evaluation of Proliferation of Osteoblast Cells / DNA Assay of CpTi Samples, which were simulated superplastic forming SPF and then subjected to immobilisation of 2mg/ml sodium alendronate. The data represents the average for each group as mean absorbance ± SD (n=8)

Total DNA of cells cultured on the Ti64 samples (Figure 4.18) showed a general increase in the response of osteoblast cell proliferation compared to the different treated titanium surfaces. The immobilisation of sodium alendronate bisphosphonate on the Ti64 samples, which were, simulated superplastic forming process (SPF) showed a significant increase in the cell proliferation activity during the 28 days.

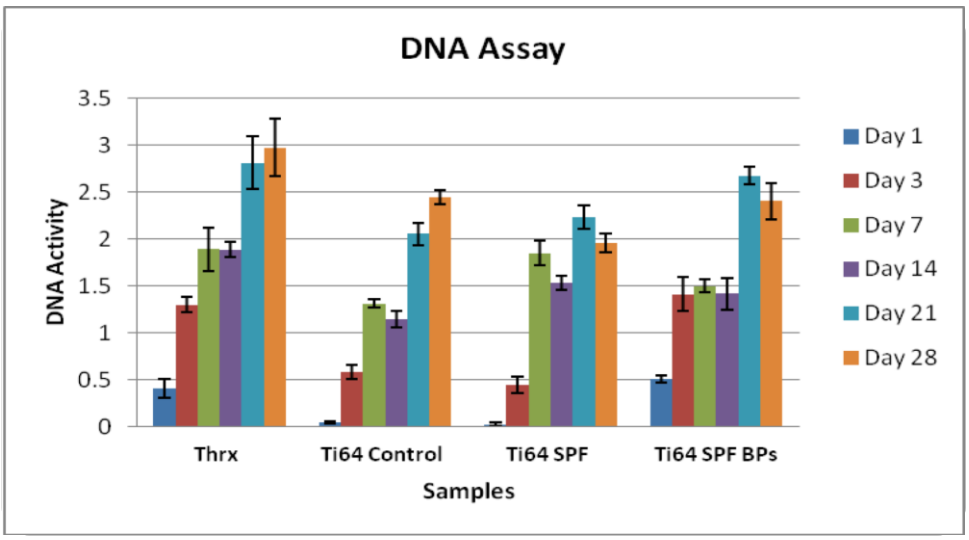

Figure 4.18: Evaluation of Proliferation of Osteoblast Cells / DNA Assay of Ti64 Samples, which, were simulated superplastic forming SPF and then subjected to immobilisation of 2mg/ml sodium alendronate. The data represents the average for each group as mean absorbance ± SD (n=8)

4.4. Discussion

There are different methods employed for the deposition of thin film coating of hydroxyapatite, such as plasma spraying [170, 171], sputtering [172], dip coating [173, 174], electrophoretic deposition [175] and electrochemical deposition [176]. As most coating techniques employ high temperatures due to post sintering requirements, this can lead to deterioration of the metallic substrate [177] and inclusion of drugs or biological molecules are not possible.

Surface topography of implant is important for the osseointegration process, and modifying the surface of implants may enhance the progress of bone formation [170, 171]. It is known that changing the surface topography influences the extent of bone formation at the implant–bone interface [172, 174, 175]. In particular, modification of implant surface through hydroxyapatite (HA) coating leads to direct chemical bonding of the implant surface with bone soon after implantation [176, 177] which enhances rapid bone formation and long-term stability because of its improved osteoconductive properties. In recent years, there has been an increasing interest in the formation of a bioactive surface layer directly on titanium substrate, which will induce apatite formation in the living environment or simulated body fluid (SBF) and this technique was investigated in this study to further localise bisphosphonate on the coated Ti surfaces. Thus, the CpTi and Ti-6Al-4V discs were prepared to obtain surfaces with an average Ra values close to 0.5 µm and then subjected to different surface treatments to follow up with immobilization of sodium alendronate. With roughness parameter kept constant at the start, the subsequent surfaces obtained were due to the different surface treatments, however, the Ra values obtained from AFM measurements showed a varied range which may be attributed to scanning of small sections of the entire surface in comparison to surface profilometry.

As expected, the immersion of the discs in simulated body fluid (SBF) irrespective of SPF treatment yielded a rougher surface that is attributed to the formation of the apatite layer (Figures 4.8 and 4.9). This is further confirmed by the SEM-EDAX that provides evidence of calcium and phosphate species; the changes at this stage due to the surface chemistry rather than the differences in surface roughness. EDAX analysis measured a range between 1.13 and 1.34 Ca/P ratios in the bioactive layer for titanium samples that were soaked in simulated body fluid (SBF) regardless of the pre-surface treatment. These Ca/P ratios much lower and vary from the stoichiometric ratio in HA of 1.67, which may be related to the other calcium phosphates such as TCP. The formation of the calcium phosphate layer thought to be induced by the super-saturation of calcium phosphate salts within the medium. A deposition process commences on immersion in the SBF solution due to a heterogeneous nucleation.

The groups that were just subjected to SPF simulation showed evidence of an interaction layer from the investment (Chapter two) and the binding of the sodium alendronate to the surface was expected to occur via the calcium phosphate layer formed as a result of the interaction of the investment material. Immobilisation of sodium alendronate on the alkaline treated and invested surfaces resulted in a lower the Ca/P ratio, which might be due to the high affinity of bisphosphonate to interact with calcium ions Ca^{++} thus resulting in a decrease in the CaP contents on the surface. The formation of an apatite layer on titanium and its alloys subjected to alkali and heat treatment has been reported in the literature [88, 168, 182]. The NaOH treatment of the titanium produces a bioactive sodium titanate layer on the surface, and when titanium immersed in SBF, it immediately releases a large amount of Na^{+} ions into the SBF via exchange with H_3O^{+} ions and causes an appreciable pH increase in the fluid, as a result of this ion exchange, the alloy formed Ti-OH groups on its surface. The Ti-OH groups then immediately incorporate calcium ions in the fluid to form a calcium titanate. The calcium titanate incorporates the phosphate ions in the fluid to form an amorphous calcium phosphate, which later converts into crystalline apatite, growing spontaneously by consuming the calcium and phosphate ions in the fluid.

Yousefpour et al. [177] investigated the formation of bioactive layer alkaline-acid treated titanium in simulated body fluid, and showed that different Ca/P ratio can be obtained according the treatment of the surface. An EDAX analysis of the bioactive layer of the different treated methods showed a Ca/P ratio 0.6 on alkaline treated surfaces with 5M NaOH stating that it could be due to other forms of calcium phosphates such as TCP. The results obtained in this study were similar with the EDAX analysis of Ca/P ratio on alkaline treated surfaces reported by Yousefpour et al. [177].

The properties of individual bisphosphonates depend on the two covalently bound side chains (-OH and $–(CH_2)_3NH_2$) attached to the central carbon atom, the -OH substituent shows additional capability to coordinate calcium, such as hydroxyl (OH) or amino (NH2), provide enhanced chemisorption to the mineral, most likely through tridentate binding to calcium [216]. In the current study, sodium alendronate bisphosphonate was immobilised on the different treated surfaces, being a most commonly used antiresorptive pharmacological agents, and it is a nitrogen-containing bisphosphonate and, unlike other bisphosphonates it does not impair mineralization. Furthermore, it

meets the requirement for a good bond formation between the surface and the molecule according to previous studies. Nancollas et al [217] demonstrated a rank order of zoledronate > alendronate> ibandronate > risedronate > etidronate > clodronate, depending on the binding affinity to synthetic hydroxyapatite (HA). The same rank was later reported for carbonated apatite by Henneman et al. and Nancollas et al. [218].

The concentration of bisphosphonates needs to be carefully determined because an increase in peri-implant bone density has been reported to be bisphosphonate concentration-dependent. Moreover, an unexpected potential adverse effect of these antiresorptive drugs is a possible association with the osteonecrosis of jaw bone [215]. Naidu et al. [219] studied the effect of different concentrations of alendronate and zendronate on osteoblast cells in vitro. He used 10^{-6} mol/L, 10^{-5} mol/L, 10^{-4} mol/L, and 10^{-3} mol/L concentrations of both BPs. It was found that the best concentration was 10^{-5} mol/L, where higher concentrations seemed to have a cytotoxic effect on the cells. A recent study by Sun et al [220] demonstrated the effect and cytotoxicity of five different concentrations of sodium alendronate on MG36 cells (Cells + 10^{-8} M, 10^{-7} M, 10^{-6} M, 10^{-5} M, 10^{-4} M). It was found that alendronate at 10^{-5} M or higher was toxic to the cells, and alendronate at 10^{-8} M to 10^{-6} M didn't affect the MG36 cells significantly. In this current study, a concentration of 2mg/ml ($6x10^{-3}$M) sodium alendronate was used to prepare the required solution to be immobilised on the treated surfaces of titanium, according to some preliminary testing on some samples.

Further analysis of the chemical characterisation of the alendronate immobilised on SPF CpTi surface was carried out using FTIR analysis. Spectra of the CpTi which were invested and subjected to immobilisation of bisphosphonate, showed a typical spectra of the bioactive layer of the treated titanium. The split bands, mainly at 917 and 1036 cm^{-1}, seem to agree with the formation of a well-crystallized apatite, and a significant concentration of amine group (NH_2) was as observed from the intensity of the stretching bands of about 1630 cm^{-1}, which is an indication of the presence of alendronate.

The roughness parameter obtained using the profilometer for the different treated titanium surfaces in this study showed homogenous surfaces with an average Ra values close to 0.5 µm. Different values have been observed between the samples due to the different treatments that the surfaces were subjected. The CpTi control had the highest Ra of ~0.404 µm followed by the Ti64 SPF SBF of 0.431 and the CpTi simulated superplastic forming process (SPF), which were immersed in SBF solution of 0.389 µm compared to the other samples. The average roughness of the CpTi discs

after the various treatments indicate that the SPF procedure decreases the Ra value, which may be due to the formation of an interaction layer with the investment, however the alloy shows the opposite trend. It is possible that the temperature of the SPF simulation (900° C) alters the chemical composition and forms of the titanium and its alloy which obviously affecting the surface roughness of the titanium. CpTi is a dimorphic allotrope whose hexagonal alpha form changes into a body-centred cubic (lattice) β form at 882 °C and remains fairly constant for the β form until reaching the melting temperature (1668 °C). While the Ti64 alloy is an alpha-beta metal which contains both phases. Usually, the expectation would be that the alloy grades would show reduced ductilities compared with the CpTi. However, at high temperatures, an unexpected behaviour is observed in Ti64 in the SPF condition, because of an interesting change in deformation mechanism leading to expectedly high ductilities resembling those of amorphous glasses rather than crystalline metals. As these surfaces are invested in phosphate bonded investment (Deguvest) the magnesia content (and presumably phosphate also) becomes soluble in the metal starting in the range between 750 °C and 1300 °C which is lower than the melting temperature of the titanium, and this reaction layer can alter the surface roughness of the surface according to the ductility of the metal at higher temperature.

Thus, the surface roughness parameters evaluated by Ra value were generally higher on the Ti64 surfaces than the CpTi ones. The invested Ti64 titanium discs showed a high surface roughness compared to the CpTi invested ones, as well as compared to the control as expected due to the formation of an interaction layer that is non-uniform. The interaction of the discs with simulated body fluid lead to a rougher surface attributed to the deposition of the apatite layer, however, the chelation of the alendronate over the entire surface may result in lowering the average roughness.

With roughness parameter kept constant, the Ra values obtained from AFM measurements showed a varied range between 0.08 and 0.213 µm. These values are lower than the values obtained using the profilometer instrument, which may be attributed to scanning of small sections i.e. 20 µm x 20 µm of the entire surface in comparison to surface profilometry, where the line measurement was about 4 mm. Therefore, it is probable that the area measured with AFM contains within the valley, bump, or fell on the flat surface. A study by Bathomarco et al. [196] has shown that roughness is a scale dependent parameter, where they showed that the roughness value in all their titanium samples presents a similar trend, i.e. the roughness of all samples is seen to increase for scan length in the range from 10 µm to approximately 50 µm. they concluded that only when the scan size/length exceeded 50 µm, the surface roughness becomes constant and is independent on the scanning length.

In this study, the viability, proliferation and differentiation evaluation of primary aHOB cells on the different treated titanium samples were examined for cell growth, changes in metabolic activity and biocompatibility. MTT test, allowed the indirect cytotoxicity to be assessed, and retention of phenotypic characteristics was determined by measuring alkaline phosphatase activity and DNA for cell turnover and growth. Indirect cytotoxicity tests performed) showed a reduction in cellular metabolic activity following exposure of cells for 72 hours in eluants. This reduction was possibly due to some toxic leachables or contaminant released from the test materials. This toxic materials leaching are likely to be either the grinding media from the cleaning process, or the investment material debris from the die or the mould, or the presence of Na^+ ions from NaOH treatments, which may not have been cleaned sufficiently from the surface. However, the eluants released from the test materials in the 24 and 72 hours eluted media did not show any detrimental effect on the aHOB cells, as the cells continued to proliferate and remained metabolically active.

The expression of alkaline phosphatase ALP was used as one of the aHOB phenotypic biochemical marker of differentiation on the titanium surfaces. aHOB cell differentiation was observed on all different treated titanium surfaces, as indicated by ALP production. The expression of ALP over the observation period of 28 days indicated that the osteoblasts on the control surface and the invested surfaces reached a peak on day 28, except for the CpTi and Ti64 NaOH treated surfaces, which were immersed in SBF in which they reached a peak earlier between day 7 and day 21. This is most probably due to the presence of apatite-like layer on the surface of these samples, which was induced by the SBF solution, as this layer can provide a favourable surface to enhance the osteoblast differentiation earlier than cells cultured on the other test surfaces. These findings are in accordance with a very recent study by Lee et al. [198], which showed that heat treated titanium alloy surfaces exhibited a higher ALP activity than non-heated surfaces. The bisphosphonate immobilised surfaces which were pre-treated with NaOH and immersed in SBF, showed a significant increase in ALP activity at day 28 compared to the non immobilised one, while there was a significant decrease in ALP activity after day 21 on invested surfaces which where immobilised with bisphosphonate.

The cellular proliferation behaviour of aHOB cells was evaluated by measuring total DNA synthesis. The results of the DNA production for the current study demonstrated that aHOB cells on the invested titanium samples was increased throughout the entire period of investigation and comparable with that of negative control (Thx). The DNA activity of aHOB cells on the NaOH pre-treated Ti64 surfaces which were immersed in SBF for 7 days and subjected to immobilisation of bisphosphonate showed a significant increase at day 3 and a significant decrease at day 21 and day 28 compared to the non-immobilised surfaces, which were observed as well on the NaOH pre-treated surfaces which were immersed in SBF for 10 days. Where the immobilisation of sodium alendronate on the CpTi and Ti64 samples simulated superplastic forming process (SPF) seems to significantly increase the cell proliferation activity during the 28 days, as the immobilisation of alendronate on simulated superplastic forming surfaces significantly increased the DNA activity of osteoblast cells on these surfaces at days 3,21 and 28. This might be due to the surface chemistry of the titanium in contact with investment materials, which may have influenced the aHOB cell adhesion and proliferation. The presence of elements such as phosphorus (P) and magnesium (Mg) on invested titanium surfaces may have contributed to the aHOB cell proliferation behaviour on these surfaces. This is particularly true due to the fact that Mg is an important element for human body function. Studies have shown that the Mg is one of many important elements required for the cell adhesion and proliferation [9].

Most of the studies in the literature [143, 163, 203] are in vivo studies investigating the effect and mechanism of bisphosphonates on living bone tissues, while very few studies investigated the effect of bisphosphonate in vitro on titanium and titanium alloy. Moon et al [138] studied the inhibitory effect of the immobilization of alendronate on initial adherence of osteoclastic cells on titanium surfaces. Bisphosphonates have recently been shown to enhance the proliferation, differentiation, and bone-forming activity of osteoblasts directly [221]. Early studies showed that osteoblastic cells derived from neonatal mice treated with the bisphosphonate incadronate inhibit the differentiation of bone marrow or irritation osteoclast precursors into mature osteoclasts [222]. Also, osteoblastic cells pre-treated with various bisphosphonates inhibited resorption by rat mature osteoclasts [223]. Recently more studies were carried out on the effect of BPs on osteoblastic function, for example Boanini et al [216] demonstrated the effect of zoledronate containing hydroxyapatite nanocrystals (HA-ZOL) on osteoblast-like MG-63 cells and human osteoclasts. It was found that the beneficial

influence of bisphosphonates on osteoblast proliferation and differentiation is enhanced when the tests are performed in co-cultures. There are some conflicting studies in the literature. Some studies revealed that culture of osteoblastic cells in the presence of bisphosphonates increased proliferation, stimulated differentiation towards the osteoblastic lineage, and enhanced mineralization [224, 225]. However, other studies showed that bisphosphonates decreased proliferation and inhibit osteoblast differentiation and mineralization [226, 227], or that they inhibited proliferation and increased differentiation [228]. This obvious contradiction is explained by the fact that growth and pro-differentiation effects are exerted at lower concentrations of bisphosphonates ranging from 10^{-9} M to 10^{-6} M, whereas the inhibitory effects are found at concentrations higher than 10^{-5} M [214]. Although the primary action of bisphosphonates is the inhibition of osteoclastic bone resorption [203], there is increasing evidence that bisphosphonates also interact with osteoblasts. The pharmacological mechanism of action of the amino-bisphosphonates relies on interference with the mevalonate pathway through the inhibition of farnesyl pyrophosphate (FPP) synthase enzyme [163].

In conclusion, it was observed that immobilisation of bisphosphonate on alkaline treated surfaces may reduce the cell proliferation, which might be due to the presence of the Na^+ ions, however bisphosphonate immobilised on invested surfaces enhanced the cell proliferation thus enhancing the bone formation.

CHAPTER FIVE

Surface Modification of Commercially Pure Titanium using the Electrohydrodynamic Method

5.1. Introduction

Despite the desirable properties of titanium, surface modification techniques have progressed towards mimicking host bone characteristics to enhance the bone-implant interface. Surface modification technologies, such as grit blasting, chemical etching, plasma spraying, pulsed laser deposition (PLD), and magnetron-sputtering techniques are often utilized to improve the osseointegration ability of titanium as discussed in detail in chapter one. The review of literature highlights several drawbacks associated with each of these methods such as delamination, porous surfaces and non-uniform crystallinity [5, 79].

Direct inorganic coatings constituting of calcium phosphates have been attempted to alter the surface of titanium with plasma spraying techniques (VPS) currently being the most common method for CaP coatings [229]. This method is capable of producing adequate coatings commercially, but VPS requires high temperatures, which means that biological agents such as growth factors, proteins and antibiotics cannot be incorporated into the coating as it is being manufactured, thus there are several inherent limitations that prevent further optimization [107]. In addition, the coatings are also un-patterned, so cannot exploit the observed control and guidance of primary human osteoblast cells onto controlled topographies on titanium substrates. Moreover, a coating thickness of 50-200 μm can result varying in bond strength, non-uniformity of coating density and microcracks from the grit-blast pre-treatment. These can introduce defects that serve as crack initiators in vivo, shortening function, service life and hinder further improvements by patterning of the surface coating [109].

Recently, a new technique, template-assisted electrohydrodynamic atomization (TAEA) spraying, using the principles of electrohydrodynamic atomization spraying, which is an electrically driven jet-based deposition method, has been of considerable interest for surface coatings[9]. The principal behind the process is described in chapter one. Typical coatings for metallic orthopaedic implants are hydroxyapatite (HA) bioceramic coatings, which have been used successfully in orthopaedic applications for several decades to improve biological response in vivo [116]. Ceramic coatings can be successfully applied via VPS due to their high melting points. However, if the coating process temperature is reduced to ambient temperature conditions, a greater range of materials could be used, including biodegradable polymers. Polymers are widely used biomaterials, thus a natural progression of work on template-assisted electrohydrodynamic atomization (TAEA) has potential applications in joint prosthesis coatings, scaffolds for hard and soft tissue engineering, low wear interfaces and orthopaedic fixation tool. Bioactive polymer coatings have exhibited bone-bonding

properties and cell-mediated osteogenesis comparable with that of HA and other calcium-phosphate coatings [116].

Bioactive glasses such as 45S5 Bioglass® is known to develop a mechanically strong interface with bone through the dissolution of the glass network, via the formation of a silica-rich gel. As a consequence a substantial amount of research has focussed on bioactive glasses and glass ceramics for non-load bearing applications in bone healing. 45S5 Bioglass® has been used in over a million patients to repair bone defects in orthopaedics and maxillofacial surgery [230, 231]. One of the commercial success of the clinical application of Bioglass® is its function as an active repair agent in toothpaste, under the name NovaMin® marketed by GlaxoSmithKline, UK. However, Bioglass coatings are not very common due to the fact that at high temperatures the glass undergoes crystallisation. Thus a number of methods such as the synthesis of sol-gel glass, free form fabrication and foaming methods have been used to develop scaffolds for bone substitutes. As described the electrohydrodynamic method does not require high temperatures, thus this method was used to study its potential for coating 45S5 Bioglass® on titanium surfaces.

The aim of the present study was to firstly analyse the responses of three different cell types namely alveolar HOB's, femur HOB's and HOS cells to alendronate as cases of BP-ONJ have been reported in patients on BP therapy. The effect on alendronate on the different cell populations may provide some data that may reflect specific responses and different impact as observed in clinical cases.

In the present study we have used the recently emerging technique of electrohydrodynamic spraying to treat the surface of titanium and generate thin coatings and subsequently use the coatings to tether bisphosphonate molecules. Bioactive 45S5 Bioglass® was used as the coating due to its bone bonding ability and the presence of calcium acting as binding sites for the bisphosphonate. The co-deposition of Bioglass® and bisphosphonate (alendronate sodium salt) was carried out using two jets with the EHD equipment and the effect on cellular activity was studied. As surface topography and the chemistry of the coating are important determinants of the cellular response, the overall aim was to establish a facile method coating of titanium to enhance osseointegration and bone healing. This study is expected to yield an optimized method of enhancing osseointegration of implants, especially where there is compromised bone healing.

5.2. Materials and Methodology

5.2.1. Preparation of Titanium Samples

Test samples were obtained using 150mmX150mm and 0.5 mm thickness commercially pure titanium stock sheet (CpTi), and prepared for treatment as previously described in chapter two. The CpTi discs were assigned into three experimental groups (Figure 5.1). The first group received no further treatment, i.e. uncoated CpTi, to be used as material control (Ti Uncoated). The second group consisted of discs to be coated with Bioglass® only (Ti + BG) and the third group of discs to be coated with Bioglass® and subsequently immobilized with sodium alendronate (Ti + BG + BP).

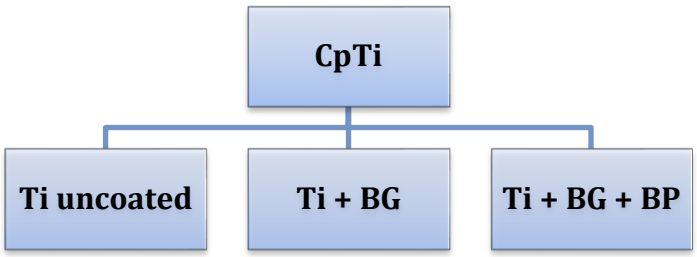

Figure 5.1. Schematic illustration of the experimental group investigated in this study, Ti: Titanium, BG: Bioglass, BPs: Bisphosphonate (sodium alendronate)

5.2.2. Electrohydrodynamic Deposition of Bioglass®

The aim of this process was to create a layer of coating consisting of fine Bioglass® particles physically embedded on Ti surface. 45S5 Bioglass® powder with chemical composition 45.0% SiO_2, 6.0% P_2O_5, 24.5% CaO, 24.5% Na_2O (in weight %) was used. The particle size was < 26.32µm. A 25 wt. % Bioglass® suspension was preapred using benzyl alcohol (Sigma) as a liquid carrier to achieve electrohydrodynamic spraying. Poly (ethyl glycol) (PEG) (Sigma) in chip form (Mn 1900 – 2200) was added to suspension (1g/ 3.33g of Bioglass®) to enhance the dispersion of Bioglass® particles in benzyl alcohol, effectively functioning as a surfactant. The suspension was stirred electronically for 10 minutes before introducing it in the container for EHDA spraying. EHDA spraying settings were determined in preliminary runs and kept constant for stable multi-jet spraying mode; needle size: 15 gauge spinal tap needle, flow rate: 50 µl/min, voltage: 19.00kv, distance from needle tip to ground electrode: 3 cm, collecting distance: 10cm. spraying time was kept at 7 minutes. A high-speed camera was used to observe jetting from needle tip. After spraying, substrates were left to dry at room temperature for 1 hour.

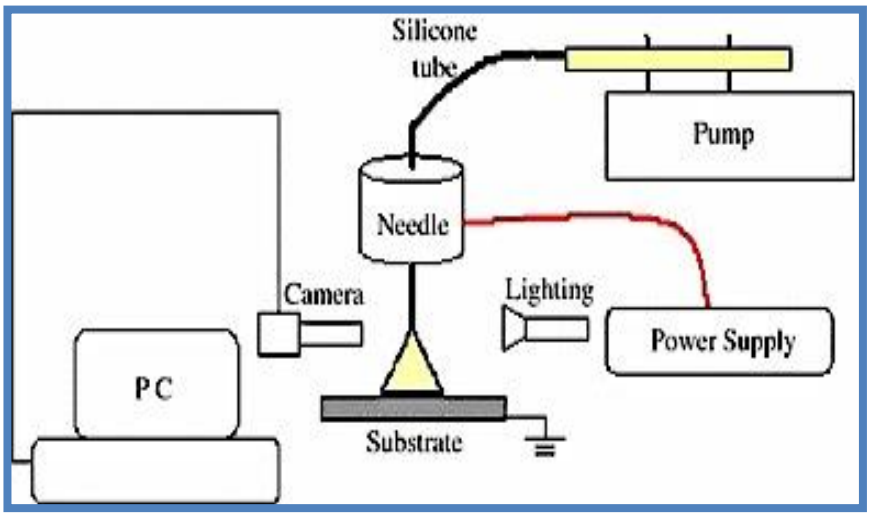

Figure 5.2: Schematic diagram illustrating EHDA process of depositing Bioglass® coating, where the coating solution is sprayed through the needle onto the surface of the substrate under predetermined conditions and power supply. [9]

5.2.3. Immobilization of Alendronate Bisphosphonate

Sodium alendronate (Calcibiochem 126855), a bisphosphonate drug was immobilized on Bioglass® coated titanium surfaces utilizing the micro-seeding technique. Solutions of desired concentration were prepared by dissolving in distilled water. 100µl of this solution was then gently pipetted directly on to the coated surfaces. This volume was enough to cover the entire disc without spilling off, thus all elements remain on the Ti disc. Discs were then oven dried at 37°C. A concentration of 2mg/ml was used for initial biocompatibility testing. Optimal alendronate bisphosphonate concentration was determined in preliminary tests by assessing cell viability at different alendronate concentrations. An alendronate concentration of 0.125mg/ml was then chosen for subsequent cell culture experiments. The experimental test samples were then sterilized by autoclaving using Priorclave autoclave at 121°C for 15 minutes. Samples were kept sealed until further analysis.

5.2.4 Surface Characterization

5.2.4.1. Scanning Electron Microscopy (SEM) and Energy-Dispersive X-Ray Spectroscopy (EDAX)

SEM/EDAX analysis was used to assess morphology and the chemical composition of coatings on all experimental groups. The technique was previously described in chapter two.

5.2.4.2. Raman Spectroscopy

Raman spectroscopy was used to analyze the nature of surface layer on the titanium discs, to determine their chemical composition as previously described in chapter two. In this study, the Raman spectroscopy measurement was performed on the titanium surfaces using the Renishaw inVia Raman microscope system (Renishaw plc, Wotton-under-Edge, UK).

5.2.5. In-vitro Biological Evaluation

Biocompatibility testing was conducted using osteogenic cells from three sources; alveolar and femur primary osteoblast (HOB) cells (non-commercial), and human osteosarcoma (HOS) cells - TE85 cells ECACC (European collection of cell cultures, Salisbury). Biocompatibility was assessed by MTT and live-dead staining, which were described previously in chapter two. Also, in order to optimize alendronate concentration, the effect of varying concentrations of alendronate on cells was investigated using MTT assays. Primary human alveolar osteoblast (aHOB) cells were used for subsequent cell culture experiments at a density of $1x10^5$ cells/ml.

5.2.5.1. Cell Viability as assessed by the MTT Assay

MTT assay was performed as an indirect test of material toxicity and cell viability by culturing cells in medium containing leachables from sample surface (eluants) for 24h and 72h time points. The method was previously described in chapter two.

5.2.5.2. Cell Viability as Assessed by Live-Dead Immune Fluorescence

Direct material cytotoxicity and cell viability was measured by live/dead staining using a cytotoxicity kit (L-3224) from Invitrogen, UK, for 24h and 72h time points. The method was previously described in chapter two.

5.2.5.3. Cellular response to sodium alendronate concentration

An initial solution of 2mg/ml of sodium alendronate was successively double diluted in distilled water. The following concentrations were used: 2mg/ml, 1mg/ml, 0.5mg/ml, 0.25mg/ml, 0.125mg/ml, and 0.0625mg/ml in accordance with previously described MTT method. 100µl of each of the alendronate concentration was added to separate tubes containing 5ml of fresh DMEM and mixed with pipette, then 100µl of resulting mix was used as eluant, replacing normal DMEM in 96-well plate after 24 hours incubation of cell culture. Cells were exposed for 24 and 72 hours.

5.2.5.4. Cytoskeletal Staining

Direct cytoskeletal analysis was performed using immunofluorescent labeling. Microtubule filaments were visualized using direct anti-β-tubulin staining. Substrates were removed from culture medium in wells and fixed in 4% formaldehyde at 4^0C overnight. The fixative was washed 3 times in PBS before incubating samples with permeabilising buffer for 10 minutes at 4°C. Non-specific sites were then blocked using 1% bovine serum albumin BSA (Sigma A4503) for 15 minutes at 37°C. Microtubule conjugated stain was then added onto the subtsrates, and incubated at 37°C for 1 hour. Residual stains were washed 3 times with PBS-tween (Sigma) at 5-minute intervals. Nuclei was counter stained with DAPI (4',6- diamidino-2-phenylindole) (Sigma D8417) for 5 minutes. Cells were then visualized under a confocal microscope.

5.2.5.5. Total DNA Production

Primary aHOB cell proliferation activity was illustrated by measuring total DNA production on test surfaces over a period of 21 days. The technique is described in chapter two.

5.2.5.6. Alkaline Phosphatase (ALP) Activity

To determine the differentiation potential of the cells, the ALP activity was quantified since it is one of the earliest markers of the differentiation of osteoblasts. ALP activity was measured over a period of 21 days as previously described in chapter two.

5.2.5.7. ALP/DNA Ratio

This is an indicative assessment of the amount of the ALP activity per cell. Variations caused by any differences in culture conditions can thus be eliminated using this approach. Both were measured from cell lysates.

5.2.5.8. Alizarin Red Staining

Alizarin red S (ARS) staining was used to evaluate calcium-rich deposits by cells in culture thus it was employed to qualitatively display mineral deposition activity. Culture medium was removed and samples washed with PBS (approximately 1ml per well). PBS was removed and cells were fixed in 1ml formal saline for 15 minutes, after which formal saline was removed and cells washed with 1ml distilled water. The samples were then stained with 1ml of 1% Alizarin Red S stain (Sigma A5533) for 5 minutes, subsequently removed and samples washed 5 times with 50% ethanol (approximately 1ml per well) and left to dry. Images were acquired using a digital camera.

5.2.6. Statistical Analysis

The data was statistically analysed using analysis of variance (ANOVA) for assessing the significance level of the differences between the experimental groups. All statistical analysis was performed with commercial statistical software GraphPad Prism (version 6.0c). The probability of p being below 0.05 was considered to be statistically significant. Results were represented graphically as mean values with standard deviation.

5.3. Results

5.3.1. Surface Characterization

5.3.1.1. Scanning Electron Microscopy (SEM) and Energy Dispersive X-Ray Spectroscopy (EDAX)

Qualitative surface characterization of the titanium surface topography was visualised using electron microscopy (SEM). The SEM images of the surface morphologies of the CpTi tested samples are shown in Figures 5.3.

A

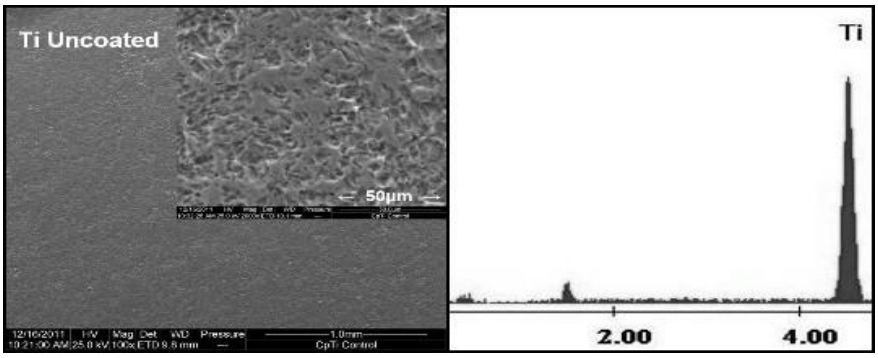

B

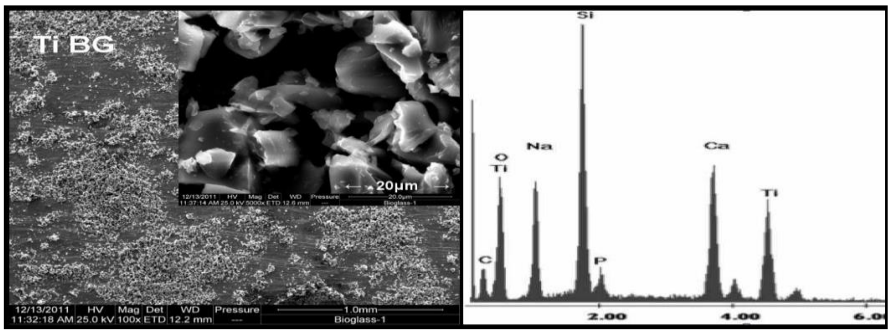

C

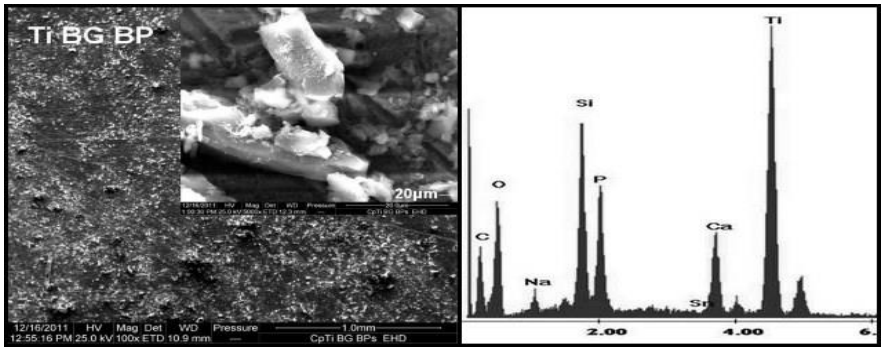

Figure 5.3: SEM images and EDAX analysis. A: The micrograph of CpTi as received at magnifications of 100x with the insert showing a magnification of 2000x. B: CpTi specimen coated with Bioglass® 45S5 using EHDA process that shows the irregular particles embedded on the surface. C: CpTi coated with Bioglass® 45S5 by EHDA and treated with alendronate (B and C show 100x magnification in main image with an insertat 5000x magnification in top right corner and EDAX analysis on right hand)

The uncoated Ti sample and revealed a uniform micro-roughened Ti surface (Figure 5.2.A), the BG Ti coated showed a fairly non-uniform coating with over approximately 60% is observed. Bioglass® particles appear to be in aggregated in patches across the surface (Figure 5.2.B). The surface morphology of BP treated group SEM image showed that the BG density is observed to be much less, and the BG particles are much more dispersed although more uniformly across the Ti surface. 5000x zoom reveals particles, which appear to be less embedded on Ti surface. The EDAX analysis of the BG and BG BP groups showed the presence of Ca, P and Si on the surface.

5.3.1.2. Raman Spectroscopy Analysis

Raman high resolution scanning of the different titanium sample surfaces were measured in order to determine the chemical composition of the treated surfaces after EHD treatment and immobilisation of alendronate sodium bisphosphonate. Raman scans of the uncoated Ti, BG Ti and BG BP Ti surfaces are illustrated in Figure 5.4.

Characteristic peaks associated with calcium-phosphate groups are observed on Bioglass® (BG) coated samples (Figure 5.4.B and C). Concerning silicate glasses such as BG, the Raman spectrum bands are obtained within the region 850 – 1200 cm^{-1}, which are associated with asymmetric and symmetric stretching vibrations of silica network. These peaks are clearly visible in Figure 3.4.B, which is the Bioglass (BG) coated group (without alendronate BP).

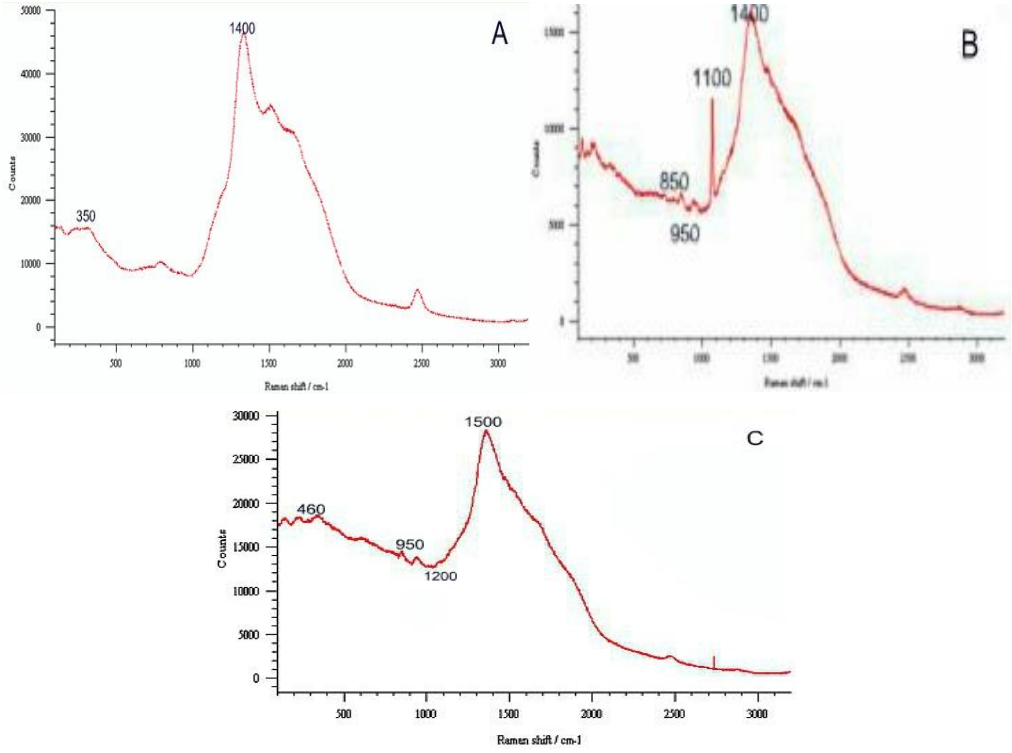

Figure 5.4: Raman spectra obtained on: (A) Ti-Uncoated surface, (B) Ti surface coated with Bioglass® (BG) and (c) Ti surface coated with Bioglass® and alendronate sodium immobilized (BG BP).

5.3.2. Cellular Response to Titanium Modified Surfaces

5.3.2.1. Evaluation of Cytotoxicity Indirect Method (MTT) on aHOB Cells

This assay was used to measure the effect of any potential toxic leachables from the surface treatments carried out on the Ti specimens on cellular metabolic activity. Among Ti substrates, cell viability was highest on the uncoated group. Cell metabolic activity was reduced with BG coating, and reduced even further in alendronate sodium BP immobilized groups. In the uncoated group, cell metabolic activity showed an increase after 72 hours exposure. This was also observed in BG coated groups. However, the viability reduced sharply after 72 hours in the alendronate sodium BP immobilized group. These findings were consistent at both elution times.

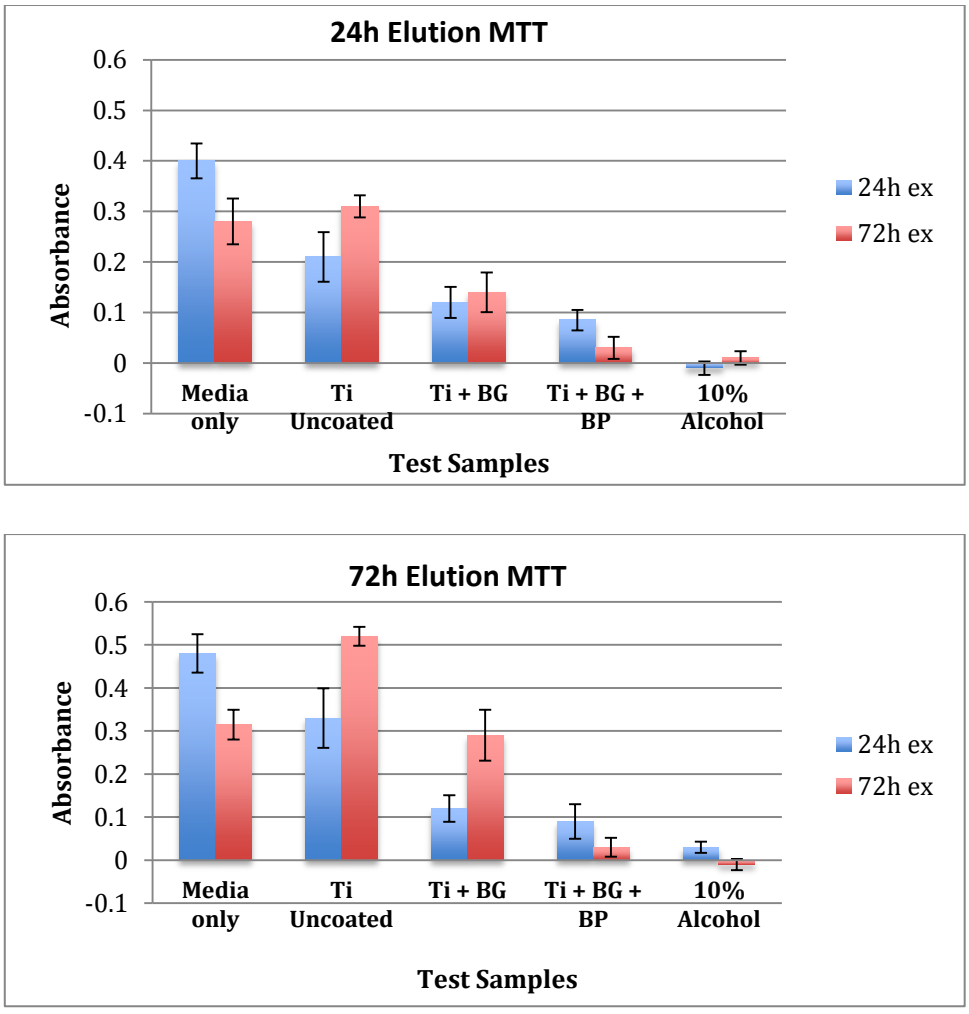

Figure 5.5: Evaluation of Cytotoxicity Indirect Method/ MTT 24h and 72h elution times of the test samples on aHOB cells; showing levels of intensity of absorbance at 570nm of the test samples at 24 and 72 exposures, expressed as mean absorbance ± S.D (n=3); the statistical significance was predetermined at $p<0.05$.

5.3.2.2. Evaluation of Cytotoxicity Indirect Method (MTT) on HOS Cells

The MTT graphs in Figure 5.6 indicates that the highest metabolic activity was observed on Ti uncoated surface. While the positive control (media only) showed an increase in the cell metabolic activity as expected after 72 h exposure compared to the other groups. However, the Bioglass® coated surfaces (Ti+BG) appeared to inhibit the cell metabolic activity compared to the control group, and further reduction was observed with immobilization of alendronate sodium BP on these surfaces.

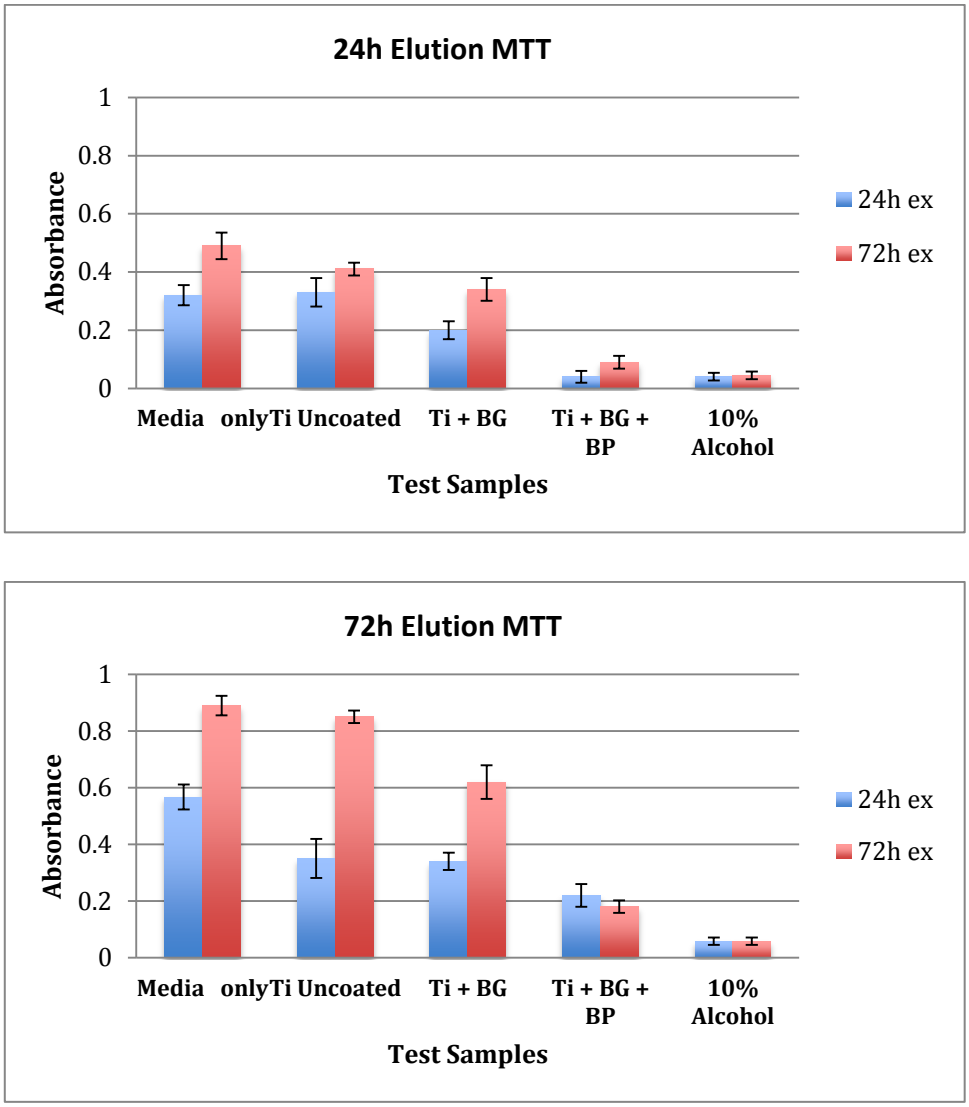

Figure 5.6: Evaluation of Cytotoxicity Indirect Method/ MTT 24h and 72h elution times of the test samples on HOS cells; showing levels of intensity of absorbance at 570nm of the test samples at 24h and 72h exposures, expressed as mean absorbance ± S.D (n=3); the statistical significance was predetermined at $p<0.05$.

5.3.2.3. Cellular response to Sodium Alendronate concentration using MTT assay

The MTT assay was carried out using three different cell types firstly to assess if bisphosphonates induced a different response in different cell types. The cell types used in this test were: alveolar HOB, femur HOB and HOS cells.

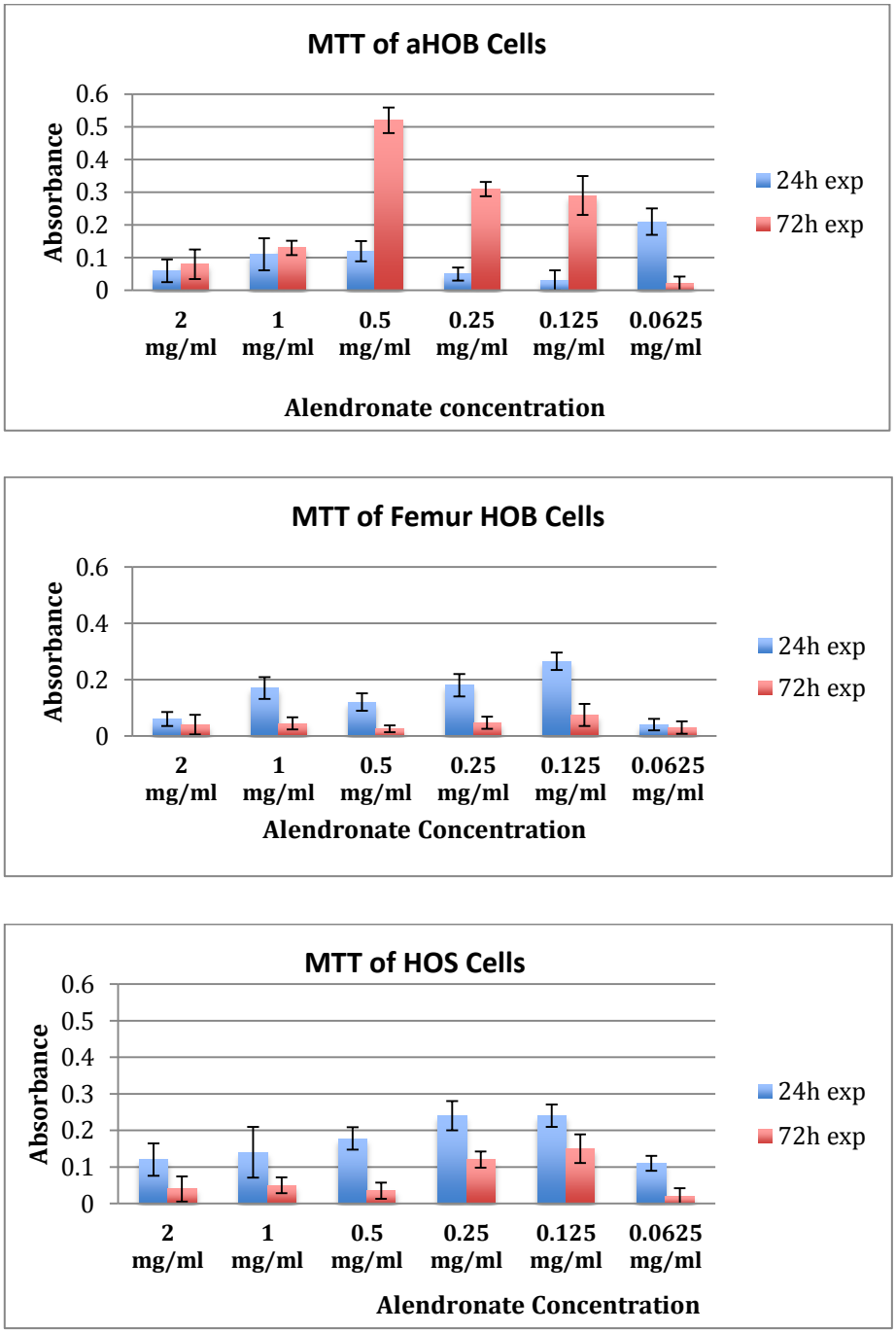

Figure 5.7: Evaluation of Cytotoxicity Indirect Method/ MTT 24 and 72 hour Exposure of alveolar HOBs, femur HOBs, and HOS cells cultured in different concentrations of sodium alendronate (BP). Showing levels of intensity of absorbance at 570nm of the test samples at 24h and 72 elutions, expressed as mean absorbance ± S.D (n=3); t statistical significance was predetermined at $p<0.05$.

The MTT graphs in Figure 5.7 showed that the femur HOBs and HOS cells largely displayed a similar pattern. Cell viability was seen to increase with reducing concentrations of alendronate sodium bisphosphonate up until 0.125mg/ml. At 72 hours exposure, viability decreases in all concentrations. In alveolar HOBs however, the cell metabolic activity peaks in 0.5mg/ml before tailing off. At most concentrations, 72-hour exposure resulted in increased cell viability. It was observed that concentration range between 0.5mg/ml and 0.0125mg/ml of alendronate appeared to increase the cell metabolic activity compared to lower or higher concentrations used in this test.

5.3.2.4. Assessment of alveolar HOB cells viability – Live and Dead Staining Assay

Comparing the experimental groups Ti + BG and Ti + BG + BP to the uncoated group, the density of dead cells in both BG coated and alendronate BP immobilized group was considerably high at 24 and 72 hours. Importantly and only observed in this cell type, very few dead cells were observed at day 7. Cell viability was lower in BG coated samples compared to uncoated (Figure 5.8).

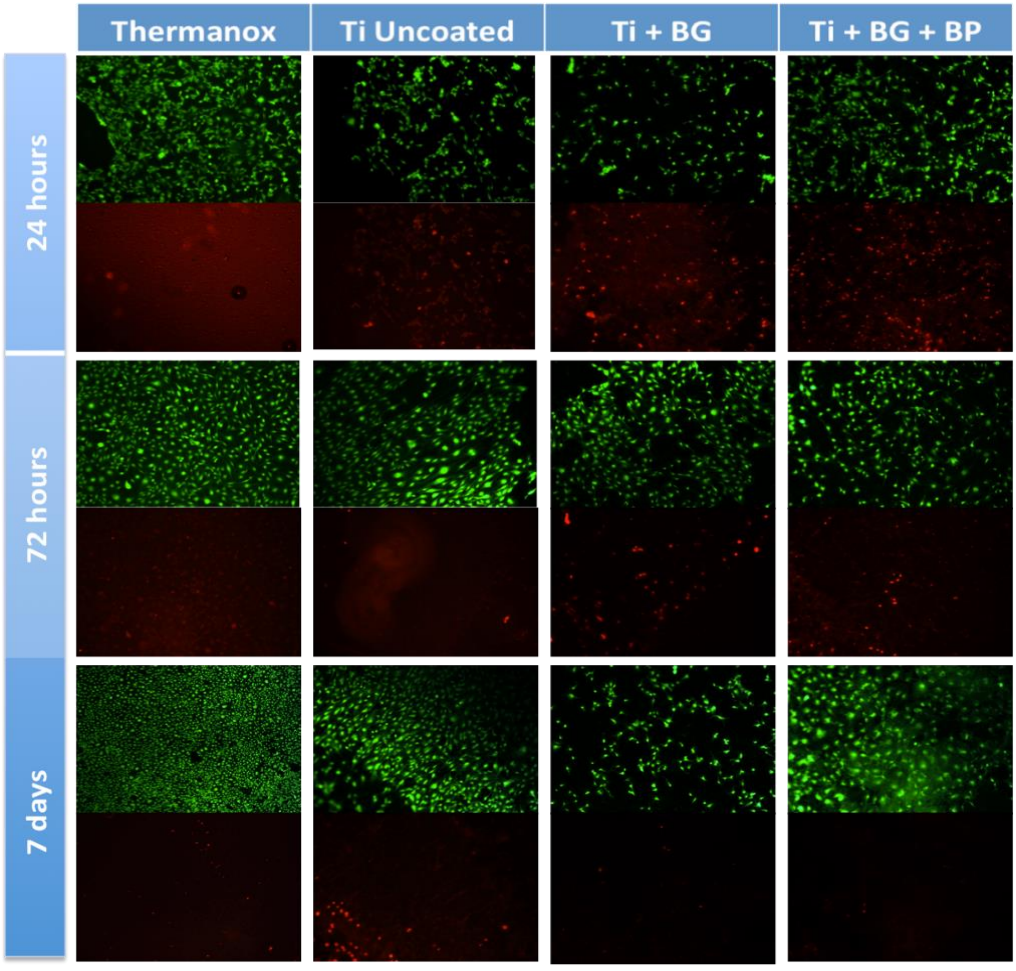

Figure 5.8: Live (green) and dead (red) fluorescence staining (Ethidium Homodimer-1) of aHOB cells exposed for 24, 72 hours and 7 days on CpTi test samples (Thermanox®= nontoxic control)

5.3.2.5. Assessment of femur HOB cells viability – Live and Dead Staining Assay

At 24 hours, cell viability was particularly low in the two BG coated groups. Cell viability was considerably increased across all groups at 72 hours. However, in contrast, cell viability was reduced at day 7 in alendronate BP containing group. (Figure 5.9)

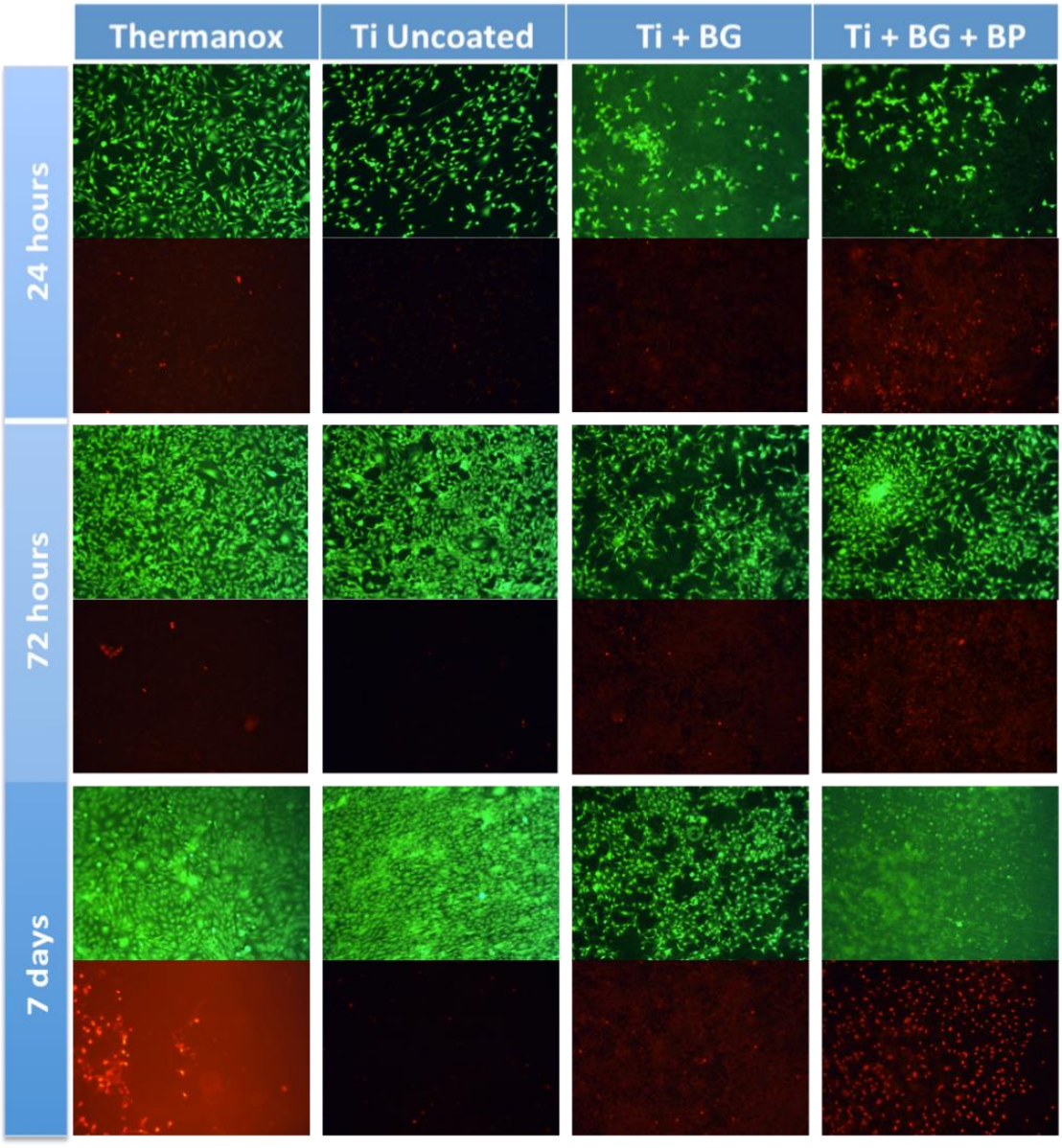

Figure 5.9: Live (green) and dead (red) fluorescence staining (Ethidium Homodimer-1) of femur HOB cells exposed for 24, 72 hours and 7 days on CpTi test samples (Thermanox®= non-toxic control)

5.3.2.6. Assessment of HOS cells viability – Live and Dead Staining Assay

The HOS cells viability similar to aHOB cells viability on the test samples. However, a higher number of dead cells were observed on the alendronate BP group, which increased by day 7 compared to the other groups (Figure 5.10).

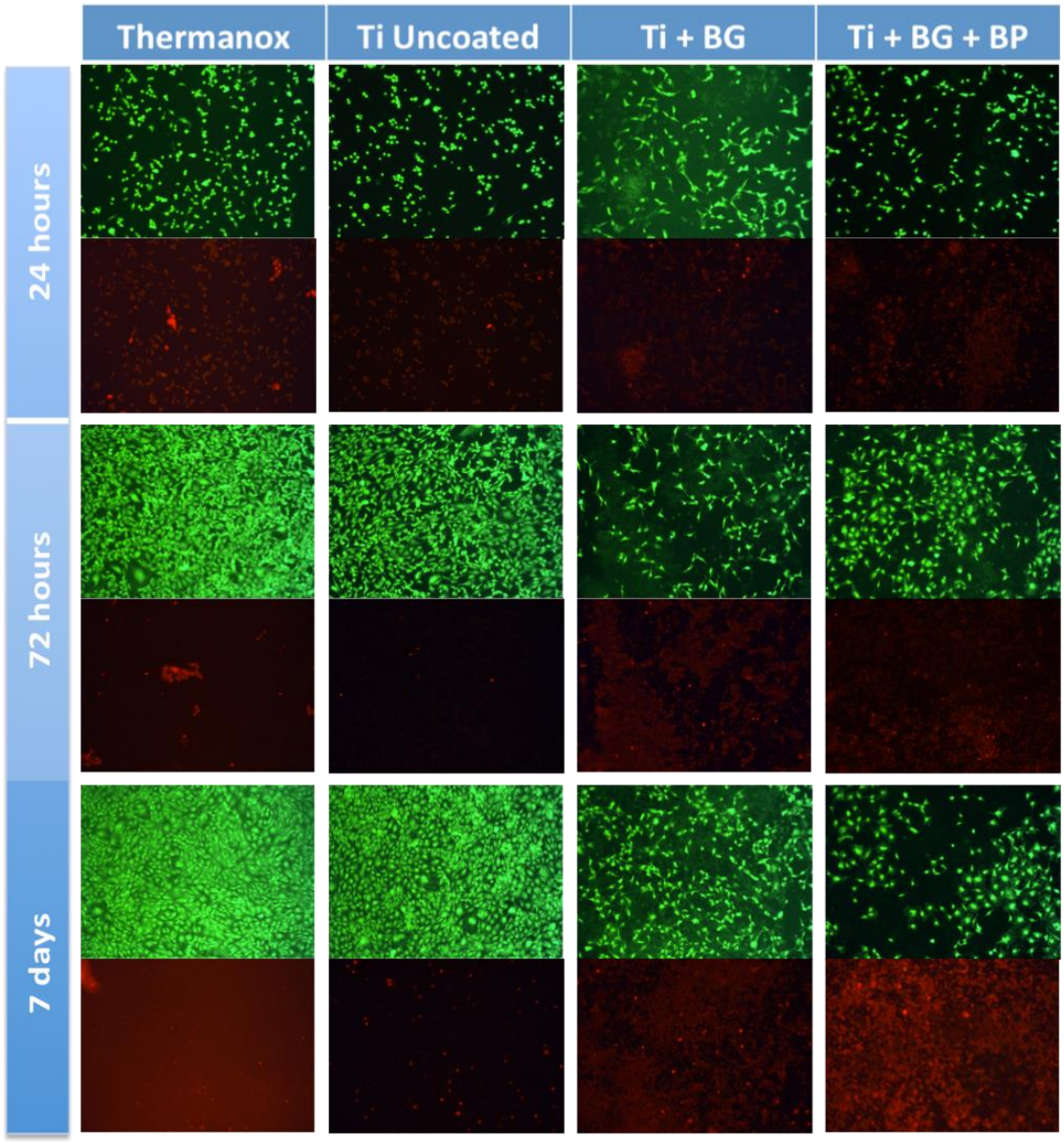

Figure 5.10: Live (green) and dead (red) fluorescence staining (Ethidium Homodimer-1) of femur HOB cells exposed for 24, 72 hours and 7 days on CpTi test samples (Thermanox®= nontoxic control)

5.3.2.7. Cytoskeletal Staining

Gross differences in HOB cell morphology and density were observed across the three Ti surfaces. On the uncoated surface, cytoskeletal-staining revealed widely spread, interconnected filaments. Cell attachment at multiple focal points was observed. On Bioglass® (BG) coated surfaces, cell density was significantly reduced and filaments were less widely spread. However, in the sodium alendronate immobilized surface a lower cell density was observed with almost no spread of filaments.

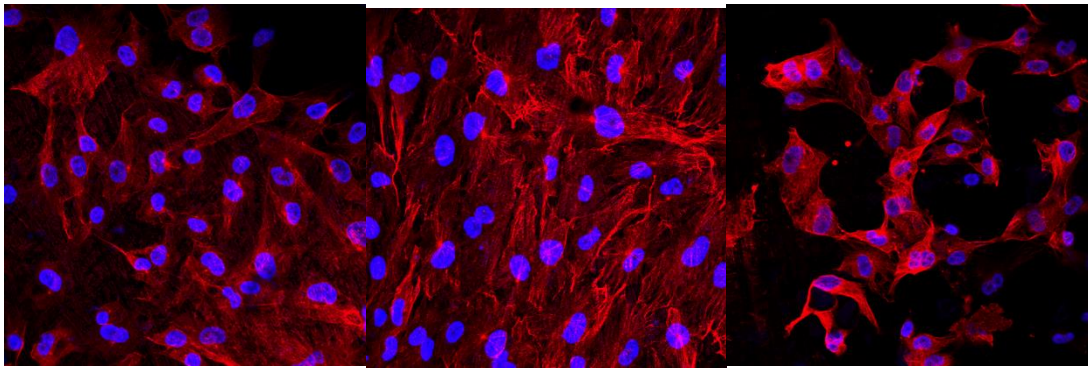

A B C

Figure 5.11: Immunofluorescent staining of cytoskeletal structure showing cell morphology at x20 magnification. Microtubule is stained with anti-β-tubulin (red). Nuclei are counter stained with DAPI (blue). A) HOB cells staining on uncoated Ti surfaces, B) HOB cells staining on BG coated surfaces, and C) HOB cells staining on BG+BPs coated surfaces.

5.3.2.8. Cell Proliferation as Assessed by Total DNA Production

As shown in Figure 5.12, there was a general increase in total DNA production peaking at day 14 for most material groups and dropping sharply by day 21. The only slight variation was in the Bioglass® coated group, which peaked at day 7 instead, decreasing thereafter. The non- material control group (TMX) showed an increasing trend with only a slight drop in day 14, but continued to increase, peaking at day 21, thus contradicting the general trend observed in the material groups. At day one, all the material (Ti) groups produced similar amount of DNA, about 0.2ng/ml DNA. There are notable differences however in subsequent time periods. DNA produced in the uncoated titanium group appeared to be consistently higher than the Bioglass®-coated group at all time periods. This was particularly evident in days 7 and 21. By day 21, DNA produced in BG-coated groups was less than half that produced on uncoated Ti. There appeared to be higher DNA production in the Bioglass alendronate sodium BP treated groups (Ti + BG + BP) compared to Bioglass coated group without alendronate (Ti + BG), particularly at days 14 and 21. The difference in cell proliferation was

increased by fifty percent by day 21. At this time point, cell proliferation in the alendronate BP treated group was similar to the uncoated Ti group. However, cell proliferation in the uncoated Ti was relatively higher compared to other interventions. Statistical analyses, however, showed that the differences among intervention groups and uncoated-Ti are not statistically significant.

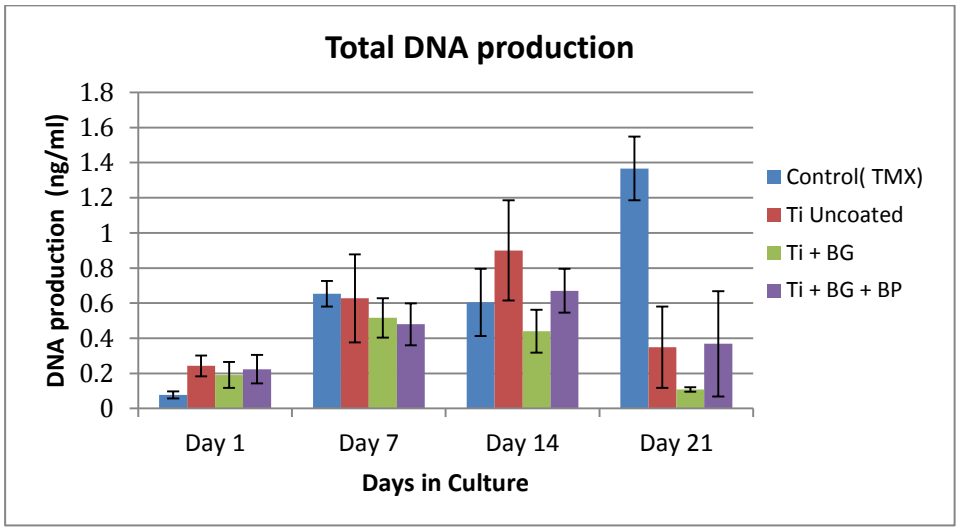

Figure 5.12: Evaluation of Proliferation of aHOB Cells / DNA Assay of CpTi titanium discs The data represents the average for each group as mean absorbance ± SD (n=3); the statistical significance was predetermined at p<0.05

5.3.2.9. Cell Differentiation as Assessed by Alkaline Phosphatase (ALP) Activity

As shown in Figure 5.13, the ALP activity in all material groups increased from day 1 to day 7, peaking on this day. A drop was observed at day 14 in these groups, however not below the initial levels at day 1. A slight increase was observed in most groups by day 21. This trend was similar in TMX, but a more marked increase was observed at day 21 in this group. At day 1 all material groups showed similar levels of ALP at about 1.5 µg/ml. There were notable differences in subsequent time points. ALP appears to be consistently higher in Uncoated-Ti than in BG-coated discs. This was particularly noticeable at day 14. Also, at most time points (apart from day 14), ALP activity of cells appeared to be further reduced in BP treated- Bioglass®-coated discs, which is especially observable in day 7. At day 14, there was a slight increase in ALP in the alendronate BP-treated group above the untreated Bioglass®-coated group. This increase however was not higher than ALP activity in uncoated-Ti. There was no statistically significant difference among the groups across all time points.

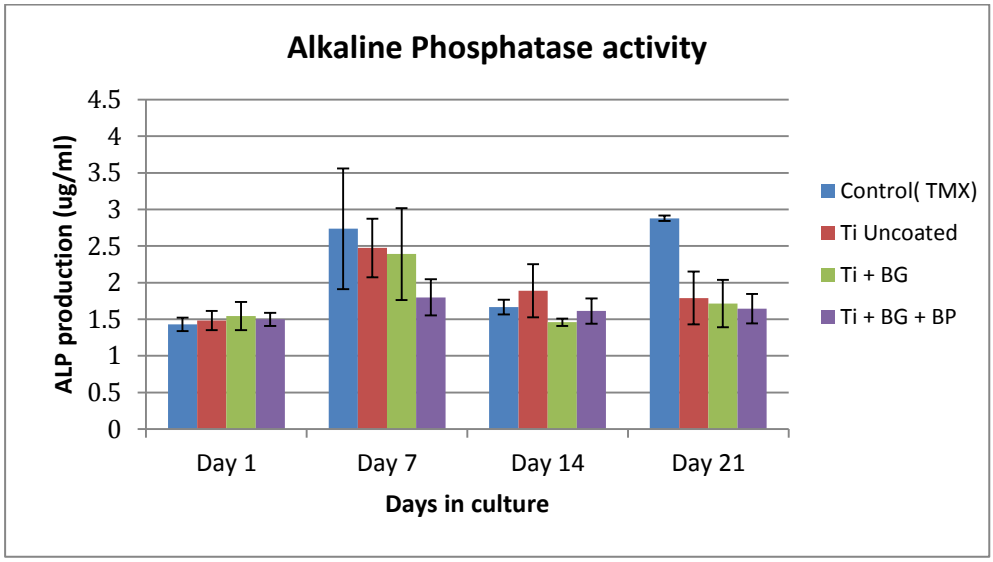

Figure 5.13: Evaluation of Proliferation of aHOB Cells / ALP Assay of CpTi titanium discs The data represents the average for each group as mean absorbance ± SD (n=3), and the statistical significance was predetermined at p<0.05

5.3.2.10. ALP/DNA Ratio

Determination of the ALP/DNA ratio indicates more precisely the amount of ALP activity per cell. As shown in Figure 5.14, in all tested groups, there was a downward trend in ALP/DNA activity up until day 14. At day 21, a sharp rise was observed in ALP/DNA in these groups. This increase was not seen in the non-material control (TMX), in which there was a consistent downward trend in ALP/DNA until day 21. At all time points, there were variable ALP/DNA findings within the test groups. Firstly it can be observed that the BG coated-group showed the highest ALP:DNA ratio at all time points. At day 21, this group displayed the highest increase in ALP/DNA, almost doubling that of day 1. The BG-coated Ti discs showed an increase in ALP/DNA ratio compared to the uncoated-Ti group. However, the groups that were further treated with alendronate BP seemed to counter this improvement in ALP/DNA, rendering this group highly similar to the uncoated-Ti group.

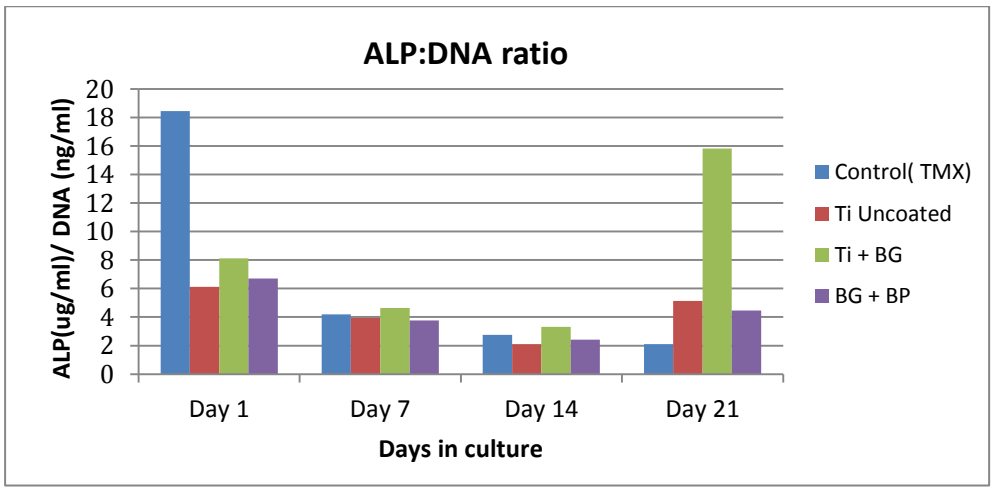

Figure 5.14: Alkaline phosphatase/ DNA activity in HOB cells, deduced from separate ALP and DNA cultures over 21 days.

Total DNA and ALP activity graphs of the test samples at day 14 were illustrated showing the trend and behaviour of cell activity at each one. However, there was no statistically significant difference among the groups for both DNA and ALP means.

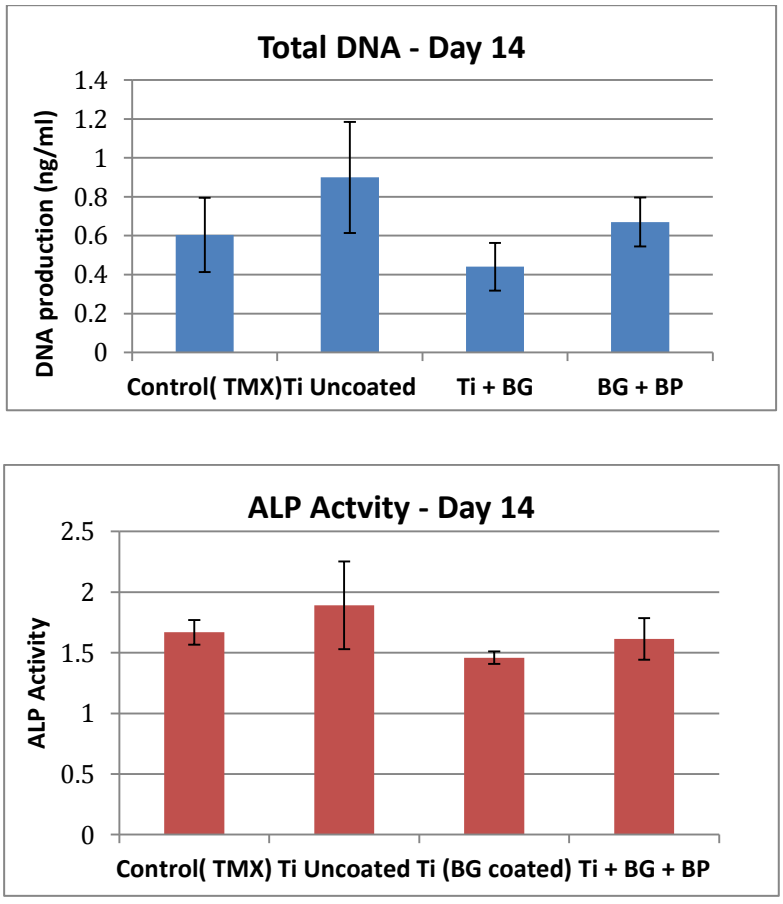

Figure 5.15: Total DNA production and ALP activity for the control and test samples at day 14 (extracted from Figures 5.11 and 5.12)

5.3.2.11. Osteoblast Mineral Deposition by Alizarin Red staining

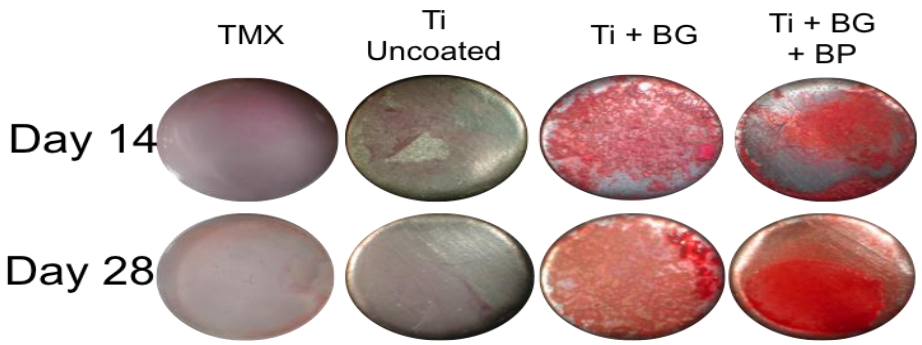

Figure 5.17: Alizarin Red Qualitative analysis of HOB cell mineral (calcium) deposition. Mineral (Calcium) stained in red. (n=2, one representative disc is displayed).

Bioglass coated Ti discs showed an enhanced staining indicating a higher calcium deposition. Addition of sodium alendronate to this group appeared to reduce mineral content, especially observable at day 14. However, mineral content at both time points in BP treated group was still higher compared to the uncoated-Ti group. The only easily observable change in mineral content between the two time points was a slight increase in staining in the BP-treated group.

5.4. Discussion

Electrohydrodynamic atomization (EHDA) spraying was used to create Bioglass® coatings on commercially pure Ti and the SEM and EDAX analysis revealed topography and chemistry of the test groups. The uncoated Ti sample revealed a uniform micro-roughened Ti surface, while the surface of the Ti substrate coated with BG, showed a fairly uniform coating, but with some evidence of agglomeration of Bioglass® particles on the surface and few areas of non-coated surfaces. This may be related to the spraying mode used by the EHDA process (referring to the appearance of suspension spray at the needle tip) or the lack of breakdown of the Bioglass® particles present in the suspension in benzyl alcohol. A multijet mode was predominantly used which resulted in particles being sprayed in multiple directions to cover the surface of the discs. A stable cone jet mode has been suggested for optimizing fine particle spray [131], however, a steady multijet mode was more readily achieved in this study, which yielded Ti substrates with coatings over majority of the surface.

Figure 5.2 shown at a high magnification revealed the surface morphology obtained after EHDA coating, which shows multilayered angular granular particles of various sizes. Comparing this to Bioglass® coatings obtained by Altomare et al. [131] via HVSFS, there were remarkable differences. Powder form BG sprayed with HVSFS underwent remarkable changes in their morphology to form more flattened layers. However, that was due to the high temperature spraying conditions with thermal pretreatment of Ti substrates, which is not the case in EHDA as the particles are embedded on the surface and not subjected to any high temperatures thus remaining in the glassy form. The surface morphology of the alendronate treated group showed that the particles were much more uniformly dispersed across the Ti surface, which may be related to the method of immobilizing alendronate onto the disc surfaces. Ideally, microseeding method employed in this study should result in all surface contents remaining on the surface after seeding, however some dispersion of loosely bound Bioglass® particles may be dislodged during the process of interaction between the alendronate solution, thus a more uniform appearance result. However, this also highlights one of the limitations of the EHDA process where all particles may not be tightly bound on the surface.

The surface roughness of uncoated Ti substrates as received had Ra value of ~0.404μm.This roughness is low, compared to reported values for good machined dental implants, which have been shown to lie between 0.5 and 1.0μm [232]. This low roughness is likely to have an effect on cellular response but may also affect BG

deposition. BG particle size was < 26.3µm, considerably larger than grooves on Ti substrate (Maximum valley depth, R_V = 1.298). This is likely to result in low rates of BG particles impingement into Ti surface. Thus, it is proposed that a rougher surface, may improve observed results in the current study. The EHDA process is recorded to be effective for depositing nano-sized particles. Li et al. [9] achieved a much more uniform coating of nano-hydroxyapatite on to Ti by EHDA.

EDAX analysis of Ti coated with BG and Ti coated with BG and BP revealed the chemical nature of both groups (Figure 5.2.B and C). The chemical composition of 45S5 Bioglass® is 45.0% SiO_2, 6.0% P_2O_5, 24.5% CaO, 24.5% Na_2O. A corresponding peak for each element is observed in the spectra. There are also identifiable peaks for Ti and TiO_2 as expected (Titanium forms an oxide layer on its surface). The coated samples with Bioglass® showed a particularly high intensity peak for Si and a higher Si:P ratio as expected due to the composition of the glass compared to the Bioglass® tethered alendronate. The intensity of the Si peak was much lower, and there was a higher P (Phosphorous) peak in the alendronate containing specimens as the chelation of alendronate with the calcium from the Bioglass® masks some of the Si peaks.

Raman spectroscopy was conducted for further surface chemical analysis. Characteristic peaks associated with calcium-phosphate groups are observed on Bioglass® coated samples (Figure 5.3.B and C) of major interest, relating to silicate glasses such as BG are bands within the region 850 – 1200 cm^{-1}, which are associated with asymmetric and symmetric stretching vibrations of silica network. These peaks are clearly visible in Figure 3.5.B, which is the BG coated group (without alendronate BP). Observable differences in peaks, including an absent peak in the 1000 cm^{-1} region may be indicative of structural alteration owing to the addition of BP. In general the, surface analysis via SEM/EDAX and Raman confirmed the presence of a coating, morphologically and chemically consistent with 45S5 Bioglass®. Notable chemical differences between BG coated and alendronate sodium BP immobilized groups confirm the presence of the alendronate. However, further chemical analysis is necessary to confirm the presence and analyze the interactions of immobilized alendronate sodium BP. Physically; interfacial bonding between metal and BG coating also needs to be analyzed. This is highly important especially for practical applications.

Several formulations of bioactive glasses have been proposed as bone graft and bone contact materials, after the first formulations proposed by Hench in the late 1960s [230]. They show the ability to bond directly to bone [233] possessing osteoconductive and osteostimulative properties [234]. It is essential that implant materials should be

biocompatible, thus any modification to surfaces of implants need to be investigated for their cytotoxicity.

The two main properties of bisphosphonates is the ability to strongly bind to bone due to the high affinity for hydroxyapatite and inhibit osteoclast function. The function of bisphosphonate is to inhibit bone reabsorption and increase bone mineral density, the reason for its use in patients with bone dysfunction. Necrotic bone in the oral cavity and the occurrence of inflammatory reaction in soft tissue in patients receiving oral bisphosphonates is an emerging complication associated with both cancer and osteoporosis care, which is often referred to as the osteonecrosis of the jaw, ONJ [13, 131]. Although no clear explanation of this observation is documented yet, some recent studies on in vitro evaluation of the effect of bisphosphonates also report the effect on different cell lines and cell types to highlight any differences and thus to provide an explanation for ONJ, however, to date there is no consensus on this issue. In the current study, firstly the dose response to alendronate was established on three cell types namely, alveolar HOB's, femoral human osteoblast like cells and human osteosarcoma cells that showed similar trends for femur HOBs and HOS however a difference was observed with the alveolar HOB's. The alveolar HOB's showed that the concentration of 0.125mg/ml at 24 hours elution was cytotoxic, however, further work is required to confirm this trend. Although different sensitivity to concentration of alendronate has already been reported between murine and human cells [235], such a trend has not been described for different cells sourced from the same species. One of the reasons could be that cell sourced from the same species may or may not exhibit any inter sensitivity to the amount of bisphosphonate, thus the results obtained from one cell type cannot be extrapolated to different cell types used for cytocompatibility testing. Thus, only alveolar HOBs were used for further work done this study. However this preliminary work does not provide sufficient explanation for the necrosis observed in the jaw although the alveolar HOB's did exhibit a different dose dependency in comparison to the femur HOBs or HOS cells.

The MTT assay to ascertain the effect of eluants from the coatings with and without bisphosphonate on the three different cell types showed that the trends observed with alveolar HOBs, femur HOB cells and HOS cells mirrored each other with cell viability decreasing with the presence of Bioglass® and Bioglass® with alendronate. These results indicated that the samples coated with Bioglass are more than likely releasing leachables, which reduce the cell metabolic activity, however, a longer exposure of 72 hours both in the 24 and 72 hour eluants indicated an improvement. One explanation for this observation is that Bioglass coatings can release sodium ions as it is a sodium containing glass, which creates a highly alkaline environment that can cause a lowering

in the cell viability. Although Bioglass is bioactive and biocompatible and has been extensively used clinically, the non-clearance of ionic species in a static environment as in cell culture conditions can be attributed to this observation. Altomare et al. [131] who successfully deposited layers of Bioglass® via high-velocity suspension flame spraying technique (HVSFS) reported no such detrimental effect on cell viability via MTT assay, whilst Acil et al. [236] showed in a study of the cytotoxic effects of three different bisphosphonates in-vitro on human gingival fibroblasts, osteoblasts and osteogenic sarcoma cells, that these bisphosphonates had inhibitory effect on collagen production and cell proliferation. The contrast from the results of this study and the coatings reported using HVSFS can be accounted by the fact that the HVSFS-deposited coatings were further allowed to interact with SBF that resulted in the deposition of a stable apatite layer thereby decreasing the solubility of the underlying glass structure.

Generally, a dose related response to alendronate concentration was observed, with higher doses resulting in lower cellular viability. These results directly implicate that alendronate is somehow inhibiting the cell metabolic activity when localised on Bioglass®. Moon et al. [138] reported the immobilization of alendronate at a concentration of 1 and 5 mg/ml on the surface of heparin grafted Ti discs and in vitro tests revealed enhanced effects on osteoblast cells in contrast to the results of this study. Cell proliferation was also reported to increase with higher alendronate concentration and it was suggested that alendronate-immobilized Ti might be a bioactive implant with to enhance osteoblast differentiation in addition to inhibiting osteoclast differentiation. Thus it is clear that the elution from the Bioglass® /alendronate coatings was released as the result of exchange of ions and not retained over a period of time as was expected.

Direct qualitative cytotoxicity testing with live-dead cell staining showed similar trends to the results (Figures 5.8, 5.9 and 5.10) obtained from the MTT assays. The alveolar HOBS, femur HOBs and HOS cells, cultured on the uncoated, Bioglass® coated and Bioglass® coated with alendronate on CpTi also demonstrated a similar trend for each of the cell type with the control group exhibiting higher numbers of live cells (green) in comparison to the experimental groups. No apparent differences were observed at day 7, cell viabilities for the Bioglass® coated samples were lower than that of uncoated samples across all cell types. In most cell types, the density of live cells in the alendronate sodium BP containing samples was even lower, and a high number of dead cells was observed. However, a qualitative visualization still suggests the presence of a large number of live cells in the experimental groups, although, the number of dead cells was seen to rise. As explained earlier, Bioglass® in the first few

hours of contact with aqueous media, can rapidly exchange Na^+ and Ca^{2+} with H_3O^+ from the solution whilst the Si–O–Si bonds are progressively broken, with loss of soluble silica in the form of $Si(OH)_4$, thus creating an alkaline environment, which may cause cell death. Supporting this observation, it has been shown that bioactive glass particles when immersed in water produce alkalinity linked with a decrease in cell number [237].

Bone development can be divided into three key stages: proliferation, extracellular maturation and mineralization [238]. Corresponding to these stages are peaks in gene expression levels of specific proteins. In this study, proliferation was measured through total DNA production (Figure 5.11). Extracellular maturation involves the secretion of several proteins, which are highly localized in bone including ALP, osteocalcin and type 1 collagen. In this study, ALP activity was measured to demonstrate this differentiation phase (Figure 5.12). A plot of ALP/DNA was made as a more accurate guide of ALP activity per cell.

Comparing the BG coated material to uncoated Ti, both total DNA and ALP activity appeared to be consistently higher in uncoated Ti. This indicates a superior proliferation and differentiation on uncoated Ti surfaces. The ALP activity of osteoblasts is inversely proportional to the amount of calcium in the medium. Since alendronate is known to precipitate divalent metal ions such as calcium, the concentration of calcium in the medium decreases with increasing concentration of the alendronate, which may be one of the factors causing a decrease in ALP activity. However, the situation may be different in an in vivo environment, where the decrease in calcium concentration in the presence of alendronate would probably be counter balanced by calcium homeostasis. Interestingly, however, ALP/DNA was consistently higher for cells cultured on the bioglass coated groups and at day 21 it was more than double that of uncoated Ti discs. This possibly suggests that cells cultured on BG coated groups were quicker to differentiate than uncoated groups.

Comparing BG coated with alendronate sodium BP immobilized groups; total DNA production is highly similar or even higher in alendronate sodium BP groups, although it is still inferior to uncoated Ti. ALP activity was mostly slightly lower in BP groups, apart from in day 14 where a slight increase is observed. Correspondingly, ALP/DNA was consistently lower in alendronate sodium BP immobilized group. It appears that the addition of alendronate sodium BP curbs the early differentiation noticed in Bioglass® coated sample (BG).

Calcium staining was particularly high in BG coated and BP treated groups. This is likely due to intrinsic calcium content of BG on both surfaces. Nonetheless, particularly high calcium deposition in the BG coated group at day 28 was consistent with high ALP expression seen at day 14.

In summary, the study showed that EHDA was a viable method for coating titanium substrates as confirmed by surfaces characterization with SEM/EDAX and Raman spectra. However, the coatings were able to interact with the surrounding medium leaching ions, which confirmed that the Bioglass® coating does not undergo any changes due to the EHDA process, but an in vitro study was probably not the best determinant due to the concentration of leachables ions. Sodium alendronate immobilized by microseeding on to coated titanium surfaces showed inferior cytotoxic effects measured in vitro in comparison to the uncoated CpTi samples. However, Bioglass® coated samples showed some positive effect on osteoblast differentiation assessed by cell proliferation and differentiation assays, however, this was not found to be the case in bisphosphonate groups.

CHAPTER SIX

Conclusion and Future Work

6.1. Conclusion

During the last 25 years, commercially pure titanium and titanium alloys have been used to make dental and orthopaedic implants, maxillofacial prosthesis and occasionally used to fabricate removable denture frameworks due to their excellent biocompatibility, corrosion resistance and mechanical properties. To ensure the successful fabrication of prosthetic components much emphasis has been given to fundamental research on titanium, such as titanium castings, alloying titanium, casting technology, machinability, wear resistance, bonding to porcelain, prosthetic composites and denture-base resins. Compared with other metals the advantages of titanium include its lightweight and excellent biocompatibility.

Implant integration in patients especially with compromised bone healing continues to pose a challenge, which has seen a resurgence of interest in efforts to improve osseointegration via surface modifications techniques and bioengineered approaches [239]. Numerous methods have been explored to improve the osseointegration of dental and maxillofacial implants, and the literature review in this thesis highlights the methods of surface modification of titanium and titanium alloys. The review indicates that there has been considerable research on surface modification techniques to improve the hard tissue compatibility of titanium either using coatings of hydroxyapatite, titanium oxide, calcium titanate with various morphologies, biofunctionalization by various techniques such as dry and wet processes and tethering of biofunctional molecules. Other approaches include include deposition of polymers such as poly(ethylene glycol) to the metal surface to control the adsorption of proteins and adhesion of cells, platelets, and bacteria.

Titanium and titanium alloys are well suited for manufacturing medical and maxillofacial devices. The general method of fabrication involves casting, machining, cold and hot forming such as superplastic forming (SPF) techniques. Superplastic forming is a method of forming titanium which is suited for devising complex and customisable implant shapes, using relatively low-cost investment materials, which are employed as a mould/die during the process. The process involves investing the titanium or its alloys in investment materials and is known to create an interaction layer, which was shown to have beneficial effects [240]. This study established that both the interaction layer and its treatment further with simulated body fluids created a favourable interaction layer on the titanium surfaces, which induced the formation of apatite like layer on the surfaces when soaked in SBF solution. The interaction layer so formed was stable and not lost after physical methods of cleaning, thus can be considered to be a quick and

inexpensive method of surface modification of titanium implants, during processing itself, which can enhance the bone healing and result in improved osseointegration. In addition as the device is manufactured by the process that causes the interaction layer to form, it can be concluded that all surfaces of the device is covered with the layer unlike the limitations of some coating methods. The in vitro cytocompatibility studies clearly demonstrated that the surfaces that resulted after SPF forming were biocompatible.

Literature findings report that the treatment of titanium and its alloys with sodium hydroxide and then subjected to heat treatment forms a bioactive layer, however in this study it was found that the heat treatment was not essential and subsequent interaction with simulated body fluid of the sodium hydroxide treated surfaces enhanced in vitro cytocompatibility.

Bisphosphonates are well known potent inhibitors of osteoclast activity and are widely used to treat metabolic bone diseases. Recent evidence from in vitro and in vivo studies indicates that bisphosphonates may additionally promote osteoblastic bone formation. The surface modification of CpTi and Ti64 achieved with SPF and sodium hydroxide treatment and further treatment with SBF were further used to immobilize alendronate successfully, which yielded a simple method of incorporating bisphosphonates on implant surfaces, without causing any damage to the drug as no heat treatment or chemical crosslinking was required.

Finally EHDA was established to be a viable method for coating titanium substrates without the conversion of the active glass phase and could be used to tether alendronate on Ti substrates. However, the coatings were able to interact with the surrounding medium leaching ions, and the in vitro study showed a detrimental effect on cytotoxicity that was attributed to the alkaline environment in the media determinant due to the leaching of ions from bioglass that also caused the alendronate to be leached quickly in the cell culture medium.

Based on the cellular response to the investment treated titanium samples, sodium hydroxide treated samples followed by SBF treatment it can be concluded that these surfaces provide favourable conditions for cell growth, proliferation and differentiation when compared to the non-invested samples.

6.2. Future Work

1. The effect of using titanium discs with different roughness for superplastic forming and study its effect on the formation of the interaction layer, which will help elucidate if thicker interaction layers are detrimental towards cellular response.

2. The use of XPS and X ray diffraction to analyse the surface chemistry of the modified titanium surfaces.

3. The use of sand blasting to create surfaces with greater roughness prior to EHDA coatings to allow a better binding of the bioactive glass particles and study the effect of heat treatment followed by EHDA deposition prior to interaction with bisphosphonates.

4. In vivo biocompatibility of the bioglass/bisphosphonate coated Ti discs to establish the effect of the coating in a living system that will provide more insight into the bone response and also to be able to predict the bone-to-implant response.

The future studies will then provide a clinically relevant study to establish if implants coated with bioactive glass and bisphosphonates may potentially compensate for the deleterious effects of particulate wear debris at the bone–implant interface, by encouraging increased numbers of cells committed to the osteoblastic phenotype, and thus improve the longevity of joint replacements.

CHAPTER SEVEN

References

References

1. Sieniawski, J., et al., *Microstructure and Mechanical Properties of High Strength Two-Phase Titanium Alloys*. Titanium Alloys - Advances in Properties Control. 2013.
2. Pelaez, M., et al., *A review on the visible light active titanium dioxide photocatalysts for environmental applications.* Applied Catalysis B: Environmental, 2012. **125**(0): p. 331-349.
3. Kurella, A. and N.B. Dahotre, *Review paper: Surface Modification for Bioimplants: The Role of Laser Surface Engineering.* Journal of Biomaterials Applications, 2005. **20**(1): p. 5-50.
4. Bonet, J., et al., *Numerical simulation of the superplastic forming of dental and medical prostheses.* Biomech Model Mechanobiol, 2002. **1**(3): p. 177-96.
5. Liu, X., P.K. Chu, and C. Ding, *Surface modification of titanium, titanium alloys, and related materials for biomedical applications.* Materials Science and Engineering: R: Reports, 2004. **47**(3–4): p. 49-121.
6. Li, X., et al., *A novel jet-based nano-hydroxyapatite patterning technique for osteoblast guidance.* J R Soc Interface, 2010. **7**(42): p. 189-97.
7. Michaelson, M.D. and M.R. Smith, *Bisphosphonates for treatment and prevention of bone metastases.* J Clin Oncol, 2005. **23**(32): p. 8219-24.
8. Russell, R.G.G., *Bisphosphonates: Mode of Action and Pharmacology.* Pediatrics, 2007. **119**(Supplement 2): p. S150-S162.
9. Li, X., J. Huang, and M. Edirisinghe, *Development of nano-hydroxyapatite coating by electrohydrodynamic atomization spraying.* J Mater Sci Mater Med, 2008. **19**(4): p. 1545-51.
10. McCracken, M., *Dental Implant Materials: Commercially Pure Titanium and Titanium Alloys.* Journal of Prosthodontics, 1999. **8**(1): p. 40-43.
11. Niinomi, M., *Mechanical properties of biomedical titanium alloys.* Materials Science and Engineering: A, 1998. **243**(1–2): p. 231-236.
12. Narayanan, R., et al., *Calcium phosphate-based coatings on titanium and its alloys.* J Biomed Mater Res B Appl Biomater, 2008. **85**(1): p. 279-99.
13. Kokubo, T., et al., *Solutions able to reproduce in vivo surface-structure changes in bioactive glass-ceramic A-W.* J Biomed Mater Res, 1990. **24**(6): p. 721-34.
14. Yamazoe, J., et al., *The development of Ti alloys for dental implant with high corrosion resistance and mechanical strength.* Dent Mater J, 2007. **26**(2): p. 260-7.
15. Desai, S., B. Bidanda, and P. Bártolo, *Metallic and Ceramic Biomaterials: Current and Future Developments*, in *Bio-Materials and Prototyping Applications in Medicine*, P. Bártolo and B. Bidanda, Editors. 2008, Springer US. p. 1-14.
16. Ada Council On Scientific, A., *Titanium applications in dentistry.* The Journal of the American Dental Association, 2003. **134**(3): p. 347-349.
17. Wilson, W. and P. Chye Khoon, *Titanium Alloys in Orthopaedics*. Titanium Alloys - Advances in Properties Control. 2013.
18. Sergueeva, A.V., et al., *Advanced mechanical properties of pure titanium with ultrafine grained structure.* Scripta Materialia, 2001. **45**(7): p. 747-752.
19. Kuroda, D., et al., *Design and mechanical properties of new β type titanium alloys for implant materials.* Materials Science and Engineering: A, 1998. **243**(1–2): p. 244-249.
20. Palmquist, A., et al., *Titanium oral implants: surface characteristics, interface biology and clinical outcome.* J R Soc Interface, 2010. **7 Suppl 5**: p. S515-27.
21. Jorge, J., et al., *Titanium in Dentistry: Historical Development, State of the Art and Future Perspectives.* The Journal of Indian Prosthodontic Society, 2013. **13**(2): p. 71-77.
22. Neiva, R., H.-L. Wang, and J. Geng, *Introduction to Implant Dentistry*, in *Application of the Finite Element Method in Implant Dentistry*, J. Geng, W. Yan, and W. Xu, Editors. 2008, Springer Berlin Heidelberg. p. 42-60.
23. Branemark, P.I., et al., *Intra-osseous anchorage of dental prostheses. I. Experimental studies.* Scand J Plast Reconstr Surg, 1969. **3**(2): p. 81-100.
24. Branemark, P.I., et al., *Osseointegrated implants in the treatment of the edentulous jaw. Experience from a 10-year period.* Scand J Plast Reconstr Surg Suppl, 1977. **16**: p. 1-132.

25. ADA COUNCIL ON SCIENTIFIC AFFAIRS, *Titanium applications in dentistry.* J Am Dent Assoc, 2003. **134**(3): p. 347-349.
26. Wakabayashi, N. and M. Ai, *A short-term clinical follow-up study of superplastic titanium alloy for major connectors of removable partial dentures.* The Journal of Prosthetic Dentistry, 1997. **77**(6): p. 583-587.
27. Hatamleh, M.M. and D.C. Watts, *Bonding of maxillofacial silicone elastomers to an acrylic substrate.* Dental Materials, 2010. **26**(4): p. 387-395.
28. Hatamleh, M.M. and D.C. Watts, *Mechanical properties and bonding of maxillofacial silicone elastomers.* Dental Materials, 2010. **26**(2): p. 185-191.
29. Lausmaa, J., *Surface spectroscopic characterization of titanium implant materials.* Journal of Electron Spectroscopy and Related Phenomena, 1996. **81**(3): p. 343-361.
30. Lee, M.-J., J.-H. Kim, and Y.-T. Park, *Surface Modification Reaction of Photocatalytic Titanium Dioxide with Triethoxysilane for Improving Dispersibility.* Bulletin of the Korean Chemical Society, 2010. **31**(5): p. 1275-1279.
31. Bhattacharyya, A. and J.A. Eades, *Use of an energy filter to improve the spatial resolution of electron backscatter diffraction.* Scanning, 2009. **31**(3): p. 114-21.
32. Leyens, C., ed. *Titanium and Titanium Alloys: Fundamentals and Applications*. 2003, John Wiley & Sons.
33. Witkowski, S., F. Komine, and T. Gerds, *Marginal accuracy of titanium copings fabricated by casting and CAD/CAM techniques.* The Journal of Prosthetic Dentistry, 2006. **96**(1): p. 47-52.
34. Fuster-Torres, M.Á., *CAD / CAM dental systems in implant dentistry: Update.* Med Oral Patol Oral Cir Bucal, 2009. **14**(3): p. 141-5.
35. Soo, S., R. Palmer, and R.V. Curtis, *Measurement of the setting and thermal expansion of dental investments used for the superplastic forming of dental implant superstructures.* Dental materials : official publication of the Academy of Dental Materials, 2001. **17**(3): p. 247-252.
36. Curtis, R.V., *The suitability of dental investment materials as dies for superplastic forming of medical and dental prostheses.* Materialwissenschaft und Werkstofftechnik, 2008. **39**(4-5): p. 322-326.
37. Barnes, A.J., *Superplastic Forming 40 Years and Still Growing.* Journal of Materials Engineering and Performance, 2007. **16**(4): p. 440-454.
38. Soo, S., et al., *The longitudinal accuracy of fit of titanium implant superstructures superplastically formed on investment models.* Dent Mater, 2004. **20**(3): p. 269-76.
39. Todd, R.I., *Critical review of mechanism of superplastic deformation in fine grained metallic materials.* Materials Science and Technology, 2000. **16**(11-12): p. 1287-1294.
40. Curtis, R.V., ed. *Dental biomaterials Imaging, testing and modelling*. 1st ed. 2008, Woodhead Publishing Limited.
41. Low, D.S., M. V., *Mechanical properties of dental investment materials.* Journal of Materials Science: Materials in Medicine, 2000. **11**(7): p. 399-405.
42. Allan, F.C. and K. Asgar, *Reaction of Cobalt-Chromium Casting Alloy with Investment.* Journal of Dental Research, 1966. **45**(5): p. 1516-1528.
43. Neiman, R. and A.C. Sarma, *Setting and thermal reactions of phosphate investments.* J Dent Res, 1980. **59**(9): p. 1478-85.
44. Neiman, R. and A.C. Sarma, *Setting and Thermal Reactions of Phosphate Investments.* Journal of Dental Research, 1980. **59**(9): p. 1478-1485.
45. Soudee, E. and J. Pera, *Mechanism of setting reaction in magnesia-phosphate cements.* Cement and Concrete Research, 2000. **30**(2): p. 315-321.
46. Scrimgeour, S.N., J.A. Chudek, and C.H. Lloyd, *The determination of phosphorus containing compounds in dental casting investment products by 31P solid-state MAS-NMR spectroscopy.* Dent Mater, 2007. **23**(4): p. 415-24.
47. Scrimgeour, S.N., et al., *(31)P solid-state MAS-NMR spectroscopy of the compounds that form in phosphate-bonded dental casting investment materials during setting.* Dent Mater, 2007. **23**(8): p. 934-43.
48. Scrimgeour, S.N., J.A. Chudek, and C.H. Lloyd, *The determination of phosphorus containing compounds in dental casting investment products by 31P solid-state MAS-NMR spectroscopy.* Dental Materials, 2007. **23**(4): p. 415-424.
49. Scrimgeour, S.N., et al., *31P solid-state MAS-NMR spectroscopy of the compounds that form in phosphate-bonded dental casting investment materials during setting.* Dental Materials, 2007. **23**(8): p. 934-943.
50. Yan, M., *Gypsum-bonded alumina dental investment for high fusing casting.* Dent Mater J, 1998. **17**: p. 174-185.

51. Meng, Y., *Study of resin bonded calcia investment: Part 3. Hardness of titanium castings.* Dent Mater J, 2004. **23**: p. 46-52.
52. Chew, C.L., et al., *Investment strength as a function of time and temperature.* Journal of Dentistry, 1999. **27**(4): p. 297-302.
53. Takahashi, J., et al., *Casting Pure Titanium into Commercial Phosphate-bonded SiO2 Investment Molds.* Journal of Dental Research, 1990. **69**(12): p. 1800-1805.
54. Cai, Z., et al., *In vitro corrosion resistance of titanium made using different fabrication methods.* Biomaterials, 1999. **20**(2): p. 183-190.
55. Eliopoulos, D., S. Zinelis, and T. Papadopoulos, *The effect of investment material type on the contamination zone and mechanical properties of commercially pure titanium castings.* The Journal of Prosthetic Dentistry, 2005. **94**(6): p. 539-548.
56. Ferenczi, A.M., et al., *Casted titanium for dental applications: an XPS and SEM study.* Biomaterials, 1998. **19**(16): p. 1513-1515.
57. Luo, X.P., et al., *Titanium casting into phosphate bonded investment with zirconite.* Dental Materials, 2002. **18**(7): p. 512-515.
58. Atwood, R.C., P.D. Lee, and R.V. Curtis, *Modeling the surface contamination of dental titanium investment castings.* Dental Materials, 2005. **21**(2): p. 178-186.
59. Syverud, M., T. Okabe, and H. Hero, *Casting of Ti-6Al-4V alloy compared with pure Ti in an Ar-arc casting machine.* Eur J Oral Sci, 1995. **103**(5): p. 327-30.
60. Larsson, C., et al., *Bone response to surface-modified titanium implants: studies on the early tissue response to machined and electropolished implants with different oxide thicknesses.* Biomaterials, 1996. **17**(6): p. 605-16.
61. Liu, X., P.K. Chu, and C. Ding, *Surface modification of titanium, titanium alloys, and related materials for biomedical applications.* Materials Science and Engineering: R: Reports, 2004. **47**(3-4): p. 49-121.
62. Wall, I., et al., *Modified titanium surfaces promote accelerated osteogenic differentiation of mesenchymal stromal cells in vitro.* Bone, 2009. **45**(1): p. 17-26.
63. Kajiwara, H., et al., *The bisphosphonate pamidronate on the surface of titanium stimulates bone formation around tibial implants in rats.* Biomaterials, 2005. **26**(6): p. 581-587.
64. Browne, M. and P.J. Gregson, *Surface modification of titanium alloy implants.* Biomaterials, 1994. **15**(11): p. 894-8.
65. Albrektsson, T. and A. Wennerberg, *Oral implant surfaces: Part 1--review focusing on topographic and chemical properties of different surfaces and in vivo responses to them.* Int J Prosthodont, 2004. **17**(5): p. 536-43.
66. Ronold, H.J. and J.E. Ellingsen, *Effect of micro-roughness produced by TiO2 blasting--tensile testing of bone attachment by using coin-shaped implants.* Biomaterials, 2002. **23**(21): p. 4211-9.
67. Fini, M., et al., *Biomechanical and histomorphometric investigations on two morphologically differing titanium surfaces with and without fluorohydroxyapatite coating: an experimental study in sheep tibiae.* Biomaterials, 2003. **24**(19): p. 3183-3192.
68. Yan, W.-Q., et al., *Apatite layer-coated titanium for use as bone bonding implants.* Biomaterials, 1997. **18**(17): p. 1185-1190.
69. Kim, H., et al., *The biocompatibility of SLA-treated titanium implants.* Biomed Mater, 2008. **3**(2): p. 025011.
70. Hu, X., et al., *Surface bioactivity modification of titanium by CO2 plasma treatment and induction of hydroxyapatite: In vitro and in vivo studies.* Applied Surface Science, 2011. **257**(6): p. 1813-1823.
71. Sobieszczyk, S., *Surface modifications of ti and its alloys.* Advances in Materials Sciences, 2010. **10**(1): p. 29-42.
72. Citeau, A., et al., *In vitro biological effects of titanium rough surface obtained by calcium phosphate grid blasting.* Biomaterials, 2005. **26**(2): p. 157-65.
73. Variola, F., et al., *Improving Biocompatibility of Implantable Metals by Nanoscale Modification of Surfaces: An Overview of Strategies, Fabrication Methods, and Challenges.* Small, 2009. **5**(9): p. 996-1006.
74. Lu, X., Z. Zhao, and Y. Leng, *Biomimetic calcium phosphate coatings on nitric-acid-treated titanium surfaces.* Materials Science and Engineering: C, 2007. **27**(4): p. 700-708.
75. Takeuchi, M., et al., *Acid pretreatment of titanium implants.* Biomaterials, 2003. **24**(10): p. 1821-1827.
76. Wen, H.B., et al., *Fast precipitation of calcium phosphate layers on titanium induced by simple chemical treatments.* Biomaterials, 1997. **18**(22): p. 1471-1478.

77. Kim, H.-M., et al., *Preparation of bioactive Ti and its alloys via simple chemical surface treatment.* Journal of Biomedical Materials Research, 1996. **32**(3): p. 409-417.
78. Li, P. and K. de Groot, *Calcium phosphate formation within sol-gel prepared titania in vitro and in vivo.* Journal of Biomedical Materials Research, 1993. **27**(12): p. 1495-1500.
79. Sobieszczyk, S., *Surface Modifications of Ti and its Alloys.* Advances in Materials Science, 2010. **10**(1): p. 23.
80. Brendel, T., A. Engel, and C. Rüssel, *Hydroxyapatite coatings by a polymeric route.* Journal of Materials Science: Materials in Medicine, 1992. **3**(3): p. 175-179.
81. Kim, H.-W., et al., *Hydroxyapatite coating on titanium substrate with titania buffer layer processed by sol–gel method.* Biomaterials, 2004. **25**(13): p. 2533-2538.
82. Cui, X., et al., *Preparation of bioactive titania films on titanium metal via anodic oxidation.* Dental Materials, 2009. **25**(1): p. 80-86.
83. Ishizawa, H. and M. Ogino, *Formation and characterization of anodic titanium oxide films containing Ca and P.* Journal of Biomedical Materials Research, 1995. **29**(1): p. 65-72.
84. Nie, X., A. Leyland, and A. Matthews, *Deposition of layered bioceramic hydroxyapatite/TiO2 coatings on titanium alloys using a hybrid technique of micro-arc oxidation and electrophoresis.* Surface and Coatings Technology, 2000. **125**(1–3): p. 407-414.
85. Gotfredsen, K., E. Hjorting-Hansen, and E. Budtz-Jorgensen, *Clinical and radiographic evaluation of submerged and nonsubmerged implants in monkeys.* Int J Prosthodont, 1990. **3**(5): p. 463-9.
86. Buser, D., et al., *Enhanced bone apposition to a chemically modified SLA titanium surface.* J Dent Res, 2004. **83**(7): p. 529-33.
87. Kokubo, T., *In Vivo Apatite Formation Induced on Titanium Metal and Its Alloys by Chemical Treatment.* Key Engineering Materials, 2000. **192**(1): p. 3-6.
88. Kim, H.M., et al., *Preparation of bioactive Ti and its alloys via simple chemical surface treatment.* J Biomed Mater Res, 1996. **32**(3): p. 409-17.
89. Kim, K.H. and N. Ramaswamy, *Electrochemical surface modification of titanium in dentistry.* Dent Mater J, 2009. **28**(1): p. 20-36.
90. Rudnev, V.S., et al., *Anodic spark deposition of P, Me(II) or Me(III) containing coatings on aluminium and titanium alloys in electrolytes with polyphosphate complexes.* Journal of Electroanalytical Chemistry, 2001. **497**(1-2): p. 150-158.
91. Del Curto, B., et al., *Anodic Spark Deposition treatments to increase reliability of Ti6Al4V modular prostheses.* J Appl Biomater Biomech, 2009. **7**(3): p. 153-9.
92. Li, L.-H., et al., *Improved biological performance of Ti implants due to surface modification by micro-arc oxidation.* Biomaterials, 2004. **25**(14): p. 2867-2875.
93. Sandrini, E., et al., *In vitro assessment of the osteointegrative potential of a novel multiphase anodic spark deposition coating for orthopaedic and dental implants.* Journal of Biomedical Materials Research Part B: Applied Biomaterials, 2005. **73B**(2): p. 392-399.
94. Chiesa, R., et al., *Osteointegration of titanium and its alloys by anodic spark deposition and other electrochemical techniques: a review.* J Appl Biomater Biomech, 2003. **1**(2): p. 91-107.
95. Kim, H.-W., et al., *Hydroxyapatite coating on titanium substrate with titania buffer layer processed by sol-gel method.* Biomaterials, 2004. **25**(13): p. 2533-2538.
96. Metikos-Hukovic, M., et al., *An in vitro study of Ti and Ti-alloys coated with sol-gel derived hydroxyapatite coatings.* Surface and Coatings Technology, 2003. **165**(1): p. 40-50.
97. Xu, W., et al., *Sol-gel derived HA/TiO2 double coatings on Ti scaffolds for orthopaedic applications.* Transactions of Nonferrous Metals Society of China, 2006. **16**(Supplement 1): p. s209-s216.
98. Zhang, W., C. Wang, and W. Liu, *Characterization and tribological investigation of sol-gel ceramic films on Ti-6Al-4V.* Wear, 2006. **260**(4-5): p. 379-386.
99. Zhao, Y., et al., *Preparation of Ti---Si mixed oxides by sol-gel one step hydrolysis.* Catalysis Today, 2004. **93-95**: p. 583-588.
100. Jones, A.C., ed. *Chemical Vapour Deposition, Precursors, Processes and Applications*. 2008, RSC Publishing.
101. Nolan, M.G., et al., *One step process for chemical vapour deposition of titanium dioxide thin films incorporating controlled structure nanoparticles.* Thin Solid Films, 2006. **515**(4): p. 1956-1962.
102. Puleo, D.A. and A. Nanci, *Understanding and controlling the bone-implant interface.* Biomaterials, 1999. **20**(23-24): p. 2311-2321.

103. Morra, M., *Biochemical modification of titanium surfaces: peptides and ECM proteins.* Eur Cell Mater, 2006. **12**: p. 1-15.
104. Puleo, D.A., R.A. Kissling, and M.S. Sheu, *A technique to immobilize bioactive proteins, including bone morphogenetic protein-4 (BMP-4), on titanium alloy.* Biomaterials, 2002. **23**(9): p. 2079-2087.
105. Heimann, R.B., *Thermal spraying of biomaterials.* Surface and Coatings Technology, 2006. **201**(5): p. 2012-2019.
106. Yip, C.S., et al., *Thermal spraying of Ti---6Al---4V/hydroxyapatite composites coatings: powder processing and post-spray treatment.* Journal of Materials Processing Technology, 1997. **65**(1-3): p. 73-79.
107. Liu, X., et al., *Plasma surface modification of titanium for hard tissue replacements.* Surface and Coatings Technology, 2004. **186**(1–2): p. 227-233.
108. Gabbi, C., et al., *Bioactive glass coating: physicochemical aspects and biological findings.* Biomaterials, 1995. **16**(7): p. 515-520.
109. Liu, X., C. Ding, and Z. Wang, *Apatite formed on the surface of plasma-sprayed wollastonite coating immersed in simulated body fluid.* Biomaterials, 2001. **22**(14): p. 2007-2012.
110. Helmersson, U., et al., *Ionized physical vapor deposition (IPVD): A review of technology and applications.* Thin Solid Films, 2006. **513**(1-2): p. 1-24.
111. Montie, T.C., K. Kelly-Wintenberg, and J.R. Roth, *An overview of research using the one atmosphere uniform glow discharge plasma (OAUGDP) for sterilization of surfaces and materials.* Plasma Science, IEEE Transactions on, 2000. **28**(1): p. 41-50.
112. Chu, P.K., *Recent applications of plasma-based ion implantation and deposition to microelectronic, nano-structured, and biomedical materials.* Surface and Coatings Technology, 2010. **204**(18-19): p. 2853-2863.
113. Hanawa, T., et al., *Early bone formation around calcium-ion-implanted titanium inserted into rat tibia.* Journal of Biomedical Materials Research, 1997. **36**(1): p. 131-136.
114. Loinaz, A., et al., *Effects of plasma immersion ion implantation of oxygen on mechanical properties and microstructure of Ti6Al4V.* Surface and Coatings Technology, 1998. **103-104**: p. 262-267.
115. Xie, Y., et al., *Improvement of surface bioactivity on titanium by water and hydrogen plasma immersion ion implantation.* Biomaterials, 2005. **26**(31): p. 6129-35.
116. Li, X., J. Huang, and M.J. Edirisinghe, *Novel patterning of nano-bioceramics: template-assisted electrohydrodynamic atomization spraying.* Journal of The Royal Society Interface, 2008. **5**(19): p. 253-257.
117. BONFIELD, W., et al., *ELECTROHYDRODYNAMIC PROCESSING OF CALCIUM PHOSPHATES: COATING AND PATTERNING FOR MEDICAL IMPLANTS.* Nano LIFE, 2012. **02**(01): p. 1250008.
118. Prawel, D.A., et al., *Electrohydrodynamic atomization technique for applying phospholipid coatings to titanium implant materials.* Materials Letters, 2013. **97**(0): p. 81-85.
119. Huang, J., et al., *Electrohydrodynamic deposition of nanotitanium doped hydroxyapatite coating for medical and dental applications.* J Mater Sci Mater Med, 2011. **22**(3): p. 491-6.
120. de Jonge, L.T., et al., *The osteogenic effect of electrosprayed nanoscale collagen/calcium phosphate coatings on titanium.* Biomaterials, 2010. **31**(9): p. 2461-2469.
121. Niinomi, M., *Recent research and development in titanium alloys for biomedical applications and healthcare goods.* Science and Technology of Advanced Materials, 2003. **4**(5): p. 445.
122. Rey, C., *Calcium phosphate biomaterials and bone mineral. Differences in composition, structures and properties.* Biomaterials, 1990. **11**: p. 13-5.
123. de Jonge, L.T., et al., *Organic-inorganic surface modifications for titanium implant surfaces.* Pharm Res, 2008. **25**(10): p. 2357-69.
124. Leeuwenburgh, S.C., et al., *In vitro and in vivo reactivity of porous, electrosprayed calcium phosphate coatings.* Biomaterials, 2006. **27**(18): p. 3368-78.
125. Paital, S.R. and N.B. Dahotre, *Calcium phosphate coatings for bio-implant applications: Materials, performance factors, and methodologies.* Materials Science and Engineering: R: Reports, 2009. **66**(1–3): p. 1-70.
126. Stan, G.E., et al., *Highly adherent bioactive glass thin films synthetized by magnetron sputtering at low temperature.* J Mater Sci Mater Med, 2011. **22**(12): p. 2693-710.
127. Oonishi, H., et al., *Comparative bone growth behavior in granules of bioceramic materials of various sizes.* J Biomed Mater Res, 1999. **44**(1): p. 31-43.

128. Bolelli, G., et al., *Influence of the manufacturing process on the crystallization behavior of a CZS glass system.* Journal of Non-Crystalline Solids, 2005. **351**(30–32): p. 2537-2546.
129. Gomez-Vega, J.M., et al., *Bioactive glass coatings with hydroxyapatite and Bioglass particles on Ti-based implants. 1. Processing.* Biomaterials, 2000. **21**(2): p. 105-11.
130. Gupta, R. and A. Kumar, *Bioactive materials for biomedical applications using sol-gel technology.* Biomed Mater, 2008. **3**(3): p. 034005.
131. Altomare, L., et al., *Microstructure and in vitro behaviour of 45S5 bioglass coatings deposited by high velocity suspension flame spraying (HVSFS).* J Mater Sci Mater Med, 2011. **22**(5): p. 1303-19.
132. Bierbaum, S., et al., *Modification of Ti6AL4V surfaces using collagen I, III, and fibronectin. II. Influence on osteoblast responses.* J Biomed Mater Res A, 2003. **67**(2): p. 431-8.
133. Wahl, D.A. and J.T. Czernuszka, *Collagen-hydroxyapatite composites for hard tissue repair.* Eur Cell Mater, 2006. **11**: p. 43-56.
134. Russell, R.G.G. and M.J. Rogers, *Bisphosphonates: from the laboratory to the clinic and back again.* Bone, 1999. **25**(1): p. 97-106.
135. McLeod, K., et al., *Adsorption of bisphosphonate onto hydroxyapatite using a novel co-precipitation technique for bone growth enhancement.* J Biomed Mater Res A, 2006. **79**(2): p. 271-81.
136. Giger, E.V., B. Castagner, and J.C. Leroux, *Biomedical applications of bisphosphonates.* J Control Release, 2013. **167**(2): p. 175-88.
137. Marx, R.E., *Pamidronate (Aredia) and zoledronate (Zometa) induced avascular necrosis of the jaws: a growing epidemic.* J Oral Maxillofac Surg, 2003. **61**(9): p. 1115-7.
138. Moon, H.J., et al., *Effect of heparin and alendronate coating on titanium surfaces on inhibition of osteoclast and enhancement of osteoblast function.* Biochem Biophys Res Commun, 2011. **413**(2): p. 194-200.
139. Ezra, A. and G. Golomb, *Administration routes and delivery systems of bisphosphonates for the treatment of bone resorption.* Adv Drug Deliv Rev, 2000. **42**(3): p. 175-95.
140. Fleisch, H., *Bisphosphonates: mechanisms of action.* Endocr Rev, 1998. **19**(1): p. 80-100.
141. Wermelin, K., et al., *Bisphosphonate coating on titanium screws increases mechanical fixation in rat tibia after two weeks.* J Biomed Mater Res A, 2008. **86**(1): p. 220-7.
142. Singhatanadgit, W., *Biological Responses to New Advanced Surface Modifications of Endosseous Medical Implants.* Bone and Tissue Regeneration Insights, 2009. **2**(1566-BTRI-Biological-Responses-to-New-Advanced-Surface-Modifications-of-Endosseo.pdf): p. 1-11.
143. Gao, Y., et al., *The effect of surface immobilized bisphosphonates on the fixation of hydroxyapatite-coated titanium implants in ovariectomized rats.* Biomaterials, 2009. **30**(9): p. 1790-6.
144. Greiner, S.H., et al., *Local application of zoledronic acid incorporated in a poly(D,L-lactide)-coated implant accelerates fracture healing in rats.* Acta Orthop, 2008. **79**(5): p. 717-25.
145. Stadelmann, V.A., et al., *Prediction of bone density around orthopedic implants delivering bisphosphonate.* J Biomech, 2009. **42**(9): p. 1206-11.
146. Moon, H.-J., et al., *Effect of heparin and alendronate coating on titanium surfaces on inhibition of osteoclast and enhancement of osteoblast function.* Biochemical and Biophysical Research Communications, 2011. **413**(2): p. 194-200.
147. S.Anil, P.S.A., H. Alghamdi and J.A. Jansen *Dental Implant Surface Enhancement and Osseointegration*, in *Dental Implant Surface Enhancement and Osseointegration, Implant Dentistry - A Rapidly Evolving Practice*, P.I. Turkyilmaz, Editor. 2011. p. 83-110.
148. Huang, Y.H., et al., *Bone formation at titanium porous oxide (TiUnite) oral implants in type IV bone.* Clin Oral Implants Res, 2005. **16**(1): p. 105-11.
149. Soskolne, W.A., et al., *The effect of titanium surface roughness on the adhesion of monocytes and their secretion of TNF-alpha and PGE2.* Clin Oral Implants Res, 2002. **13**(1): p. 86-93.
150. Albrektsson, T., et al., *Osseointegrated titanium implants. Requirements for ensuring a long-lasting, direct bone-to-implant anchorage in man.* Acta Orthop Scand, 1981. **52**(2): p. 155-70.
151. Zhao, G., et al., *Osteoblast-like cells are sensitive to submicron-scale surface structure.* Clin Oral Implants Res, 2006. **17**(3): p. 258-64.

152. Cochran, D.L., et al., *The use of reduced healing times on ITI implants with a sandblasted and acid-etched (SLA) surface: early results from clinical trials on ITI SLA implants.* Clin Oral Implants Res, 2002. **13**(2): p. 144-53.
153. Buser, D., et al., *Interface shear strength of titanium implants with a sandblasted and acid-etched surface: a biomechanical study in the maxilla of miniature pigs.* J Biomed Mater Res, 1999. **45**(2): p. 75-83.
154. Anselme, K., et al., *The relative influence of the topography and chemistry of TiAl6V4 surfaces on osteoblastic cell behaviour.* Biomaterials, 2000. **21**(15): p. 1567-77.
155. Shalabi, M.M., et al., *Implant surface roughness and bone healing: a systematic review.* J Dent Res, 2006. **85**(6): p. 496-500.
156. Huang, H.H., et al., *Effect of surface roughness of ground titanium on initial cell adhesion.* Biomol Eng, 2004. **21**(3-5): p. 93-7.
157. Deligianni, D.D., et al., *Effect of surface roughness of the titanium alloy Ti–6Al–4V on human bone marrow cell response and on protein adsorption.* Biomaterials, 2001. **22**(11): p. 1241-1251.
158. Dowling, D.P., et al., *Effect of Surface Wettability and Topography on the Adhesion of Osteosarcoma Cells on Plasma-modified Polystyrene.* Journal of Biomaterials Applications, 2011. **26**(3): p. 327-347.
159. Sul, Y.T., et al., *Optimum surface properties of oxidized implants for reinforcement of osseointegration: surface chemistry, oxide thickness, porosity, roughness, and crystal structure.* Int J Oral Maxillofac Implants, 2005. **20**(3): p. 349-59.
160. Wakabayashi, N. and M. Ai, *A short-term clinical follow-up study of superplastic titanium alloy for major connectors of removable partial dentures.* J Prosthet Dent, 1997. **77**(6): p. 583-7.
161. Hatamleh, M.M. and D.C. Watts, *Mechanical properties and bonding of maxillofacial silicone elastomers.* Dent Mater, 2010. **26**(2): p. 185-91.
162. Hatamleh, M.M. and D.C. Watts, *Bonding of maxillofacial silicone elastomers to an acrylic substrate.* Dent Mater, 2010. **26**(4): p. 387-95.
163. Kajiwara, H., et al., *The bisphosphonate pamidronate on the surface of titanium stimulates bone formation around tibial implants in rats.* Biomaterials, 2005. **26**(6): p. 581-7.
164. Oh, S.-H., et al., *Growth of nano-scale hydroxyapatite using chemically treated titanium oxide nanotubes.* Biomaterials, 2005. **26**(24): p. 4938-4943.
165. Rocha, S.S.d., et al., *Effect of phosphate-bonded investments on titanium reaction layer and crown fit.* Brazilian Oral Research, 2010. **24**: p. 147-152.
166. Omar, R.A., et al., *Titanium Alloys for Dental and Mixillofacial Applications*. 2011: University of London.
167. Allan, F.C. and K. Asgar, *Reaction of cobalt-chromium casting alloy with investment.* J Dent Res, 1966. **45**(5): p. 1516-28.
168. Jager, M., et al., *Osteoblast differentiation onto different biometals with an endoprosthetic surface topography in vitro.* J Biomed Mater Res A, 2008. **86**(1): p. 61-75.
169. Di-Silvio, L. and N. Gurav, *Osteoblasts*, in *Human Cell Culture*, M. Koller, B. Palsson, and J.W. Masters, Editors. 2002, Springer Netherlands. p. 221-241.
170. Filiaggi, M.J., N.A. Coombs, and R.M. Pilliar, *Characterization of the interface in the plasma-sprayed HA coating/Ti-6Al-4V implant system.* J Biomed Mater Res, 1991. **25**(10): p. 1211-29.
171. Hayashi, K., T. Mashima, and K. Uenoyama, *The effect of hydroxyapatite coating on bony ingrowth into grooved titanium implants.* Biomaterials, 1999. **20**(2): p. 111-9.
172. Lacefield, W.R., *Hydroxyapatite Coatings.* Annals of the New York Academy of Sciences, 1988. **523**(1): p. 72-80.
173. Evans, S.L., K.R. Lawes, and P.J. Gregson, *Layered, adhesively bonded hydroxyapatite coatings for orthopaedic implants.* Journal of Materials Science: Materials in Medicine, 1994. **5**(6-7): p. 495-499.
174. Boulton, L.M., et al., *Adhesively bonded hydroxyapatite coating.* Materials Letters, 1991. **12**(1–2): p. 1-6.
175. Wei, M., et al., *Solution ripening of hydroxyapatite nanoparticles: effects on electrophoretic deposition.* J Biomed Mater Res, 1999. **45**(1): p. 11-9.
176. Kikuchi, S. and J. Takebe, *Characterization of the surface deposition on anodized-hydrothermally treated commercially pure titanium after immersion in simulated body fluid.* J Prosthodont Res, 2010. **54**(2): p. 70-7.
177. Yousefpour, M., et al., *Bioactive layer formation on alkaline-acid treated titanium in simulated body fluid.* Materials & Design, 2007. **28**(7): p. 2154-2159.

178. Dalgarno, K.W., et al., *Mass customization of medical devices and implants: state of the art and future directions.* Virtual and Physical Prototyping, 2006. **1**(3): p. 137-145.
179. Combes, C. and C. Rey, *Amorphous calcium phosphates: Synthesis, properties and uses in biomaterials.* Acta Biomaterialia, 2010. **6**(9): p. 3362-3378.
180. Takadama, H., et al., *TEM-EDX study of mechanism of bonelike apatite formation on bioactive titanium metal in simulated body fluid.* J Biomed Mater Res, 2001. **57**(3): p. 441-8.
181. Vanzillotta, P.S., et al., *Improvement of in vitro titanium bioactivity by three different surface treatments.* Dental Materials, 2006. **22**(3): p. 275-282.
182. Lee, B.-H., et al., *Surface modification by alkali and heat treatments in titanium alloys.* Journal of Biomedical Materials Research, 2002. **61**(3): p. 466-473.
183. Wang, X.X., et al., *Apatite deposition on thermally and anodically oxidized titanium surfaces in a simulated body fluid.* Biomaterials, 2003. **24**(25): p. 4631-7.
184. Combes, C. and C. Rey, *Amorphous calcium phosphates: synthesis, properties and uses in biomaterials.* Acta Biomater, 2010. **6**(9): p. 3362-78.
185. Kokubo, T. and S. Yamaguchi, *Novel Bioactive Titanate Layers Formed on Ti Metal and Its Alloys by Chemical Treatments.* Materials, 2009. **3**(1): p. 48-63.
186. Yang, G.-l., et al., *Effects of biomimetically and electrochemically deposited nano-hydroxyapatite coatings on osseointegration of porous titanium implants.* Oral Surgery, Oral Medicine, Oral Pathology, Oral Radiology, and Endodontology, 2009. **107**(6): p. 782-789.
187. Bathomarco, R.V., et al., *Atomic force microscopy analysis of different surface treatments of Ti dental implant surfaces.* Applied Surface Science, 2004. **233**(1–4): p. 29-34.
188. Hamouda, I.M., et al., *Alkali and heat treatment of titanium implant material for bioactivity.* Int J Oral Maxillofac Implants, 2012. **27**(4): p. 776-84.
189. Nishiguchi, S., et al., *Titanium metals form direct bonding to bone after alkali and heat treatments.* Biomaterials, 2001. **22**(18): p. 2525-2533.
190. Fawzy, A.S. and M.A. Amer, *An in vitro and in vivo evaluation of bioactive titanium implants following sodium removal treatment.* Dental Materials, 2009. **25**(1): p. 48-57.
191. Uchida, M., et al., *Effect of water treatment on the apatite-forming ability of NaOH-treated titanium metal.* J Biomed Mater Res, 2002. **63**(5): p. 522-30.
192. Fujibayashi, S., et al., *Bioactive titanium: effect of sodium removal on the bone-bonding ability of bioactive titanium prepared by alkali and heat treatment.* J Biomed Mater Res, 2001. **56**(4): p. 562-70.
193. Takemoto, M., et al., *Mechanical properties and osteoconductivity of porous bioactive titanium.* Biomaterials, 2005. **26**(30): p. 6014-23.
194. Lee, M.H., J.H. Kang, and S.W. Lee, *The effect of surface microgrooves and anodic oxidation on the surface characteristics of titanium and the osteogenic activity of human periodontal ligament cells.* Archives of Oral Biology, 2013. **58**(1): p. 59-66.
195. Paul, W. and C.P. Sharma, *Effect of calcium, zinc and magnesium on the attachment and spreading of osteoblast like cells onto ceramic matrices.* J Mater Sci Mater Med, 2007. **18**(5): p. 699-703.
196. Feng, B., et al., *Characterization of surface oxide films on titanium and bioactivity.* J Mater Sci Mater Med, 2002. **13**(5): p. 457-64.
197. Vanzillotta, P.S., et al., *Improvement of in vitro titanium bioactivity by three different surface treatments.* Dental materials : official publication of the Academy of Dental Materials, 2006. **22**(3): p. 275-282.
198. Chosa, N., et al., *Characterization of apatite formed on alkaline-heat-treated Ti.* J Dent Res, 2004. **83**(6): p. 465-9.
199. Kokubo, T., et al., *Spontaneous Formation of Bonelike Apatite Layer on Chemically Treated Titanium Metals.* Journal of the American Ceramic Society, 1996. **79**(4): p. 1127-1129.
200. Kokubo, T., et al., *REVIEW Bioactive metals: preparation and properties.* Journal of Materials Science: Materials in Medicine, 2004. **15**(2): p. 99-107.
201. M. Ravelingien , S.M., J. Luyten , V. Meynen , E. Vinck , Ch. Vervaet , J.-P. Remon *Influence of Heat Treatment on the In Vitro Bioactivity of Alkali-treated Titanium Surfaces.* Ceramics-Silikáty, 2010. **54**(3): p. 241-247.
202. Chen, Y., et al., *Effect of Ti–OH formation on bioactivity of vacuum plasma sprayed titanium coating after chemical treatment.* Surface and Coatings Technology, 2007. **202**(3): p. 494-498.

203. Abtahi, J., P. Tengvall, and P. Aspenberg, *A bisphosphonate-coating improves the fixation of metal implants in human bone. A randomized trial of dental implants.* Bone, 2012. **50**(5): p. 1148-1151.
204. Lee, T.C., et al., *Bone morphogenetic protein gene therapy using a fibrin scaffold for a rabbit spinal-fusion experiment.* Neurosurgery, 2006. **58**(2): p. 373-80; discussion 373-80.
205. Sellers, R.S., D. Peluso, and E.A. Morris, *The effect of recombinant human bone morphogenetic protein-2 (rhBMP-2) on the healing of full-thickness defects of articular cartilage.* J Bone Joint Surg Am, 1997. **79**(10): p. 1452-63.
206. Kim, S.E., et al., *The effect of immobilization of heparin and bone morphogenic protein-2 (BMP-2) to titanium surfaces on inflammation and osteoblast function.* Biomaterials, 2011. **32**(2): p. 366-73.
207. Palmquist, A., et al., *Titanium oral implants: surface characteristics, interface biology and clinical outcome.* Journal of The Royal Society Interface, 2010.
208. Im, G.I., et al., *Osteoblast proliferation and maturation by bisphosphonates.* Biomaterials, 2004. **25**(18): p. 4105-15.
209. Josse, S., et al., *Novel biomaterials for bisphosphonate delivery.* Biomaterials, 2005. **26**(14): p. 2073-80.
210. Faucheux, C., et al., *Controlled release of bisphosphonate from a calcium phosphate biomaterial inhibits osteoclastic resorption in vitro.* J Biomed Mater Res A, 2009. **89**(1): p. 46-56.
211. Yoshinari, M., et al., *Immobilization of bisphosphonates on surface modified titanium.* Biomaterials, 2001. **22**(7): p. 709-15.
212. Meraw, S.J. and C.M. Reeve, *Qualitative analysis of peripheral peri-implant bone and influence of alendronate sodium on early bone regeneration.* J Periodontol, 1999. **70**(10): p. 1228-33.
213. Meraw, S.J., C.M. Reeve, and P.C. Wollan, *Use of alendronate in peri-implant defect regeneration.* J Periodontol, 1999. **70**(2): p. 151-8.
214. Bellido, T. and L.I. Plotkin, *Novel actions of bisphosphonates in bone: preservation of osteoblast and osteocyte viability.* Bone, 2011. **49**(1): p. 50-5.
215. Peter, B., et al., *Calcium phosphate drug delivery system: influence of local zoledronate release on bone implant osteointegration.* Bone, 2005. **36**(1): p. 52-60.
216. Boanini, E., et al., *The effect of zoledronate-hydroxyapatite nanocomposites on osteoclasts and osteoblast-like cells in vitro.* Biomaterials, 2012. **33**(2): p. 722-30.
217. Nancollas, G.H., et al., *Novel insights into actions of bisphosphonates on bone: differences in interactions with hydroxyapatite.* Bone, 2006. **38**(5): p. 617-27.
218. Henneman, Z.J., et al., *Bisphosphonate binding affinity as assessed by inhibition of carbonated apatite dissolution in vitro.* Journal of Biomedical Materials Research Part A, 2008. **85A**(4): p. 993-1000.
219. Naidu, A., et al., *The effects of bisphosphonates on osteoblasts in vitro.* Oral surgery, oral medicine, oral pathology, oral radiology, and endodontics, 2008. **106**(1): p. 5-13.
220. Sun, J., et al., *Effects of alendronate on human osteoblast-like MG63 cells and matrix metalloproteinases.* Arch Oral Biol, 2012. **57**(6): p. 728-36.
221. Garcia-Moreno, C., et al., *Effect of alendronate on cultured normal human osteoblasts.* Bone, 1998. **22**(3): p. 233-9.
222. Nishikawa, M., et al., *Bisphosphonates act on osteoblastic cells and inhibit osteoclast formation in mouse marrow cultures.* Bone, 1996. **18**(1): p. 9-14.
223. Sahni, M., et al., *Bisphosphonates act on rat bone resorption through the mediation of osteoblasts.* J Clin Invest, 1993. **91**(5): p. 2004-11.
224. Itoh, F., et al., *Clodronate stimulates osteoblast differentiation in ST2 and MC3T3-E1 cells and rat organ cultures.* Eur J Pharmacol, 2003. **477**(1): p. 9-16.
225. D'Aoust, P., et al., *Etidronate (HEBP) promotes osteoblast differentiation and wound closure in rat calvaria.* Cell Tissue Res, 2000. **302**(3): p. 353-63.
226. Tsuchimoto, M., et al., *Alendronate modulates osteogenesis of human osteoblastic cells in vitro.* Jpn J Pharmacol, 1994. **66**(1): p. 25-33.
227. Idris, A.I., et al., *Aminobisphosphonates cause osteoblast apoptosis and inhibit bone nodule formation in vitro.* Calcif Tissue Int, 2008. **82**(3): p. 191-201.
228. Reinholz, G.G., et al., *Bisphosphonates directly regulate cell proliferation, differentiation, and gene expression in human osteoblasts.* Cancer Res, 2000. **60**(21): p. 6001-7.
229. Surmenev, R.A., *A review of plasma-assisted methods for calcium phosphate-based coatings fabrication.* Surface and Coatings Technology, 2012. **206**(8–9): p. 2035-2056.

230. L.L. Hench, J.R.J., M.B. Fenn *Bioactive materials for gene control*, in *New materials and technologies for healthcare*, J.R.J. L.L. Hench, M.B. Fenn Editor. 2011: World Scientific, Singapore p. 25–48.
231. Jones, J.R., *Review of bioactive glass: from Hench to hybrids.* Acta Biomater, 2013. **9**(1): p. 4457-86.
232. Elias, C.N., et al., *Relationship between surface properties (roughness, wettability and morphology) of titanium and dental implant removal torque.* J Mech Behav Biomed Mater, 2008. **1**(3): p. 234-42.
233. Kokubo, T., *Bioactive glass ceramics: properties and applications.* Biomaterials, 1991. **12**(2): p. 155-163.
234. Farooq, I.I., Zonera; Farooq, Umer; Leghari, Ali; Ali, Humera, *Bioactive Glass: A Material for the Future.* World Journal of Dentistry April 2012. **3**(2): p. 199.
235. Yamaguchi, K., et al., *Involvement of interleukin-1 in the inflammatory actions of aminobisphosphonates in mice.* Br J Pharmacol, 2000. **130**(7): p. 1646-54.
236. Acil, Y., et al., *The cytotoxic effects of three different bisphosphonates in-vitro on human gingival fibroblasts, osteoblasts and osteogenic sarcoma cells.* J Craniomaxillofac Surg, 2012. **40**(8): p. e229-35.
237. Misra, S.K., et al., *Comparison of nanoscale and microscale bioactive glass on the properties of P(3HB)/Bioglass composites.* Biomaterials, 2008. **29**(12): p. 1750-61.
238. Lian, J.B. and G.S. Stein, *Concepts of osteoblast growth and differentiation: basis for modulation of bone cell development and tissue formation.* Crit Rev Oral Biol Med, 1992. **3**(3): p. 269-305.
239. Vandamme, K., et al., *In vivo molecular evidence of delayed titanium implant osseointegration in compromised bone.* Biomaterials, 2011. **32**(14): p. 3547-54.
240. Omar, R.A., *Titanium Alloys for Dental and Maxillofacial Applications*, in *Department of Biomaterials, Biomimetics & Biophotonics*. 2011, King's College London: London UK. p. 249.

CHAPTER EIGHT

Appendices

8.1. Introduction

This section of experiment is describing the gene expression analysis, which has been done, on the different coated and treated surfaces using the electrohdyrodynamic method from chapter 5. The coated surfaces included untreated titanium surfaces, Bioglass coated surfaces, and Bioglass bisphosphonate coated surfaces. Although the results showed poor recognition of the desired genes on the coated surfaces, which maybe due to the toxice leachables from the bioglass during the coating process, but it was important to state this analysis and showed these results in the appendix.

8.2. Materials and Methodology

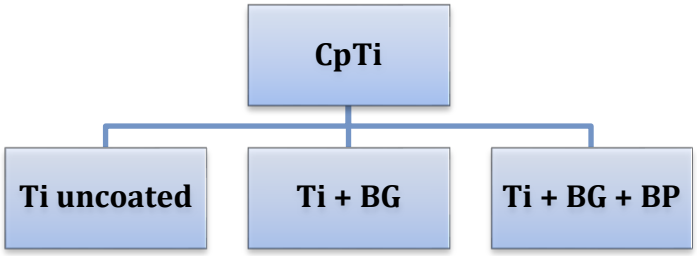

Figure 8.1. Schematic illustration of the experimental group investigated in this study, Ti: Titanium, BG: Bioglass, BPs: Bisphosphonate (sodium alendronate)

8.2.1. Gene Expression Analysis

8.2.1.1. RNA Extraction from Cultured Cells

Reagent preparation: TRI reagent was prepared by mixing 250µl of nuclease-free water with 750µl % ethanol per ml of TRI reagent solution.

RNA extraction: Cell culture medium was removed from the wells and 1ml of TRI Reagent (Ambion® AM9738) was added in a fume cupboard before placing at -80°C freezer for at least of 24 hours (to maximize RNA yield). Samples were then thawed at room temperature before transferring TRI Reagent containing cells into a 2ml phase

lock heavy gel tube (S Prime 2302830). 200µl of chloroform (Sigma C2432) was added to each sample tube and then shaken vigorously for a few seconds and left to stand for one minute. Samples were then centrifuged at 12,000 rpm for 15 minutes at 4°C. The resulting aqueous phase from each tube was transferred to a 1.5ml eppendorf tube and 0.5ml of propan-2-ol (Sigma I9516) was added to each sample before being left to precipitate over night at -80°C. Immediately after removing from the -80°C freezer, the samples were centrifuged at 20,000 rpm for 20 minutes at 4°C. Supernatants were removed carefully in order not to disturb the RNA pellet. 1ml of 75% ethanol (Sigma E7023) was added and samples were vortexed for a few seconds and subsequently re-centrifuged at 4°C for 5 minutes at 7,500 rpm. Ethanol was then removed taking care not to extricate any observable RNA pellets, after which they were dried at room temperature for 10 minutes. 10 µl of molecular water is then added to the samples and kept at -80°C for at least 24 hours.

8.2.1.2. Quantification of Extracted RNA and Quantity Analysis

RNA concentration was determined using the Qubit RNA BR Assay Kit (Q10210) and read using the Qubit Fluorometer 2.0 (Q32866) where the amount of RNA is given by ng/µl. RNA quality was analyzed using Agilent RNA 6000 Nano (5067.1511) protocol and kit containing microfluidic chips, gel matrix and dye, ladder and marker. RNA integrity number (RIN) and 28s:18s ribosomal RNA ratio were obtained for quality analysis.

8.2.1.3. Reverse Transcriptase of RNA to cDNA

Complementary DNA (cDNA) was produced using a modified protocol from the Applied Biosystems High Capacity Reverse Transcriptase Kit (4368814). A master mix was prepared for each sample by mixing 2µl 10x RT Buffer, 0.8µl 25x dNTp Buffer, 2µl 10x RT Random Primer and 1µl Multiscribe Reverse Transcriptase. The mix was vortexed before aliquoting 5.8µl of the mixture into a PCR tube. After making up final volumes of 20 µl in each tube, samples were placed into the bench top Veriti Thermal Cycler for conversion to cDNA via a cDNA programe.

8.2.1.4. PCR Amplification

PCR reactions were performed using specific primer sets. These primers are; alkaline phosphatise (ALP) collagen type I, Osteocalcin (OSC), Runt-related transcription factor 2 (RUNX2), and Glyceraldehyde 3-phosphate dehydrogenase (GAPDH) which was used as a positive control, and nuclease-free water was used as a negative control. These primers' sequences and length are summarized in Table 5.1. 1µl of DNA

template was used in all of the PCR reactions. DNA was amplified using mixture of 12.5µl of GoTaq Green Master Mix 2x (Promega M7118) with 1µl of both forward and reverse primers (GAPDH primer F and GAPDH primer R). Samples were put into the bench top thermal cycler programmed running a PCR program.

Gene Product	Primer Sequence	Length (Base Pairs)
ALP	F5'-CCA CGT CTT CAC ATT TGG TG-3' R5'-AGA CTG CGC CTG GTA GTT GT- 5'	196bp
OSC	F5'-ATG AGA GCC CTC ACA CTC CT-3' R5'-CAA GGG GAA GAG GAA AGA AG-3'	377bp
RUNX2	F5'-CAG ACC AGC AGC ACT CCA TA- 3' R5'-CAG CGT CAA CAC CAT CAT TC- 3'	170bp
GAPDH	F5'-ACC ACA GTC CAT GCC ATC AC-3' R5'-TCC ACC ACC CTG TTG CTG TA-5'	452bp

Table 8.1: Primer sequences for RT-PCR, ALP: alkaline phosphatase, OSC: osteocalcin, RUNX2: Runt-related transcription factor 2, and GAPDH: Glyceraldehyde 3-phosphate dehydrogenase

8.2.1.5. Gel Electrophoresis

PCR product sizes were assessed by gel electrophoresis in 2% agarose gels made from Bioline Agarose Gel tablets (BIO-41028) and and 10x Tris Acetate-Ethylenediaminetetraacetic acid (TAE) in the amounts specified in the Bioline product protocol. 5µ-10µl of each sample was used to run gel electrophoresis alongside 10µl of DNA Ladder (PCRsizer100 base pair, Norgen Biotek Corporation 11400). Images were obtained using programmed software running along with the machine.

7.3. Results and Discussion

Day 14 was selected as a key time period, representative of HOB cell differentiation. Qualitative analysis of cell differentiation by PCR from RNA extracted directly from material and control at day 14 was carried out.

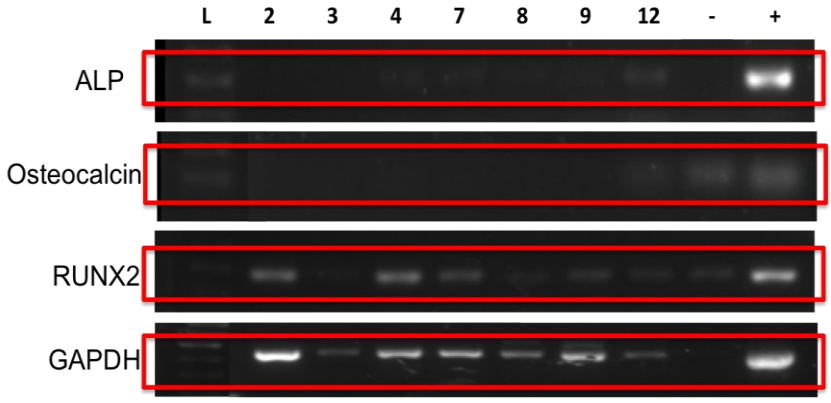

L **Ladder**	**2, 3** **Control (TMX)**	**7, 8, 9** **Ti + BG**	**+ Control**
	4 **Ti Uncoated**	**12** **Ti + BG + BP**	**- Control**

Figure 8.2: Gene expression of four different genes: ALP, Osteocalcin, RUNX2 and GAPDH (as a control) from RNA extracted at day 14. The table represents the corresponding bands to the tested samples.

Considering ALP (an early marker of osteoblast activity) gene expression, there was no observable band in the non-material control (TMX) as seen in lanes 2 and 3. Faint bands were observed in other lanes 4 – 12 which include uncoated-Ti, Ti + BG and Ti + BG + BP. The strongest band compared to the positive control was in lane 12, which was the alendronate BP-treated-Bioglass coated group. There were no observable bands indicating osteocalcin (a late marker of osteoblastic activity) gene expression in most groups. A very faint band was evident in lane 12 (alendronate BP-treated-BG-coated group). RUNX2 (a marker for osteoblast differentiation) bands were observed across all groups. As a control, GAPDH (a general marker for metabolic and non-metabolic cell activity) expression was seen with bands in all groups (apart from the negative control).

Day 14 was selected as a key period, representative of HOB cell differentiation. Qualitative analysis of cell differentiation was carried out by PCR from RNA extracted from the cells cultured on test samples. Alendronate sodium BP immobilized group displayed the strongest ALP band indicating early differentiation in this group. Indeed this correlates with the observed ALP/DNA data. Visible bands in negative control groups are attributed to contamination from positive control. Thus, analysis of the faint band of OSC in BP group (lane 12) cannot be conclusive.